Valerio Magnasco

Models for Bonding in Chemistry

$\Delta E/10^{6}E_h$

VdW

R/a_0
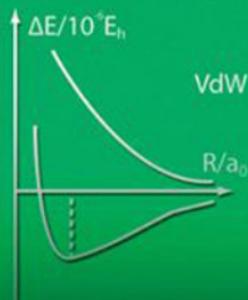
Models for Bonding
in Chemistry

Models for Bonding in Chemistry

in Chemistry

Valerio Magnasco
University of Genoa, Italy

To Deryk

Contents

Preface

Experimental evidence shows that molecules are not like 'liquid droplets' of electrons, but have a structure made of bonds and lone pairs directed in space. Even at its most elementary level, any successful theory of bonding in chemistry should explain why atoms are or are not bonded in molecules, the structure and shape of molecules in space and how molecules interact at long range. Even if modern molecular quantum mechanics offers the natural basis for very elaborate numerical calculations, models of bonding avoiding the more mathematical aspects of the subject in the spirit of Coulson's *Valence* are still of conceptual interest for providing an elementary description of valence and its implications for the electronic structure of molecules. This is the aim of this concise book, which grew from a series of lectures delivered by the author at the University of Genoa, based on original research work by the author and his group from the early 1990s to the present day. The book should serve as a complement to a 20-hour university lecture course in Physical and Quantum Chemistry.

The book consists of two parts, where essentially two models have been proposed, mostly requiring the solution of quadratic equations with real roots. Part 1 explains forces acting at *short range*, typical of localized or delocalized chemical bonds in molecules or solids; Part 2 explains forces acting at *long range*, between closed-shell atoms or molecules, resulting in the so-called van der Waals (VdW) molecules. An electrostatic model is further derived for H-bonded and VdW dimers, which explains in a simple way the angular shape of the dimers in terms of the first two permanent electric moments of the monomers.

The contents of the book is as follows. After a short self-contained mathematical introduction, Chapter 1 presents the essential elements of the variation approach to either total or second-order molecular energies,

the system of atomic units (au) necessary to simplify all mathematical expressions, and an introductory description of the electron distribution in molecules, with particular emphasis on the nature of the quantum mechanical exchange-overlap densities and their importance in determining the nature of chemical bonds and Pauli repulsions.

The contents of Part 1 is based on such premises. Using mostly 2×2 Hückel secular equations, Chapter 2 introduces a model of bonding in homonuclear and heteronuclear diatomics, multiple and delocalized bonds in hydrocarbons, and the stereochemistry of chemical bonds in polyatomic molecules; in a word, a model of the *strong* first-order interactions originating in the chemical bond. Hybridization effects and their importance in determining shape and charge distribution in first-row hydrides (CH_4, HF, H_2O and NH_3) are examined in some detail in Section 2.7.

In Chapter 3, the Hückel model of linear and closed polyene chains is used to explain the origin of band structure in the one-dimensional crystal, outlining the importance of the nature of the electronic bands in determining the different properties of insulators, conductors, semiconductors and superconductors.

Turning to Part 2, after a short introduction to stationary Rayleigh–Schrödinger (RS) perturbation theory and its use for the classification of long-range intermolecular forces, Chapter 4 deals with a simple two-state model of *weak* interactions, introducing the reader to an easy way of understanding second-order electric properties of molecules and VdW bonding between closed shells. The chapter ends with a short outline of the temperature-dependent Keesom interactions in polar gases.

Finally, Chapter 5 studies the structure of H-bonded dimers and the nature of the hydrogen bond, which has a strength *intermediate* between a VdW bond and a weak chemical bond. Besides a qualitative MO approach based on HOMO-LUMO charge transfer from an electron donor to an electron acceptor molecule, a quantitative electrostatic approach is presented, suggesting an electrostatic model which works even at its simplest pictorial level.

A list of alphabetically ordered references, and author and subject indices complete the book.

The book is dedicated to the memory of my old friend and colleague Deryk Wynn Davies, who died on 27 February 2008. I wish to thank my colleagues Gian Franco Musso and Giuseppe Figari for useful discussions on different topics of this subject, Paolo Lazzeretti and Stefano Pelloni for

some calculations using the SYSMO programme at the University of Modena and Reggio, and my son Mario who prepared the drawings on the computer. Finally, I acknowledge the support of the Italian Ministry for Education University and Research (MIUR) and the University of Genoa.

1

Mathematical Foundations

In physics and chemistry it is not possible to develop any useful model of matter without a basic knowledge of some elementary mathematics. This involves use of some elements of linear algebra, such as the solution of algebraic equations (at least quadratic), the solution of systems of linear equations, and a few elements on matrices and determinants.

1.1 MATRICES AND SYSTEMS OF LINEAR EQUATIONS

We start from matrices, limiting ourselves to the case of a *square matrix* of order two, namely a matrix involving two rows and two columns. Let us denote this matrix by the boldface capital letter $\mathbf{A}$:

$$\mathbf{A} = \begin{pmatrix} A_{11} & A_{12} \\ A_{21} & A_{22} \end{pmatrix} \tag{1.1}$$

where A_{ij} is a number called the *ij*th *element* of matrix **A**. The elements A_{ii} $(j = i)$ are called diagonal elements. We are interested mostly in *symmetric* matrices, for which $A_{21} = A_{12}$. If $A_{21} = A_{12} = 0$, the matrix is *diagonal*. Properties of a square matrix **A** are its *trace*(tr **A** = $A_{11} + A_{22}$), the sum of its diagonal elements, and its *determinant*, denoted by $|\mathbf{A}| = \det \mathbf{A}$, a number that can be evaluated from its elements by the rule:

$$|\mathbf{A}| = A_{11}A_{22} - A_{12}A_{21} \tag{1.2}$$

Two 2×2 matrices can be multiplied rows by columns by the rule:

$$\mathbf{AB} = \mathbf{C} \tag{1.3}$$

$$\begin{pmatrix} A_{11} & A_{12} \\ A_{21} & A_{22} \end{pmatrix} \begin{pmatrix} B_{11} & B_{12} \\ B_{21} & B_{22} \end{pmatrix} = \begin{pmatrix} C_{11} & C_{12} \\ C_{21} & C_{22} \end{pmatrix} \tag{1.4}$$

the elements of the product matrix **C** being:

$$\begin{cases} C_{11} = A_{11}B_{11} + A_{12}B_{21}, & C_{12} = A_{11}B_{12} + A_{12}B_{22}, \\ C_{21} = A_{21}B_{11} + A_{22}B_{21}, & C_{22} = A_{21}B_{12} + A_{22}B_{22}. \end{cases} \tag{1.5}$$

So, we are led to the *matrix multiplication rule:*

$$C_{ij} = \sum_{\kappa=1}^{2} A_{i\kappa}B_{\kappa j} \tag{1.6}$$

If matrix **B** is a simple number a, Equation (1.6) shows that *all* elements of matrix **A** must be multiplied by this number. Instead, for $a|\mathbf{A}|$, we have from Equation (1.2):

$$a|\mathbf{A}| = a(A_{11}A_{22} - A_{12}A_{21}) = \begin{vmatrix} aA_{11} & aA_{12} \\ A_{21} & A_{22} \end{vmatrix} = \begin{vmatrix} aA_{11} & A_{12} \\ aA_{21} & A_{22} \end{vmatrix}, \tag{1.7}$$

so that, multiplying a determinant by a number is equivalent to multiplying just *one* row (or *one* column) by that number.

We can have also *rectangular* matrices, where the number of rows is different from the number of columns. Particularly important is the 2×1 *column vector* **c**:

$$\mathbf{c} = \begin{pmatrix} c_{11} \\ c_{21} \end{pmatrix} = \begin{pmatrix} c_1 \\ c_2 \end{pmatrix} \tag{1.8}$$

or the 1×2 *row vector* $\tilde{\mathbf{c}}$:

$$\tilde{\mathbf{c}} = (\,c_{11} \quad c_{12}\,) = (\,c_1 \quad c_2\,) \tag{1.9}$$

where the tilde $\tilde{\ }$ means interchanging columns by rows or vice versa (the *transposed* matrix).

The linear *inhomogeneous* system:

$$\begin{cases} A_{11}c_1 + A_{12}c_2 = b_1 \\ A_{21}c_1 + A_{22}c_2 = b_2 \end{cases} \tag{1.10}$$

can be easily rewritten in matrix form using matrix multiplication rule (1.3) as:

$$\mathbf{Ac} = \mathbf{b} \tag{1.11}$$

where $\mathbf{c}$ and $\mathbf{b}$ are 2×1 column vectors.

Equation (1.10) is a system of two algebraic equations linear in the *unknowns* c_1 and c_2, the elements of matrix $\mathbf{A}$ being the *coefficients* of the linear combination. Particular importance has the case where $\mathbf{b}$ is proportional to $\mathbf{c}$ through a number λ:

$$\mathbf{Ac} = \lambda\mathbf{c} \tag{1.12}$$

which is known as the *eigenvalue equation* for matrix $\mathbf{A}$. λ is called an *eigenvalue* and $\mathbf{c}$ an *eigenvector* of the square matrix $\mathbf{A}$. Equation (1.12) is equally well written as the *homogeneous* system:

$$(\mathbf{A} - \lambda\mathbf{1})\mathbf{c} = \mathbf{0} \tag{1.13}$$

where $\mathbf{1}$ is the 2×2 diagonal matrix having 1 along the diagonal, called the *identity* matrix, and $\mathbf{0}$ is the zero vector matrix, a 2×1 column of zeros. Written explicitly, the homogeneous system (Equation 1.13) is:

$$\begin{cases} (A_{11} - \lambda)c_1 + A_{12}c_2 = 0 \\ A_{21}c_1 + (A_{22} - \lambda)c_2 = 0 \end{cases} \tag{1.14}$$

Elementary algebra then says that the system of equations (1.14) has acceptable solutions if and only if the determinant of the coefficients vanishes, namely if:

$$|\mathbf{A} - \lambda\mathbf{1}| = \begin{vmatrix} A_{11} - \lambda & A_{12} \\ A_{21} & A_{22} - \lambda \end{vmatrix} = 0 \tag{1.15}$$

Equation (1.15) is known as the *secular equation* for matrix $\mathbf{A}$. If we expand the determinant according to the rule of Equation (1.2), we obtain

for a symmetric matrix $\mathbf{A}$:

$$(A_{11}-\lambda)(A_{22}-\lambda)-A_{12}{}^2 = 0 \tag{1.16}$$

giving the *quadratic* equation in λ:

$$\lambda^2-(A_{11}+A_{22})\lambda+A_{11}A_{22}-A_{12}{}^2 = 0 \tag{1.17}$$

which has the two *real*[1] solutions (the eigenvalues, the roots of the equation):

$$\begin{cases} \lambda_1 = \dfrac{A_{11}+A_{22}}{2} + \dfrac{\Delta}{2} \\[2ex] \lambda_2 = \dfrac{A_{11}+A_{22}}{2} - \dfrac{\Delta}{2} \end{cases} \tag{1.18}$$

where Δ is the *positive* quantity:

$$\Delta = \left[(A_{22}-A_{11})^2 + 4A_{12}{}^2\right]^{1/2} > 0 \tag{1.19}$$

Inserting each root in turn in the homogeneous system (Equation 1.14), we obtain the corresponding solutions (the eigenvectors, our unknowns):

$$\begin{cases} c_{11} = \left(\dfrac{\Delta+(A_{22}-A_{11})}{2\Delta}\right)^{1/2}, & c_{21} = \left(\dfrac{\Delta-(A_{22}-A_{11})}{2\Delta}\right)^{1/2} \\[3ex] c_{12} = -\left(\dfrac{\Delta-(A_{22}-A_{11})}{2\Delta}\right)^{1/2}, & c_{22} = \left(\dfrac{\Delta+(A_{22}-A_{11})}{2\Delta}\right)^{1/2} \end{cases} \tag{1.20}$$

where the second index (a column index, shown in bold type in Equations 1.20) specifies the eigenvalue to which the eigenvector refers. All such results can be collected in the 2×2 square matrices:

$$\Lambda = \begin{pmatrix} \lambda_1 & 0 \\ 0 & \lambda_2 \end{pmatrix}, \quad \mathbf{C} = (\, \mathbf{c}_1 \quad \mathbf{c}_2 \,) = \begin{pmatrix} c_{11} & c_{12} \\ c_{21} & c_{22} \end{pmatrix} \tag{1.21}$$

the first being the diagonal matrix of the eigenvalues (the *roots* of our secular equation 1.17), the second the row matrix of the eigenvectors (the *unknowns* of the homogeneous system 1.14). Matrix multiplication rule shows that:

$$\tilde{\mathbf{C}}\mathbf{A}\mathbf{C} = \Lambda, \quad \tilde{\mathbf{C}}\mathbf{C} = \mathbf{C}\tilde{\mathbf{C}} = 1 \tag{1.22}$$

---

[1]This is a mathematical property of real symmetric matrices.

We usually say that the first of Equations (1.22) expresses the *diagonalization* of the symmetric matrix **A** through a transformation with the complete matrix of its eigenvectors, while the second equations express the *normalization* of the coefficients (i.e., the resulting vectors are chosen to have modulus 1).[2]

Equations (18–20) simplify noticeably in the case $A_{22} = A_{11} = \alpha$. Then, putting $A_{12} = A_{21} = \beta$, we obtain:

$$\begin{cases} \lambda_1 = \alpha + \beta, \quad \lambda_2 = \alpha - \beta \\ \mathbf{c}_1 = \begin{pmatrix} 1/\sqrt{2} \\ 1/\sqrt{2} \end{pmatrix}, \quad \mathbf{c}_2 = \begin{pmatrix} -1/\sqrt{2} \\ 1/\sqrt{2} \end{pmatrix} \end{cases} \quad (1.23)$$

Occasionally, we shall need to solve the so called *pseudosecular equation* for the symmetric matrix **A** arising from the *pseudoeigenvalue equation*:

$$\mathbf{Ac} = \lambda \mathbf{Sc} \Rightarrow |\mathbf{A} - \lambda \mathbf{S}| = \begin{vmatrix} A_{11} - \lambda & A_{12} - \lambda S \\ A_{21} - \lambda S & A_{22} - \lambda \end{vmatrix} = 0 \quad (1.24)$$

where **S** is the *overlap matrix*:

$$\mathbf{S} = \begin{pmatrix} S_{11} & S_{12} \\ S_{21} & S_{22} \end{pmatrix} = \begin{pmatrix} 1 & S \\ S & 1 \end{pmatrix} \quad (1.25)$$

Solution of Equation (1.24) then gives:

$$\begin{cases} \lambda_1 = \dfrac{A_{11} + A_{22} - 2A_{12}S}{2(1 - S^2)} - \dfrac{\Delta}{2(1 - S^2)} \\ \lambda_2 = \dfrac{A_{11} + A_{22} - 2A_{12}S}{2(1 - S^2)} + \dfrac{\Delta}{2(1 - S^2)} \end{cases} \quad (1.26)$$

$$\Delta = \left[(A_{22} - A_{11})^2 + 4(A_{12} - A_{11}S)(A_{12} - A_{22}S) \right]^{1/2} > 0 \quad (1.27)$$

The eigenvectors corresponding to the roots (Equations 1.26) are rather complicated (Magnasco, 2007), so we shall content ourselves here by giving only the results for $A_{22} = A_{11} = \alpha$ and $A_{21} = A_{12} = \beta$:

---

[2]The length of the vectors. A matrix satisfying the second of Equations (1.22) is said to be an *orthogonal* matrix.

$$\begin{cases} \lambda_1 = \dfrac{\alpha+\beta}{1+S}, & \mathbf{c}_{11} = (2+2S)^{-1/2}, & \mathbf{c}_{21} = (2+2S)^{-1/2} \\[3mm] \lambda_2 = \dfrac{\alpha-\beta}{1-S}, & \mathbf{c}_{12} = -(2-2S)^{-1/2}, & \mathbf{c}_{22} = (2-2S)^{-1/2} \end{cases} \tag{1.28}$$

under these assumptions, these are the elements of the square matrices Λ and $\mathbf{C}$ (Equations 1.21). Matrix multiplication shows that these matrices satisfy the generalization of Equations (1.22):

$$\tilde{\mathbf{C}}\mathbf{A}\mathbf{C} = \Lambda, \quad \tilde{\mathbf{C}}\mathbf{S}\mathbf{C} = \mathbf{C}\mathbf{S}\tilde{\mathbf{C}} = \mathbf{1} \tag{1.29}$$

so that matrices $\mathbf{A}$ and $\mathbf{S}$ are simultaneously diagonalized under the transformation with the orthogonal matrix $\mathbf{C}$.

All previous results can be extended to square symmetric matrices of order N, in which case the solution of the corresponding secular equations must be found by numerical methods, unless use can be made of symmetry arguments.

1.2   PROPERTIES OF EIGENVALUES AND EIGENVECTORS

It is of interest to stress some properties hidden in the eigenvalues $(\lambda_1 \quad \lambda_2)$ and eigenvectors $\begin{pmatrix} \mathbf{c}_1 \\ \mathbf{c}_2 \end{pmatrix}$, (Equations 1.23), of the symmetric matrix $\mathbf{A}$ of order 2 with $A_{22} = A_{11} = \alpha$ and $A_{21} = A_{12} = \beta$.

In fact, Equation (1.17) can be written:

$$(\lambda_1-\lambda)(\lambda_2-\lambda) = \lambda_1\lambda_2-(\lambda_1 + \lambda_2)\lambda + \lambda^2 = 0 \tag{1.30}$$

so that:

$$\lambda_1\lambda_2 = A_{11}A_{22}-A_{12}{}^2 = \alpha^2-\beta^2 = \det \mathbf{A} \tag{1.31}$$

$$\lambda_1 + \lambda_2 = A_{11} + A_{22} = 2\alpha = \operatorname{tr} \mathbf{A} \tag{1.32}$$

In Equation (1.17), therefore, the coefficient of λ^0, the determinant of matrix $\mathbf{A}$, is expressible as the *product* of the two eigenvalues; the coefficient of λ, the trace of matrix $\mathbf{A}$, is expressible as the *sum* of the two eigenvalues.

From the eigenvectors of Equations (1.23) we can construct the two square symmetric matrices of order 2:

$$P_1 = c_1 \tilde{c}_1 = \begin{pmatrix} \dfrac{1}{\sqrt{2}} \\[2ex] \dfrac{1}{\sqrt{2}} \end{pmatrix} \begin{pmatrix} \dfrac{1}{\sqrt{2}} & \dfrac{1}{\sqrt{2}} \end{pmatrix} = \begin{pmatrix} \dfrac{1}{2} & \dfrac{1}{2} \\[2ex] \dfrac{1}{2} & \dfrac{1}{2} \end{pmatrix} \qquad (1.33)$$

$$P_2 = c_2 \tilde{c}_2 = \begin{pmatrix} -\dfrac{1}{\sqrt{2}} \\[2ex] \dfrac{1}{\sqrt{2}} \end{pmatrix} \begin{pmatrix} -\dfrac{1}{\sqrt{2}} & \dfrac{1}{\sqrt{2}} \end{pmatrix} = \begin{pmatrix} \dfrac{1}{2} & -\dfrac{1}{2} \\[2ex] -\dfrac{1}{2} & \dfrac{1}{2} \end{pmatrix} \qquad (1.34)$$

The two matrices P_1 and P_2 do not admit inverse (the determinants of both are zero) and have the properties:

$$P_1{}^2 = \begin{pmatrix} \dfrac{1}{2} & \dfrac{1}{2} \\[2ex] \dfrac{1}{2} & \dfrac{1}{2} \end{pmatrix} \begin{pmatrix} \dfrac{1}{2} & \dfrac{1}{2} \\[2ex] \dfrac{1}{2} & \dfrac{1}{2} \end{pmatrix} = \begin{pmatrix} \dfrac{1}{2} & \dfrac{1}{2} \\[2ex] \dfrac{1}{2} & \dfrac{1}{2} \end{pmatrix} = P_1 \qquad (1.35)$$

$$P_2{}^2 = \begin{pmatrix} \dfrac{1}{2} & -\dfrac{1}{2} \\[2ex] -\dfrac{1}{2} & \dfrac{1}{2} \end{pmatrix} \begin{pmatrix} \dfrac{1}{2} & -\dfrac{1}{2} \\[2ex] -\dfrac{1}{2} & \dfrac{1}{2} \end{pmatrix} = \begin{pmatrix} \dfrac{1}{2} & -\dfrac{1}{2} \\[2ex] -\dfrac{1}{2} & \dfrac{1}{2} \end{pmatrix} = P_2 \qquad (1.36)$$

$$P_1 P_2 = \begin{pmatrix} \dfrac{1}{2} & \dfrac{1}{2} \\[2ex] \dfrac{1}{2} & \dfrac{1}{2} \end{pmatrix} \begin{pmatrix} \dfrac{1}{2} & -\dfrac{1}{2} \\[2ex] -\dfrac{1}{2} & \dfrac{1}{2} \end{pmatrix} = \begin{pmatrix} 0 & 0 \\ 0 & 0 \end{pmatrix} = 0 \qquad (1.37)$$

$$P_2 P_1 = \begin{pmatrix} \dfrac{1}{2} & -\dfrac{1}{2} \\[2ex] -\dfrac{1}{2} & \dfrac{1}{2} \end{pmatrix} \begin{pmatrix} \dfrac{1}{2} & \dfrac{1}{2} \\[2ex] \dfrac{1}{2} & \dfrac{1}{2} \end{pmatrix} = \begin{pmatrix} 0 & 0 \\ 0 & 0 \end{pmatrix} = 0 \qquad (1.38)$$

$$\mathbf{P}_1 + \mathbf{P}_2 = \begin{pmatrix} \dfrac{1}{2} & \dfrac{1}{2} \\[2mm] \dfrac{1}{2} & \dfrac{1}{2} \end{pmatrix} + \begin{pmatrix} \dfrac{1}{2} & -\dfrac{1}{2} \\[2mm] -\dfrac{1}{2} & \dfrac{1}{2} \end{pmatrix} = \begin{pmatrix} 1 & 0 \\ 0 & 1 \end{pmatrix} = \mathbf{1} \qquad (1.39)$$

In mathematics, matrices having these properties (idempotency, mutual exclusivity, completeness[3]) are called *projectors*. In fact, acting on matrix $\mathbf{C}$ of Equation (1.21)

$$\mathbf{P}_1 \mathbf{C} = \mathbf{P}_1 \mathbf{c}_1 + \mathbf{P}_1 \mathbf{c}_2 = \mathbf{c}_1 \qquad (1.40)$$

since:

$$\mathbf{P}_1 \mathbf{c}_1 = \begin{pmatrix} \dfrac{1}{2} & \dfrac{1}{2} \\[2mm] \dfrac{1}{2} & \dfrac{1}{2} \end{pmatrix} \begin{pmatrix} \dfrac{1}{\sqrt{2}} \\[2mm] \dfrac{1}{\sqrt{2}} \end{pmatrix} = \begin{pmatrix} \dfrac{1}{2}\dfrac{1}{\sqrt{2}} + \dfrac{1}{2}\dfrac{1}{\sqrt{2}} \\[2mm] \dfrac{1}{2}\dfrac{1}{\sqrt{2}} + \dfrac{1}{2}\dfrac{1}{\sqrt{2}} \end{pmatrix} = \begin{pmatrix} \dfrac{1}{\sqrt{2}} \\[2mm] \dfrac{1}{\sqrt{2}} \end{pmatrix} = \mathbf{c}_1 \quad (1.41)$$

$$\mathbf{P}_1 \mathbf{c}_2 = \begin{pmatrix} \dfrac{1}{2} & \dfrac{1}{2} \\[2mm] \dfrac{1}{2} & \dfrac{1}{2} \end{pmatrix} \begin{pmatrix} -\dfrac{1}{\sqrt{2}} \\[2mm] \dfrac{1}{\sqrt{2}} \end{pmatrix} = \begin{pmatrix} -\dfrac{1}{2}\dfrac{1}{\sqrt{2}} + \dfrac{1}{2}\dfrac{1}{\sqrt{2}} \\[2mm] -\dfrac{1}{2}\dfrac{1}{\sqrt{2}} + \dfrac{1}{2}\dfrac{1}{\sqrt{2}} \end{pmatrix} = \begin{pmatrix} 0 \\ 0 \end{pmatrix} = \mathbf{0}$$

$$(1.42)$$

so that, acting on the complete matrix $\mathbf{C}$ of the eigenvectors, $\mathbf{P}_1$ selects its eigenvector $\mathbf{c}_1$, at the same time annihilating $\mathbf{c}_2$. In the same way:

$$\mathbf{P}_2 \mathbf{C} = \mathbf{P}_2 \mathbf{c}_1 + \mathbf{P}_2 \mathbf{c}_2 = \mathbf{c}_2 \qquad (1.43)$$

This makes evident the projector properties of matrices $\mathbf{P}_1$ and $\mathbf{P}_2$.

Furthermore, matrices $\mathbf{P}_1$ and $\mathbf{P}_2$ allow one to write matrix $\mathbf{A}$ in the so-called *canonical* form:

$$\mathbf{A} = \lambda_1 \mathbf{P}_1 + \lambda_2 \mathbf{P}_2 \qquad (1.44)$$

---

[3]Often referred to as resolution of the identity.

Equation (1.44) is easily verified:

$$\begin{cases} \lambda_1 \mathbf{P}_1 + \lambda_2 \mathbf{P}_2 = (\alpha + \beta) \begin{pmatrix} \dfrac{1}{2} & \dfrac{1}{2} \\[2mm] \dfrac{1}{2} & \dfrac{1}{2} \end{pmatrix} + (\alpha - \beta) \begin{pmatrix} \dfrac{1}{2} & -\dfrac{1}{2} \\[2mm] -\dfrac{1}{2} & \dfrac{1}{2} \end{pmatrix} \\[8mm] = \begin{pmatrix} \dfrac{\alpha+\beta}{2} + \dfrac{\alpha-\beta}{2} & \dfrac{\alpha+\beta}{2} - \dfrac{\alpha-\beta}{2} \\[4mm] \dfrac{\alpha+\beta}{2} - \dfrac{\alpha-\beta}{2} & \dfrac{\alpha+\beta}{2} + \dfrac{\alpha-\beta}{2} \end{pmatrix} = \begin{pmatrix} \alpha & \beta \\ \beta & \alpha \end{pmatrix} = \mathbf{A} \end{cases} \tag{1.45}$$

The same holds true for any analytical function[4]F of matrix $\mathbf{A}$:

$$F(\mathbf{A}) = F(\lambda_1)\mathbf{P}_1 + F(\lambda_2)\mathbf{P}_2 \tag{1.46}$$

Therefore, it is easy to calculate, say, the inverse or the square root of matrix $\mathbf{A}$. For instance, we obtain for the *inverse* matrix $(F = {}^{-1})$:

$$\begin{cases} \lambda_1{}^{-1}\mathbf{P}_1 + \lambda_2{}^{-1}\mathbf{P}_2 = \begin{pmatrix} \dfrac{1}{2(\alpha+\beta)} & \dfrac{1}{2(\alpha+\beta)} \\[4mm] \dfrac{1}{2(\alpha+\beta)} & \dfrac{1}{2(\alpha+\beta)} \end{pmatrix} + \begin{pmatrix} \dfrac{1}{2(\alpha-\beta)} & -\dfrac{1}{2(\alpha-\beta)} \\[4mm] -\dfrac{1}{2(\alpha-\beta)} & \dfrac{1}{2(\alpha-\beta)} \end{pmatrix} \\[10mm] = \dfrac{1}{2(\alpha^2-\beta^2)} \begin{pmatrix} (\alpha-\beta)+(\alpha+\beta) & (\alpha-\beta)-(\alpha+\beta) \\ (\alpha-\beta)-(\alpha+\beta) & (\alpha-\beta)+(\alpha+\beta) \end{pmatrix} = \dfrac{1}{2(\alpha^2-\beta^2)} \begin{pmatrix} 2\alpha & -2\beta \\ -2\beta & 2\alpha \end{pmatrix} \\[8mm] = \dfrac{1}{\alpha^2-\beta^2} \begin{pmatrix} \alpha & -\beta \\ -\beta & \alpha \end{pmatrix} = \mathbf{A}^{-1} \end{cases} \tag{1.47}$$

and we obtain the usual result for the inverse matrix $(\mathbf{A}^{-1}\mathbf{A} = \mathbf{A}\mathbf{A}^{-1} = \mathbf{1})$.

In the same way, provided $\sqrt{\lambda_1}$ and $\sqrt{\lambda_2}$ are positive, we can calculate the *square root* of matrix $\mathbf{A}\left(F = \sqrt{\ }\right)$:

$$\begin{cases} \sqrt{\mathbf{A}} = \sqrt{\alpha+\beta}\,\mathbf{P}_1 + \sqrt{\alpha-\beta}\,\mathbf{P}_2 \\[4mm] = \dfrac{1}{2} \begin{pmatrix} \sqrt{\alpha+\beta}+\sqrt{\alpha-\beta} & \sqrt{\alpha+\beta}-\sqrt{\alpha-\beta} \\ \sqrt{\alpha+\beta}-\sqrt{\alpha-\beta} & \sqrt{\alpha+\beta}+\sqrt{\alpha-\beta} \end{pmatrix} = \begin{pmatrix} \dfrac{A+B}{2} & \dfrac{A-B}{2} \\[4mm] \dfrac{A-B}{2} & \dfrac{A+B}{2} \end{pmatrix} \end{cases} \tag{1.48}$$

---

[4]Any function expressible as a power series, e.g. inverse, square root, exponential.

where we have put:

$$A = \sqrt{\alpha + \beta}, \quad B = \sqrt{\alpha - \beta} \tag{1.49}$$

Then, we can easily check that:

$$
\begin{cases}
\sqrt{\mathbf{A}}\sqrt{\mathbf{A}} = \dfrac{1}{4} \begin{pmatrix} A+B & A-B \\ A-B & A+B \end{pmatrix} \begin{pmatrix} A+B & A-B \\ A-B & A+B \end{pmatrix} \\[2mm]
\qquad = \dfrac{1}{4} \begin{pmatrix} (A+B)^2 + (A-B)^2 & 2(A^2-B^2) \\ 2(A^2-B^2) & (A-B)^2 + (A+B)^2 \end{pmatrix} \\[2mm]
\qquad = \dfrac{1}{4} \begin{pmatrix} 2(A^2+B^2) & 2(A^2-B^2) \\ 2(A^2-B^2) & 2(A^2+B^2) \end{pmatrix} = \dfrac{1}{4} \begin{pmatrix} 4\alpha & 4\beta \\ 4\beta & 4\alpha \end{pmatrix} = \mathbf{A}
\end{cases}
\tag{1.50}
$$

as it must be. These examples show how far we can go when eigenvalues and eigenvectors of a symmetric matrix are known.

1.3   VARIATIONAL APPROXIMATIONS

For our description of atoms and molecules, we rely on the *orbital model*, where atoms or molecules are described by one or more point-like positively charged nuclei surrounded by a cloud of negatively charged electrons, whose density is distributed in space in terms of atomic orbitals (one-centre, AOs) or molecular orbitals (multicentre, MOs) $\psi(\mathbf{r})$, one-electron wavefunctions, such that

$$|\psi(\mathbf{r})|^2 d\mathbf{r} \tag{1.51}$$

gives the probability of finding at $d\mathbf{r}$ an electron in state $\psi(\mathbf{r})$, provided $\psi(\mathbf{r})$ satisfies the *normalization* condition:

$$\int d\mathbf{r} |\psi(\mathbf{r})|^2 = 1 \tag{1.52}$$

the integration being extended over all space. The AOs are functions of the space point $\mathbf{r}$ in the three spherical coordinates (r, θ, φ) that depend on the three quantum numbers n, l, m and have radial and angular dependence. As well known, they are classified as $1s, 2s, 2p, 3s, 3p, 3d$, etc. and we shall
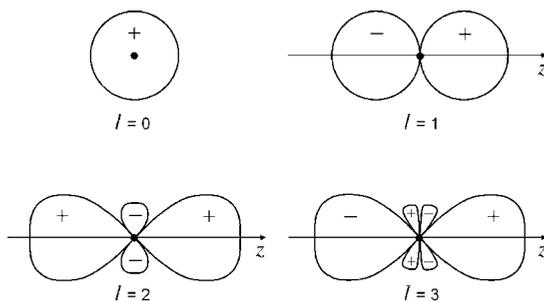
Figure 1.1 Polar diagrams of the angular part of *s*, *p*, *d*, and *f* AOs with $m = 0$. Reprinted from Magnasco, V., Methods of Molecular Quatum Mechanics: An Introduction to Electronic Molecular Structure. Copyright (2009) with permission from John Wiley and Sons
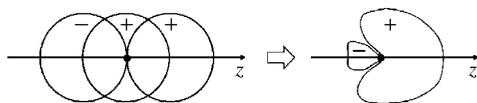
Figure 1.2 Schematic drawing of the formation of an *sp* hybrid AO

assume that they are real *regular*[5] functions showing an exponential (Slater-type, STO) or gaussian (GTO) radial decay. Figure 1.1 shows schematically the polar diagrams of the angular parts of *s*, *p*, *d*, and *f* AOs with $l = 0, 1, 2, 3$, respectively, and $m = 0$.

Hybrid orbitals are AOs mixed on the same centre (e.g. *s* and *p*). Figure 1.2 sketches the formation of an *sp* hybrid directed along the *z* axis (right of the figure) from the mixing of a spherical 2*s* orbital with a $2p_z$ orbital (left of the figure). Because its form is nonsymmetric with respect to the nucleus on which it is centred, the hybrid AO acquires an intrinsic dipole moment, called by Coulson (1961) the *atomic dipole*, which is very important in the theoretical interpretation of the observed dipole moment in the molecule (see the case of first-row hydrides in Chapter 2). We are not interested in further details about AOs here, but more can be learned elsewhere (Magnasco, 2007, 2009a).

The AOs are obtained by solving some kind of differential Schrödinger-type eigenvalue equation, which for a single electron can be written:

$$\hat{H}\psi = \varepsilon\psi \tag{1.53}$$

---

[5]A *regular* function is a mathematical function satisfying the three conditions of being: (i) single-valued; (ii) continuous with its first derivatives; and (iii) quadratically integrable, i.e. vanishing at infinity.

where $\hat{H} = \hat{T} + V$ is the total (kinetic + potential) energy or *Hamiltonian* operator[6], ψ a wavefunction (the *eigenfunction* of Equation 1.53), and ε (the *eigenvalue*) an orbital energy. In our model, $\hat{H}$ will be replaced by a symbol H, where we suppress the caret characterizing the operator.

Since equations as (1.53) are difficult to solve exactly, practically all results in the applications of quantum mechanics to chemistry rely on a general method of approximation due to Rayleigh and known as the *variational method* (Magnasco, 2007, 2009a), which we summarize briefly in the following.

Let φ be a normalized[7] regular *trial* (or *variational*) function. We define the Rayleigh ratio as the functional:[8]

$$\varepsilon[\varphi] = \frac{\int dx\, \varphi^*(x) H\varphi(x)}{\int dx\, \varphi^*(x)\varphi(x)} = \frac{\langle\varphi|H|\varphi\rangle}{\langle\varphi|\varphi\rangle} \qquad (1.54)$$

where x are the electronic coordinates, $\varphi^*(x)$ the function complex conjugate to $\varphi(x)$, and H the Hamiltonian of the system. In the last term on the right-hand side of the equation we have introduced the so-called Dirac notation for the integrals. Then, the Rayleigh variational principle states that, if E_0 is the *true* energy of the ground state (the state of lowest energy):

$$\varepsilon[\varphi] \geq E_0 \qquad (1.55)$$

In other words, any approximate energy must lie *above* the true energy of the ground state, giving an *upper bound* to the electronic energy. Variational approximations to energy and wavefunction can then be simply worked out by introducing some *variational parameters* $\{c\}$ in the trial function φ, then evaluating the integrals in the functional (1.54), in order to obtain an ordinary function of the parameters $\{c\}$ that can be *minimized* against these parameters. Therefore, for a single parameter c:

$$\varepsilon[\varphi] = \frac{\int dx\, \varphi^*(x, c) H\varphi(x, c)}{\int dx\, \varphi^*(x, c)\varphi(x, c)} = \varepsilon(c) \Rightarrow \min \qquad (1.56)$$

The necessary condition for the minimum of $\varepsilon(c)$ will be:

$$\frac{d\varepsilon}{dc} = 0 \Rightarrow c_{\min} \qquad (1.57)$$

---

[6] An operator is a rule changing a regular function into another one, and is denoted by the caret sign ^.
[7] A function satisfying Equation (1.52).
[8] A function of function $\varphi(x)$.

an algebraic equation which must be solved for the *best* value of parameter c, giving in this way the best variational energy and wavefunction.

The most interesting application for our purposes is to construct MOs by the linear combination of atomic orbitals (LCAO) method, where the variable parameters are the coefficients of the linear combination of some basic orbitals $\{\chi\}^9$ (Ritz method). It can be shown that, in this case, *the best orbitals are obtained by solving the eigenvalue equation for matrix* **H**:

$$\mathbf{Hc} = \varepsilon \mathbf{c} \Rightarrow (\mathbf{H} - \varepsilon \mathbf{1})\mathbf{c} = 0 \qquad (1.58)$$

where:

$$H_{ij} = \langle \chi_i | H | \chi_j \rangle, \quad S_{ij} = \langle \chi_i | \chi_j \rangle = \delta_{ij} \qquad (1.59)$$

For molecules, all elements of matrix **H** are negative numbers. The homogeneous system (Equation 1.58) has nontrivial solutions if and only if:

$$|\mathbf{H} - \varepsilon \mathbf{1}| = 0 \qquad (1.60)$$

The solution of the secular equation (1.60) for our simple case of a 2×2 symmetric matrix **H** (a basis of *two* AOs) yields as *best* values for the variational energy the *two* real roots (eigenvalues) ε_1 and ε_2, that are usually written in ascending order, with the corresponding *two* eigenvectors $\mathbf{c}_1$ and $\mathbf{c}_2$ determining the *two* molecular orbitals φ_1 and φ_2 (Equations 18–20 with $\lambda = \varepsilon$, or the simpler Equations 1.23 when the diagonal elements are equal):

$$\begin{cases} \varepsilon_1 \leq \varepsilon_2 \\ \mathbf{c}_1, \mathbf{c}_2 \\ \varphi_1, \varphi_2 \end{cases} \qquad (1.61)$$

$\varepsilon < 0$ means *bonding*, $\varepsilon > 0$ means *antibonding*, with a corresponding notation for the resulting MOs.

The same procedure can be applied to find approximations to the second-order energy E_2 of Section 4.2 of Chapter 4 in the context of the Hylleraas variational method (Magnasco, 2007, 2009a), as we shall illustrate in the simple case of two functions. We start from a convenient set of basis functions $\boldsymbol{\chi}$ written as the (1×2) row vector:

$$\boldsymbol{\chi} = (\chi_1 \quad \chi_2) \qquad (1.62)$$

---

[9]Assumed normalized and orthogonal to each other, namely $\langle \chi_i | \chi_j \rangle = \delta_{ij}$, where δ is the Kronecker' symbol ($=1$ for $j = i, = 0$ for $j \neq i$).

possibly orthonormal in themselves but necessarily *orthogonal* to ψ_0. We shall assume that:

$$\boldsymbol{\chi}^\dagger\boldsymbol{\chi} = \mathbf{1}, \quad \boldsymbol{\chi}^\dagger\psi_0 = \mathbf{0} \tag{1.63}$$

If the $\boldsymbol{\chi}$s are not orthogonal they must first be orthogonalized by the Schmidt method (Magnasco, 2007). Then, we construct the matrices:

$$\mathbf{M} = \boldsymbol{\chi}^\dagger(\hat{H}_0 - E_0)\boldsymbol{\chi} \tag{1.64}$$

the (2×2) Hermitian matrix of the *excitation energies*, and:

$$\boldsymbol{\mu} = \boldsymbol{\chi}^\dagger(\hat{H}_1\psi_0) \tag{1.65}$$

the (2×1) column vector of the transition moments.

By expanding the first-order function ψ_1 in the *finite* set of the $\boldsymbol{\chi}$s, we can write:

$$\psi_1 = \boldsymbol{\chi}\mathbf{C} = \sum_{\kappa=1}^{2} \chi_\kappa C_\kappa \tag{1.66}$$

$$E_2 = \mathbf{C}^\dagger\mathbf{M}\mathbf{C} + \mathbf{C}^\dagger\boldsymbol{\mu} + \boldsymbol{\mu}^\dagger\mathbf{C} \tag{1.67}$$

which is minimum for:

$$\frac{\delta E_2}{\delta\mathbf{C}^\dagger} = \mathbf{M}\mathbf{C} + \boldsymbol{\mu} = \mathbf{0} \Rightarrow \mathbf{C}(\text{best}) = -\mathbf{M}^{-1}\boldsymbol{\mu} \tag{1.68}$$

giving as *best* variational approximation to the second-order energy E_2:

$$E_2(\text{best}) = -\boldsymbol{\mu}^\dagger\mathbf{M}^{-1}\boldsymbol{\mu} \tag{1.69}$$

The symmetric matrix $\mathbf{M}$ can be reduced to *diagonal* form by a unitary transfomation[10] $\mathbf{U}$ among its basis functions $\boldsymbol{\chi}$:

$$\boldsymbol{\psi} = \boldsymbol{\chi}\mathbf{U}, \quad \mathbf{U}^\dagger\mathbf{M}\mathbf{U} = \boldsymbol{\varepsilon}, \quad \mathbf{U}^\dagger\boldsymbol{\mu} = \boldsymbol{\mu}_\psi \tag{1.70}$$

where $\boldsymbol{\varepsilon}$ is here the (2×2) diagonal matrix of the (positive) *excitation energies*:

$$\boldsymbol{\varepsilon} = \begin{pmatrix} \varepsilon_1 & 0 \\ 0 & \varepsilon_2 \end{pmatrix} \tag{1.71}$$

---

[10] A unitary matrix $\mathbf{U}$ satisfies $\mathbf{U}^{-1} = \mathbf{U}^\dagger$, where $\mathbf{U}^{-1}$ is the inverse and $\mathbf{U}^\dagger = (\tilde{\mathbf{U}})^*$ the adjoint matrix (Magnasco, 2007). A matrix is said Hermitian if $\mathbf{U} = \mathbf{U}^\dagger$. For *real* elements, unitary and orthogonal matrices coincide, so that we can use either of them indistinctly.

The ψs are called *pseudostates*, and give best E_2 in the form:

$$E_2(\text{best}) = -\boldsymbol{\mu}_\psi^\dagger \boldsymbol{\varepsilon}^{-1} \boldsymbol{\mu}_\psi = -\sum_{\kappa=1}^{2} \frac{|\langle \psi_\kappa | \hat{H}_1 | \psi_0 \rangle|^2}{\varepsilon_\kappa} \tag{1.72}$$

which is known as *sum-over-pseudostates* expression. Equation (1.72) has the same form as the analogous expression that would arise from the discrete *eigenstates* of $\hat{H}_0$, but with definitely better convergence properties, reducing the infinite summation to a sum of a *finite* number of terms, and avoiding the need of considering the contribution from the continuous part of the spectrum (Magnasco, 2007).

1.4 ATOMIC UNITS

To get rid of all fundamental physical constants in our mathematical formulae we shall introduce consistently a system of *atomic units* (au), by putting:

$$e = \hbar = m = 4\pi\varepsilon_0 = 1 \tag{1.73}$$

The basic atomic units are obtained from the SI values of the fundamental physical constants given in Table 1.1 (Mohr and Taylor, 2003).

The basic au of charge, length, energy and time are then expressed by:

$$
\begin{cases}
\text{Charge} & e = 1.602\,176 \times 10^{-19}\,\text{C} \\[2mm]
\text{Length, } Bohr & a_0 = 4\pi\varepsilon_0 \dfrac{\hbar^2}{me^2} = 5.291\,772 \times 10^{-11}\,\text{m} \\[3mm]
\text{Energy, } Hartree & E_h = \dfrac{1}{4\pi\varepsilon_0} \dfrac{e^2}{a_0} = 4.359\,744 \times 10^{-18}\,\text{J} \\[3mm]
\text{Time} & \tau = \dfrac{\hbar}{E_h} = 2.418\,884 \times 10^{-17}\,\text{s}
\end{cases}
\tag{1.74}
$$

When the atomic unit of energy is referred to molar quantities, we have the different SI equivalents:

$$
\begin{cases}
N_A E_h = 2625.499\,\text{kJ}\,\text{mol}^{-1} = 27.211\,38\,\text{eV}\,\text{mol}^{-1} \\[2mm]
\quad = 219.474\,6 \times 10^3\,\text{cm}^{-1}\,\text{mol}^{-1} = 315.774\,6 \times 10^3\,\text{K}\,\text{mol}^{-1}
\end{cases}
\tag{1.75}
$$

Table 1.1 Fundamental physical constants

Physical quantity	Value in SI units
Elementary charge	$e = 1.602\,176 \times 10^{-19}$ C
Electron mass	$m = 9.109\,382 \times 10^{-31}$ kg
Reduced Planck's constant	$\hbar = 1.054\,572 \times 10^{-34}$ J s
Vacuum permittivity	$4\pi\varepsilon_0 = 1.112\,650$ J^{-1} C^2 m^{-1}
Light velocity in vacuum	$c = 2.997\,925 \times 10^8$ m s^{-1}
Avogadro number	$N_A = 6.022\,142 \times 10^{23}$ mol^{-1}
Boltzmann constant	$k = 1.380\,650 \times 10^{-23}$ J K^{-1}

with the submultiples:

$$10^{-3}E_h = mE_h \quad [\text{milliHartree}] \tag{1.76}$$

$$10^{-6}E_h = \mu E_h \quad [\text{microHartree}] \tag{1.77}$$

etc. The milliHartree is the characteristic unit for the energy of the chemical bond, the microHartree is that for the energy of the Van der Waals bond. The hydrogen bond has an intermediate energy, corresponding to that of a weak chemical bond.

The basic au for dipole, quadrupole and octupole electric moments are given as:

$$\begin{cases} \text{Dipole moment}, ea_0 & = 8.478 \times 10^{-30} \text{ C} \times \text{m} \\ & = 2.542 \times 10^{-18} \text{ esu} \times \text{cm} = 2.542 \text{ D} \\ \text{Quadrupole moment}, ea_0{}^2 & = 4.486 \times 10^{-40} \text{ C} \times \text{m}^2 \\ & = 1.345 \times 10^{-26} \text{ esu} \times \text{cm}^2 = 1.345 \text{ B} \\ \text{Octupole moment}, ea_0{}^3 & = 2.374 \times 10^{-50} \text{ C} \times \text{m}^3 \\ & = 7.117 \times 10^{-35} \text{ esu} \times \text{cm}^3 \end{cases} \tag{1.78}$$

In the expressions above, D is the Debye unit of electric dipole moment, and B the Buckingham unit for the electric quadrupole moment.

At the end of a calculation in atomic units, as we shall usually do, the actual SI values can be obtained by taking into account the SI equivalents (1.74) and (1.78). As an example, we give below the calculation of the SI equivalent of the Hartree unit to seven significant figures:

$$
\begin{cases}
E_h = \dfrac{1}{4\pi\varepsilon_0}\dfrac{e^2}{a_0} = \dfrac{me^4}{(4\pi\varepsilon_0)^2\hbar^2} \\[3mm]
\quad = \dfrac{9.109\,382 \times 10^{-31} \times (1.602\,176 \times 10^{-19})^4}{(1.112\,650 \times 10^{-10})^2 \times (1.054\,571 \times 10^{-34})^2}\dfrac{\text{kg C}^4}{\text{C}^4\,\text{m}^{-2}\,\text{J}^2\,\text{s}^2} \\[3mm]
\quad = 4.359\,744 \times 10^{-18}\ \text{J.}
\end{cases}
\tag{1.79}
$$

1.5 THE ELECTRON DISTRIBUTION IN MOLECULES

The one-electron spatial function $P(\mathbf{r})$ describing the distribution of the electrons (the *electron density*) in the doubly occupied MO $\phi(\mathbf{r})$:

$$
\phi(\mathbf{r}) = \chi_A(\mathbf{r})c_A + \chi_B(\mathbf{r})c_B = \frac{\chi_A(\mathbf{r}) + \lambda\chi_B(\mathbf{r})}{\sqrt{1 + \lambda^2 + 2\lambda S}}
\tag{1.80}
$$

where $\lambda = c_B/c_A$ denotes here the *polarity parameter* of the bond orbital and $S = \langle\chi_A|\chi_B\rangle$ the *overlap* integral, is simply given by:

$$
P(\mathbf{r}) = \rho^{\alpha}(\mathbf{r}) + \rho^{\beta}(\mathbf{r}) = 2\phi(\mathbf{r})\phi^*(\mathbf{r}) = 2|\phi(\mathbf{r})|^2
\tag{1.81}
$$

the factor 2 comes from the equal contribution of electrons with either spin (α = spin-up, β = spin-down).

   The electron density can be further analysed in terms of elementary contributions from the AOs, giving the so-called *population analysis*,[11] which shows how the electrons are distributed between the different atomic orbitals in the molecule. We obtain from Equation (1.81):

$$
P(\mathbf{r}) = q_A\chi_A^{\,2}(\mathbf{r}) + q_B\chi_B^{\,2}(\mathbf{r}) + q_{AB}\frac{\chi_A(\mathbf{r})\chi_B(\mathbf{r})}{S} + q_{BA}\frac{\chi_B(\mathbf{r})\chi_A(\mathbf{r})}{S}
\tag{1.82}
$$

where $\chi_A^2(\mathbf{r})$ and $\chi_B^2(\mathbf{r})$ are *atomic densities*, $\frac{\chi_A(\mathbf{r})\chi_B(\mathbf{r})}{S}$ and $\frac{\chi_B(\mathbf{r})\chi_A(\mathbf{r})}{S}$ are *overlap densities*, all normalized to 1, while the coefficients:

$$
q_A = \frac{2}{1 + \lambda^2 + 2\lambda S}, \quad q_B = \frac{2\lambda^2}{1 + \lambda^2 + 2\lambda S}
\tag{1.83}
$$

---

[11]The extension to *N*-electron LCAO-MO wave functions is due to Mulliken (1955).

are *atomic charges*, and:

$$q_{AB} = q_{BA} = \frac{2\lambda S}{1 + \lambda^2 + 2\lambda S} \tag{1.84}$$

overlap charges. The charges are normalized so that:

$$q_A + q_B + q_{AB} + q_{BA} = \frac{2 + 2\lambda^2 + 4\lambda S}{1 + \lambda^2 + 2\lambda S} = 2 \tag{1.85}$$

the total number of electrons in the bond orbital $\phi(\mathbf{r})$.

For a *homopolar* bond, $\lambda = 1$:

$$q_A = q_B = \frac{1}{1+S} \quad q_{AB} = q_{BA} = \frac{S}{1+S} \tag{1.86}$$

so that for $S > 0$, in the bond, the charge on the atoms is decreased, electrons being transferred to the region between nuclei to an extent described by q_{AB} and q_{BA}. This reduces internuclear repulsion and means *bonding.*

For a *heteropolar* bond, $\lambda \neq 1$, and we define *gross charges* on A and B as:

$$Q_A = q_A + q_{AB} = \frac{2 + 2\lambda S}{1 + \lambda^2 + 2\lambda S} \tag{1.87}$$

$$Q_B = q_B + q_{BA} = \frac{2\lambda^2 + 2\lambda S}{1 + \lambda^2 + 2\lambda S} \tag{1.88}$$

and *formal charges* on A and B as:

$$\delta_A = 1 - Q_A = \frac{\lambda^2 - 1}{1 + \lambda^2 + 2\lambda S} \tag{1.89}$$

$$\delta_B = 1 - Q_B = -\frac{\lambda^2 - 1}{1 + \lambda^2 + 2\lambda S} \tag{1.90}$$

If $\lambda > 1$, $\delta_A = \delta > 0$, $\delta_B = -\delta_A = -\delta < 0$, and we have the dipole $A^{+\delta}B^{-\delta}$ (e.g. the LiH molecule).

In our model, an essential role will be assigned to the *exchange-overlap densities* (Magnasco and McWeeny, 1991; Magnasco, 2007, 2008, 2009a):

$$\chi_A(\mathbf{r})\chi_B(\mathbf{r}) - S\chi_A^2(\mathbf{r}), \quad \chi_B(\mathbf{r})\chi_A(\mathbf{r}) - S\chi_B^2(\mathbf{r}) \tag{1.91}$$

which have the properties:

$$\int d\mathbf{r}[\chi_A(\mathbf{r})\chi_B(\mathbf{r}) - S\chi_A^2(\mathbf{r})] = 0, \quad \int d\mathbf{r}[\chi_B(\mathbf{r})\chi_A(\mathbf{r}) - S\chi_B^2(\mathbf{r})] = 0 \tag{1.92}$$

1.6 EXCHANGE-OVERLAP DENSITIES AND THE CHEMICAL BOND

This section aims to illustrate the origin of the quantum mechanical exchange-overlap densities and their different behaviour in the case of the chemical bond in ground state H_2 and the Pauli repulsion in He_2. We choose as starting point for the $^1\Sigma_g^+$ ground state of the systems the normalized Heitler–London (HL) wave functions (Magnasco, 2008):

$$\Psi(H_2) = \frac{||a\bar{b}|| + ||b\bar{a}||}{\sqrt{2 + 2S^2}} = \frac{a(\mathbf{r}_1)b(\mathbf{r}_2) + b(\mathbf{r}_1)a(\mathbf{r}_2)}{\sqrt{2 + 2S^2}} \frac{\alpha(s_1)\beta(s_2) - \beta(s_1)\alpha(s_2)}{\sqrt{2}}$$

$$(1.93)$$

$$\Psi(He_2) = ||a\bar{a}b\bar{b}|| = ||a(\mathbf{r}_1)\alpha(s_1) \quad a(\mathbf{r}_2)\beta(s_2) \quad b(\mathbf{r}_3)\alpha(s_3) \quad b(\mathbf{r}_4)\beta(s_4)||$$

$$(1.94)$$

where $\mathbf{r}$ and s are space and spin variables, the bar denotes β spin, $a(\mathbf{r}) = 1s_A(\mathbf{r})$ and $b(\mathbf{r}) = 1s_B(\mathbf{r})$ are AOs centred at A and B, the double bar standing for a normalized Slater determinant (Magnasco, 2007, 2009a)[12].

If $\mathbf{x} = \mathbf{r}s$ denotes the space-spin variable, we recall from first principles (Magnasco, 2007, 2009a) that, for a normalized N-electron wavefunction satisfying the Pauli antisymmetry principle, the one-electron density function is defined as:

$$\rho(\mathbf{x}; \mathbf{x}) = N \int d\mathbf{x}_2 d\mathbf{x}_3 \cdots d\mathbf{x}_N \Psi(\mathbf{x}, \mathbf{x}_2, \cdots, \mathbf{x}_N)\Psi^*(\mathbf{x}, \mathbf{x}_2, \cdots, \mathbf{x}_N)$$

$$(1.95)$$

where the first set of variables in ρ comes from Ψ, the second from Ψ^*. The physical meaning of ρ is:

$$\rho(\mathbf{x}; \mathbf{x})d\mathbf{x} = \text{probability of finding an electron at } d\mathbf{x} \qquad (1.96)$$

where $d\mathbf{x} = d\mathbf{r}ds$ is an elementary volume at a *fixed* point in space-spin space. In this way, ρ determines the probability distribution in space of

---

[12]It should be remarked that, while the Heitler–London function (1.93) for H_2 is a two-determinant wave function, the Heitler–London function (1.94) for He_2 is a single determinant wave function, so that in this case HL and MO approaches coincide.

electrons of either spin. If:

$$\begin{cases} \rho^{\alpha}(\mathbf{r};\mathbf{r})d\mathbf{r} = \text{probability of finding at } d\mathbf{r} \ an \text{ electron with spin } \alpha \\ \rho^{\beta}(\mathbf{r};\mathbf{r})d\mathbf{r} = \text{probability of finding at } d\mathbf{r} \ an \text{ electron with spin } \beta \end{cases}$$
(1.97)

with $\rho^{\alpha}(\mathbf{r};\mathbf{r}) = \rho^{\alpha}(\mathbf{r})$ and $\rho^{\beta}(\mathbf{r};\mathbf{r}) = \rho^{\beta}(\mathbf{r})$ the (spatial) coefficients of $\alpha(s)\alpha^{*}(s)$ and $\beta(s)\beta^{*}(s)$ in ρ, the (spatial) *electron density*, as observed from experiment, is defined as:

$$P(\mathbf{r};\mathbf{r}) = \rho^{\alpha}(\mathbf{r};\mathbf{r}) + \rho^{\beta}(\mathbf{r};\mathbf{r})$$
(1.98)

The electron densities for the ${}^{1}\Sigma_{g}^{+}$ states of H_2 and He_2 resulting from these Heitler–London wave functions are then:

$$\begin{cases} P(\mathbf{r};\mathbf{r}) = \rho^{\alpha}(\mathbf{r};\mathbf{r}) + \rho^{\beta}(\mathbf{r};\mathbf{r}) \\ \quad = \dfrac{a(\mathbf{r})a^{*}(\mathbf{r}) + b(\mathbf{r})b^{*}(\mathbf{r}) + S[a(\mathbf{r})b^{*}(\mathbf{r}) + b(\mathbf{r})a^{*}(\mathbf{r})]}{1+S^2} \end{cases}$$
(1.99)

for the two-electron system H_2, and:

$$\begin{cases} P(\mathbf{r};\mathbf{r}) = \rho^{\alpha}(\mathbf{r};\mathbf{r}) + \rho^{\beta}(\mathbf{r};\mathbf{r}) \\ \quad = 2\dfrac{a(\mathbf{r})a^{*}(\mathbf{r}) + b(\mathbf{r})b^{*}(\mathbf{r}) - S[a(\mathbf{r})b^{*}(\mathbf{r}) + b(\mathbf{r})a^{*}(\mathbf{r})]}{1-S^2} \end{cases}$$
(1.100)

for the four-electron system He_2.

We give in detail below the calculation of the electron density for the Heitler–London wavefunction (1.93) of ground state H_2, when $a(\mathbf{r})$, $b(\mathbf{r})$, $\alpha(s)$, $\beta(s)$ are all normalized to one:

$$\rho(\mathbf{x}_1;\mathbf{x}_1) = 2\int d\mathbf{x}_2 \frac{\dfrac{a(\mathbf{r}_1)b(\mathbf{r}_2)+b(\mathbf{r}_1)a(\mathbf{r}_2)}{\sqrt{2+2S^2}}\ \dfrac{\alpha(s_1)\beta(s_2)-\beta(s_1)\alpha(s_2)}{\sqrt{2}}}{\dfrac{[a(\mathbf{r}_1)b(\mathbf{r}_2)+b(\mathbf{r}_1)a(\mathbf{r}_2)]^{*}}{\sqrt{2+2S^2}}\ \dfrac{[\alpha(s_1)\beta(s_2)-\beta(s_1)\alpha(s_2)]^{*}}{\sqrt{2}}}$$

$$= (2+2S^2)^{-1}\int d\mathbf{r}_2 \frac{[a(\mathbf{r}_1)b(\mathbf{r}_2)+b(\mathbf{r}_1)a(\mathbf{r}_2)]}{[a^{*}(\mathbf{r}_1)b^{*}(\mathbf{r}_2)+b^{*}(\mathbf{r}_1)a^{*}(\mathbf{r}_2)]}\int ds_2 \frac{[\alpha(s_1)\beta(s_2)-\beta(s_1)\alpha(s_2)]}{[\alpha^{*}(s_1)\beta^{*}(s_2)-\beta^{*}(s_1)\alpha^{*}(s_2)]}$$

$$= \frac{a(\mathbf{r}_1)a^{*}(\mathbf{r}_1)+b(\mathbf{r}_1)b^{*}(\mathbf{r}_1)+S[a(\mathbf{r}_1)b^{*}(\mathbf{r}_1)+b(\mathbf{r}_1)a^{*}(\mathbf{r}_1)]}{2+2S^2}[\alpha(s_1)\alpha^{*}(s_1)+\beta(s_1)\beta^{*}(s_1)]$$

so that:

$$\rho^{\alpha}(\mathbf{r}_1;\mathbf{r}_1)=\rho^{\beta}(\mathbf{r}_1;\mathbf{r}_1)=\frac{a(\mathbf{r}_1)a^*(\mathbf{r}_1)+b(\mathbf{r}_1)b^*(\mathbf{r}_1)+S[a(\mathbf{r}_1)b^*(\mathbf{r}_1)+b(\mathbf{r}_1)a^*(\mathbf{r}_1)]}{2+2S^2}$$

(1.101)

and we obtain the result of Equation (1.99) if we leave out the now useless suffix 1 on the space-spin variables.

(i) The $^1\Sigma_g^+$ state of H_2 (two-electron interaction)

The *spinless* 1-electron density (Equation 1.99) satisfies the conservation relation:

$$\int dr P(\mathbf{r};\mathbf{r}) = 2$$

(1.102)

the total number of electrons in H_2.

Using the identity:

$$(1+S^2)^{-1} = 1-S^2(1+S^2)^{-1}$$

(1.103)

we see that the electron density (real orbitals) can be *partitioned* into:

$$\begin{cases} P(\mathbf{r};\mathbf{r})= [a^2(\mathbf{r})+b^2(\mathbf{r})]+\dfrac{S}{1+S^2}\Big\{ [a(\mathbf{r})b(\mathbf{r})-Sa^2(\mathbf{r})]+ [b(\mathbf{r})a(\mathbf{r})-Sb^2(\mathbf{r})]\Big\} \\ = P^{cb}(\mathbf{r};\mathbf{r})+P^{exch-ov}(\mathbf{r};\mathbf{r}) \end{cases}$$

(1.104)

where:

$$P^{cb}(\mathbf{r};\mathbf{r})= a^2(\mathbf{r})+b^2(\mathbf{r})= P^{cl}(\mathbf{r};\mathbf{r})$$

(1.105)

is the *quasi-classical* contribution to the molecular density, and:

$$P^{exch-ov}(\mathbf{r};\mathbf{r})=\frac{S}{1+S^2}\Big\{ [a(\mathbf{r})b(\mathbf{r})-Sa^2(\mathbf{r})]+ [b(\mathbf{r})a(\mathbf{r})-Sb^2(\mathbf{r})]\Big\}= P^I(\mathbf{r};\mathbf{r})$$

(1.106)

the quantum mechanical *exchange-overlap* (or *interference*) density. Equations (1.105) and (1.106) satisfy the relations:

$$\int dr P^{cl}(\mathbf{r};\mathbf{r})= \int dr[a^2(\mathbf{r})+b^2(\mathbf{r})]=2$$

(1.107)

the number of electrons in the H_2 molecule, and:

$$\begin{cases} \int d\mathbf{r}\, P^{exch-ov}(\mathbf{r};\mathbf{r}) \\ = \dfrac{S}{1+S^2} \int d\mathbf{r} \Big\{ [a(\mathbf{r})b(\mathbf{r}) - Sa^2(\mathbf{r})] + [b(\mathbf{r})a(\mathbf{r}) - Sb^2(\mathbf{r})] \Big\} \\ = \dfrac{S}{1+S^2}(2S - 2S) = 0 \end{cases} \qquad (1.108)$$

in agreement with Equations (1.92). However, the energy changes associated with the quantum mechanical exchange-overlap component (Equation 1.106) of the interaction energy are the greatest contributors to the energy of the chemical bond (see Table 1.2).

Equations (1.105) and (1.106) are the Heitler–London counterpart of the corresponding quantities (Equations 3.4 and 3.5 on page 340 of Ruedenberg's paper (1962), which refers to a LCAO-MO wave function. Ruedenberg calls Equation (1.106) 'the modification of the quasi-classical density due to the *interference* effect', while we, more literally, speak of *exchange*$[a(\mathbf{r})b(\mathbf{r})]$, $[b(\mathbf{r})a(\mathbf{r})]$ and *overlap*$[-Sa^2(\mathbf{r})]$, $[-Sb^2(\mathbf{r})]$ densities.

Finally, it is worth noting that, while:

$$q_A{}^{cl} = q_b{}^{cl} = 1 \qquad (1.109)$$

is the classical electron charge on separate A and B (one electron on each H atom),

$$q_{AB}{}^{exch-ov} = q_{BA}{}^{exch-ov} = \frac{S}{1+S^2} > 0 \qquad (1.110)$$

is the fraction of electronic charge transferred in the bond region, due to what Ruedenberg calls the 'constructive interference', and which means *bonding*.

Table 1.2 Optimized bond energies and their components ($10^{-3}E_h$) for ground state H_2

R/a_0	ΔE^{cb}	$\Delta E^{exch-ov}$	$\Delta E(^1\Sigma_g{}^+)$
1	15.85	−104.43	−88.58
1.2	−9.93	−119.03	−128.96
1.4	−19.42	−119.63	−139.05
1.6	−21.83	−112.54	−134.37
1.8	−21.08	−101.60	−122.68
2	−18.99	−89.02	−108.01
4	−1.68	−9.68	−11.36
6	−0.06	−0.45	−0.51
8	-0.00_2	-0.01_5	-0.01_7

So, a complete equivalence exists between our notation (Magnasco and McWeeny, 1991; Magnasco, 2004a, 2007, 2008, 2009a) and that of Ruedenberg (1962).

(ii) The $^1\Sigma_g^+$ state of He_2 (four-electron interaction)
    The same argument can be applied to the electron density (Equation 1.100), which satisfies the conservation relation:

$$\int d\mathbf{r}\, P(\mathbf{r};\mathbf{r}) = 4 \tag{1.111}$$

the total number of electrons in He_2.
    Using the identity:

$$(1-S^2)^{-1} = 1 + S^2(1-S^2)^{-1} \tag{1.112}$$

the electron density (real orbitals) can be *partitioned* into:

$$\begin{cases} P(\mathbf{r};\mathbf{r}) = 2\left[a^2(\mathbf{r})+b^2(\mathbf{r})\right] - \dfrac{2S}{1-S^2}\left\{\left[a(\mathbf{r})b(\mathbf{r})-Sa^2(\mathbf{r})\right] + \left[b(\mathbf{r})a(\mathbf{r})-Sb^2(\mathbf{r})\right]\right\} \\ = P^{cb}(\mathbf{r};\mathbf{r}) + P^{exch-ov}(\mathbf{r};\mathbf{r}), \end{cases} \tag{1.113}$$

where:

$$P^{cb}(\mathbf{r};\mathbf{r}) = 2[a^2(\mathbf{r})+b^2(\mathbf{r})] = P^{cl}(\mathbf{r};\mathbf{r}) \tag{1.114}$$

is the *quasi-classical* contribution to the molecular density, and:

$$\begin{cases} P^{exch-ov}(\mathbf{r};\mathbf{r}) = \\ = -\dfrac{2S}{1-S^2}\left\{\left[a(\mathbf{r})b(\mathbf{r})-Sa^2(\mathbf{r})\right] + \left[b(\mathbf{r})a(\mathbf{r})-Sb^2(\mathbf{r})\right]\right\} = P^{I}(\mathbf{r};\mathbf{r}) \end{cases} \tag{1.115}$$

the quantum mechanical *exchange-overlap* (or *interference*) density. Even in this case it is evident that:

$$\int d\mathbf{r}\, P^{cl}(\mathbf{r};\mathbf{r}) = 4 \tag{1.116}$$

$$\int d\mathbf{r}\, P^{exch-ov}(\mathbf{r};\mathbf{r}) = 0 \tag{1.117}$$

While the 'exchange-overlap' (or 'interference') density still does not give any contribution to the electron population, it is now at the origin of

Table 1.3 Optimized Pauli repulsions and their components ($10^{-3}E_h$) for the He–He interaction in the medium range

R/a_0	ΔE^{cb}	$\Delta E^{exch-ov}$	$\Delta E(^1\Sigma_g^+)$
2	−27.28	163.90	136.62
2.5	−7.55	50.22	42.67
3	−1.93	14.89	12.96
3.5	−0.47	4.27	3.80
4	−0.11	1.18	1.07
4.5	−0.02	0.32	0.30
5	−0.00$_5$	0.08	0.07$_5$

the *strong repulsion* occurring at short range between two neutral He atoms (Pauli repulsion, see Table 1.3), since in this case:

$$q_{AB}^{exch-ov} = q_{BA}^{exch-ov} = -\frac{2S}{1-S^2} < 0 \qquad (1.118)$$

so that, now, electrons escape from the region between the nuclei, giving what Ruedenberg calls 'a destructive interference'. The same behaviour occurs for the triplet $^3\Sigma_u^+$ excited state of H_2.

Hence, we conclude, first, that there is a complete equivalence between Ruedenberg's (1962) and our formulation (Magnasco and McWeeny, 1991; Magnasco, 2004a, 2007, 2008, 2009a) in terms of quantum densities, and, next, that the different behaviour of the quantum 'exchange-overlap' (or 'interference') density for the $^1\Sigma_g^+$ states of H_2 (chemical bonding) and He_2 (Pauli repulsion) is evident from the opposite signs of the $q_{AB}^{exch-ov}$ terms occurring in H_2 and He_2. The latter originate the main contribution to the respective $\Delta E^{exch-ov}$ components of the bond energy in H_2 (*attractive* contribution) and of the Pauli repulsion in He_2 (*repulsive* contribution).

Numerical values of the interaction energies for these Heitler–London wavefunctions, taken from Magnasco (2008), are given in Tables 1.2 and 1.3. The energies are optimized variationally with respect to the values of the orbital exponents c_0 of the atomic 1s STOs on A and B.

It can be seen from Table 1.2 that the optimized value resulting for the bond energy of H_2 at the equilibrium bond length, $\Delta E_e(^1\Sigma_g^+) = -139.05 \times 10^{-3}E_h$ at $R_e = 1.40a_0$, is within 80% of the theoretical value $\Delta E_e(^1\Sigma_g^+) = -174.45 \times 10^{-3}E_h$ given by Wolniewicz (1993) in his accurate calculation using a 279-term expansion in spheroidal coordinates for the two electrons, including powers of the inter-electronic distance. It must be admitted that our results are particularly satisfying for such a simple wavefunction!

The He–He optimized Pauli repulsion at medium range resulting from Table 1.3 at $R = 3a_0$, $\Delta E(^1\Sigma_g^+) = 12.96 \times 10^{-3}E_h$, turns out to be within 96% of the accurate result $\Delta E(^1\Sigma_g^+) = 13.52 \times 10^{-3}E_h$, obtained by Liu and McLean (1973) from an accurate SCF Hartree–Fock calculation using a $4s3p2d1f$ basis of STOs on each centre. At $R = 4a_0$, the optimized result, $\Delta E(^1\Sigma_g^+) = 1.07 \times 10^{-3}E_h$, is still within 80% of the accurate value given by the same authors, $\Delta E(^1\Sigma_g^+) = 1.35 \times 10^{-3}E_h$. Apparently, our results would be even better when compared with experiment[13] (Feltgen et al., 1982), but in this case we must expect that our SCF values, underestimating the interaction, compensate in part for the effect of the attractive London forces not considered in the calculation.

These numerical results confirm the validity of our simple analysis based on the exchange-overlap densities either for the chemical bond (H_2) or the Pauli repulsion (He–He). Even at the simple MO level, which we know to behave correctly in the bond region (Magnasco, 2007, 2009a), a model representing at its best such quantum densities in terms of the single one-electron Hückel parameter $[(\beta - \alpha S)/(1 + S)] < 0$ (Magnasco, 2004a) is expected to give a qualitatively correct representation of the chemical bond and its properties. This is what we want to present in the next chapter.

---

[13]Our calculated value at $R = 3.5a_0$ would exceed by less than 2% the experimental value of $\Delta E = 3.74 \times 10^{-3}E_h$.

Part 1

Short-range Interactions

2

The Chemical Bond

The multicentre one-electron space functions $\phi(\mathbf{r})$ describing electron distribution in molecules are called molecular orbitals (MOs). In the independent-particle approximation convenient MOs are constructed by the linear combination of atomic orbitals (LCAO) with coefficients determined by the Ritz method of Chapter 1.

2.1   AN ELEMENTARY MOLECULAR ORBITAL MODEL

Consider the formation of two two-centre MOs obtained from two normalized nonorthogonal real AOs, $\chi_1(\mathbf{r})$ on atom A and $\chi_2(\mathbf{r})$ on atom B:

$$\phi_1(\mathbf{r}) = \chi_1(\mathbf{r})C_{11} + \chi_2(\mathbf{r})C_{21} = C_{11}(\chi_1 + \lambda_1\chi_2) \tag{2.1}$$

where:

$$\lambda_1 = \frac{C_{21}}{C_{11}} \tag{2.2}$$

is the *polarity parameter* of MO ϕ_1 with C_{11} a normalization factor, and:

$$\phi_2(\mathbf{r}) = \chi_2(\mathbf{r})C_{22} + \chi_1(\mathbf{r})C_{12} = C_{22}(\chi_2 + \lambda_2\chi_1) \tag{2.3}$$

with:

$$\lambda_2 = \frac{C_{12}}{C_{22}} \tag{2.4}$$

the polarity parameter of MO ϕ_2.

We now introduce a simple Hückel theory including overlap (Magnasco, 2002, 2004a, 2007, 2009a). The elements of the Hückel secular determinant are given in terms of just two negative unspecified parameters, the diagonal element α (the Coulomb or atomic integral) and the off-diagonal element β (the bond integral).

Optimization of the linear coefficients in this simple Hückel scheme including overlap gives the 2×2 pseudosecular equation:

$$\begin{vmatrix} \alpha_1 - \varepsilon & \beta - \varepsilon S \\ \beta - \varepsilon S & \alpha_2 - \varepsilon \end{vmatrix} = 0 \qquad (2.5)$$

where $\alpha_1 < 0, \alpha_2 < 0$ are *atomic* integrals specifying the energy levels of AOs χ_1 and χ_2; $\beta < 0$ the *bond* integral describing formation of a bond between χ_1 and χ_2;

$$S = \int d\mathbf{r}\, \chi_1(\mathbf{r})\chi_2(\mathbf{r}) = \langle \chi_1 | \chi_2 \rangle \qquad (2.6)$$

the *overlap* integral giving the superposition between the normalized AOs χ_1 and χ_2. S depends in an exponentially decreasing way on the internuclear distance R between atoms A and B. It is important to note that β depends on S and that no bond can be formed between AOs for which $S = 0$ by symmetry.

According to Equations (1.26) and (1.27) with:

$$A_{11} = \alpha_1,\ A_{22} = \alpha_2,\ A_{12} = A_{21} = \beta,\ \lambda_1 = \varepsilon_1,\ \lambda_2 = \varepsilon_2 \qquad (2.7)$$

solution of Equation (2.5) gives the real roots:

$$\varepsilon_1 = \frac{\alpha_1 + \alpha_2 - 2\beta S - \Delta}{2(1 - S^2)} \qquad (2.8)$$

$$\varepsilon_2 = \frac{\alpha_1 + \alpha_2 - 2\beta S + \Delta}{2(1 - S^2)} \qquad (2.9)$$

with:

$$\Delta = [(\alpha_2 - \alpha_1)^2 + 4(\beta - \alpha_1 S)(\beta - \alpha_2 S)]^{1/2} > 0 \qquad (2.10)$$

The roots ε_i of the pseudosecular equation are called *molecular orbital energies*, while the differences $\Delta\varepsilon_i = \varepsilon_i - \alpha_i$ are assumed to give the contribution of the *i*th MO to the *bond energy*. The energy of the chemical bond will, in general, depend on β, α_1, α_2, and S. The solutions become particularly simple in the two cases schematically shown in Figure 2.1.

If $\alpha_1 = \alpha_2 = \alpha$, we have *degeneracy* of the atomic levels, and we obtain for orbital energies and MOs the following results:

$$\varepsilon_1 = \frac{\alpha + \beta}{1 + S} = \alpha + \frac{\beta - \alpha S}{1 + S} \qquad (2.11)$$
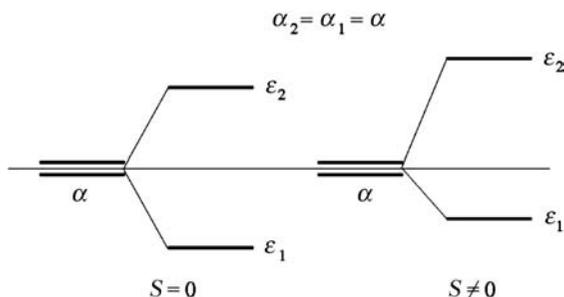
Figure 2.1 Bonding and antibonding molecular splittings for a first-order interaction
(*β large*)

is the orbital energy for the *bonding* MO ϕ_1;

$$\Delta\varepsilon_1 = \varepsilon_1 - \alpha = \frac{\beta - \alpha S}{1 + S} < 0 \qquad (2.12)$$

the *attractive* bonding orbital interaction;

$$\phi_1 = \frac{\chi_1 + \chi_2}{\sqrt{2 + 2S}}, \quad \lambda_1 = 1 \qquad (2.13)$$

the normalized bonding MO;

$$\varepsilon_2 = \frac{\alpha - \beta}{1 - S} = \alpha - \frac{\beta - \alpha S}{1 - S} \qquad (2.14)$$

the orbital energy for the *antibonding* MO ϕ_2;

$$\Delta\varepsilon_2 = \varepsilon_2 - \alpha = -\frac{\beta - \alpha S}{1 - S} > 0 \qquad (2.15)$$

the *repulsive* antibonding orbital interaction;

$$\phi_2 = \frac{\chi_2 - \chi_1}{\sqrt{2 - 2S}}, \quad \lambda_2 = -1 \qquad (2.16)$$

the normalized antibonding MO.

We notice that the resulting MOs are normalized and orthogonal:

$$\begin{cases} \langle \phi_1 | \phi_1 \rangle = \left\langle \dfrac{\chi_1 + \chi_2}{\sqrt{2 + 2S}} \middle| \dfrac{\chi_1 + \chi_2}{\sqrt{2 + 2S}} \right\rangle = \dfrac{2 + 2S}{2 + 2S} = 1 \\[4mm] \langle \phi_2 | \phi_2 \rangle = \left\langle \dfrac{\chi_2 - \chi_1}{\sqrt{2 - 2S}} \middle| \dfrac{\chi_2 - \chi_1}{\sqrt{2 - 2S}} \right\rangle = \dfrac{2 - 2S}{2 - 2S} = 1 \\[4mm] \langle \phi_1 | \phi_2 \rangle \propto \langle \chi_1 + \chi_2 | \chi_2 - \chi_1 \rangle = -1 + 1 = 0 \end{cases} \qquad (2.17)$$

$$\alpha_2 - \alpha_1 > 0$$
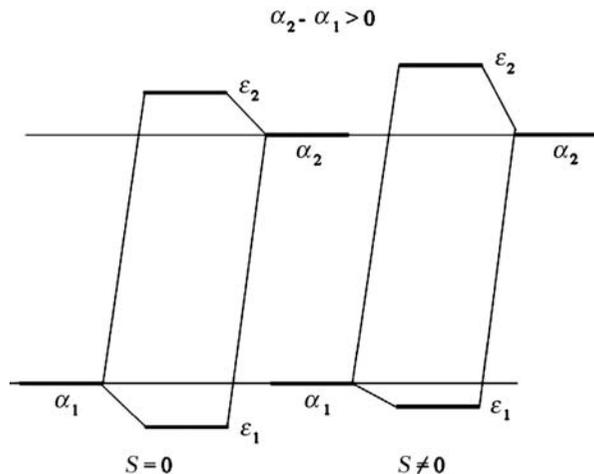
Figure 2.2 Bonding and antibonding molecular splittings for a second-order interaction (β *small*)

and that ϕ_2 has a nodal plane at the midpoint of the internuclear axis whereas ϕ_1 has no nodes. For $S \neq 0$ (right-hand side of Figure 2.1) the molecular levels are asymmetric with respect to the atomic levels, the bonding level being less bonding, the antibonding level is more antibonding than the case $S = 0$ (left-hand side of Figure 2.1) where splitting is symmetric. Finally, we observe that the orbital interaction energy is *first order* in β (*strong* interaction).

If $|\beta| \ll (\alpha_2 - \alpha_1) > 0$ (Figure 2.2), the two atomic energy levels have sensibly different energies, so that the interaction β is *small*.

If we assume α_1 to be the deepest level, using a Taylor expansion for the square root, we have:

$$
\left\{
\begin{aligned}
\Delta &= (\alpha_2 - \alpha_1)\left[1 + \frac{4(\beta - \alpha_1 S)(\beta - \alpha_2 S)}{(\alpha_2 - \alpha_1)^2}\right]^{1/2} \\[2mm]
&\approx (\alpha_2 - \alpha_1)\left[1 + \frac{2(\beta - \alpha_1 S)(\beta - \alpha_2 S)}{(\alpha_2 - \alpha_1)^2}\right] \\[2mm]
&= (\alpha_2 - \alpha_1) + \frac{2(\beta - \alpha_1 S)(\beta - \alpha_2 S)}{\alpha_2 - \alpha_1}
\end{aligned}
\right.
\qquad (2.18)
$$

so that, substituting in the previous equations, we obtain:

$$\varepsilon_1 \approx \alpha_1 - \frac{(\beta - \alpha_1 S)^2}{\alpha_2 - \alpha_1} \qquad (2.19)$$

the orbital energy of the bonding MO;

$$\Delta\varepsilon_1 \approx \varepsilon_1 - \alpha_1 = -\frac{(\beta - \alpha_1 S)^2}{\alpha_2 - \alpha_1} < 0 \qquad (2.20)$$

the *attractive* bonding orbital interaction;

$$\phi_1 = \frac{\chi_1 + \lambda_1 \chi_2}{\sqrt{1 + \lambda_1^2 + 2\lambda_1 S}}, \quad \lambda_1 \approx -\frac{\beta - \alpha_1 S}{\alpha_2 - \alpha_1} > 0 \text{ small} \qquad (2.21)$$

the normalized bonding MO, little different from χ_1;

$$\varepsilon_2 \approx \alpha_2 + \frac{(\beta - \alpha_2 S)^2}{\alpha_2 - \alpha_1} \qquad (2.22)$$

the orbital energy of the antibonding MO;

$$\Delta\varepsilon_2 \approx \varepsilon_2 - \alpha_2 = +\frac{(\beta - \alpha_2 S)^2}{\alpha_2 - \alpha_1} > 0 \qquad (2.23)$$

the *repulsive* antibonding orbital interaction;

$$\phi_2 = \frac{\chi_2 + \lambda_2 \chi_1}{\sqrt{1 + \lambda_2^2 + 2\lambda_2 S}}, \quad \lambda_2 \approx \frac{\beta - \alpha_2 S}{\alpha_2 - \alpha_1} < 0 \text{ small} \qquad (2.24)$$

the normalized antibonding MO, little different from χ_2. The greater the difference $\Delta\alpha = \alpha_2 - \alpha_1$ the smaller the orbital interaction: this explains why *the chemical bond always occurs at the valence level*, where energy differences between AOs are smaller. The interaction is now *second order* in β.

2.2 BOND ENERGIES AND PAULI REPULSIONS IN HOMONUCLEAR DIATOMICS

According to our simple model, in a *homonuclear diatomic*, the energy of a chemical bond (in short, the *bond energy*) is obtained by adding at the valence level the contributions from the different MOs that are occupied
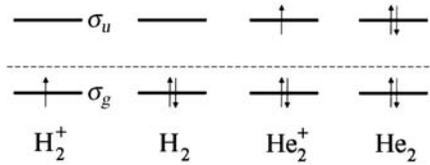
Figure 2.3 Electron configurations in first-row homonuclear diatomics originating one-electron (H_2^+), two-electron (H_2), three-electron (He_2^+) chemical bonds and Pauli repulsion in He_2

by electrons according to the *aufbau* principle (Walker and Straw, 1966). In the absence of degeneracy, in each molecular level we put two electrons with opposite spin so as to satisfy the Pauli exclusion principle. So, we obtain for the bonds in the simplest molecules built from atoms having one or two $1s$ electrons in their valence shell (H, He) the results shown in Figure 2.3.

2.2.1 The Hydrogen Molecular Ion H_2^+ $(N = 1)$

$$\Delta E = \frac{\beta - \alpha S}{1 + S} < 0 \qquad (2.25)$$

This is the energy of the one-electron bond in our model.

2.2.2 The Hydrogen Molecule H_2 $(N = 2)$

$$\Delta E = 2\frac{\beta - \alpha S}{1 + S} < 0 \qquad (2.26)$$

so that the energy of the two-electron bond in H_2 should be *twice* that of the one-electron bond in H_2^+.

2.2.3 The Helium Molecular Ion He_2^+ $(N = 3)$

$$\Delta E = 2\frac{\beta - \alpha S}{1 + S} - \frac{\beta - \alpha S}{1 - S} = \frac{2(1 - S) - (1 + S)}{1 - S^2}(\beta - \alpha S) = \frac{1 - 3S}{1 - S^2}(\beta - \alpha S) < 0 \qquad (2.27)$$

For small S, the three-electron bond energy in He_2^+ should be not far from (better, a little less than) that of H_2^+.

Table 2.1 Bond distances (a_0) and bond strengths (E_h) observed in first-row homonuclear diatomics

Molecule	R/a_0	$D/10^{-3}E_h$	Ratio	Model
H_2^+	2.0	102.6	1	1
H_2	1.4	174.4	1.7	2
He_2^+	2.04	90.8	0.9	1
He_2	3.0	−13.5	–	Repulsion

2.2.4   The Helium Molecule He_2 ($N = 4$)

$$\Delta E = 2\frac{\beta-\alpha S}{1+S} - 2\frac{\beta-\alpha S}{1-S} = \frac{2(1-S)-2(1+S)}{1-S^2}(\beta-\alpha S) = -\frac{4S}{1-S^2}(\beta-\alpha S) > 0$$

$$(2.28)$$

so that, for the interaction between two ground state He atoms, the model predicts repulsion between the atoms (the so-called *Pauli repulsion*), and no chemical bond can be formed. So, the diatomic molecule He_2 cannot exist in the usual region of chemical bonds[1].

This is exactly what is observed by experiment (Huber and Herzberg, 1979). In Table 2.1 we give the bond distances and the bond strengths (in atomic units) measured for the ground states of H_2^+, H_2, He_2^+, and the accurate Pauli repulsion energy calculated at $R = 3a_0$ for He_2 by Liu and McLean (1973). The bond strengths D reported in the table are obtained at the bottom of the potential energy curve, and correspond to the negative of the bond energies ΔE of our model ($D = -\Delta E$)

The results of our model are seen to agree well with experiment, and were confirmed by ab initio calculations on the same systems (Magnasco, 2008). It was shown there that the single one-electron bond energy parameter $(\beta-\alpha S)$ occurring in Equations (25–28) is just the model representation of the one-electron part of the exchange-overlap component of the interaction due to the exchange-overlap densities $[a(\mathbf{r})b(\mathbf{r})-Sa^2(\mathbf{r})]$ on A and $[b(\mathbf{r})a(\mathbf{r})-Sb^2(\mathbf{r})]$ on B.

The naïve extension of the model to the bonds of the second-row homonuclear diatomics (Li_2^+, Li_2, Be_2^+, Be_2), mostly involving overlap

---

[1] At the rather large internuclear distance of $5.63a_0$, the potential energy curve of the He($1s^2$)-He($1s^2$) interaction shows a shallow minimum of $-33.4 \times 10^{-6}E_h$ corresponding to the formation of a so-called Van der Waals bond. This is possible since, at this large distance, the *small* Pauli repulsion between closed shells is overbalanced by a *small* London attraction (see Chapter 4).

between easily polarizable $2s$ AOs, is however not immediately possible, because, at variance with H_2^+ and H_2, Li_2^+ $(D = 47.3 \times 10^{-3}E_h)$ is more stable than $Li_2(D = 38.6 \times 10^{-3}E_h)$ as a result of the sensibly stronger polarization effects of the valence $2s$ electrons compared with $1s$ $(\alpha_{Li} = 168a_0^3, \alpha_H = 4.5a_0^3)$ (Kutzelnigg, 1991), not accounted for in our model. However, the model correctly predicts Be_2 to be a van der Waals molecule, like its lighter homologue, He_2.

What is rather surprising is that a similar trend for bond lengths and bond strengths is observed when filling 1 through 8 electrons in the doubly degenerate valence π levels in the ground states of the series C_2^+, C_2, N_2^+, N_2, O_2^+, O_2, F_2^+, F_2 (Magnasco, 2004a). The maximum bond strength occurs for the triple bond in N_2 $(N_\pi = 4, D = 358.7 \times 10^{-3}E_h)$, lying in between N_2^+ $(N_\pi = 3, D = 237.9 \times 10^{-3}E_h)$ and O_2^+ $(N_\pi = 5, D = 242.4 \times 10^{-3}E_h)$ which have rather similar bond strengths, while the π system of F_2, containing a complete shell of 8 electrons, exhibits a Pauli repulsion that reduces the strength of the underlying σ bond $(D = 62.1 \times 10^{-3}E_h)$.

2.3   MULTIPLE BONDS

In diatomic molecules, it is customary to assume the z axis along the bond direction connecting atom A (chosen at the origin of the interatomic coordinate system) to atom B, a distance R apart, while axes x and y are perpendicular to it. Bonds directed along the internuclear axis z are called σ *bonds*, bonds perpendicular to the z axis (hence having the two equivalent orthogonal directions of axes x and y) are called π *bonds*. Multiple bonds have either σ and π bonds, the ordinary *double* bond (e.g. in ethylene) having four electrons in the configuration $\sigma^2\pi^2$, the ordinary *triple* bond (e.g. in N_2 and C_2H_2) six electrons in the configuration $\sigma^2\pi^4$. However, we have just seen that we can also have chemical bonds involving either one electron (H_2^+) or three electrons (He_2^+), so deviating from the classical Lewis bond that consists of an electron pair (H_2). So, we can also speak of three-electron σ bonds (as in He_2^+), and of three-electron π bonds (as for the triplet ground state of O_2), as shown in Figure 2.4.

It should be noted that, because of the invariance properties of the density function with respect to a unitary transformation among its orbitals, the σ–π description of double or triple bonds in terms of nonequivalent orbitals is not the only possible one; a description in terms of two or three equivalent *bent* banana bonds is possible as well. It is
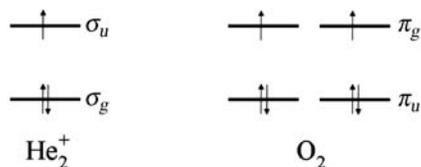
Figure 2.4 Ground state electron configurations originating the three-electron σ bond in He_2^+ (Σ_u^+), and the two three-electron π bonds in $O_2(\Sigma_g^-)$
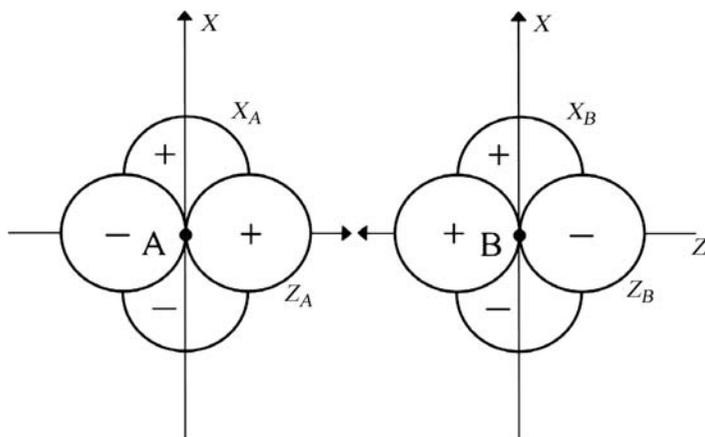
Figure 2.5 The four basic AOs needed for the $\sigma^2\pi^2$ description of the double bond

important to stress that *the two descriptions are physically equivalent.* We shall show this by an energy calculation for the simple MO description of the double bond.

2.3.1 $\sigma^2\pi^2$ Description of the Double Bond

Let us consider the four basic AOs (z_A, z_B, x_A, x_B) or $(\sigma_A, \sigma_B, \pi_{xA}, \pi_{xB})$, where $2p_z = z = \sigma$ are AOs directed along the internuclear axis, and $2p_x = x = \pi_x$ (= π for short) AOs perpendicular to it[2]. We choose two coordinate systems, a right-handed one on A and a left-handed on B (Figure 2.5), so that $S_{\sigma\sigma}$ elementary overlap is positive.

---

[2] A nomenclature borrowed from diatomic molecules.
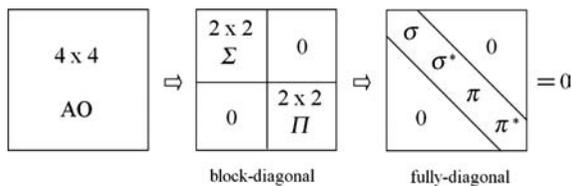
Figure 2.6 Factorization and diagonalization of the Hückel secular equation for a double bond

If we then construct Hückel MOs using the LCAO method, assuming for simplicity orthonormal[3] basic AOs, we must solve the secular equation of Figure 2.6. After diagonalization of the Hückel matrix, we get:

$$\begin{cases} \sigma = \dfrac{1}{\sqrt{2}}(z_A + z_B), & \sigma^* = \dfrac{1}{\sqrt{2}}(z_A - z_B) \\[2ex] \pi = \dfrac{1}{\sqrt{2}}(x_A + x_B), & \pi^* = \dfrac{1}{\sqrt{2}}(x_A - x_B) \end{cases} \qquad (2.29)$$

the MOs in the first column being *bonding*, those in the second column *antibonding*. We concentrate our attention only in bonding orbitals.

Let us examine the structure of the block-diagonal matrix describing orbital interaction within the Hückel scheme:

$$\begin{pmatrix} \alpha_\sigma & \beta_{\sigma\sigma} \\ \beta_{\sigma\sigma} & \alpha_\sigma \end{pmatrix}, \qquad \begin{pmatrix} \alpha_\pi & \beta_{\pi\pi} \\ \beta_{\pi\pi} & \alpha_\pi \end{pmatrix} \qquad (2.30)$$

$$\Sigma\text{-matrix} \qquad\quad \Pi\text{-matrix}$$

where the αs are Coulomb integrals and the βs bond (interaction) integrals. As already said, in Hückel-type theories (Magnasco, 2002, Magnasco, 2004a) α is taken to be an *atomic* quantity (roughly the negative of the ionization potential of an electron in the orbital), while β is taken proportional to the overlap $S_{\mu\nu}$ between the two interacting orbitals χ_μ and χ_ν via a constant β_0:

$$\beta_{\mu\nu} = \beta_0 S_{\mu\nu}, \quad S_{\mu\nu} = \langle \chi_\mu | \chi_\nu \rangle \qquad (2.31)$$

---

[3] Remember that orthogonal does not mean not interacting (Magnasco, 2004a).
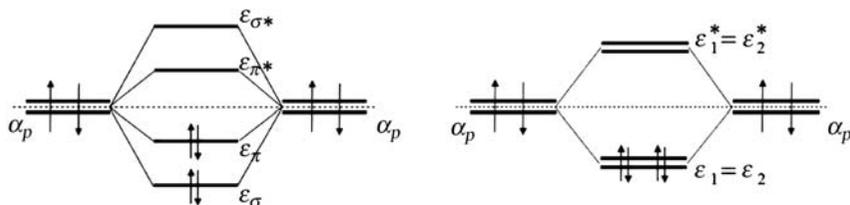
Figure 2.7 Diagram of the MO orbital energies ($S=0$) for the carbon-carbon interaction in the $\sigma^2\pi^2$ description of the double bond (left) and in the equivalent $B_1^2 B_2^2$ bent bond description (right)

To get the MOs we solve the two quadratic equations:

$$\begin{vmatrix} \alpha_p-\varepsilon & \beta_{\sigma\sigma} \\ \beta_{\sigma\sigma} & \alpha_p-\varepsilon \end{vmatrix} = 0, \quad \begin{vmatrix} \alpha_p-\varepsilon & \beta_{\pi\pi} \\ \beta_{\pi\pi} & \alpha_p-\varepsilon \end{vmatrix} = 0 \qquad (2.32)$$

having roots:

$$\begin{cases} \varepsilon_\sigma = \alpha_p + \beta_{\sigma\sigma}, & \varepsilon_{\sigma^*} = \alpha_p - \beta_{\sigma\sigma} \\ \varepsilon_\pi = \alpha_p + \beta_{\pi\pi}, & \varepsilon_{\pi^*} = \alpha_p - \beta_{\pi\pi} \end{cases} \qquad (2.33)$$

the first being Σ molecular orbital energies, the second Π molecular orbital energies. Then, when there is interaction between A and B, we get for the orbital energies the diagram on the left-hand side of Figure 2.7.

We have the total Hückel energy:

$$E = 2\varepsilon_\sigma + 2\varepsilon_\pi \qquad (2.34)$$

giving as bond energy for the $\sigma^2\pi^2$ *double bond*:

$$\Delta E = 2\beta_{\sigma\sigma} + 2\beta_{\pi\pi} \qquad (2.35)$$

Since $\beta_{\pi\pi} < \beta_{\sigma\sigma}$, *the bond energy of the double bond is lower than the bond energy corresponding to two separate single σ bonds*. This is the first result obtained from MO theory.

2.3.2 $B_1^2 B_2^2$ Bent (or Banana) Description of the Double Bond

Since the σ and π MOs are mathematical functions obtained in principle as solutions of a differential equation, describing the motion of a single electron in the field provided by nuclei and all remaining electrons, we

can mix them through a linear combination without changing the mathematical solutions themselves. In other words, the new MOs obtained from linear combination of σ and π will still be a solution of the *same* differential equation, the electron density being invariant against this transformation. The simplest combination is then:

$$
\begin{cases}
B_1 = \dfrac{1}{\sqrt{2}}(\sigma + \pi) = \dfrac{1}{\sqrt{2}}\left[\dfrac{1}{\sqrt{2}}(z_A + x_A) + \dfrac{1}{\sqrt{2}}(z_B + x_B)\right] = \dfrac{1}{\sqrt{2}}(p_{A1} + p_{B1}) \\[4mm]
B_2 = \dfrac{1}{\sqrt{2}}(\sigma - \pi) = \dfrac{1}{\sqrt{2}}\left[\dfrac{1}{\sqrt{2}}(z_A - x_A) + \dfrac{1}{\sqrt{2}}(z_B - x_B)\right] = \dfrac{1}{\sqrt{2}}(p_{A2} + p_{B2})
\end{cases}
$$

$$(2.36)$$

where p_{A1} is a $2p$ orbital on A making an angle of $\theta = 45°$ with respect to the internuclear z axis, p_{A2} a $2p$ orbital on A making an angle of $\theta = -45°$ with respect to the internuclear z axis, etc. In matrix form:

$$
(B_1\, B_2) = (\sigma\, \pi)
\begin{pmatrix}
\dfrac{1}{\sqrt{2}} & \dfrac{1}{\sqrt{2}} \\[3mm]
\dfrac{1}{\sqrt{2}} & -\dfrac{1}{\sqrt{2}}
\end{pmatrix}
= (\sigma\, \pi)\mathbf{U}
\qquad (2.37)
$$

where

$$
\mathbf{U}\,\tilde{\mathbf{U}} = \tilde{\mathbf{U}}\mathbf{U} = 1 \qquad (2.38)
$$

so that the transformation U connecting the two descriptions is given by an *orthogonal*[4] matrix.

The orbitals B_1 and B_2 obtained in this way describe the double bond in terms of two equivalent *bent bonds* making an angle of $2\theta = 90°$ between them (each bent bond makes an angle of $\theta = 45°$ with the internuclear axis) as shown in Figure 2.8.

From a geometrical point of view, B_1 and B_2 are obtained by a rotation of $180°$ around the z axis, but, although the individual form of the MOs is changed, *the physical situation is unchanged* as we can easily see by evaluating the molecular energy in the *new* basis. Since the two bond orbitals are equivalent (under reflection across the yz plane) their asso-

---

[4]This transformation leaves the length of the vectors invariant.
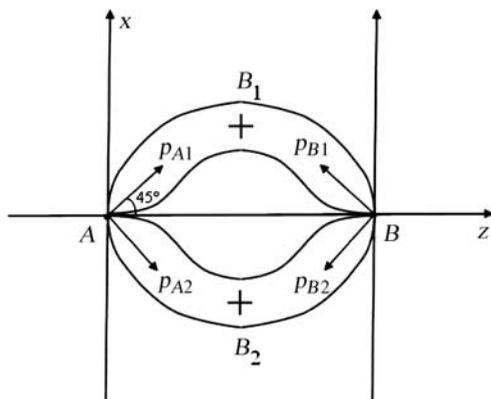
Figure 2.8 Equivalent bent (or banana) bond description of the double bond

ciated energy levels are degenerate:

$$\begin{cases} \varepsilon_1 = \langle B_1|H|B_1\rangle = \dfrac{1}{2}\langle \sigma+\pi|H|\sigma+\pi\rangle = \dfrac{1}{2}\left(\varepsilon_\sigma+\varepsilon_\pi\right) \\[4mm] \varepsilon_2 = \langle B_2|H|B_2\rangle = \dfrac{1}{2}\langle \sigma-\pi|H|\sigma-\pi\rangle = \dfrac{1}{2}\left(\varepsilon_\sigma+\varepsilon_\pi\right) = \varepsilon_1 \end{cases} \qquad (2.39)$$

We have two degenerate levels of energy $\varepsilon_2 = \varepsilon_1$ equal to the *arithmetic mean* of the previous σ and π levels (right-hand side of Figure 2.7). We finally obtain:

$$\begin{cases} E = 2\varepsilon_1 + 2\varepsilon_2 = 4\varepsilon_1 = 2\varepsilon_\sigma + 2\varepsilon_\pi \\[2mm] \Delta E = 2\beta_{\sigma\sigma} + 2\beta_{\pi\pi} \end{cases} \qquad (2.40)$$

the same result as before. Molecular and bond energy are therefore unchanged. *The σ–π and B_1–B_2 representation of the double bond describe the same physical situation*[5]. This is the second result obtained from the quantum mechanical description of the chemical bond. We have no experimental way of distinguishing between the two.

2.3.3 Hybridization Effects

We now turn to examination of hybridization effects. We allow for sp^2 hybridization of the orbitals lying in the zx molecular plane (e.g. ethylene).

---

[5] This is true only for the MO approximation. Ab initio VB calculations by Palke (1986) on ethylene show the equivalent banana bond description of the double bond in terms of equivalent nonorthogonal hybrids to be more stable than the σ–π description.
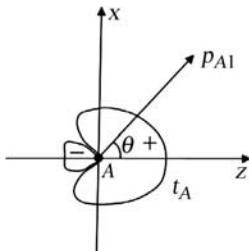
Figure 2.9 t_A is an sp^2 hybrid directed along the z axis

Let:

$$t = \frac{s + \sqrt{2}z}{\sqrt{3}} \tag{2.41}$$

be a normalized sp² hybrid on the *same* atom. Then, t_A is an sp² hybrid on A directed along the z axis (Figure 2.9).

In the σ–π description of the double bond we must solve the secular equation (2.5) in the basis $(t_A t_B\, x_A x_B)$, assuming $S = 0$ as before, getting after diagonalization the molecular orbitals:

$$\begin{cases} \sigma = \dfrac{1}{\sqrt{2}}(t_A + t_B), \quad \sigma^* = \dfrac{1}{\sqrt{2}}(t_A - t_B) \\[2mm] \pi = \dfrac{1}{\sqrt{2}}(x_A + x_B), \quad \pi^* = \dfrac{1}{\sqrt{2}}(x_A - x_B) \end{cases} \tag{2.42}$$

where only σ MOs are changed by hybridization. We have now for the σ bonding orbital energy:

$$\varepsilon_\sigma = \frac{1}{2}\langle t_A + t_B|H|t_A + t_B\rangle = \alpha_t + \beta_{tt} \tag{2.43}$$

where:

$$\alpha_t = \langle t_A|H|t_A\rangle = \frac{1}{3}\langle s_A + \sqrt{2}z_A|H|s_A + \sqrt{2}z_A\rangle = \frac{1}{3}(\alpha_s + 2\alpha_p) \tag{2.44}$$

$$\begin{cases} \beta_{tt} = \langle t_A|H|t_B\rangle = \dfrac{1}{3}\langle s_A + \sqrt{2}z_A|H|s_B + \sqrt{2}z_B\rangle \\[3mm] \qquad = \dfrac{1}{3}(\beta_{ss} + 2\beta_{\sigma\sigma} + 2\sqrt{2}\beta_{s\sigma}) \end{cases} \tag{2.45}$$

whereas the π bonding energy is unchanged:

$$\varepsilon_\pi = \alpha_p + \beta_{\pi\pi}. \tag{2.46}$$

Hybridization introduces further Coulomb (α_s) and bond (β_{ss} and $\beta_{s\sigma}$) integrals. So, we have, for total and bond energy of the double bond accounting for hybridization:

$$\left\{ \begin{aligned} E &= 2\varepsilon_\sigma + 2\varepsilon_\pi = 2(\alpha_t + \beta_{tt}) + 2(\alpha_p + \beta_{\pi\pi}) \\ &= \left(\frac{2}{3}\alpha_s + \frac{10}{3}\alpha_p \right) + \frac{2}{3}\beta_{ss} + \frac{4}{3}\beta_{\sigma\sigma} + \frac{4\sqrt{2}}{3}\beta_{s\sigma} + 2\beta_{\pi\pi} \\ \Delta E &= \frac{2}{3}\beta_{ss} + \frac{4}{3}\beta_{\sigma\sigma} + \frac{4\sqrt{2}}{3}\beta_{s\sigma} + 2\beta_{\pi\pi} \end{aligned} \right. \tag{2.47}$$

Bond energy *increases with hybridization* for two reasons: (i) since $\beta_{ss} > \beta_{\sigma\sigma}$ and (ii) because the additional term $\beta_{s\sigma}$ is quite large (Pople and Santry, 1964, 1965).

A guess of the energy resulting for the double bond in ethylene ($R_{CC} = 2.55a_0$) can be made assuming nodeless Slater-type orbitals (STOs) with $c_s = c_p = 1.625$ using overlap values taken from the literature (Pople and Santry, 1965) and assuming $\beta_0 \approx -3\,\text{eV} = -69.1\,\text{kcal mol}^{-1}$, giving the numbers collected in Tables 2.2 and 2.3.

We then obtain the results (kcal mol^{-1}):

$$\left\{ \begin{aligned} \Delta E_\pi &= 2\beta_{\pi\pi} = -36.6 \\ \Delta E_\sigma &= \left\{ \begin{aligned} &2\beta_{\sigma\sigma} = -45.0 \\ &\frac{2}{3}\beta_{ss} + \frac{4}{3}\beta_{\sigma\sigma} + \frac{4\sqrt{2}}{3}\beta_{s\sigma} + 2\beta_{\pi\pi} = -106.0 \end{aligned} \right. \end{aligned} \right. \tag{2.48}$$

Table 2.2 Overlap integrals between carbon STOs

S_{ss}	$S_{s\sigma}$	$S_{\sigma\sigma}$	$S_{\pi\pi}$
0.431	0.430	0.326	0.265

Table 2.3 Bond integrals between carbon STOs

Energy unit	β_{ss}	$\beta_{s\sigma}$	$\beta_{\sigma\sigma}$	$\beta_{\pi\pi}$
eV	−1.29	−1.29	−0.98	−0.79
kcal mol^{-1}	−29.8	−29.8	−22.5	−18.3

Table 2.4 Bond strength D (kcal mol^{-1}) of the $C = C$ double bond in ethylene

No hybridization	sp^2 hybridization
81.6	142.6

giving for the bond energy of the $C=C$ *double bond* in ethylene the results of Table 2.4.

There is a gain of 61.0 kcal mol^{-1} due to sp^2 hybridization, since the overlap between *bonding* hybrids is stronger than that pertaining to the elementary overlaps (Magnasco, 2007, Magnasco, 2009a). Coulson (1961) gives for the bond strengths:

$$
\begin{cases}
C-C \approx 83 \text{ kcal mol}^{-1} \\
C=C \approx 146 \text{ kcal mol}^{-1}
\end{cases}
\tag{2.49}
$$

in excellent agreement with our estimate here.

Table 2.5 collects some typical values of bond strengths in hydrocarbons taken from Coulson's book (Coulson, 1961).

Turning to the bent bonds description, we have:

$$
\begin{cases}
B_1 = \dfrac{1}{\sqrt{2}}(\sigma+\pi) = \dfrac{1}{\sqrt{2}}\left[\dfrac{1}{\sqrt{2}}(t_A+x_A) + \dfrac{1}{\sqrt{2}}(t_B+x_B)\right] = \dfrac{1}{\sqrt{2}}(b_{A1}+b_{B1}) \\[4mm]
B_2 = \dfrac{1}{\sqrt{2}}(\sigma-\pi) = \dfrac{1}{\sqrt{2}}\left[\dfrac{1}{\sqrt{2}}(t_A-x_A) + \dfrac{1}{\sqrt{2}}(t_B-x_B)\right] = \dfrac{1}{\sqrt{2}}(b_{A2}+b_{B2})
\end{cases}
\tag{2.50}
$$

Table 2.5 Bond strengths D (kcal mol^{-1}) of some bonds in hydrocarbons

Bond	Bond strength	Hybridization
C−C single	83	sp^3
C=C double	146	$sp^2+\pi$
C≡C triple	201	$sp+\pi^2$
C−H in CH_4	103	sp^3
C−H in C_2H_4	106	sp^2
C−H in C_2H_2	121	sp

where:

$$\begin{cases} b_{A1} = \dfrac{1}{\sqrt{2}}(t_A + x_A) = \dfrac{1}{\sqrt{6}}\left(s_A + \sqrt{5}p_{A1}\right) \\[4mm] p_{A1} = \sqrt{\dfrac{2}{5}}\left(z_A + \sqrt{\dfrac{3}{2}}x_A\right). \end{cases} \tag{2.51}$$

b_{A1} is the *hybrid* orbital on A engaged in the B_1 bond orbital, p_{A1} a normalized $2p$ orbital on A making an angle of $\theta = 50.8°$ with the internuclear z axis. The interbond angle between the pair of bent bonds amounts now to $2\theta = 101.6°$ when sp^2 hybridization is included. In fact:

$$\begin{cases} \tan\theta = \dfrac{\text{coefficient of } x_A}{\text{coefficient of } z_A} = \sqrt{\dfrac{3}{2}} = 1.2247 \\[4mm] \theta = 50.8° \end{cases} \tag{2.52}$$

Hence, hybridization increases the angle between the bent bonds. This is the third result given by the quantum mechanical description of the double bond, namely, *hybridization increases the angle between the bent bonds, increasing overlap and therefore increasing the bond strength.*

2.3.4 Triple Bonds

The level occupancy of the bonding MOs originating the typical *triple bond* in ground state N_2 is shown in Figure 2.10. Six valence electrons fill in the nondegenerate σ level and the doubly degenerate π level, giving the configuration $\sigma^2\pi^4$. The same is true for the triple bond in ground state acetylene C_2H_2.
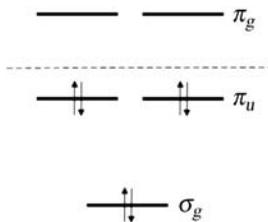

Figure 2.10 Schematic $\sigma_g{}^2\pi_u{}^4$ ground state configuration of the valence electrons originating the triple bond in N_2 and C_2H_2

$$H—C\equiv C—H \qquad H—C\equiv N\!\!<\!\!:$$

$$:\!\!>\!\!O\equiv O\!\!<\!\!: \qquad :\!\!>\!\!N\equiv O\!\!<\!\!:$$

$$:\!\!>\!\!N\equiv N\!\!<\!\!: \qquad :\!\!>\!\!\overset{-}{C}\equiv \overset{+}{O}\!\!<\!\!:$$
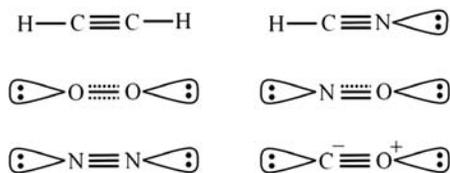
Figure 2.11 Schematic drawing of the triple bonds occurring in some diatomics and in linear polyatomic molecules (σ lone pairs are also sketched)

The *equivalent bent bonds* description of the triple bond is obtained using the same arguments used before for the double bond. Three equivalent bond orbitals B_1, B_2, B_3 are obtained by the linear mixing of σ, π_x, π_y:

$$\begin{cases} B_1 = \dfrac{1}{\sqrt{3}}\sigma + \dfrac{\sqrt{2}}{\sqrt{3}}\pi_x \\[2mm] B_2 = \dfrac{1}{\sqrt{3}}\sigma - \dfrac{1}{\sqrt{6}}\pi_x + \dfrac{1}{\sqrt{2}}\pi_y \\[2mm] B_3 = \dfrac{1}{\sqrt{3}}\sigma - \dfrac{1}{\sqrt{6}}\pi_x - \dfrac{1}{\sqrt{2}}\pi_y \end{cases} \qquad (2.53)$$

the transformation coefficients between the two sets being the elements of an orthogonal matrix. Again, *the two descriptions are physically equivalent*.

A schematic drawing of different sorts of triple bonds is shown in Figure 2.11, centrosymmetric linear molecules (C_2H_2) and homonuclear diatomics (O_2, N_2) being given on the left, noncentrosymmetric linear molecules (HCN) and heteronuclear diatomics (NO, CO) on the right.

As already said, ground state O_2 has two *three-electron* π bonds (dotted in the Figure), NO an ordinary two-electron π bond and a *three-electron π* bond, while CO has an *ionic* triple bond (Magnasco, 2007, Magnasco, 2009a). UV photoelectron spectra (Murrell *et al.*, 1985) show that the correct electron configurations of the ground states are $2\sigma_u^2\,1\pi_u^4\,3\sigma_g^2$ for $N_2(^1\Sigma_g^+)$, $3\sigma_g^2 1\pi_u^4 1\pi_g^2$ for $O_2(^3\Sigma_g^-)$, and $5\sigma^2\,1\pi^4 2\pi$ for NO($^2\Pi$). The order of electron levels in Figure 2.10 is therefore purely schematic.

2.4   THE THREE-CENTRE DOUBLE BOND IN DIBORANE

Electron diffraction studies (Bartell and Carroll, 1965) show that diborane B_2H_6 has a D_{2h} structure like that of ethylene C_2H_4 (Herzberg, 1945),
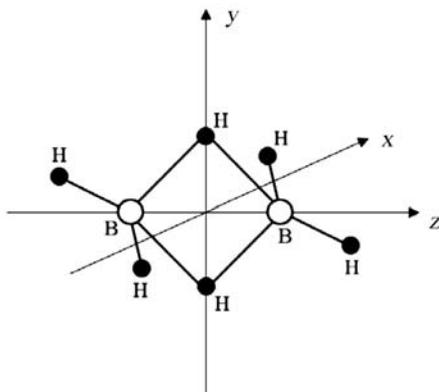
Figure 2.12 Structure of diborane B_2H_6. The two three-centre BHB bonds lie in the yz plane

in which two three-centre bent BHB bonds replace the double bond in ethylene as shown in Figure 2.12. From a theoretical standpoint, uniform localization (Magnasco and Perico, 1968) of the MO-SCF wavefunction of Palke and Lipscomb (1966) also gives strong support to the similarity between diborane and ethylene[6].

With its 16 electrons B_2H_6 is an electron-deficient molecule having the ground state MO electron configuration[7]:

$$B_2H_6 \, (^1A_g): \; 1a_u^2 \, 1a_g^2 \, 2a_g^2 \, 2a_u^2 \, 1b_{2u}^2 \, 1b_{3u}^2 \, 3a_g^2 \, 1b_{2g}^2 \qquad (2.54)$$

which can be compared with that of the ground state of the isoelectronic ethylene molecule:[8]

$$C_2H_4 \, (^1A_g): \; 1a_g^2 \, 1a_u^2 \, 2a_g^2 \, 2a_u^2 \, 1b_{3u}^2 \, 3a_g^2 \, 1b_{2g}^2 \, 1b_{2u}^2 \qquad (2.55)$$

The first five ionization potentials observed from UV photoelectron spectroscopy[9] for the two molecules (B_2H_6: Lloyd and Lynaugh, 1970; C_2H_4: Branton *et al.*, 1970) are compared in Table 2.6 with the negative of the orbital energies resulting from the theoretical MO-SCF calculations

---

[6] It is found that the total $2p$-character is 0.905 for the bond hybrids engaged in the three-centre bonds and 0.777 for those forming the coplanar B−H bonds in diborane, the corresponding values for ethylene being 0.911 for C−C and 0.787 for C−H (so giving a large deviation from the ideal sp^2 hybrids, which have a $2p$-content of $\sqrt{2}/\sqrt{3} = 0.816$). The calculated interbond angle in diborane is 92.6°.

[7] For the notation, see Magnasco (Magnasco, 2007, 2009a).

[8] In the electron configuration of both molecules we have shown the π orbital in bold.

[9] The 'fingerprints' of the molecule.

Table 2.6 Comparison between vertical UV ionization potentials and theoretical MO-SCF results (eV) for the A_g ground states of diborane and ethylene

MOs	B_2H_6		MOs	C_2H_4	
	Experimental[a]	Theoretical[b]		Experimental[c]	Theoretical[b]
$1b_{2g}$	11.89	13.25	**$1b_{2u}$**	10.51	10.09
$3a_g$	13.30	14.56	$1b_{2g}$	12.46	13.77
$1b_{3u}$	13.91	15.24	$3a_g$	14.46	15.28
$1b_{2u}$	14.75	15.68	$1b_{3u}$	15.78	17.52
$2a_u$	16.11	17.86	$2a_u$	18.87	21.29

[a] Lloyd and Lynaugh 1970.
[b] Palke and Lipscomb 1966.
[c] Branton *et al.* 1970.

by Palke and Lipscomb (1966) assuming the validity of Koopmans' theorem:

$$I_i \approx -\varepsilon_i \tag{2.56}$$

Even if the quantitative agreement between the two sets of data is rather unsatisfactory,[10] nonetheless both experiment and calculation show that the π bonding level in both molecules is:

$$\begin{cases} \varepsilon(1b_{2u}) = \varepsilon_\pi \approx -14.5 \text{ eV} & \text{for diborane} \\ \varepsilon(1b_{2u}) = \varepsilon_\pi \approx -11.0 \text{ eV} & \text{for ethylene} \end{cases} \tag{2.57}$$

so that we can say that the two protons entering the three-centre double bonds in diborane *stabilize* the double bond, the π energy level in diborane now appearing as the fourth ionization potential instead of the first, as observed in ethylene.

2.5   THE HETEROPOLAR BOND

In the following, we extend our method to consideration of the *heteropolar* chemical bond. New aspects are now that: (i) both atomic energy difference $\alpha_2 - \alpha_1$ and bond integral β do contribute to the bond energy, often being of the same order of magnitude; and (ii) the molecular charge distribution is asymmetric so that it generates an electric dipole moment. Assuming for simplicity orthogonal AOs (remember Footnote 3), the

---

[10] Not accounting for any correlation energy, theoretical MO calculations heavily overestimate ionization potentials.

fundamental quantities entering the model, the atomic energy difference $\alpha_2 - \alpha_1$ and the bond integral β, can be determined for each molecule using the experimental values of its atomization energy D and its electric dipole moment μ. We shall shortly discuss below some results obtained for the two-electron σ bonds occurring in the ground states of the first-row series of diatomic hydrides (Magnasco, 2003).

The linear combination of two normalized real nonorthogonal fixed AOs, $\chi_1(\mathbf{r})$ on atom A and $\chi_2(\mathbf{r})$ on atom B, with coefficients determined by the Ritz method, gives rise to two orthogonal two-centre MOs having the normalized form:

$$\begin{cases} \phi_1 = \dfrac{\chi_1 + \lambda\chi_2}{\sqrt{1 + \lambda^2 + 2\lambda S}} & \text{bonding MO} \\[4mm] \phi_2 = \dfrac{(1 + \lambda S)\chi_2 - (\lambda + S)\chi_1}{\sqrt{(1 - S^2)(1 + \lambda^2 + 2\lambda S)}} & \text{antibonding MO} \end{cases} \tag{2.58}$$

with orbital energies:

$$\begin{cases} \varepsilon_1 = \dfrac{\alpha_1 + \alpha_2 - 2\beta S - \Delta}{2(1 - S^2)} \\[4mm] \varepsilon_2 = \dfrac{\alpha_1 + \alpha_2 - 2\beta S + \Delta}{2(1 - S^2)} \end{cases} \tag{2.59}$$

where:

$$\Delta = \left[(\alpha_2 - \alpha_1)^2 + 4(\beta - \alpha_1 S)(\beta - \alpha_2 S) \right]^{1/2} > 0 \tag{2.60}$$

λ is the *unique*[11] polarity parameter, given by (see later Equation 2.106):

$$\lambda = \frac{\Delta - (\alpha_2 - \alpha_1)}{2|\beta - \alpha_2 S|} = \sqrt{\frac{\Delta - (\alpha_2 - \alpha_1)}{\Delta + (\alpha_2 - \alpha_1)}} \sqrt{\frac{|\beta - \alpha_1 S|}{|\beta - \alpha_2 S|}} \tag{2.61}$$

As before, according to this simple model, the bond energy in *heteronuclear diatomics* is obtained by adding, at the valence level, the contributions from the different MOs which are occupied by electrons according to the *aufbau* principle.

---

[11] The orthogonality constraint between the resulting MOs gives λ as the only independent variational parameter.

If n_i is the number of electrons occupying the ith MO ϕ_i, n_i^0 the number of electrons in the ith AO χ_i in the separated atoms, we define the *bond energy* as:

$$\Delta E = \sum_i^{occ} n_i \varepsilon_i - \sum_i^{occ} n_i^0 \alpha_i \tag{2.62}$$

which, for homonuclear diatomics, reduces to the expression used in Section 2.1:

$$\Delta E = \sum_i^{occ} n_i(\varepsilon_i - \alpha) = \sum_i^{occ} n_i \Delta \varepsilon_i \tag{2.63}$$

The filling of electrons into the MO levels has now more possibilities than in the previous homonuclear case. These cases are fully described elsewhere (Magnasco, 2003).

Apart from their asymptotic form for $0 < |\beta| < \alpha_2 - \alpha_1$ (Equations 2.20 and 2.23 in Section 2.1), the general expressions for the orbital interaction energies of the heteropolar MOs are rather complicated in the case of nonorthogonal AOs. For the sake of simplicity, we shall content ourselves with the simpler expressions occurring in the case of orthogonality between the interacting AOs χ_1 and χ_2. Under this assumption, Equations (2.58) simplify to:

$$\begin{cases} \phi_1 = \dfrac{\chi_1 + \lambda \chi_2}{\sqrt{1+\lambda^2}} & \text{bonding MO} \\[4mm] \phi_2 = \dfrac{\chi_2 - \lambda \chi_1}{\sqrt{1+\lambda^2}} & \text{antibonding MO} \end{cases} \tag{2.64}$$

with the orbital energies:

$$\varepsilon_1 = \frac{\alpha_1 + \alpha_2}{2} - \frac{\Delta}{2}, \quad \varepsilon_2 = \frac{\alpha_1 + \alpha_2}{2} + \frac{\Delta}{2} \tag{2.65}$$

where now:

$$\Delta = [(\alpha_2 - \alpha_1)^2 + 4\beta^2]^{1/2} > 0 \tag{2.66}$$

We observe that, in this case, the splitting of the molecular levels upon interaction is *symmetric* with respect to the arithmetic mean of the atomic levels (Figure 2.13).

Table 2.7 collects the bond energies ΔE for the eight possible ways of filling electrons into the MO levels resulting for a heteronuclear σ system
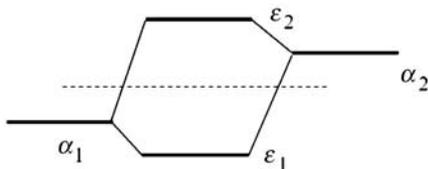
Figure 2.13 For $S = 0$, the first-order splitting of the molecular energy levels in a heteronuclear diatomic is symmetric with respect to the arithmetical mean of the atomic levels (dashed line)

in the case of orthogonal AOs, starting from the lowest bonding MO up to a maximum of four electrons, with a short comment on the nature of the interaction. There are twice as many levels in the heteronuclear system compared with the homonuclear system. Without any loss of generality we have assumed $\alpha_2 - \alpha_1 > 0$ (atom A having the deepest atomic energy level). We see that the bond energy will depend in this case on just two parameters, the atomic energy difference $\alpha_2 - \alpha_1$ and the bond integral $|\beta|$.

The series of first-row diatomic hydrides having a two-electron σ bond (HeH$^+$, LiH, BH, CH, NH, OH, FH) will now be examined in some detail in order to analyse the systematic behaviour of our model in a case of physically occurring molecules. In the case of orthogonal AOs, as already said, the two fundamental quantities of the model, the atomic energy difference $\alpha_2 - \alpha_1$ and the bond integral $|\beta|$, can be determined

Table 2.7 Model bond energies resulting for N-electron heteronuclear σ–systems assuming $\alpha_2 - \alpha_1 > 0$ (orthogonal AOs)

N	Case	n_1^0	n_2^0	ΔE	Nature of the interaction
1	(i)	1	0	$\dfrac{\alpha_2 - \alpha_1}{2} - \dfrac{\Delta}{2}$	Little bonding
	(ii)	0	1	$-\dfrac{\alpha_2 - \alpha_1}{2} - \dfrac{\Delta}{2}$	Bonding
2	(iii)	1	1	$-\Delta$	Bonding
	(iv)	2	0	$(\alpha_2 - \alpha_1) - \Delta$	Little bonding CT (A$^+$B$^-$)
	(v)	0	2	$-(\alpha_2 - \alpha_1) - \Delta$	Bonding CT (A$^-$B$^+$)
3	(vi)	2	1	$\dfrac{\alpha_2 - \alpha_1}{2} - \dfrac{\Delta}{2}$	Little bonding
	(vii)	1	2	$-\dfrac{\alpha_2 - \alpha_1}{2} - \dfrac{\Delta}{2}$	Bonding
4	(viii)	3	3	0	Non-bonding

using experimentally observed quantities for the ground states such as the atomization energy $|D_e|$ and the electric dipole moment μ.

The polarity parameter is:

$$\lambda = \frac{\Delta - (\alpha_2 - \alpha_1)}{2|\beta|} \tag{2.67}$$

We now look at the distribution of the electronic charge, which, for two electrons in the bonding MO of an XH system, gives the atomic charges:

$$q_X = \frac{2}{\lambda^2 + 1}, \quad q_H = \frac{2\lambda^2}{\lambda^2 + 1}, \quad q_X + q_H = 2 \tag{2.68}$$

The formal charges on the interacting atoms for $\lambda < 1$ are:

$$\text{on } X: \ \delta_X = 1 - q_X = \frac{\lambda^2 - 1}{\lambda^2 + 1} = -|\delta| \tag{2.69}$$

$$\text{on } H: \ \delta_H = 1 - q_H = -\frac{\lambda^2 - 1}{\lambda^2 + 1} = +|\delta| \tag{2.70}$$

For $\lambda < 1$, $\delta_X < 0$, and electronic charge will be transferred from H to X, as expected on electronegativity grounds (Coulson, 1961) from C to F. The formal charge $|\delta|$ is independently derived from the experimentally observed values of the vibrationless electric dipole moment[12] μ, when its entire value is attributed to the heteropolar dipole:

$$|\mu| = |\mu_H| = |\delta| R_e, \tag{2.71}$$

so that we obtain for the polarity parameter[13] in the case $\lambda < 1$:

$$\lambda = \left(\frac{1 - |\delta|}{1 + |\delta|} \right)^{1/2} \tag{2.72}$$

We are now in a position to determine the values of our two unknown parameters $\alpha_2 - \alpha_1$ and $|\beta|$ from observed experimental data. If $\left| D_o^o \right|$ is the dissociation energy (Huber and Herzberg, 1979; Feller and Dixon, 2001) and ω_e the vibrational frequency of the ground vibrational level,

---

[12] As usual, we assume $\mu > 0$ when the direction of the dipole is from $-|\delta|$ to $+|\delta|$. Calculated Hartree–Fock values of μ corrected for correlation effects generally agree with experimental results (see text).

[13] For $\lambda > 1$ the signs in the expression for λ must be reversed.

$|D_e| = |D_o{}^o| + \frac{1}{2}\omega_e$ is the experimental atomization energy of XH observed from molecular spectra. Then:

$$\alpha_2 - \alpha_1 = -|D_e|\frac{\lambda^2 - 1}{\lambda^2 + 1} \tag{2.73}$$

is the atomic energy difference, obtained as the admissible solution of the quadratic equation:

$$(\lambda^2 + 1)(\alpha_2 - \alpha_1)^2 - 2|D_e|(\alpha_2 - \alpha_1) - (\lambda^2 - 1)D_e^2 = 0 \tag{2.74}$$

The bond energy parameter is then given by:

$$|\beta| = \frac{1}{2}[D_e{}^2 - (\alpha_2 - \alpha_1)^2]^{1/2} \tag{2.75}$$

The formal charge $|\delta|$, the polarity parameter λ, the atomic energy difference $\alpha_2 - \alpha_1$ and the bond energy parameter $|\beta|$ resulting from the experimental bond distances R_e, the atomization energies $|D_e|$, and the SCF values for the electric dipole moments μ of the ground states of first-row diatomic hydrides, are given in atomic units in Table 2.8. In the series, all molecules have at the valence level a two-electron heteropolar σ bond and a number of σ or π lone pairs and unpaired π electrons. Apart from the first two terms in the series, the bond energy increases with decreasing bond distance and the regular increase of the electronegativity difference of atom X with respect to H. LiH has an unusually long bond distance, with a rather large bond energy and a very large dipole moment.

While further details are left elsewhere (Magnasco, 2003), we shall content ourselves here to remark that the model atomic energy differences $\alpha_2 - \alpha_1$ are seen to follow the Mulliken electronegativity scale (Coulson, 1961; McWeeny, 1979), α_H being the deepest atomic level for LiH,

Table 2.8 Two-electron σ bonds occurring in the ground state of first-row diatomic hydrides

Molecule	R_e/a_0	$|D_e|/E_h$	$|\mu|/ea_0$	$|\delta|/e$	λ	$\alpha_2-\alpha_1/E_h$	$|\beta|/E_h$
HeH$^+$	1.46	0.075	0.49	0.33	0.710	0.025	0.0353
LiH	3.015	0.092	2.36	0.78	2.844	−0.072	0.0288
BH	2.32	0.133	0.68	0.29	0.742	0.039	0.0636
CH	2.12	0.133	0.62	0.29	0.742	0.039	0.0650
NH	1.96	0.136	0.64	0.32	0.718	0.043	0.0696
OH	1.83	0.169	0.70	0.38	0.670	0.064	0.0782
FH	1.73	0.224	0.76	0.44	0.624	0.099	0.1005

the reverse being true for the remaining hydrides ($\alpha_H - \alpha_X > 0$). It is apparent that the model parameter $\alpha_H - \alpha_X$ accounts in some way for atom electronegativities within the bond. The bond energy parameter $|\beta|$ has the same order of magnitude of $\alpha_2 - \alpha_1$ and, apart from LiH, regularly increases from HeH$^+$ to FH.

2.6   STEREOCHEMISTRY OF POLYATOMIC MOLECULES

The structure in space of polyatomic molecules depends on the stereochemistry of their chemical bonds through the principle of maximum overlap (Magnasco, 2005).

2.6.1   The Molecular Orbital Model of Directed Valency

In the following, we shall use our model description of the chemical bond to show that *bonding is strongest for AOs maximizing the strength of the exchange-overlap component of the bond energy*. Making the usual assumptions typical of elementary Hückel theory including overlap, we shall show that the Hückel energy of the two-electron bond is minimized for orbitals having maximum overlap.

Let b_A be a directed orbital (atomic or hybrid) centred at the nucleus of atom A and making an angle θ with the interbond axis A–B directed along z from A to B, and χ_B a spherical orbital on atom B a distance R apart. Then, overlap S_{AB} and bond integral β_{AB} can be written as:

$$S_{AB} = S\cos\theta, \quad \beta_{AB} = \beta\cos\theta \tag{2.76}$$

where S and β are integrals characteristic of the bond A–B, which depend on R, but are independent of the orientation θ.

The pseudosecular equation for the corresponding bond orbital ϕ in a one-electron Hückel-type approximation including overlap can then be written as:

$$\begin{vmatrix} \alpha_A - \varepsilon & (\beta - \varepsilon S)\cos\theta \\ (\beta - \varepsilon S)\cos\theta & \alpha_B - \varepsilon \end{vmatrix} = 0 \tag{2.77}$$

which expands to the quadratic equation in ε:

$$(1 - S^2\cos^2\theta)\varepsilon^2 - (\alpha_A + \alpha_B - 2\beta S\cos^2\theta)\varepsilon + (\alpha_A\alpha_B - \beta^2\cos^2\theta) = 0 \tag{2.78}$$

where α_A, α_B, and β are all negative energy quantities having the usual meaning, the first two being interpreted as atomic integrals pertaining to orbitals b_A and χ_B, while β is the bond integral depending on the nature of A and B.

The two real roots are:

$$\varepsilon_- = \frac{\alpha_A + \alpha_B - 2\beta S \cos^2\theta - \Delta}{2(1 - S^2 \cos^2\theta)} \qquad (2.79)$$

the *bonding* root, and:

$$\varepsilon_+ = \frac{\alpha_A + \alpha_B - 2\beta S \cos^2\theta + \Delta}{2(1 - S^2 \cos^2\theta)} \qquad (2.80)$$

the *antibonding* root, with:

$$\Delta = [(\alpha_B - \alpha_A)^2 + 4(\beta - \alpha_A S)(\beta - \alpha_B S)\cos^2\theta]^{1/2} > 0 \qquad (2.81)$$

To examine the dependence of the orbital energies ε on θ, it is convenient to consider the determinantal Equation (2.77) as an *implicit function* of the two variables θ and ε:

$$f(\theta, \varepsilon) = (\alpha_A - \varepsilon)(\alpha_B - \varepsilon) - (\beta - \varepsilon S)^2 \cos^2\theta = 0 \qquad (2.82)$$

From the derivation rules for implicit functions (Smirnov, 1993) it follows:

$$df = \left(\frac{\partial f}{\partial \theta}\right)_\varepsilon d\theta + \left(\frac{\partial f}{\partial \varepsilon}\right)_\theta d\varepsilon = 0 \qquad (2.83)$$

$$\frac{d\varepsilon}{d\theta} = -\frac{\left(\dfrac{\partial f}{\partial \theta}\right)_\varepsilon}{\left(\dfrac{\partial f}{\partial \varepsilon}\right)_\theta} = -\frac{f_\theta}{f_\varepsilon} \qquad (2.84)$$

provided:

$$f_\varepsilon = \left(\frac{\partial f}{\partial \varepsilon}\right)_\theta \neq 0 \qquad (2.85)$$

and, using the Schwartz equality for the second partial derivatives:

$$\frac{d^2\varepsilon}{d\theta^2} = -\frac{f_{\theta\theta}(f_\varepsilon)^2 + f_{\varepsilon\varepsilon}(f_\theta)^2 - 2f_{\theta\varepsilon}f_\theta f_\varepsilon}{(f_\varepsilon)^3} \qquad (2.86)$$

When the calculation of the second derivative involves a *stationarity* point for ε, which implies:

$$f_\theta = \left(\frac{\partial f}{\partial \theta}\right)_\varepsilon = 0 \tag{2.87}$$

expression (2.86) simplifies to:

$$\frac{d^2\varepsilon}{d\theta^2} = -\frac{f_{\theta\theta}}{f_\varepsilon} \tag{2.88}$$

provided both members are evaluated at the stationarity point for ε.

From Equation (2.82), we easily obtain:

$$f_\theta = \left(\frac{\partial f}{\partial \theta}\right)_\varepsilon = (\beta - \varepsilon S)^2 \sin 2\theta \tag{2.89}$$

$$f_{\theta\theta} = \left(\frac{\partial^2 f}{\partial \theta^2}\right)_\varepsilon = 2(\beta - \varepsilon S)^2 \cos 2\theta \tag{2.90}$$

$$f_\varepsilon = \left(\frac{\partial f}{\partial \varepsilon}\right)_\theta = 2\varepsilon(1 - S^2 \cos^2\theta) - (\alpha_A + \alpha_B - 2\beta S \cos^2\theta) \tag{2.91}$$

For the lowest root (Equation 2.79), $\varepsilon = \varepsilon_-$, we have:

$$(f_\theta)_{\varepsilon_-} = (\beta - \varepsilon_- S)^2 \sin 2\theta \tag{2.92}$$

$$(f_\varepsilon)_{\varepsilon_-} = -\Delta, \tag{2.93}$$

so that Equations (2.84) and (2.86) become:

$$\frac{d\varepsilon_-}{d\theta} = \frac{(\beta - \varepsilon_- S)^2 \sin 2\theta}{\Delta} \tag{2.94}$$

$$\frac{d^2\varepsilon_-}{d\theta^2} = \frac{2(\beta - \varepsilon_- S)^2 \cos 2\theta}{\Delta} \tag{2.95}$$

The stationarity condition of ε_- with respect to θ says that:

$$\frac{d\varepsilon_-}{d\theta} = 0 \tag{2.96}$$

for $\theta = 0$, so that:

$$\left(\frac{d^2\varepsilon_-}{d\theta^2}\right)_{\theta=0} = \frac{2(\beta - \varepsilon_- S)^2}{\Delta} > 0 \tag{2.97}$$

provided both numerator and denominator are evaluated at $\theta = 0$. From Equations (2.96) and (2.97) it follows that $\theta = 0$ is a stationarity point for which ε_- has a true *minimum* value.

Hence, the Hückel energy for the two electrons in the bond orbital ϕ:

$$\left\{ \begin{aligned} E_-(\theta = 0) &= 2\varepsilon_-(\theta = 0) \\[2ex] &= \frac{\alpha_A + \alpha_B - 2\beta S - \left[(\alpha_B - \alpha_A)^2 + 4(\beta - \alpha_A S)(\beta - \alpha_B S)\right]^{1/2}}{1 - S^2} \end{aligned} \right. \tag{2.98}$$

has a minimum for $\theta = 0$, corresponding to a *maximum strength* for the straight A−B bond. In the same way, it can be shown that $\theta = 0$, corresponds to a maximum for $E_+ = 2\varepsilon_+$.

For orthogonal AOs, such as those of the original Hückel theory, $S = 0$, and Equations (2.94) and (2.95) become:

$$\frac{d\varepsilon_-}{d\theta} = \frac{\beta^2 \sin 2\theta}{\Delta}, \quad \frac{d^2\varepsilon_-}{d\theta^2} = \frac{2\beta^2 \cos 2\theta}{\Delta} \tag{2.99}$$

and the same conclusions still hold.

2.6.2   Analysis of the MO Bond Energy

In our MO model, the bond energy defined as:

$$\left\{ \begin{aligned} \Delta E_- \;&=\; 2\varepsilon_- - (\alpha_A + \alpha_B) \\[2ex] &= -\frac{S}{1 - S^2 \cos^2\theta}\left\{[(\beta - \alpha_A S) + (\beta - \alpha_B S)]\cos^2\theta\right\} \\[2ex] &\quad - \frac{\Delta}{1 - S^2 \cos^2\theta} \end{aligned} \right. \tag{2.100}$$

consists of two terms, the last being the *bonding* term (< 0, attractive), the first a repulsive term (> 0) *correcting* for nonorthogonality.

For $\theta = 0$, if:

$$\alpha_A = \alpha_B = \alpha \tag{2.101}$$

$$\Delta = \left[4(\beta - \alpha S)^2\right]^{1/2} = 2|\beta - \alpha S| > 0 \tag{2.102}$$

the bond energy becomes:

$$
\begin{cases}
\Delta E_-(\theta = 0) = -\dfrac{2S}{1-S^2}(\beta - \alpha S) - \dfrac{2|\beta - \alpha S|}{1-S^2} \\[3mm]
\qquad\qquad = -\dfrac{2S}{1-S^2}(\beta - \alpha S) + \dfrac{2(\beta - \alpha S)}{1-S^2} \\[3mm]
\qquad\qquad = 2\dfrac{\beta - \alpha S}{1+S}
\end{cases}
\tag{2.103}
$$

as it must be for homonuclear bonding. Hence, the correction term in Equation (2.100) is essential in order to avoid overestimation of the bond energy. This is in agreement with the well- known asymmetric splitting of the MO levels occurring in Hückel theory for $S \neq 0$, where nonorthogonality of the basic AOs yields a bonding level *less* bonding, and an antibonding level *more* antibonding, than those of the symmetric splitting occurring for $S = 0$.

As far as the bonding term in Equation (2.100) is concerned, Equation (2.81) shows that Δ, in turn, depends: (i) on the atomic energy difference $(\alpha_B - \alpha_A)$; and (ii) on the product of bond energy integrals, $(\beta - \alpha_A S)(\beta - \alpha_B S)\cos^2\theta$, arising from the *exchange-overlap densities* $[a(\mathbf{r})b(\mathbf{r}) - Sa^2(\mathbf{r})]$ on A and $[b(\mathbf{r})a(\mathbf{r}) - Sb^2(\mathbf{r})]$ on B, respectively, and which contains all dependence of Δ on the orientation θ. So, it is apparent that the MO description of bonding and of its directional properties in the general case $B \neq A$ involves a rather complicated dependence (through the square root defining Δ) on such exchange-overlap densities. On the other hand, both factors above contribute to the determination of the polarity parameter λ of the bonding MO ϕ (Magnasco, 2003):

$$
\phi = \frac{b_A + \lambda\chi_B}{\sqrt{1 + \lambda^2 + 2\lambda S\cos\theta}}
\tag{2.104}
$$

Rather than from the homogeneous system corresponding to the pseudosecular equation (2.77), it is convenient to obtain λ for the lowest eigenvalue ε_- as the appropriate solution of the quadratic equation[14]:

$$
(\beta - \alpha_B S)\cos\theta\,\lambda^2 - (\alpha_B - \alpha_A)\lambda - (\beta - \alpha_A S)\cos\theta = 0
\tag{2.105}
$$

$$
\lambda = \frac{(\alpha_B - \alpha_A) - \Delta}{2(\beta - \alpha_B S)\cos\theta} = \sqrt{\frac{\Delta - (\alpha_B - \alpha_A)}{\Delta + (\alpha_B - \alpha_A)}}\sqrt{\frac{|\beta - \alpha_A S|}{|\beta - \alpha_B S|}}
\tag{2.106}
$$

---

[14] Arising from the matrix formulation of the *full* 2×2 non-orthogonal eigenvalue problem (Magnasco, 2007).

Equation (2.106) allows then for the MO description of the electric dipole moment μ of the bond.

As a matter of fact, Hückel theory including overlap appropriately describes the physically relevant part of the interaction in this region, showing that the possibility of forming a chemical bond lies in the *attractive* nature of the one-electron part of the exchange-overlap component of the interaction energy (Magnasco and McWeeny, 1991). We have already seen that these considerations correctly explain the nature of the bonding in the series of homonuclear diatomics H_2^+, H_2, He_2^+, He_2, with their further extension to the homonuclear diatomics of the first row (Magnasco, 2004a), which involve π bonding as well, and to the heteropolar bond in the orthogonal approximation (Magnasco, 2003). All these effects are the same in determining the straight bond when directed orbitals overlap.

2.7 *sp*-HYBRIDIZATION EFFECTS IN FIRST-ROW HYDRIDES

At the simplest physical level, not taking hybridization into account, we need a 1×2 row vector basis for describing formation of the F–H bond in HF $(z\,h)$, the O–H bond in H_2O $\left(z\,h_z = \dfrac{1}{\sqrt{2}}(h_1 + h_2) \right)$, and the N–H bond in $NH_3 \left(z\,h_z = \dfrac{1}{\sqrt{3}}(h_1 + h_2 + h_3) \right)$, the first belonging to Σ symmetry, the last two to A_1 symmetry. As a final step in our Hückel calculation, all cases involve diagonalization of a 2×2 Hückel matrix, which is trivial.

Admitting *sp* hybridization, for Σ, C_{2v}, and C_{3v} molecular symmetries, the s and z functions always belong to the *same* symmetry (Table 2.9), so that the row basis vector is now 1×3 giving a 3×3 Hückel matrix, whose diagonalization is not so easy.

For the higher T_d symmetry of the methane molecule, CH_4, s and z belong to *different* symmetries (Table 2.9), so that the 1×8 row basis vector $(s\,h_s\;z\,h_z\;x\,h_x\;y\,h_y)$ generates an 8×8 Hückel matrix which shows complete factorization into four 2×2 orthogonal noninteracting blocks, belonging to A_1, T_{2z}, T_{2x}, and T_{2y} symmetries, respectively. So, the higher symmetry of CH_4 much simplifies the problem, and will be treated first (Magnasco, 2004a). For the remaining hydrides (HF, H_2O, NH_3) we are faced with the solution of a 3×3 Hückel secular equation, which we shall pursue numerically for HF (Magnasco, 2009d) and analytically for H_2O

Table 2.9 Symmetries of atomic bases involving *sz*-mixing in first-row hydrides

Molecule	AO basis	Symmetry
HF	$(s\,z\,h)$	Σ
H_2O	$\left(s\,z\,h_z = \dfrac{1}{\sqrt{2}}(h_1 + h_2)\right)$	A_1
NH_3	$\left(s\,z\,h_z = \dfrac{1}{\sqrt{3}}(h_1 + h_2 + h_3)\right)$	A_1
CH_4	$\left(s\,h_s = \dfrac{1}{2}(h_1 + h_2 + h_3 + h_4)\right)$	A_1
	$\left(z\,h_z = \dfrac{1}{2}(h_1 - h_2 - h_3 + h_4)\right)$	T_{2z}

(Magnasco, 2009b) and NH_3 (Magnasco, 2009c). For all polyatomic molecules, we shall show that *sp* hybridization opens the interbond angle beyond 90° and that minimization of the valence Hückel energy against the hybridization parameter yields straight bonds satisfying the principle of maximum overlap.

2.7.1 The Methane Molecule

We now apply our model to investigate the formation of four C–H bonds in the methane molecule CH_4 of symmetry T_d (Magnasco, 2004a). For this molecule, tetrahedral sp^3 hybridization is completely determined by molecular symmetry. We use the usual notation for the eight valence AOs, calling s, x, y, z the 2s and 2p orbitals on C, and h_1, h_2, h_3, h_4 the 1s orbitals on the H atoms at the vertices of the tetrahedron (Figure 2.14). Molecular
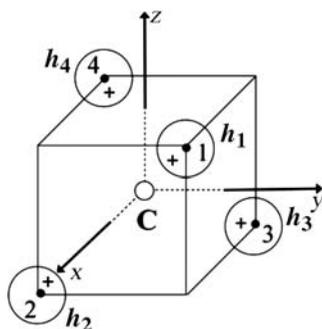

Figure 2.14   The cube circumscribing the tetrahedral CH_4 molecule

symmetry suggests to use combinations of H orbitals transforming as (s, x, y, z), which we can write by inspection:

$$\begin{cases} h_s = \dfrac{1}{2}(h_1 + h_2 + h_3 + h_4) \\[1.5em] h_x = \dfrac{1}{2}(h_1 + h_2 - h_3 - h_4) \\[1.5em] h_y = \dfrac{1}{2}(h_1 - h_2 + h_3 - h_4) \\[1.5em] h_z = \dfrac{1}{2}(h_1 - h_2 - h_3 + h_4) \end{cases} \tag{2.107}$$

The four (unnormalized) bonding MOs are then appropriately written as:

$$\begin{cases} a_1 \propto s + \lambda h_s \\ t_{2x} \propto x + \mu h_x \\ t_{2y} \propto y + \mu h_y \\ t_{2z} \propto z + \mu h_z \end{cases} \tag{2.108}$$

where the coefficients (polarity parameters) are found by solving the four 2×2 Hückel secular equations:

$$\begin{vmatrix} H_{ss} - \varepsilon & H_{sh_s} \\ H_{sh_s} & H_{h_s h_s} - \varepsilon \end{vmatrix} = 0 \qquad \begin{vmatrix} H_{zz} - \varepsilon & H_{zh_z} \\ H_{zh_z} & H_{h_z h_z} - \varepsilon \end{vmatrix} = 0. \tag{2.109}$$

$$\text{Symmetry } A_1 \qquad\qquad\qquad \text{Symmetry } T_2\,(x, y, z)$$

The calculation of the matrix elements follows as usual, giving:

$$\begin{cases} H_{ss} = \alpha_s & H_{sh_s} = 2\beta_{sh} & H_{h_s h_s} = \alpha_h + 3\beta_{hh} \approx \alpha_h \\ H_{zz} = \alpha_p & H_{zh_z} = 2\beta_{zh} & H_{h_z h_z} = \alpha_h - \beta_{hh} \approx \alpha_h \end{cases} \tag{2.110}$$

with similar expressions for the remaining x, y components, and where β_{hh} is neglected as usual in Hückel theory.[15] The β integrals involving (x, y, z) AOs on carbon can be expressed in terms of the more convenient set (σ, π_x, π_y), where σ is a p–orbital directed along the CH_1 bond, and the π's are orbitals perpendicular to it:

---

[15] H atoms in CH_4 are not adjacent atoms.

$$\begin{cases} x = \dfrac{1}{\sqrt{2}}\sin\theta \cdot \sigma + \dfrac{1}{\sqrt{2}}\cos\theta \cdot \pi_x - \dfrac{1}{\sqrt{2}}\pi_y \\[3mm] y = \dfrac{1}{\sqrt{2}}\sin\theta \cdot \sigma + \dfrac{1}{\sqrt{2}}\cos\theta \cdot \pi_x + \dfrac{1}{\sqrt{2}}\pi_y \\[3mm] z = \cos\theta \cdot \sigma - \sin\theta \cdot \pi_x \end{cases} \qquad (2.111)$$

2θ being the interbond (valence) angle. Then:

$$\beta_{xh} = \beta_{yh} = \beta_{ph}\frac{1}{\sqrt{2}}\sin\theta \qquad \beta_{zh} = \beta_{ph}\cos\theta \qquad (2.112)$$

where β_{ph} is a quantity characteristic of the bond.

The lowest roots of the secular equations will give the Hückel energy of the eight valence electrons as a function of angle θ:

$$\begin{cases} \begin{aligned} E(\theta) \;=\; & 2\sum_{i}^{occ}\varepsilon_i = (\alpha_s + \alpha_h) + 3(\alpha_p + \alpha_h) \\[2mm] & -\Big[(\alpha_s-\alpha_h)^2 + 16\beta_{sh}^2\Big]^{1/2} - \Big[(\alpha_p-\alpha_h)^2 + 16\beta_{xh}^2\Big]^{1/2} \\[2mm] & -\Big[(\alpha_p-\alpha_h)^2 + 16\beta_{yh}^2\Big]^{1/2} - \Big[(\alpha_p-\alpha_h)^2 + 16\beta_{zh}^2\Big]^{1/2} \\[2mm] =\; & (\alpha_s + 3\alpha_p + 4\alpha_h) \\[2mm] & -\Big[(\alpha_s-\alpha_h)^2 + 16\beta_{sh}^2\Big]^{1/2} \\[2mm] & -2\Big[(\alpha_p-\alpha_h)^2 + 8\beta_{ph}^2\sin^2\theta\Big]^{1/2} \\[2mm] & -\Big[(\alpha_p-\alpha_h)^2 + 16\beta_{ph}^2\cos^2\theta\Big]^{1/2} \end{aligned} \end{cases} \qquad (2.113)$$

which has an absolute minimum $\left(\dfrac{dE}{d\theta} = 0,\ \left(\dfrac{d^2E}{d\theta^2}\right)_{2\theta=109.5^\circ} > 0\right)$ for:

$$\begin{cases} \cos^2\theta = \dfrac{1}{2}\sin^2\theta \\[3mm] \cos\theta = \dfrac{1}{\sqrt{3}},\ \sin\theta = \dfrac{\sqrt{2}}{\sqrt{3}} \Rightarrow 2\theta = 109.5^\circ \end{cases} \qquad (2.114)$$

i.e. the tetrahedral angle.

The resulting MOs are symmetry MOs, *delocalized* over the entire molecule. As it will be shown for H_2O, a description more adherent to the chemical picture of four *localized* C−H bonds can be obtained in terms of the orthogonal transformation[16] connecting occupied MOs, the first relation being:

$$\begin{cases} B_1 = \dfrac{1}{2}(a_1 + t_{2x} + t_{2y} + t_{2z}) \\[2mm] \quad = \dfrac{1}{2}\left[s + (x+y+z) + \dfrac{\lambda+3\mu}{2}h_1 + \dfrac{\lambda-\mu}{2}(h_2 + h_3 + h_4) \right] \quad (2.115) \\[2mm] \quad = \dfrac{1}{2}\left[s + \sqrt{3}p_1 + \dfrac{\lambda+3\mu}{2}h_1 + \dfrac{\lambda-\mu}{2}(h_2 + h_3 + h_4) \right] \end{cases}$$

and so forth for B_2, B_3, B_4. If $\lambda \approx \mu$, we obtain:

$$B_1 \approx \frac{s + \sqrt{3}p_1}{2} + \lambda h_1 = t_1 + \lambda h_1 \qquad (2.116)$$

a *localized* CH_1 bond orbital, where $p_1 = \dfrac{1}{\sqrt{3}}(x+y+z)$ is a $2p$–orbital on C pointing along the (111) diagonal of the cube, and:

$$t_1 = \frac{s + \sqrt{3}p_1}{2} \qquad (2.117)$$

a tetrahedral sp^3 *hybrid* on C (25% s, 75% p). So, the usual chemical picture of the CH_4 molecule in terms of four equivalent C−H bonds having tetrahedral symmetry is simply recovered from the requirement of Hückel's lowest energy for the valence shell.

2.7.2   The Hydrogen Fluoride Molecule

2.7.2.1   MO Theory Without Hybridization

As usual, we choose the F atom at the origin of the coordinate system with the H atom placed on the positive z axis at the experimental bond distance $R_e = 1.73a_o$ (Huber and Herzberg, 1979).

---

[16] Which leaves invariant the whole physical description. A general transformation from canonical to localized MOs was given time ago by Magnasco and Perico (Magnasco and Perico, 1967, 1968). See also Magnasco (2007).

We start by considering that, in the first approximation, only the appropriate $2p$ AO on fluorine ($2p_z$, in short denoted by z) contributes to the bonding with the $1s$ AO of hydrogen (in short, h). Two electrons are placed in the undistorted σ F lone pair s^2, and four electrons in the two π F lone pairs x^2y^2. As usual in elementary Hückel theory, for the sake of simplicity, we do not consider *explicitly* the overlap between basic AOs (which are hence assumed orthonormal), but still maintain their *implicit* dependence on overlap in the bond integral[17] $|\beta|$ (Magnasco, 2004a). The bonding MO is then given by the Ritz method as:

$$\sigma = zC_1 + hC_2 = \frac{z + \lambda h}{\sqrt{\lambda^2 + 1}} \qquad (2.118)$$

where

$$\lambda = \left(\frac{C_2}{C_1}\right)_1$$

is the polarity parameter. The coefficients are obtained from the lowest root of the 2×2 Hückel secular equation:

$$\begin{vmatrix} H_{zz} - \varepsilon & H_{zh} \\ H_{zh} & H_{hh} - \varepsilon \end{vmatrix} = 0 \qquad (2.119)$$

Hückel matrix elements are:

$$H_{zz} = \alpha_p, \quad H_{hh} = \alpha_h, \quad H_{zh} = \beta \qquad (2.120)$$

all elements being negative quantities. Roots are:

$$2\varepsilon = (\alpha_p + \alpha_h) \pm \Delta \qquad (2.121)$$

$$\Delta = [(\alpha_p - \alpha_h)^2 + 4\beta^2]^{1/2} > 0 \qquad (2.122)$$

so that the Hückel energy for the valence electron configuration $s^2\sigma^2x^2y^2$ of ground state HF will be:

$$E(HF, {}^1\Sigma^+) = 2\alpha_s + 4\alpha_p + (\alpha_p + \alpha_h) - \Delta \qquad (2.123)$$

The bond energy is then (Magnasco, 2003):

$$\Delta E(HF, {}^1\Sigma^+) = E(HF, {}^1\Sigma^+) - 2\alpha_s - 5\alpha_p - \alpha_h = -\Delta = -|D| \qquad (2.124)$$

---

[17] Orthogonal does not mean not interacting (Footnote 3). This is tantamount to keeping only the exchange part of the exchange-overlap interaction (Magnasco, 2002, 2004a).

where $|D| = |D_o^o| + \frac{1}{2}\omega_e$ is the experimental atomization energy of HF(Σ^+) observed from molecular spectra (Huber and Herzberg, 1979), $|D_o^o| = 0.235\,E_h$ the dissociation energy and $\omega_e \approx 4138\,\text{cm}^{-1} \approx 0.019E_h$ the vibrational frequency of the vibrational ground level $v = 0$. So, we shall use $|D| = 0.245E_h$.

The polarity parameter for ground state HF is then calculated to be:

$$\lambda = \left(\frac{C_2}{C_1}\right)_1 = \frac{\varepsilon_1 - \alpha_p}{\beta} = \frac{(\alpha_p - \alpha_h) + \Delta}{2|\beta|} \qquad (2.125)$$

We now look at the distribution of the two electrons in the σ bonding MO, which gives the atomic charges:

$$q_F = \frac{2}{\lambda^2 + 1}, \quad q_H = \frac{2\lambda^2}{\lambda^2 + 1}, \quad q_F + q_H = 2 \qquad (2.126)$$

The formal charges on the interacting atoms are:

$$\text{on } F: \ \delta_F = 1 - q_F = \frac{\lambda^2 - 1}{\lambda^2 + 1} = -|\delta| \qquad (2.127)$$

$$\text{on } H: \ \delta_H = 1 - q_H = -\frac{\lambda^2 - 1}{\lambda^2 + 1} = +|\delta| \qquad (2.128)$$

For $\lambda < 1$, $\delta_F < 0$, and electronic charge will be transferred from H to F, as expected on electronegativity grounds. As we said before, the formal charge $|\delta|$ can be independently derived from the experimentally observed value (Muenter and Klemperer, 1970; Sileo and Cool, 1976) of the vibrationless electric dipole moment[18] ($\mu = 0.72\,ea_o$), if we attribute the entire value of the dipole to its heteropolar component $|\mu_H|$ (Magnasco, 2003):

$$|\mu| = |\mu_H| = |\delta|R_e, \quad |\delta| = 0.42 \qquad (2.129)$$

so that we obtain for the polarity parameter in the case of simple p bonding:

$$\lambda = \left(\frac{1 - |\delta|}{1 + |\delta|}\right)^{1/2} = 0.64 \qquad (2.130)$$

---

[18] As usual, we assume $\mu > 0$ when the direction of the dipole is from $-|\delta|$ to $+|\delta|$. Calculated Hartree–Fock values of μ ($0.756ea_o$) (Christiansen and McCullough, 1977; Sundholm *et al.*, 1985) corrected for correlation effects ($-0.043ea_o$) (Werner and Meyer, 1976; Amos, 1982) agree with the experimental result.

As we did before, we are now in the position to determine entirely from observed experimental data the values of our two unknown parameters $|\alpha_p - \alpha_h|$ and $|\beta|$. In fact, if we put:

$$\alpha_p - \alpha_h = A, \quad 2|\beta| = B \tag{2.131}$$

we find that the values of A are the solutions of the quadratic Equation (2.74). The roots are:

$$A = \begin{cases} -|D| \\ |D|\left(\dfrac{\lambda^2 - 1}{\lambda^2 + 1}\right) = -|\delta| \cdot |D| \end{cases} \tag{2.132}$$

Both roots are real and negative, as it should be. We must discard the first root, which would give $|\beta| = 0$. For the remaining root:

$$\begin{cases} A = \alpha_p - \alpha_h = -0.42 \times 0.245 = -0.1029 E_h \\ B = 2|\beta| = 0.2214 E_h \\ |\beta| = 0.1107 E_h = 69.5 \, \text{kcal mol}^{-1} \end{cases} \tag{2.133}$$

Even if the resulting values of $|\alpha_p - \alpha_h|$ and $|\beta|$ are of the *same* order of magnitude, the contribution to the radicand from the bond integral is about five times larger than that arising from the atomic energy difference. It is interesting to notice that the case under consideration is not included in the two extreme cases analysed by us previously (Magnasco, 2004a), and that the value resulting for $\alpha_p - \alpha_h$ lies roughly midway between the one-term ($-0.0264 E_h$) and the two-term ($-0.2239 E_h$) SCF values for STOs (Clementi and Roetti, 1974). This is fairly reasonable in view of the simplicity of our assumptions.

2.7.2.2 Admitting Full Mixing Within Σ Symmetry

As a second step, we admit full mixing of s and z AOs on fluorine within Σ symmetry. The Hückel matrix will be:

$$\mathbf{H} = \begin{pmatrix} H_{ss} & 0 & H_{sh} \\ 0 & H_{zz} & H_{zh} \\ H_{sh} & H_{zh} & H_{hh} \end{pmatrix} \tag{2.134}$$

where:

$$\begin{cases} H_{ss} = \alpha_s, \quad H_{zz} = \alpha_p \\ H_{sh} = \beta_{sh}, \quad H_{zh} = \beta_{zh} = \beta_{\sigma h} \end{cases} \tag{2.135}$$

giving the complete 3×3 Hückel secular equation:

$$\begin{vmatrix} \alpha_s - \varepsilon & 0 & \beta_{sh} \\ 0 & \alpha_p - \varepsilon & \beta_{\sigma h} \\ \beta_{sh} & \beta_{\sigma h} & \alpha_h - \varepsilon \end{vmatrix} = 0 \tag{2.136}$$

Expanding the determinant gives the cubic equation:

$$(\alpha_s - \varepsilon)[(\alpha_p - \varepsilon)(\alpha_h - \varepsilon) - \beta_{\sigma h}^2] - (\alpha_p - \varepsilon)\beta_{sh}^2 = 0 \tag{2.137}$$

$$\varepsilon^3 + p\varepsilon^2 + q\varepsilon + r = 0 \tag{2.138}$$

where:

$$\begin{cases} p = -(\alpha_s + \alpha_p + \alpha_h) \\ q = (\alpha_s + \alpha_p)\alpha_h + \alpha_s\alpha_p - \beta_{sh}^2 - \beta_{\sigma h}^2 \\ r = \alpha_s\beta_{\sigma h}^2 + \alpha_p\beta_{sh}^2 - \alpha_s\alpha_p\alpha_h \end{cases} \tag{2.139}$$

It is well within the spirit of Hückel theory to assume for the s AO the *same* bond integral as that for the p AO, so that the properties of the F–H bond will depend just on a single parameter β and *not* on the detailed form of the fluorine AOs:

$$\beta_{sh} = \beta_{\sigma h} = \beta \tag{2.140}$$

Then:

$$\begin{cases} p = -(\alpha_s + \alpha_p + \alpha_h) \\ q = (\alpha_s + \alpha_p)\alpha_h + \alpha_s\alpha_p - 2\beta^2 \\ r = (\alpha_s + \alpha_p)\beta^2 - \alpha_s\alpha_p\alpha_h \end{cases} \tag{2.141}$$

Putting:

$$\varepsilon = x - \frac{p}{3} \tag{2.142}$$

(Abramowitz and Stegun, 1965) gives the cubic equation in x:

$$\begin{cases} x^3 + ax + b = 0 \\ a = \frac{1}{3}(3q - p^2), \quad b = \frac{1}{27}(2p^3 - 9pq + 27r) \end{cases} \quad (2.143)$$

Since $\mathbf{H}$ is Hermitian, we must have:

$$\left(\frac{b^2}{4} + \frac{a^3}{27} \right) < 0 \quad (2.144)$$

with three different *real* roots, which are easily expressed in terms of the trigonometric relations:

$$\begin{cases} x_1 = 2\sqrt{-\frac{a}{3}} \cos\frac{\phi}{3} \\[2ex] x_2 = 2\sqrt{-\frac{a}{3}} \cos\left(\frac{\phi}{3} + 120°\right) \\[2ex] x_3 = 2\sqrt{-\frac{a}{3}} \cos\left(\frac{\phi}{3} - 120°\right) \end{cases} \quad (2.145)$$

with:

$$\cos\frac{\phi}{3} = -\frac{b}{2}\sqrt{-\frac{a^3}{27}} \quad (2.146)$$

Using one-term SCF/STO values for the fluorine atom (Clementi and Roetti, 1974):

$$\varepsilon_s \approx \alpha_s = -1.43\,E_h, \quad \varepsilon_p \approx \alpha_p = -0.53\,E_h, \quad \varepsilon_h = \alpha_h = -0.5\,E_h \quad (2.147)$$

the roots of the cubic secular equation will depend in a parametric way on the values given to $|\beta|$. Assuming:[19]

$$|\beta| = 0.114 E_h = 71.5\,\text{kcal mol}^{-1} \quad (2.148)$$

gives, in atomic units:

$$\varepsilon_1 = -0.3928\,E_h, \quad \varepsilon_2 = -1.4440\,E_h, \quad \varepsilon_3 = -0.6238\,E_h. \quad (2.149)$$

---

[19] This is roughly the value assumed by $|\beta|$ in the bond-orbital approximation.

The two lowest roots, as well as $\varepsilon_p \approx \alpha_p$ are in unexpected fair agreement with the negative of the ionization potentials observed from experimental UV photoelectron spectra of ground state HF (Lempka *et al.*, 1968; Potts and Price, 1972; Price, 1974):

$$\varepsilon_2 = \varepsilon(2s) = -1.433\, E_h, \quad \varepsilon_3 = \varepsilon(3s) = -0.702\, E_h,$$
$$\varepsilon_4 = \varepsilon(1\pi) = -0.588\, E_h. \tag{2.150}$$

Therefore, the bond dissociation energy resulting from the solution of the complete cubic Hückel equation for one-term SCF/STOs and $|\beta| = 0.114 E_h$ will be:

$$\begin{cases} \Delta E(HF,{}^1\Sigma^+) = E(HF,{}^1\Sigma^+) - 2\alpha_s - 5\alpha_p - \alpha_h \\ \qquad = 2\varepsilon(2\sigma) + 3\varepsilon(3\sigma) + 4\varepsilon(1\pi) - 2\alpha_s - 5\alpha_p - \alpha_h \quad (2.151) \\ \qquad = -0.245\, E_h \end{cases}$$

in complete agreement with the assumed spectroscopic value of $|D| = 0.245\, E_h$ (Huber and Herzberg, 1979).

However, if we attempt to extract, from the calculated MOs, information on the resulting *sp* hybrids on F, we are faced with the problem that such hybrids are not orthogonal and therefore not mutually exclusive, as already observed long ago by us (Magnasco and Perico, 1967, 1968) in obtaining *localized* MOs from ab initio results.

2.7.2.3   Introducing Hybridization into Σ Symmetry

We now make the orthogonal transformation **O** of the original basis to the hybridized basis (Magnasco, 2009b; Magnasco, 2009c):

$$(l\,b\,h) = (s\,z\,h)\begin{pmatrix} \cos\omega & \sin\omega & 0 \\ -\sin\omega & \cos\omega & 0 \\ 0 & 0 & 1 \end{pmatrix} \tag{2.152}$$

which corresponds to introducing the pair of *orthogonal* hybrids (Figure 2.15):

$$\begin{cases} l = s\cos\omega - z\sin\omega & \text{lone pair hybrid} \\ b = s\sin\omega + z\cos\omega & \text{bond hybrid} \end{cases} \tag{2.153}$$

where ω is the hybridization (mixing) parameter. Putting $\omega = 0$ gives the previous case of no hybridization.
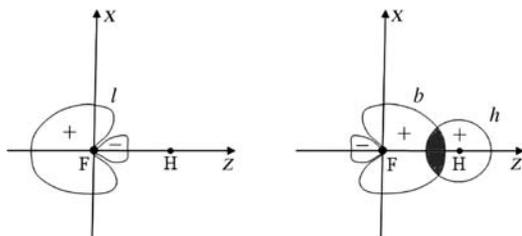
Figure 2.15   Orthogonal *sp* lone pair *l* (left) and bond hybrid *b* (right) engaged in the F–H bond[20]. Reprinted from Chemical Physics Letters, 477, Magnasco, V., *Hückel transformation theory of ground state HF*. 397–401, Copyright (2009), with permission from Elsevier

Elements of the transformed Hückel matrix are:

$$
\begin{cases}
\alpha_l = \alpha_s \cos^2\omega + \alpha_p \sin^2\omega \\[2mm]
\beta_{lb} = \dfrac{(\alpha_s - \alpha_p)}{2}\sin 2\omega \\[2mm]
\beta_{lh} = \beta(\cos\omega - \sin\omega) \\[2mm]
\alpha_b = \alpha_s \sin^2\omega + \alpha_p \cos^2\omega \\[2mm]
\beta_{bh} = \beta(\cos\omega + \sin\omega)
\end{cases}
\tag{2.154}
$$

Since the AOs of the hybridized basis are now properly directed along the *z* axis, we see that in the range $0 \leq \omega \leq 45°$ (namely, from pure *p* to equivalent digonal hybrids) β_{lh} decreases and β_{bh} increases from the value assumed for $\omega = 0$. The transformed Hückel matrix:

$$
\tilde{\mathbf{H}} = \tilde{\mathbf{O}} \mathbf{H} \mathbf{O} = \begin{pmatrix}
\alpha_l & \beta_{lb} & \beta_{lh} \\
\beta_{lb} & \alpha_b & \beta_{bh} \\
\beta_{lh} & \beta_{bh} & \alpha_h
\end{pmatrix}
\tag{2.155}
$$

therefore assumes a nearly block-diagonal form. We notice that the full cubic secular equation is *invariant* against the rotation yielding hybridization, so that the three roots are the same. If we put:

$$
\beta_{lb} = \beta_{lh} = 0
\tag{2.156}
$$

i.e. we neglect delocalization of the lone pair into the bond, this invariance is lost, and the resulting approximation is tantamount to assuming a bond orbital (BO) approach inside Hückel theory. Delocalization of the hybrid lone pair into the bond could eventually be treated as a small perturbative

---

[20] The shaded area on the right sketches the overlap region in the F–H bond orbital.

correction (Magnasco and Musso, 1981), as we did in the past in ab-initio investigations on torsional barriers in molecules (Musso and Magnasco, 1982).

The 3×3 Hückel secular equation in this approximation has the block-diagonal form:

$$\begin{vmatrix} \alpha_l & 0 & 0 \\ 0 & \alpha_b - \varepsilon & \beta_{bh} \\ 0 & \beta_{bh} & \alpha_h - \varepsilon \end{vmatrix} = 0 \tag{2.157}$$

giving the Hückel energy for the valence $l^2 \sigma^2 x^2 y^2$ electron configuration of ground state HF:

$$E(HF, \Sigma^+) = 2\alpha_l + 4\alpha_p + (\alpha_b + \alpha_h - \Delta) \tag{2.158}$$

with:

$$\Delta = [(\alpha_b - \alpha_h)^2 + 4\beta^2(1 + \sin 2\omega)]^{1/2} > 0 \tag{2.159}$$

The bond energy will now depend on ω:

$$\begin{cases} \Delta E(HF, {}^1\Sigma^+) = E(HF, {}^1\Sigma^+) - 2\alpha_s - 5\alpha_p - \alpha_h \\ = (\alpha_s - \alpha_p)(\cos^2 \omega - 1) - \Delta(\omega) = -|D| \end{cases} \tag{2.160}$$

The best value of ω can be determined by optimizing $\Delta E(\omega)$ with respect to ω, so that:

$$\frac{d\Delta E}{d\omega} = 0 \tag{2.161}$$

gives, as a necessary condition for stationarity of the energy against variations in ω, the complicated trigonometric equation:

$$\left(\frac{2|\beta|}{\alpha_s - \alpha_p} \cot 2\omega\right)^2 + 2\frac{\alpha_b - \alpha_h}{\alpha_s - \alpha_p} \cot 2\omega = 1 + \sin 2\omega \tag{2.162}$$

where:

$$\alpha_b - \alpha_h = (\alpha_s - \alpha_h) - (\alpha_s - \alpha_p)\cos^2 \omega \tag{2.163}$$

still depends on ω. Approximate solutions to this trigonometric equation can be obtained by successive approximations until the difference between the left- and right-hand sides becomes less than a predetermined threshold (say 10^{-3}). Using one-term SCF/STO values (Clementi and Roetti, 1974) for $\alpha_s, \alpha_p, \alpha_h$ and the experimental value for $|D|$, we find that

$\omega = 7.55°$ does satisfy the stationarity equation with an accuracy better than 1×10^{-5}. In the following, however, we shall content ourselves with the rounded value $\omega \approx 8°$, which means 2% mixing of s into the bond hybrid (98% p). In the range $7° \leq \omega \leq 8°$ $|\beta|$ has the practically constant value

$$|\beta| = 0.1142\, E_h = 71.7\,\text{kcal mol}^{-1}.$$

2.7.2.4 Charge Distribution in the Hybridized Basis

We now analyse the charge distribution in ground state HF resulting from the σ bond orbitals in the hybridized basis (Figure 2.15):

$$2\sigma \approx l = s\cos\omega - z\sin\omega \tag{2.164}$$

$$3\sigma \approx \frac{b + \lambda h}{\sqrt{\lambda^2 + 1}} = \frac{s\sin\omega + z\cos\omega + \lambda h}{\sqrt{\lambda^2 + 1}} \tag{2.165}$$

We have for the electron density (Magnasco, 2007, Magnasco, 2009a):

$$
\begin{cases}
P(\mathbf{r}) = 2[2\sigma(\mathbf{r})]^2 + 2[3\sigma(\mathbf{r})]^2 \\[6pt]
\quad = 2[s^2\cos^2\omega + z^2\sin^2\omega - sz\sin 2\omega \\[6pt]
\qquad + (\lambda^2 + 1)^{-1}(s^2\sin^2\omega + z^2\cos^2\omega + sz\sin 2\omega + \lambda^2 h^2)] \\[6pt]
\quad = s^2\left(2\cos^2\omega + \dfrac{2\sin^2\omega}{\lambda^2 + 1}\right) + z^2\left(2\sin^2\omega + \dfrac{2\cos^2\omega}{\lambda^2 + 1}\right) + h^2\left(\dfrac{2\lambda^2}{\lambda^2 + 1}\right) \\[12pt]
\quad + sz\left(-2\sin 2\omega\, \dfrac{\lambda^2}{\lambda^2 + 1}\right)
\end{cases}
$$

$$\tag{2.166}$$

where the first three terms contribute to the heteropolar dipole (μ_H), the last term being the contribution from the so called atomic dipole μ_A (Coulson, 1961). There is no contribution from the size effect (or homopolar) dipole moment, since we are neglecting explicit overlap between our AOs. Of course, the conservation relation holds:

$$\int \mathrm{d}\mathbf{r} P(\mathbf{r}) = 4 \tag{2.167}$$

We pass now to the calculation of the two components of the atomic dipole:

$$\begin{cases} \langle l|\mathbf{z}|l\rangle = -\sin2\omega\,(sz|\mathbf{z}) = -\sin2\omega \cdot \mu_a \\ \langle b|\mathbf{z}|b\rangle = \sin2\omega \cdot \mu_a \end{cases} \qquad (2.168)$$

where:

$$\mu_a = (sz|\mathbf{z}) \qquad (2.169)$$

is the atomic dipole along z. Using normalized one-term SCF/STOs with similar orbital exponents ($c_s \approx c_p = c \approx 2.55$) (Clementi and Roetti, 1974):

$$s = \left(\frac{c^5}{3\pi}\right)^{\frac{1}{2}}\exp(-cr)r \qquad\qquad z = \left(\frac{c^5}{\pi}\right)^{\frac{1}{2}}\exp(-cr)r\cos\theta \qquad (2.170)$$

we obtain:

$$\mu_a = \frac{5\sqrt{3}}{6}\frac{1}{c} = 0.57 \qquad (2.171)$$

a value which, as expected, is practically independent of s nonorthogonality[21].

Therefore, the contribution resulting from the atomic dipole will be:

$$\mu_A = -2\sin2\omega\,\frac{\lambda^2}{\lambda^2+1}\mu_a \qquad (2.172)$$

and we can express the experimental dipole moment μ as the *sum* of the two concurrent[22] contributions:

$$|\mu| = |\delta|R_e + |\mu_A| = -\frac{\lambda^2-1}{\lambda^2+1}R_e + 2\sin2\omega\,\frac{\lambda^2}{\lambda^2+1}\mu_a \qquad (2.173)$$

We obtain for λ^2:

$$\lambda^2 = \frac{R_e-|\mu|}{R_e + |\mu|-2\sin2\omega\,\mu_a} = 0.47 \qquad (2.174)$$

---

[21] Using $c_k = 8.65$, Schmidt orthogonalization of s against k with $S = 0.2326$ gives $\mu_a = 0.566$.
[22] The resulting atomic dipole μ_A is in the *same* sense as the heteropolar dipole $\mu_H(F^{-|\delta|}\,H^{+|\delta|})$.

for $\omega = 8°$. Hence, $\lambda = 0.685$ and:

$$|\delta| = \left|\frac{\lambda^2 - 1}{\lambda^2 + 1}\right| = 0.36 \qquad (2.175)$$

In this way, we see that little hybridization on F originates an atomic dipole ($|\mu_A| = 0.10 e a_0$) which reduces the formal charge $|\delta|$ by about 14%. This reduction is expected to be even larger with larger values of the hybridization parameter.

2.7.3 The Water Molecule

2.7.3.1 MO Description Without Hybridization

First, we recast in our notation a calculation originally done by Coulson (1961). With reference to Figures 2.16 and 2.17, we choose the molecule to lie in the yz plane. Nuclear symmetry (Magnasco, 2007, 2009a) shows that H_2O has C_{2v} symmetry, with two symmetry planes (yz and zx) whose intersection determines a C_2 binary axis directed along z. 2θ is the interbond (valence) angle.

In the simplest admissible physical description of H_2O *neglecting hybridization*, we concentrate attention on the four-electron valence problem involving $2p_z = z$, $2p_y = y$ AOs on the oxygen atom, $1s_1 = h_1$, $1s_2 = h_2$ AOs on the two hydrogen atoms, while $2s = s$ and $2p_x = x$ are doubly occupied AOs on oxygen making the two lone pairs. It
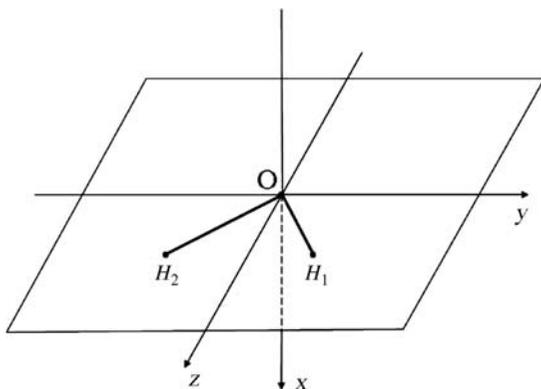
Figure 2.16   Reference coordinate system for H_2O (C_{2V} symmetry). The molecule lies in the yz plane with z the binary symmetry axis
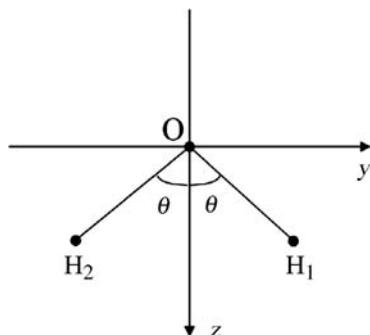
Figure 2.17 The H_2O molecule in the yz plane. 2θ is the interbond (valence) angle

is immediately evident that symmetry AOs[23] of C_{2v} symmetry are (Magnasco, 2009a):

$$
\begin{cases}
A_1 : z, h_z = \dfrac{1}{\sqrt{2}}(h_1 + h_2) \\[3mm]
B_2 : y, h_y = \dfrac{1}{\sqrt{2}}(h_1 - h_2)
\end{cases}
\tag{2.176}
$$

so that the normalized MOs[24] not interacting by symmetry are:

$$
a_1 = \frac{z + \lambda h_z}{\sqrt{1 + \lambda^2}}, \qquad b_2 = \frac{y + \mu h_y}{\sqrt{1 + \mu^2}}
\tag{2.177}
$$

The polarity parameters λ, μ and the orbital energies are found by solving the secular equations:

$$
\begin{vmatrix} H_{zz} - \varepsilon & H_{zh_z} \\ H_{zh_z} & H_{h_zh_z} - \varepsilon \end{vmatrix} = 0
\qquad
\begin{vmatrix} H_{yy} - \varepsilon & H_{yh_y} \\ H_{yh_y} & H_{h_yh_y} - \varepsilon \end{vmatrix} = 0
\tag{2.178}
$$

$$
\text{Symmetry } A_1 \qquad\qquad\qquad \text{Symmetry } B_2
$$

The matrix elements in the Hückel approximation are:

$$
\begin{cases}
H_{zz} = \alpha_p \\[2mm]
H_{zh_z} = \sqrt{2}\,\beta_{zh} \\[2mm]
H_{h_zh_z} = \alpha_h + \beta_{hh} \cong \alpha_h
\end{cases}
\tag{2.179}
$$

---

[23] The only AOs that can mix in the LCAO approximation.
[24] Neglecting overlap for brevity.

$$\begin{cases} H_{yy} = \alpha_p \\ H_{yh_y} = \sqrt{2}\beta_{yh} \\ H_{h_y h y} = \alpha_h + \beta_{hh} \cong \alpha_h \end{cases} \tag{2.180}$$

where β_{hh} is neglected in Equations (2.179) and (2.180) in the spirit of Hückel's assumptions.[25] Hence, we get the two secular equations:

$$\begin{vmatrix} \alpha_p - \varepsilon & \sqrt{2}\beta_{zh} \\ \sqrt{2}\beta_{zh} & \alpha_h - \varepsilon \end{vmatrix} = 0 \qquad \begin{vmatrix} \alpha_p - \varepsilon & \sqrt{2}\beta_{yh} \\ \sqrt{2}\beta_{yh} & \alpha_h - \varepsilon \end{vmatrix} = 0 \tag{2.181}$$

with the lowest roots:

$$\begin{cases} \varepsilon(A_1) = \dfrac{\alpha_p + \alpha_h}{2} - \dfrac{1}{2}[(\alpha_p - \alpha_h)^2 + 8\beta_{zh}^2]^{1/2} \\[4mm] \varepsilon(B_2) = \dfrac{\alpha_p + \alpha_h}{2} - \dfrac{1}{2}[(\alpha_p - \alpha_h)^2 + 8\beta_{yh}^2]^{1/2} \end{cases} \tag{2.182}$$

In the ground state, these roots correspond to energy levels doubly occupied by electrons, so we have the total Hückel energy:

$$\begin{cases} E = 2\displaystyle\sum_i^{occ} \varepsilon_i \\[4mm] \quad = 2(\alpha_p + \alpha_h) - [(\alpha_p - \alpha_h)^2 + 8\beta_{zh}^2]^{1/2} - [(\alpha_p - \alpha_h)^2 + 8\beta_{yh}^2]^{1/2} \end{cases} \tag{2.183}$$

Now, let σ be a $2p$ AO directed along the OH bond and π a $2p$ AO perpendicular to the bond. If θ is half the valence angle (Figure 2.17), we have:

$$\begin{cases} z = \sigma\cos\theta + \pi\sin\theta, \quad y = \sigma\sin\theta - \pi\cos\theta \\ \beta_{zh} = \beta_{\sigma h}\cos\theta, \qquad \beta_{yh} = \beta_{\sigma h}\sin\theta \end{cases} \tag{2.184}$$

where $\beta_{\sigma h} = \beta$ is a quantity characteristic of the OH bond, independent of the orientation. We then have for the bond energy:

$$\begin{cases} \Delta E(\theta) = -[(\alpha_p - \alpha_h)^2 + 8\beta^2\cos^2\theta]^{1/2} - [(\alpha_p - \alpha_h)^2 + 8\beta^2\sin^2\theta]^{1/2} \\ \qquad = -\Delta_1 - \Delta_2 \end{cases} \tag{2.185}$$

---

[25] H_1 and H_2 are nonadjacent atoms.

where we have put:

$$\begin{cases} \Delta_1 = [(\alpha_p - \alpha_h)^2 + 8\beta^2\cos^2\theta]^{1/2} > 0 \\ \Delta_2 = [(\alpha_p - \alpha_h)^2 + 8\beta^2\sin^2\theta]^{1/2} > 0 \end{cases} \qquad (2.186)$$

The necessary condition for the minimum of ΔE is then:

$$\frac{d\Delta E}{d\theta} = -\frac{d\Delta_1}{d\theta} - \frac{d\Delta_2}{d\theta} = 4\beta^2\frac{1}{\Delta_1}\sin 2\theta - 4\beta^2\frac{1}{\Delta_2}\sin 2\theta = 0 \qquad (2.187)$$

giving, after squaring both members,

$$\Delta_1^2 = \Delta_2^2 \Rightarrow \cos^2\theta = \sin^2\theta \Rightarrow \cos\theta = \sin\theta \Rightarrow 2\theta = 90° \qquad (2.188)$$

By evaluating the second derivative at the point $2\theta = 90°$, we find:

$$\begin{cases} \left(\frac{d^2\Delta E}{d\theta^2}\right)_{2\theta=90°} = \left[8\beta^2\cos 2\theta\left(\frac{1}{\Delta_1} - \frac{1}{\Delta_2}\right) + 16\beta^4(\sin 2\theta)^2\left(\frac{1}{\Delta_1^{\ 3}} + \frac{1}{\Delta_2^{\ 3}}\right)\right]_{2\theta=90°} \\ \qquad\qquad = 16\beta^4[(\alpha_p - \alpha_h)^2 + 4\beta^2]^{-3/2} > 0, \end{cases} \qquad (2.189)$$

so that we conclude that the Hückel bond energy in ground state H_2O has a true minimum[26] for $2\theta = 90°$.

2.7.3.2 Localized Description

The unnormalized bonding MOs (Equation 2.177) for H_2O:

$$\begin{cases} a_1 \approx z + \lambda(h_1 + h_2) \\ b_2 \approx y + \mu(h_1 - h_2) \end{cases} \qquad (2.190)$$

are *delocalized three-centre MOs* which describe the two OH bonds in the molecule, but bear no resemblance to bond functions. As already seen for the double bond, for the invariance of the MO description, we may replace symmetry MOs by their sum and difference without changing the physical description of the system. We have:

$$\begin{cases} a_1 + b_2 \propto z + y + (\lambda + \mu)h_1 + (\lambda - \mu)h_2 \\ a_1 - b_2 \propto z - y + (\lambda - \mu)h_1 + (\lambda + \mu)h_2 \end{cases} \qquad (2.191)$$

---

[26] Namely, a maximum of bond strength.
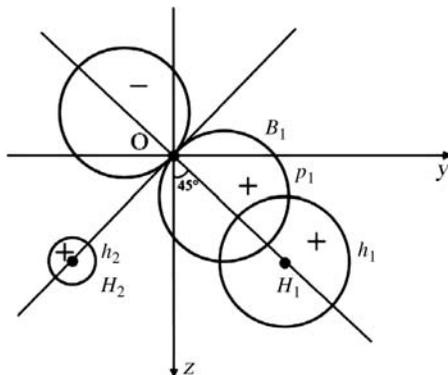
Figure 2.18 B_1 is a *localized* MO describing the OH_1 bond

namely:

$$\begin{cases} B_1 \propto \sqrt{2}p_1 + (\lambda+\mu)h_1 + (\lambda-\mu)h_2 \\ B_2 \propto \sqrt{2}p_2 + (\lambda-\mu)h_1 + (\lambda+\mu)h_2 \end{cases} \tag{2.192}$$

where:

$$p_1 = \frac{z+y}{\sqrt{2}}, \qquad p_2 = \frac{z-y}{\sqrt{2}} \tag{2.193}$$

Orbital p_1 is a $2p$ AO on oxygen making an angle of $45°$ with the z axis, p_2 a $2p$ AO on oxygen making an angle of $-45°$ with the z axis. Since now the coefficient of h_1 in B_1 is *large*, while that of h_2 is *small*,[27] B_1 describes a bond orbital essentially localized in the region of the $O-H_1$ bond (Figure 2.18), and similarly B_2, an equivalent bond orbital obtained from B_1 by rotation of $180°$ about the z symmetry axis.

2.7.3.3 Introducing Hybridization into A_1 Symmetry

Neglecting hybridization, as we did so far, the angle between p_1 and p_2 is $2\theta = 90°$, so that the resulting O–H bonds will be *bent outwards*, since the experimentally observed valence angle is about $2\theta = 105°$ (Herzberg, 1956). This is contrary to the principle of maximum overlap

---

[27] It would be zero for $\mu = \lambda$.

(Magnasco, 2005). If we choose p_1 and p_2 along the bonds, they will be no longer orthogonal, since:

$$\begin{cases} p_1 = z\cos\theta + y\sin\theta \\ p_2 = z\cos\theta - y\sin\theta \\ \langle p_1|p_2\rangle = \cos^2\theta - \sin^2\theta = \cos 2\theta \end{cases} \qquad (2.194)$$

where $\cos 2\theta = -0.25882$. However, we can restore orthogonality between the AOs on oxygen by mixing in a certain amount of $2s(=s)$ with the two $2p$ AOs, obtaining in this way *three sp^2 hybrids of C_{2v} symmetry*, directed along two equivalent O–H bonds and on the rear of the molecule in a direction bisecting the valence angle. It is easily shown that these hybrids are (Figure 2.19):

$$\begin{cases} hy_1 = 0.4534s + 0.5426z + 0.7071y \\ hy_2 = 0.4534s + 0.5426z - 0.7071y \\ hy_3 = 0.7673s - 0.6412z \end{cases} \qquad (2.195)$$

The three hybrids (Equations (2.195) allow: (i) for an interbond angle greater than $90°(\cos 2\theta < 0)$, preserving orthogonality onto the same atom; and (ii) for orbitals directed along the bonds, satisfying in this way the principle of maximum overlap and giving stronger *straight* bonds. Details of the calculation are given elsewhere (Magnasco, 2007).
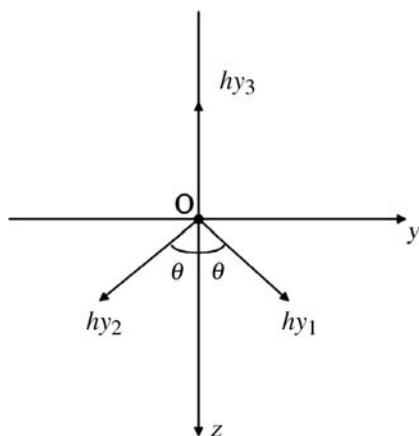
Figure 2.19   The three sp^2 hybrids in H_2O equivalent under C_{2V} symmetry

The s and p contents in the hybrids are simply obtained from the square of the respective coefficients in Equations (2.195), so that:

$$\begin{cases} 20.6\%\, s & 79.4\%\, p & \text{for hybrids engaged in the O} - \text{H bonds} \\ 58.8\%\, s & 41.2\%\, p & \text{for the hybrid lone pair} \end{cases}$$

$$(2.196)$$

This picture is close to Klessinger (1965) result obtained from *ab initio* SCF calculations using one-term STOs with orbital exponents $c_s = 2.2458$, $c_p = 2.2266$, and $c_h = 1.3$ (case III in Klessinger, 1965).

We now extend Coulson's calculation, introducing a Hückel transformation theory which transforms the $(s\, z)$ oxygen valence AOs belonging to A_1 symmetry to an ω-hybridized $(b\, l)$ set, where ω is the hybridization parameter, b the bond hybrid directed along the positive z axis, and l the lone pair hybrid directed along the negative z axis (Magnasco, 2009b). This will give an alternative derivation of hybrids (Equations (2.195).

If we allow for sp mixing onto oxygen, the Hückel matrix for the $(s\, z\, h_z)$ basis of A_1 symmetry becomes:

$$\mathbf{H} = \begin{pmatrix} \alpha_s & 0 & \sqrt{2}\beta_{sh} \\ 0 & \alpha_p & \sqrt{2}\beta_{\sigma h}\cos\theta \\ \sqrt{2}\beta_{sh} & \sqrt{2}\beta_{\sigma h}\cos\theta & \alpha_h \end{pmatrix} \qquad (2.197)$$

giving a 3×3 secular equation whose analytic solution is difficult and, what is worse, not suited for doing any useful approximation on its elements.

To proceed further, we make the orthogonal transformation $\mathbf{O}$ to the hybridized basis:

$$(l\, b\, h_z) = (s\, z\, h_z) \begin{pmatrix} \cos\omega & \sin\omega & 0 \\ -\sin\omega & \cos\omega & 0 \\ 0 & 0 & 1 \end{pmatrix} \qquad (2.198)$$

which corresponds to introducing the orthonormal hybrids (Figure 2.20):

$$\begin{cases} b = s\sin\omega + z\cos\omega & \text{bond hybrid} \\ l = s\cos\omega - z\sin\omega & \text{lone pair hybrid} \end{cases} \qquad (2.199)$$

where ω is the hybridization parameter. Putting $\omega = 0$ gives the previous case of no hybridization.

For the transformed Hückel matrix:

$$\mathbf{H}' = \tilde{\mathbf{O}}\mathbf{H}\mathbf{O} \qquad (2.200)$$
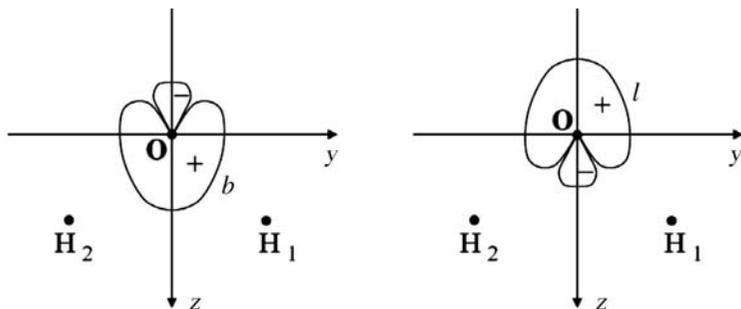
Figure 2.20 *sp* hybrids on oxygen resulting from the orthogonal transformation **O** of the original basis set of A_1 symmetry. Left, bond hybrid; right, lone pair hybrid. Reprinted from Chemical Physics Letters, 474, Magnasco, V., *On the hybridization problem in H₂O by Hückel transformation theory*. 212–216, Copyright (2009), with permission from Elsevier

where $\tilde{O}$ is the transpose of **O**, matrix elements are:

$$\begin{cases} \alpha_l = \alpha_s \cos^2\omega + \alpha_p \sin^2\omega \\ \beta_{lb} = (\alpha_s - \alpha_p)\sin\omega \cos\omega \\ \beta_{lh} = \sqrt{2}(\beta_{sh}\cos\omega - \beta_{\sigma h}\sin\omega \cos\theta) \\ \alpha_b = \alpha_s \sin^2\omega + \alpha_p \cos^2\omega \\ \beta_{bh} = \sqrt{2}(\beta_{sh}\sin\omega + \beta_{\sigma h}\cos\omega \cos\theta) \\ \alpha_h \end{cases} \quad (2.201)$$

giving the 3×3 transformed secular equation:

$$\begin{vmatrix} \alpha_l - \varepsilon & \beta_{lb} & \beta_{lh} \\ \beta_{lb} & \alpha_b - \varepsilon & \beta_{bh} \\ \beta_{lh} & \beta_{bh} & \alpha_h - \varepsilon \end{vmatrix} = 0. \quad (2.202)$$

If we make again the reasonable assumption that β_{lb} and β_{lh} are *small* compared with β_{bh} (Figure 2.20), matrix **H′** becomes nearly block-diagonal and, putting:

$$\beta_{lb} = \beta_{lh} = 0 \quad (2.203)$$

is tantamount to assuming a bond orbital (BO) model within Hückel theory. We then get the approximate roots belonging to A_1 symmetry:

$$\begin{cases} \varepsilon_1 = \alpha_l \qquad\qquad \varepsilon_2 = \dfrac{\alpha_b + \alpha_h}{2} - \dfrac{\Delta_2}{2} \qquad\qquad \varepsilon_3 = \dfrac{\alpha_b + \alpha_h}{2} + \dfrac{\Delta_2}{2} \\ \Delta_2 = [(\alpha_b - \alpha_h)^2 + 8(\beta_{sh}\sin\omega + \beta_{\sigma h}\cos\omega \cos\theta)^2]^{1/2} > 0 \end{cases}$$

$$(2.204)$$

So, the Hückel energy for the valence configuration $2a_1{}^2 3a_1{}^2 1b_2{}^2 1b_1{}^2$ of the $^1A_1$ ground state H_2O will be:

$$
\begin{cases}
E(\theta) = 2\varepsilon_1(A_1) + 2\varepsilon_2(A_1) + 2\varepsilon_1(B_2) + 2\varepsilon_1(B_1) \\[2mm]
\quad = 2(\alpha_s \cos^2\omega + \alpha_p \sin^2\omega) + (\alpha_s \sin^2\omega + \alpha_p \cos^2\omega) + 3\alpha_p + 2\alpha_H \\[2mm]
\quad - [(\alpha_b - \alpha_h)^2 + 8(\beta_{sh}\sin\omega + \beta_{\sigma h}\cos\omega\cos\theta)^2]^{1/2} \\[2mm]
\quad - [(\alpha_p - \alpha_h)^2 + 8\beta_{\sigma h}^2 \sin^2\theta]^{1/2} \\[2mm]
\quad = E^{val}(O) + 2E(H) - \Delta_2 - \Delta_3
\end{cases}
$$

$$(2.205)$$

The calculation of the first and second derivatives of $E(\theta)$ vs θ (ω considered as a parameter) gives:

$$
\begin{cases}
\dfrac{\mathrm{d}E}{\mathrm{d}\theta} = -\dfrac{\mathrm{d}\Delta_2}{\mathrm{d}\theta} - \dfrac{\mathrm{d}\Delta_3}{\mathrm{d}\theta} \\[3mm]
\quad = \dfrac{4}{\Delta_2}(\beta_{sh}\beta_{\sigma h}\sin 2\omega \sin\theta + \beta_{\sigma h}^2 \cos^2\omega \sin 2\theta) - \dfrac{4}{\Delta_3}\beta_{\sigma h}^2 \sin 2\theta
\end{cases}
$$

$$(2.206)$$

$$
\begin{cases}
\dfrac{\mathrm{d}^2 E}{\mathrm{d}\theta^2} = -\dfrac{\mathrm{d}^2\Delta_2}{\mathrm{d}\theta^2} - \dfrac{\mathrm{d}^2\Delta_3}{\mathrm{d}\theta^2} \\[3mm]
\quad = \dfrac{4}{\Delta_2}(\beta_{sh}\beta_{\sigma h}\sin 2\omega \cos\theta + 2\beta_{\sigma h}^2 \cos^2\omega \cos 2\theta) \\[3mm]
\quad + \dfrac{16}{\Delta_2{}^3}(\beta_{sh}\beta_{\sigma h}\sin 2\omega \sin\theta + \beta_{\sigma h}^2 \cos^2\omega \sin 2\theta)^2 \\[3mm]
\quad - \dfrac{8}{\Delta_3}\beta_{\sigma h}^2 \cos 2\theta + \dfrac{16}{\Delta_3^3}\beta_{\sigma h}^4(\sin 2\theta)^2
\end{cases}
$$

$$(2.207)$$

The stationarity condition for $E(\theta)$ with respect to θ gives a quartic equation in $\cos\theta = x$, whose coefficients depend in a rather complicated way on the actual values assumed by β_{sh}, $\beta_{\sigma h}$, $\alpha_b - \alpha_h$, $\alpha_p - \alpha_h$ and ω:

$$P_4(x) = Ax^4 + Bx^3 + Cx^2 + Dx + E = 0 \qquad (2.208)$$

with:

$$\begin{cases} A = 32\,\beta_{\sigma h}^4 \cos^2\omega\,(\cos^2\omega+1) \\ B = 32\,\beta_{sh}\beta_{\sigma h}^3 \sin2\omega\,(\cos^2\omega+1) \\ C = 4\,\beta_{\sigma h}^2\,\{(\alpha_b-\alpha_h)^2 + 2\beta_{sh}^2[(\sin2\omega)^2 + 4\sin^2\omega] \\ \qquad -\cos^4\omega\,[(\alpha_p-\alpha_h)^2 + 8\beta_{\sigma h}^2]\} \\ D = -4\beta_{sh}\beta_{\sigma h}\sin2\omega\cos^2\omega\,[(\alpha_p-\alpha_h)^2 + 8\beta_{\sigma h}^2] \\ E = -\beta_{sh}^2(\sin2\omega)^2\,[(\alpha_p-\alpha_h)^2 + 8\beta_{\sigma h}^2] \end{cases} \quad (2.209)$$

Putting $\beta_{sh} = \beta_{\sigma h} = \beta$ in the spirit of Hückel theory, the coefficients become, after dividing by β^2:

$$\begin{cases} A = 32\,\beta^2\cos^2\omega\,(\cos^2\omega+1) \\ B = 32\,\beta^2\sin2\omega\,(\cos^2\omega+1) \\ C = 4\,\{(\alpha_b-\alpha_h)^2 + 2\,\beta^2[(\sin2\omega)^2 + 4\sin^2\omega] - \cos^4\omega[(\alpha_p-\alpha_h)^2 + 8\beta^2]\} \\ D = -4\sin2\omega\cos^2\omega[(\alpha_p-\alpha_h)^2 + 8\beta^2] \\ E = -(\sin2\omega)^2[(\alpha_p-\alpha_h)^2 + 8\beta^2] \end{cases}$$

$$(2.210)$$

Two special cases can be immediately analysed.

(i) For $\omega = 0$ (no hybridization), $\alpha_b-\alpha_h = \alpha_p-\alpha_h$, coefficients B, D, E vanish, $A = 64\beta^2$, $C = -32\,\beta^2$, and Equation (2.208) gives:

$$2x^2 = 1, \qquad x = \cos\theta = \frac{1}{\sqrt{2}} \Rightarrow \theta = 45° \qquad (2.211)$$

as it must be.

(ii) If we put:

$$\alpha_b-\alpha_h = \alpha_p-\alpha_h = 0, \qquad (2.212)$$

(which is tantamount to assuming nonpolar bonds) dividing throughout by $8\beta^2$, the coefficients will depend only on ω:

$$\begin{cases} A = 4\cos^2\omega(\cos^2\omega+1) \\ B = 4\sin2\omega(\cos^2\omega+1) \\ C = (\sin2\omega)^2 + 4\sin^2\omega - 4\cos^4\omega \\ D = -4\sin2\omega\cos^2\omega \\ E = -(\sin2\omega)^2 \end{cases} \quad (2.213)$$

A root of the quartic equation (2.208) is given in this case by the simple trigonometric relation:

$$\cot\theta = \cos\omega \tag{2.214}$$

provided $\theta > 45°$. This shows that for $\omega \neq 0$ *the interbond angle resulting from energy optimization opens beyond 90°*.

In fact, in this case, we have ($x = \cos\theta$):

$$\cos^2\omega = \frac{x^2}{1-x^2}, \quad \sin^2\omega = \frac{1-2x^2}{1-x^2}, \quad \sin2\omega = \frac{2\sqrt{x^2-2x^4}}{1-x^2} \tag{2.215}$$

and the coefficients become:

$$\begin{cases} A = \dfrac{4x^2}{(1-x^2)^2} \\[3mm] B = 8\dfrac{\sqrt{x^2-2x^4}}{(1-x^2)^2} \\[3mm] C = 4\dfrac{1-2x^2-x^4}{(1-x^2)^2} \\[3mm] D = -8\dfrac{x^2\sqrt{x^2-2x^4}}{(1-x^2)^2} \\[3mm] E = -4\dfrac{x^2-2x^4}{(1-x^2)^2} \end{cases} \tag{2.216}$$

giving, upon substitution in Equation (2.208):

$$\begin{cases} P_4(x) = Ax^4 + Bx^3 + Cx^2 + Dx + E \\[2mm] \quad = \dfrac{4x^6 + 8x^3\sqrt{x^2-2x^4} + 4x^2 - 8x^4 - 4x^6 - 8x^3\sqrt{x^2-2x^4} - 4x^2 + 8x^4}{(1-x^2)^2} = 0 \end{cases} \tag{2.217}$$

so that $\cot\theta = \cos\omega$ is a solution satisfying the quartic equation.

We now construct two sp^2 hybrids b_1 and b_2 directed towards the H atoms simply by doing the further orthogonal transformation of the functions b (belonging to A_1 symmetry) and y (belonging to B_2 symmetry):
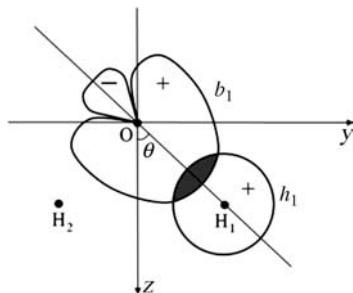
Figure 2.21 Orthogonal sp^2b_1 bond hybrid of C_{2v} symmetry on oxygen overlapping (shaded area) the h_1 orbital at $\theta = 52.5°$ to give a straight O–H bond in H_2O[28]. Reprinted from Chemical Physics Letters, 474, Magnasco, V., *On the hybridization problem in H₂O by Hückel transformation theory*. 212–216, Copyright (2009), with permission from Elsevier

$$(b_1\, b_2) = (b\, y)\begin{pmatrix} \dfrac{1}{\sqrt{2}} & \dfrac{1}{\sqrt{2}} \\[2mm] \dfrac{1}{\sqrt{2}} & -\dfrac{1}{\sqrt{2}} \end{pmatrix} \tag{2.218}$$

obtaining in this way the three orthonormal sp^2 hybrids of C_{2v} symmetry:

$$\begin{cases} b_1 = \dfrac{b+y}{\sqrt{2}} = \dfrac{1}{\sqrt{2}}(s\sin\omega + z\cos\omega + y) \\[3mm] b_2 = \dfrac{b-y}{\sqrt{2}} = \dfrac{1}{\sqrt{2}}(s\sin\omega + z\cos\omega - y) \\[3mm] l = s\cos\omega - z\sin\omega \end{cases} \tag{2.219}$$

The hybridization parameter ω, arbitrary so far, is best chosen so as the bond hybrids b_1 and b_2 point in the direction of the two O–H bonds, giving in this way strongest bonding with H $1s$ orbitals and satisfying the principle of maximum overlap. According to Equation (2.214), $2\theta = 105°$ gives $\omega \approx 40°$, and we obtain the set (Figure 2.21):

$$\begin{cases} b_1 = 0.45\,34\,36\,s + 0.54\,25\,82\,z + 0.70\,71\,06\,y = hy_1 \\[2mm] b_2 = 0.45\,34\,36\,s + 0.54\,25\,82\,z - 0.70\,71\,06\,y = hy_2 \\[2mm] l = 0.76\,73\,27\,s - 0.64\,12\,55\,z = hy_3 \end{cases} \tag{2.220}$$

---

[28] The equivalent b₂ bond hybrid is obtained by reflection of b_1 across the zx plane.

which coincides with the set of the three orthogonal sp^2 hybrids on oxygen, equivalent under C_{2v} symmetry, derived by McWeeny (1979) under the requirement of equivalence, normality and orthogonality, and given in Equations (2.195).

Consideration of the second derivative (Equation 2.207) for $\beta_{sh} = \beta_{oh} = \beta$ shows that it is *positive* for $\omega = 40°$, $2\theta = 105°$ (Section 2.9.1), so that we can conclude that, under our assumptions, sp hybridization opens the interbond angle beyond $90°$, giving hybrids which locally minimize the Hückel model energy for the valence electron configuration of ground state H_2O, and which can be chosen to give straight bonds satisfying the principle of maximum overlap.

It can be further shown (Section 2.9.2) that the trigonometric relation (Equation 2.214) is equivalent to Coulson's hybridization condition (Coulson, 1961; Magnasco, 2007) provided the lone pair hybrid $l = hy_3$ is Schmidt-orthogonalized against the bond hybrids $b_1 = hy_1$ and $b_2 = hy_2$ directed towards the hydrogen atoms H_1 and H_2.

Finally, we recall that the detailed calculations on ground state HF (Part 4 of Section 2.7.2) show that hybridization acts in the sense of reducing the main factor determining the polarity of the O−H bond. In terms of the O−H bond moment μ_{OH}, we may say that hybridization introduces a large *atomic* dipole (Coulson, 1961) reducing the heteropolar $O^{-\delta}H^{+\delta}$ component, so justifying our assumption (2.212).

An equivalent description of H_2O as a *distorted* tetrahedron of C_{2v} symmetry (two equivalent O−H bonds and two equivalent lone pairs lying in orthogonal yz and zx planes) (Torkington, 1951) can be obtained by doing a further orthogonal transformation of l and x lone pairs on oxygen, without changing our description of bonding in the water molecule.

This Hückel transformation method will now be applied in detail to the ground state of the NH_3 molecule (Magnasco, 2009c).

2.7.4   The Ammonia Molecule

2.7.4.1   MO Description Without Hybridization

The pyramidal ammonia molecule of C_{3v} symmetry has an experimental interbond angle of $2\theta \approx 107°$ (Herzberg, 1956). Its geometry is depicted in Figure 2.22. It is convenient to work in terms of the angle γ that each NH bond makes with the z symmetry axis, whose value is related to half the valence angle θ by the relation:
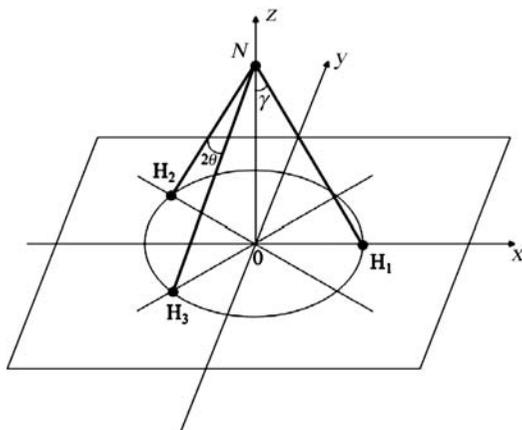
Figure 2.22 Geometry of the pyramidal NH_3 molecule of C_{3v} symmetry. Reprinted from Chemical Physics Letters, 477, Magnasco, V., *Hückel transformation theory of the hybridization problem in NH_3*. 392–396, Copyright (2009), with permission from Elsevier

$$\sin\gamma = \frac{2}{\sqrt{3}}\sin\theta \qquad (2.221)$$

Using the usual self-explanatory notation for the seven valence AOs, we call s, x, y, z the $2s$ and $2p$ orbitals on N, and h_1, h_2, h_3 the $1s$ orbitals on the H atoms (H_1 on the positive x axis).

Leaving out s for the moment, the AOs belonging to C_{3v} symmetry are (Magnasco, 2009a):

$$\begin{cases} A_1 : z, h_z = \dfrac{1}{\sqrt{3}}(h_1 + h_2 + h_3) \\[2ex] E_x : x, h_x = \dfrac{1}{\sqrt{6}}(2h_1 - h_2 - h_3) \\[2ex] E_y : y, h_y = \dfrac{1}{\sqrt{2}}(h_2 - h_3) \end{cases} \qquad (2.222)$$

so that the 6×6 Hückel secular equation can be factorized into the three 2×2 equations:

$$\begin{vmatrix} H_{zz} - \varepsilon & H_{zh_z} \\ H_{zh_z} & H_{h_z h_z} - \varepsilon \end{vmatrix} = 0 \quad \begin{vmatrix} H_{xx} - \varepsilon & H_{xh_x} \\ H_{xh_x} & H_{h_x h_x} - \varepsilon \end{vmatrix} = 0 \quad \begin{vmatrix} H_{yy} - \varepsilon & H_{yh_y} \\ H_{yh_y} & H_{h_y h_y} - \varepsilon \end{vmatrix} = 0$$

$$\text{Symmetry } A_1 \qquad\qquad \text{Symmetry } E_x \qquad\qquad\qquad \text{Symmetry } E_y$$

$$(2.223)$$

The Hückel matrix elements are:

$$\begin{cases} H_{zz} = \alpha_p \\ H_{zh_z} = -\sqrt{3}\beta_{\sigma h}\cos\gamma \\ H_{h_z h_z} = \alpha_h + 2\beta_{hh} \approx \alpha_h \end{cases} \qquad (2.224)$$

$$\begin{cases} H_{xx} = \alpha_p \\ H_{yh_y} = \dfrac{\sqrt{3}}{\sqrt{2}}\beta_{\sigma h}\sin\gamma \\ H_{h_x h_x} = \alpha_h - \beta_{hh} \approx \alpha_h \end{cases} \qquad (2.225)$$

$$\begin{cases} H_{yy} = \alpha_p \\ H_{yh_y} = \dfrac{\sqrt{3}}{\sqrt{2}}\,\beta_{\sigma h}\sin\gamma \\ H_{h_y h_y} = \alpha_h - \beta_{hh} \approx \alpha_h \end{cases} \qquad (2.226)$$

where β_{hh} is neglected as usual in Hückel theory.[29]

The three lowest roots of the secular equations give the Hückel energy of the $3a_1^2 1e_x^2 1e_y^2$ valence electron configuration of NH_3 as a function of angle γ:

$$\begin{cases} E(\gamma) = 2\varepsilon_1(A_1) + 2\varepsilon_1(E_x) + 2\varepsilon_1(E_y) \\ = 3\alpha_p + 3\alpha_h - \Delta_1 - 2\Delta_3 \end{cases} \qquad (2.227)$$

where:

$$\begin{cases} \Delta_1(\gamma) = [(\alpha_p - \alpha_h)^2 + 4H_{zh_z}^2]^{1/2} = [(\alpha_p - \alpha_h)^2 + 12\beta_{\sigma h}^2 \cos^2\gamma]^{1/2} > 0 \\ \Delta_3(\gamma) = [(\alpha_p - \alpha_h)^2 + 4H_{xh_x}^2]^{1/2} = [(\alpha_p - \alpha_h)^2 + 6\beta_{\sigma h}^2 \sin^2\gamma]^{1/2} > 0 \end{cases} \qquad (2.228)$$

Taking the first γ-derivatives of the Δs, the stationarity condition for the energy is:

$$\frac{dE}{d\gamma} = -\frac{d\Delta_1}{d\gamma} - 2\frac{d\Delta_3}{d\gamma} = 6\beta_{\sigma h}^2 \sin 2\gamma \left(\frac{1}{\Delta_1} - \frac{1}{\Delta_3}\right) = 0 \qquad (2.229)$$

---

[29] In the second of Equations (2.224) the minus sign accounts for the need of positive overlap between the z AO of nitrogen and the symmetrical sum h_z of hydrogen AOs.

giving:

$$\begin{cases} \Delta_3 = \Delta_1 \qquad \Delta_3^2 = \Delta_1^2 \\[2mm] \sin^2\gamma = 2\cos^2\gamma \qquad 3\sin^2\gamma = 2 \qquad \sin\gamma = \dfrac{\sqrt{2}}{\sqrt{3}} \Rightarrow \gamma = 54.74° \\[3mm] \sin\theta = \dfrac{\sqrt{3}}{2}\dfrac{\sqrt{2}}{\sqrt{3}} = \dfrac{1}{\sqrt{2}} \Rightarrow \theta = 45° \end{cases} \qquad (2.230)$$

so that we obtain a true minimum for $2\theta = 90°$, since the second derivative is positive there:

$$\left(\frac{d^2E}{d\gamma^2}\right)_{\theta=45°} = 48\,\beta_{\sigma h}^4[(\alpha_p - \alpha_h)^2 + 4\beta_{\sigma h}^2]^{-3/2} > 0 \qquad (2.231)$$

This is what we expect in absence of hybridization, the resulting N−H bonds being strongly bent outwards, and so very far from the principle of maximum overlap.

2.7.4.2   Introducing Hybridization into A_1 Symmetry

If we allow for sp mixing on nitrogen, the Hückel matrix for the $(s\,z\,h_z)$ basis of A_1 symmetry becomes:

$$\mathbf{H} = \begin{pmatrix} \alpha_s & 0 & \sqrt{3}\,\beta_{sh} \\ 0 & \alpha_p & -\sqrt{3}\,\beta_{\sigma h}\cos\gamma \\ \sqrt{3}\,\beta_{sh} & -\sqrt{3}\,\beta_{\sigma h}\cos\gamma & \alpha_h \end{pmatrix} \qquad (2.232)$$

giving a 3×3 secular equation whose solution is suitable only for numerical calculations (compare the previous case of HF).

We now make the orthogonal transformation $\mathbf{O}$ of the original basis to the hybridized basis:

$$(l\,b\,h_z) = (s\,z\,h_z) \begin{pmatrix} \cos\omega & \sin\omega & 0 \\ \sin\omega & -\cos\omega & 0 \\ 0 & 0 & 1 \end{pmatrix} \qquad (2.233)$$
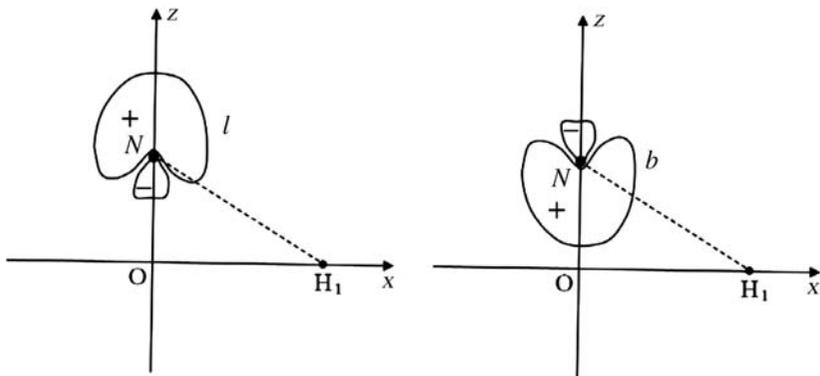
Figure 2.23 *sp* hybrids on nitrogen resulting from the orthogonal transformation O of the original basis set of A_1 symmetry. Left, lone pair hybrid *l*; right, bond hybrid *b*. Reprinted from Chemical Physics Letters, 477, Magnasco, V., *Hückel transformation theory of the hybridization problem in NH₃*. 392–396, Copyright (2009), with permission from Elsevier

which corresponds to introducing the orthonormal hybrids (Figure 2.23):

$$(l\ b\ h_z) = (s\ z\ h_z)\begin{pmatrix} \cos\omega & \sin\omega & 0 \\ \sin\omega & -\cos\omega & 0 \\ 0 & 0 & 1 \end{pmatrix} \quad (2.234)$$

where ω is the hybridization parameter. Putting $\omega = 0$ gives the previous case of no hybridization.

The transformed Hückel matrix has elements:

$$\begin{cases} \alpha_l = \alpha_s\cos^2\omega + \alpha_p\sin^2\omega \\ \beta_{lb} = \dfrac{\alpha_s - \alpha_p}{2}\sin 2\omega \\ \beta_{lh} = \sqrt{3}(\beta_{sh}\cos\omega - \beta_{\sigma h}\sin\omega\cos\gamma) \\ \alpha_b = \alpha_s\sin^2\omega + \alpha_p\cos^2\omega \\ \beta_{bh} = \sqrt{3}(\beta_{sh}\sin\omega + \beta_{\sigma h}\cos\omega\cos\gamma) \\ \alpha_h \end{cases} \quad (2.235)$$

giving the 3×3 transformed secular equation:

$$\begin{vmatrix} \alpha_l - \varepsilon & \beta_{lb} & \beta_{lh} \\ \beta_{lb} & \alpha_b - \varepsilon & \beta_{bh} \\ \beta_{lh} & \beta_{bh} & \alpha_h - \varepsilon \end{vmatrix} = 0 \quad (2.236)$$

Making the reasonable assumption that β_{lb} and β_{lh} are *small* compared with β_{bh}, the transformed matrix becomes nearly block-diagonal and, putting:

$$\beta_{lb} = \beta_{lh} = 0 \qquad (2.237)$$

we get the approximate roots belonging to A_1 symmetry:

$$\begin{cases} \varepsilon_1(A_1) = \alpha_l \quad \varepsilon_2(A_1) = \dfrac{\alpha_b + \alpha_h}{2} - \dfrac{\Delta_2}{2} \quad \varepsilon_3(A_1) = \dfrac{\alpha_b + \alpha_h}{2} + \dfrac{\Delta_2}{2} \\[2mm] \Delta_2(A_1) = [(\alpha_b - \alpha_h)^2 + 12(\beta_{sh}\sin\omega + \beta_{\sigma h}\cos\omega\cos\gamma)^2]^{1/2} \end{cases}$$
$$(2.238)$$

So, the Hückel energy for the valence configuration $2a_1^2 3a_1^2 1e_x^2 1e_y^2$ of the A_1 ground state of NH_3 will be:

$$\begin{cases} E(\gamma) = 2\varepsilon_1(A_1) + 2\varepsilon_2(A_1) + 2\varepsilon_1(E_x) + 2\varepsilon_1(E_y) \\[2mm] \qquad = 2(\alpha_s\cos^2\omega + \alpha_p\sin^2\omega) + (\alpha_s\sin^2\omega + \alpha_p\cos^2\omega) + \alpha_h + 2(\alpha_p + \alpha_h) \\[2mm] \qquad\quad -\Delta_2(A_1) - \Delta_3(E_x) - \Delta_3(E_y) \\[2mm] \qquad = E^{\mathrm{val}}(N) + 3E(H) - \Delta_2 - 2\Delta_3 \end{cases}$$
$$(2.239)$$

where Δ_2 is defined in Equation (2.238) and Δ_3 in Equation (2.228).

The calculation of the first and second derivatives of Δ_2 with respect to γ (ω considered as a parameter) gives:

$$\begin{cases} \dfrac{d\Delta_2}{d\gamma} = -\dfrac{6}{\Delta_2}(\beta_{sh}\beta_{\sigma h}\sin 2\omega\sin\gamma + \beta_{\sigma h}^2\cos^2\omega\sin 2\gamma) \\[4mm] \dfrac{d^2\Delta_2}{d\gamma^2} = -\dfrac{6}{\Delta_2}(\beta_{sh}\beta_{\sigma h}\sin 2\omega\cos\gamma + 2\beta_{\sigma h}^2\cos^2\omega\cos 2\gamma) \\[4mm] \qquad\qquad -\dfrac{36}{\Delta_2}(\beta_{sh}\beta_{\sigma h}\sin 2\omega\sin\gamma + \beta_{\sigma h}^2\cos^2\omega\sin 2\gamma)^2 \end{cases} \quad (2.240)$$

The stationarity condition for $E(\gamma)$ with respect to γ now gives a quartic equation in $\cos\gamma = x$, with coefficients which depend on the actual values assumed by β_{sh}, $\beta_{\sigma h}$, $\alpha_b - \alpha_h$, $\alpha_p - \alpha_h$ and ω:

$$P_4(x) = Ax^4 + Bx^3 + Cx^2 + Dx + E = 0 \qquad (2.241)$$

If, in the spirit of Hückel theory, we put $\beta_{sh} = \beta_{oh} = \beta$, a parameter characteristic of the N–H bond, the coefficients become after dividing by β^2:

$$
\begin{cases}
A = 24\,\beta^2 \cos^2\omega\,(\cos^2\omega + 2) \\[2mm]
B = 24\,\beta^2 \sin 2\,\omega\,(\cos^2\omega + 2) \\[2mm]
C = 4\left\{ (\alpha_b - \alpha_h)^2 + 3\,\beta^2 \left[\dfrac{1}{2}(\sin 2\,\omega)^2 + 4\sin^2\omega \right] - \cos^4\omega \left[(\alpha_p - \alpha_h)^2 + 6\,\beta^2 \right] \right\} \\[2mm]
D = -4\sin 2\,\omega \cos^2\omega\,[(\alpha_p - \alpha_h)^2 + 6\,\beta^2] \\[2mm]
E = -(\sin 2\,\omega)^2\,[(\alpha_p - \alpha_h)^2 + 6\,\beta^2].
\end{cases}
\tag{2.242}
$$

As before, we now examine the following two particular cases.

(i) For $\omega = 0$ (no hybridization), $\alpha_b - \alpha_h = \alpha_p - \alpha_h$, coefficients B, D, E vanish, $A = 72\,\beta^2$, $C = -24\,\beta^2$, and Equation (2.241) gives:

$$
\begin{cases}
3x^2 = 1, \quad x = \cos\gamma = \dfrac{1}{\sqrt{3}} \Rightarrow \gamma = 54.74° \\[3mm]
\sin\gamma = \dfrac{2}{\sqrt{3}}\sin\theta = \dfrac{\sqrt{2}}{\sqrt{3}} \Rightarrow \sin\theta = \dfrac{1}{\sqrt{2}} \Rightarrow 2\theta = 90°
\end{cases}
\tag{2.243}
$$

as it must be.

(ii) If we put:

$$
\alpha_b - \alpha_h = \alpha_p - \alpha_h = 0
\tag{2.244}
$$

(which is tantamount to assuming nonpolar bonds) dividing throughout by $6\beta^2$, the coefficients will depend only on ω, becoming:

$$
\begin{cases}
A = 4\cos^2\omega\,(\cos^2\omega + 2) \\[2mm]
B = 4\sin 2\,\omega\,(\cos^2\omega + 2) \\[2mm]
C = (\sin 2\,\omega)^2 + 8\sin^2\omega - 4\cos^4\omega \\[2mm]
D = -4\sin 2\,\omega \cos^2\omega \\[2mm]
E = -(\sin 2\,\omega)^2
\end{cases}
\tag{2.245}
$$

A root of the quartic equation (2.241) is given in this case by the simple trigonometric relation:

$$\sqrt{2}\cot\gamma = \cos\omega \tag{2.246}$$

provided $54.74° \leq \gamma \leq 90°\,(45° \leq \theta \leq 60°)$. This shows that *for $\omega \neq 0$ the interbond angle resulting from energy optimization opens beyond $90°$*.

The four p AOs directed according to C_{3v} symmetry:

$$\begin{cases} p_1 = -z\cos\gamma + x\sin\gamma \\[2mm] p_2 = -z\cos\gamma - \dfrac{1}{2}x\sin\gamma + \dfrac{\sqrt{3}}{2}y\sin\gamma \\[2mm] p_3 = -z\cos\gamma - \dfrac{1}{2}x\sin\gamma - \dfrac{\sqrt{3}}{2}y\sin\gamma \\[2mm] p_4 = z \end{cases} \tag{2.247}$$

are still normalized, but no longer orthogonal to each other:

$$\begin{cases} \langle p_1|p_2\rangle = \langle p_1|p_3\rangle = \langle p_2|p_3\rangle = \cos^2\gamma - \dfrac{1}{2}\sin^2\gamma \\[2mm] \langle p_1|p_4\rangle = \langle p_2|p_4\rangle = \langle p_3|p_4\rangle = -\cos\gamma \end{cases} \tag{2.248}$$

Orthogonality can be restored by mixing in a certain amount of s (Magnasco, 2007; Torkington, 1951):

$$\begin{cases} b_1 = as + bp_1 = \dfrac{1}{\sqrt{3}}(s\sin\omega - z\cos\omega) + \dfrac{\sqrt{2}}{\sqrt{3}}x = \dfrac{1}{\sqrt{3}}b + \dfrac{\sqrt{2}}{\sqrt{3}}x \\[3mm] b_2 = as + bp_2 = \dfrac{1}{\sqrt{3}}(s\sin\omega - z\cos\omega) - \dfrac{1}{\sqrt{6}}x + \dfrac{1}{\sqrt{2}}y = \dfrac{1}{\sqrt{3}}b - \dfrac{1}{\sqrt{6}}x + \dfrac{1}{\sqrt{2}}y \\[3mm] b_3 = as + bp_3 = \dfrac{1}{\sqrt{3}}(s\sin\omega - z\cos\omega) - \dfrac{1}{\sqrt{6}}x - \dfrac{1}{\sqrt{2}}y = \dfrac{1}{\sqrt{3}}b - \dfrac{1}{\sqrt{6}}x - \dfrac{1}{\sqrt{2}}y \end{cases} \tag{2.249}$$

$$l = cs + dp_4 = s\cos\omega + z\sin\omega \tag{2.250}$$

since:

$$a = \frac{1}{\sqrt{3}}\left(\frac{1-3\cos^2\gamma}{\sin^2\gamma}\right)^{1/2}, \quad b = \frac{\sqrt{2}}{\sqrt{3}}\frac{1}{\sin\gamma}, \quad c = \sqrt{2}\cot\gamma, \quad d = \left(\frac{1-3\cos^2\gamma}{\sin^2\gamma}\right)^{1/2} \tag{2.251}$$
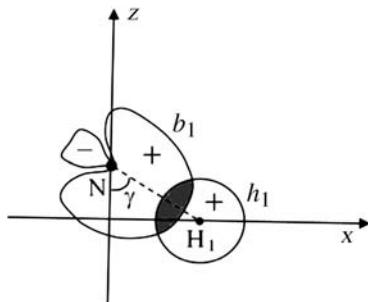
Figure 2.24 sp^3b_1 bond hybrid of C_{3v} symmetry on nitrogen overlapping (shaded area) the hydrogen h_1 orbital at $\theta = 53.5°$ to give a straight N–H$_1$ bond in NH$_3$. Reprinted from Chemical Physics Letters, 477, Magnasco, V., *Hückel transformation theory of the hybridization problem in NH$_3$*. 392–396, Copyright (2009), with permission from Elsevier

Hence, we can construct four sp^3 hybrids of C_{3v} symmetry, three directed towards the H atoms and one making the axially symmetric lone pair of Figure 2.23, simply by doing the further orthogonal transformation **U** of the functions b (belonging to A_1 symmetry) and x,y (belonging to E symmetry):

$$(b_1\, b_2\, b_3\, l) = (b\, x\, y\, l)\begin{pmatrix} \dfrac{1}{\sqrt{3}} & \dfrac{1}{\sqrt{3}} & \dfrac{1}{\sqrt{3}} & 0 \\[3mm] \dfrac{\sqrt{2}}{\sqrt{3}} & -\dfrac{1}{\sqrt{6}} & -\dfrac{1}{\sqrt{6}} & 0 \\[3mm] 0 & \dfrac{1}{\sqrt{2}} & -\dfrac{1}{\sqrt{2}} & 0 \\[3mm] 0 & 0 & 0 & 1 \end{pmatrix} = (b\, x\, y\, l)\mathbf{U} \quad (2.252)$$

where $\mathbf{U\tilde{U}} = \mathbf{\tilde{U}U} = 1$. The hybridization parameter ω, arbitrary so far, is best chosen so that the bond hybrids b_i point in the direction of the three N–H$_i$ bonds, giving in this way strongest bonding with H$_i$ 1s orbitals and satisfying the principle of maximum overlap. According to Equation (2.246), $2\theta = 107°$, $\gamma = 68.16°$ gives $\omega \approx 55.47°$, and we obtain the set (Figure 2.24 shows the b_1 bond hybrid engaged in the N–H$_1$ bond):[30]

---

[30] The equivalent hybrids b_2 and b_3 are obtained, respectively, by the anticlockwise rotation of b_1 by 120° and 240° around the z symmetry axis.

$$\begin{cases} b_1 = 0.475638\,s - 0.327264\,z + 0.816496\,x \\[6pt] b_2 = 0.475638\,s - 0.327264\,z - 0.408248\,x + 0.707107\,y \\[6pt] b_3 = 0.475638\,s - 0.327264\,z - 0.408248\,x - 0.707107\,y \\[6pt] l = 0.566848\,s - 0.823822\,z \end{cases}$$

$$(2.253)$$

which coincides with the set of four orthogonal sp^3 hybrids on nitrogen, equivalent under C_{3v} symmetry, obtainable in the standard way (Magnasco, 2007; Torkington, 1951) under the requirement of equivalence, normality and orthogonality. We have roughly a content of 22.6% s and 77.4% p in the bond hybrids, 32.1% s and 67.9% p in the lone pair.

Consideration of the second derivative of $E(\gamma)$ with respect to γ for $\beta_{sh} = \beta_{\sigma h} = \beta$ shows that it is *positive* for $\omega \approx 55.47°$, $2\theta = 107°$, so we conclude that, under our assumptions, sp hybridization opens the interbond angle beyond 90°, giving hybrids which locally minimize the Hückel model energy for the valence electron configuration of ground state NH_3, and which can be chosen to give straight bonds satisfying the principle of maximum overlap.

2.8   DELOCALIZED BONDS

We have seen so far that MOs resulting from the LCAO approximation are *delocalized* among the various nuclei in the polyatomic molecule even for the so-called saturated σ bonds. The effect of delocalization is even more important when looking to the π electron systems of conjugated and aromatic hydrocarbons, the systems for which the theory was originally developed by Hückel (1930, 1931, 1932). In the following, we shall consider four typical systems with N π electrons, two linear hydrocarbon chains, the allyl radical ($N = 3$) and the butadiene molecule ($N = 4$), and two closed hydrocarbon chains (rings), cyclobutadiene ($N = 4$) and the benzene molecule ($N = 6$). The case of the ethylene molecule, considered as a two π electron system, will however be considered first since it is the reference basis for the π bond in the theory.

The elements of the Hückel matrix are given in terms of just two negative unspecified parameters,[31] the diagonal α and the off-diagonal β for the nearest neighbours, introduced in a *topological* way as:

$$\begin{cases} H_{\mu\mu} = \alpha & \mu = 1, 2, 3, \ldots, N \\ H_{\mu\nu} = \beta & \nu = \mu \pm 1, 0 \text{ otherwise} \\ S_{\mu\nu} = \delta_{\mu\nu} \end{cases} \qquad (2.254)$$

Therefore, Hückel theory of π electron systems distinguishes only between linear chains and rings. It is useful to introduce the notation:

$$\begin{cases} \dfrac{\alpha - \varepsilon}{\beta} = -x \\[2ex] \varepsilon = \alpha + x\beta, \qquad \Delta\varepsilon = \varepsilon - \alpha = x\beta, \qquad \dfrac{\Delta\varepsilon}{\beta} = x \end{cases} \qquad (2.255)$$

so that x measures the π bond energy in units of β ($x > 0$ means *bonding*, $x < 0$ means *antibonding*).

The typical Hückel secular equations for N π electrons are then written in terms of determinants of order N, such as:

$$D_N = \begin{vmatrix} -x & 1 & 0 & \cdots & 0 & 0 & 0 \\ 1 & -x & 1 & \cdots & 0 & 0 & 0 \\ \cdots & \cdots & \cdots & \cdots & \cdots & \cdots & \cdots \\ 0 & 0 & 0 & \cdots & 1 & -x & 1 \\ 0 & 0 & 0 & \cdots & 0 & 1 & -x \end{vmatrix} \qquad (2.256)$$

for the *linear chain*, and:

$$D_N = \begin{vmatrix} -x & 1 & 0 & \cdots & 0 & 0 & 1 \\ 1 & -x & 1 & \cdots & 0 & 0 & 0 \\ \cdots & \cdots & \cdots & \cdots & \cdots & \cdots & \cdots \\ 0 & 0 & 0 & \cdots & 1 & -x & 1 \\ 1 & 0 & 0 & \cdots & 0 & 1 & -x \end{vmatrix} \qquad (2.257)$$

for the *closed chain* (the ring). The general solution of these determinantal equations is given in Chapter 3.

---

[31] Equal for all cases, at variance with what we saw for saturated systems.

2.8.1   The Ethylene Molecule

The Hückel secular equation for the π electrons in ethylene ($N = 2$):

$$D_2 = \begin{vmatrix} -x & 1 \\ 1 & -x \end{vmatrix} = 0 \qquad (2.258)$$

has the two roots (in ascending order):

$$x_1 = 1, \qquad x_2 = -1 \qquad (2.259)$$

with the corresponding MOs:

$$\phi_1 = \frac{1}{\sqrt{2}}(\chi_1 + \chi_2), \qquad \phi_2 = \frac{1}{\sqrt{2}}(\chi_2 - \chi_1) \qquad (2.260)$$

The MO diagram of the energy levels and a schematic drawing of the molecular orbitals are sketched in Figure 2.25. The highest occupied molecular orbital is called HOMO, the lowest unoccupied molecular orbital is called LUMO.

2.8.2   The Allyl Radical

The allyl radical has an unpaired π electron in a doublet ground state. For the allyl radical (linear chain with $N = 3$), expansion of the Hückel
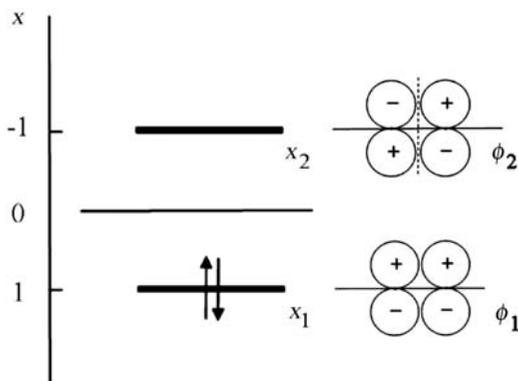
Figure 2.25   Energy levels (left) and Hückel MOs (right) for ethylene ground state ($N = 2$)
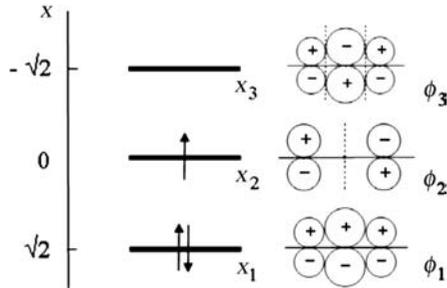
Figure 2.26 Energy levels (left) and Hückel MOs (right) for the allyl radical ground state $(N = 3)$

secular equation gives:

$$D_3 = \begin{vmatrix} -x & 1 & 0 \\ 1 & -x & 1 \\ 0 & 1 & -x \end{vmatrix} = -x(x^2-2) = 0 \qquad (2.261)$$

with the ordered roots:

$$x_1 = \sqrt{2}, \quad x_2 = 0, \qquad x_3 = -\sqrt{2} \qquad (2.262)$$

and the MOs:

$$\begin{cases} \phi_1 = \dfrac{\chi_1 + \sqrt{2}\chi_2 + \chi_3}{2} \\[2mm] \phi_2 = \dfrac{\chi_1 - \chi_3}{\sqrt{2}} \\[2mm] \phi_3 = \dfrac{\chi_1 - \sqrt{2}\chi_2 + \chi_3}{2} \end{cases} \qquad (2.263)$$

Figure 2.26 gives the diagram of the energy levels as occupied by electrons for the ground state of the allyl radical and the related Hückel molecular orbitals ϕs (ϕ_2 = HOMO, ϕ_3 = LUMO).[32]

The electron distribution of the π electrons in the allyl radical ground state is:

$$\begin{cases} P(\mathbf{r}) = \text{contribution from } \alpha \text{ and } \beta \text{ spin} \\ \quad = \rho^{\alpha}(\mathbf{r}) + \rho^{\beta}(\mathbf{r}) \\ \quad = \chi_1^2(\mathbf{r}) + \chi_2^2(\mathbf{r}) + \chi_3^2(\mathbf{r}), \end{cases} \qquad (2.264)$$

---

[32] This is true for the allyl radical ($N = 3$) and for the allyl anion ($N = 4$), but ϕ_1 = HOMO, ϕ_2 = LUMO for the allyl cation ($N = 2$).

and the spin density distribution of the unpaired α spin electron:

$$\begin{cases} P(\mathbf{r}) & = \text{ contribution from } \alpha \text{ and } \beta \text{ spin} \\ & = \rho^{\alpha}(\mathbf{r}) + \rho^{\beta}(\mathbf{r}) \\ & = \chi_1^2(\mathbf{r}) + \chi_2^2(\mathbf{r}) + \chi_3^2(\mathbf{r}) \end{cases} \qquad (2.265)$$

According to these equations, the Hückel distribution of the three π electrons is *uniform* (one electron onto each carbon atom, alternant hydrocarbon[33]), while the unpaired electron of α spin is 1/2 on atom 1 and 1/2 on atom 3, with zero probability of being found at atom 2. This spin distribution is however incorrect, since ESR experiments and theoretical VB calculations show that, if the unpaired electron has α spin, there is a nonvanishing probability of finding some β spin at the central atom.

The bond energy (in units of β) of the allyl radical is:

$$\Delta E^{\pi}(\text{allyl}) = 2\sqrt{2} = 2.828 \qquad (2.266)$$

while that of an ethylenic double bond:

$$\Delta E^{\pi}(\text{ethylene}) = 2 \qquad (2.267)$$

The difference 0.828 is an attractive stabilizing energy called the *delocalization energy* of the double bond in the allyl radical.

2.8.3   The Butadiene Molecule

The Hückel secular equation for the *linear* chain with $N = 4$ is:

$$D_4 = \begin{vmatrix} -x & 1 & 0 & 0 \\ 1 & -x & 1 & 0 \\ 0 & 1 & -x & 1 \\ \mathbf{0} & 0 & 1 & -x \end{vmatrix} = x^4 - 3x^2 + 1 = 0 \qquad (2.268)$$

where we have indicated in boldface the top right and the bottom left elements that differ from those of the *closed* chain which will be examined next. Equation (2.268) is a pseudoquartic equation that can be easily reduced to a quadratic equation by the substitution:

$$x^2 = y \Rightarrow y^2 - 3y + 1 = 0 \qquad (2.269)$$

---

[33] For the definition of alternant hydrocarbons, see Magnasco (Magnasco, 2007, 2009a).
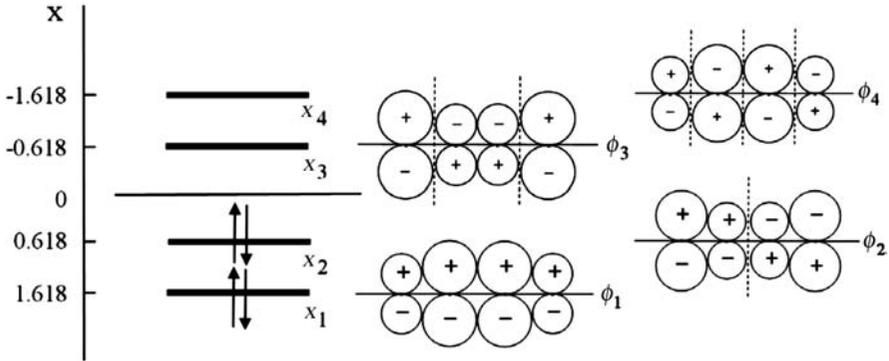
Figure 2.27 Energy levels (left) and Hückel MOs (right) for butadiene ground state $(N = 4)$

having the roots:

$$y = \frac{3 \pm \sqrt{5}}{2} = \begin{cases} y_1 = \dfrac{3 + \sqrt{5}}{2} = 2.618 \\[3mm] y_2 = \dfrac{3 - \sqrt{5}}{2} = 0.382 \end{cases} \tag{2.270}$$

So, we obtain the four roots (left-hand side of Figure 2.27):

$$\begin{cases} x_1 = \sqrt{y_1} = 1.618 \\ x_2 = \sqrt{y_2} = 0.618 \\ x_3 = -\sqrt{y_2} = -0.618 \\ x_4 = -\sqrt{y_1} = -1.618 \end{cases} \tag{2.271}$$

the first two being *bonding* levels, the last two *antibonding*.

The calculation of the MO coefficients (the eigenvectors corresponding to the four roots above) proceeds through solution of the linear homogeneous system, giving the MOs (right-hand side of Figure 2.27):

$$\begin{cases} \phi_1 = 0.371\,\chi_1 + 0.601\,(\chi_2 + \chi_3) + 0.371\,\chi_4 \\ \phi_2 = 0.601\,\chi_1 + 0.371\,(\chi_2 - \chi_3) - 0.601\,\chi_4 \\ \phi_3 = 0.601\,\chi_1 - 0.371\,(\chi_2 + \chi_3) + 0.601\,\chi_4 \\ \phi_4 = 0.371\,\chi_1 - 0.601\,\chi_2 + 0.601\,\chi_3 - 0.371\,\chi_4 \end{cases} \tag{2.272}$$

the first two being *bonding* (ϕ_2 = HOMO), the last two *antibonding* (ϕ_3 = LUMO) MOs.

Proceeding as we did for the allyl radical, it is easily seen that the electron charge distribution is uniform (one π electron onto each carbon atom, alternant hydrocarbon) and the spin density is zero, as expected for a state with $S = M_S = 0$ since the two bonding MOs are fully occupied by electrons with opposite spin. The delocalization (or conjugation) energy for linear butadiene is:

$$\Delta E^\pi(\text{butadiene}) - 2\Delta E^\pi(\text{ethylene}) = 4.472 - 4 = 0.472 \qquad (2.273)$$

and is therefore sensibly less than the conjugation energy of the allyl radical.

2.8.4   The Cyclobutadiene Molecule

The Hückel secular equation for the square *ring* with $N = 4$ is:

$$D_4 = \begin{vmatrix} -x & 1 & 0 & \mathbf{1} \\ 1 & -x & 1 & 0 \\ 0 & 1 & -x & 1 \\ \mathbf{1} & 0 & 1 & -x \end{vmatrix} = x^4 - 4x^2 = x^2(x^2 - 4) = 0 \qquad (2.274)$$

where the elements in boldface are the only ones differing from those of the *linear* chain (1 and 4 are now adjacent atoms). The roots of this equation are (left-hand side of Figure 2.28):

$$x_1 = 2, \quad x_2 = x_3 = 0, \quad x_4 = -2 \qquad (2.275)$$

For the MOs this gives:

$$\begin{cases} \phi_1 = \dfrac{1}{2}(\chi_1 + \chi_2 + \chi_3 + \chi_4) \\[2mm] \phi_2 = \phi_{2x} = \dfrac{1}{2}(\chi_1 - \chi_2 - \chi_3 + \chi_4) \propto x \\[2mm] \phi_3 = \phi_{2y} = \dfrac{1}{2}(\chi_1 + \chi_2 - \chi_3 - \chi_4) \propto y \\[2mm] \phi_4 = \dfrac{1}{2}(\chi_1 - \chi_2 + \chi_3 - \chi_4). \end{cases} \qquad (2.276)$$
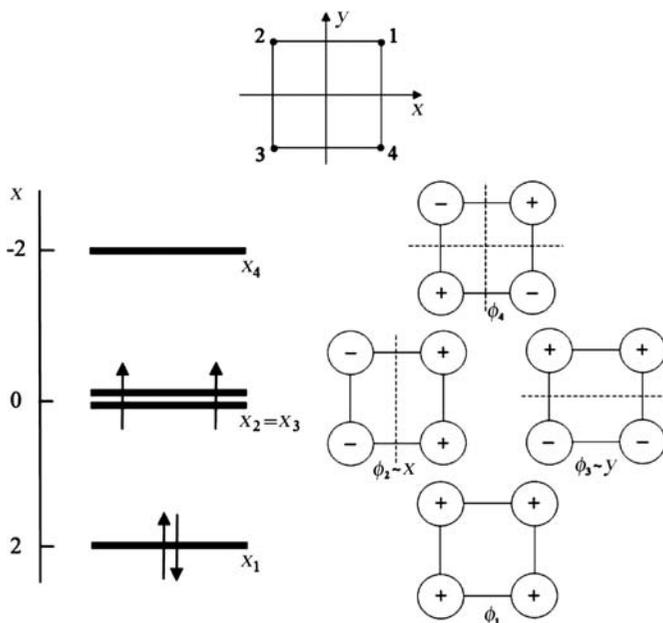
Figure 2.28 Coordinate system (top), energy levels (left) and real Hückel MOs (right) for cyclobutadiene (ring with $N = 4$)

The coordinate system, energy levels and Hückel MOs for cyclobutadiene are sketched in Figure 2.28. To simplify the drawing, the $2p\pi$ AOs in the MOs are viewed from above the zx molecular plane, so that only the signs of the upper lobes are reported. We note that ϕ_{2x} is a function having the same transformation properties as the x coordinate, yz being a *nodal* plane for this MO. ϕ_{2y} is a function having the same transformation properties as the y coordinate, zx now being the *nodal* plane for this MO. ϕ_{2x} and ϕ_{2y} are the pair of HOMO MOs belonging to the doubly degenerate energy level $\varepsilon_2 = \varepsilon_3$ which transform as the pair of basic vectors $\mathbf{e_x}$ and $\mathbf{e_y}$ of the D_{2h} symmetry (Magnasco, 2009a) to which the σ skeleton of cyclobutadiene belongs. They are therefore orthogonal and not interacting, as can be seen immediately:

$$\langle\phi_{2x}|\phi_{2y}\rangle = \frac{1}{4}\langle\chi_1 - \chi_2 - \chi_3 + \chi_4|\chi_1 + \chi_2 - \chi_3 - \chi_4\rangle = \frac{1}{4}(1 - 1 + 1 - 1) = 0$$

$$(2.277)$$

$$
\begin{cases}
\langle \phi_{2x}|H|\phi_{2y}\rangle = \dfrac{1}{4}\langle \chi_1 - \chi_2 - \chi_3 + \chi_4|H|\chi_1 + \chi_2 - \chi_3 - \chi_4\rangle \\[2mm]
\qquad\qquad = \dfrac{1}{4}[(\alpha+\beta-\beta)+(-\beta-\alpha+\beta)+(-\beta+\alpha+\beta)+(\beta-\beta-\alpha)] = 0
\end{cases}
$$

$$(2.278)$$

It is also seen that they belong to the *same* eigenvalue $\varepsilon = \alpha$:

$$
\varepsilon_{2x} = \frac{1}{4}\langle \chi_1 - \chi_2 - \chi_3 + \chi_4|H|\chi_1 - \chi_2 - \chi_3 + \chi_4\rangle = \alpha \qquad (2.279)
$$

$$
\varepsilon_{2y} = \frac{1}{4}\langle \chi_1 + \chi_2 - \chi_3 - \chi_4|H|\chi_1 + \chi_2 - \chi_3 - \chi_4\rangle = \alpha \qquad (2.280)
$$

ϕ_4 is sketched in the diagram of the upper row of Figure 2.28 and shows the existence of two nodal planes orthogonal to each other.[34] ϕ_4 is the last *antibonding* MO (LUMO).

The delocalization energy for cyclobutadiene is:

$$
\Delta E^{\pi}(\text{cyclobutadiene}) - 2\Delta E^{\pi}(\text{ethylene}) = 4 - 4 = 0 \qquad (2.281)
$$

so that, according to Hückel theory, the π electron system of cyclobutadiene has *zero* delocalization energy.

2.8.5 The Benzene Molecule

The Hückel secular equation for the *closed* chain (ring) with $N = 6$ is:

$$
D_6 = \begin{vmatrix}
-x & 1 & 0 & 0 & 0 & 1 \\
1 & -x & 1 & 0 & 0 & 0 \\
0 & 1 & -x & 1 & 0 & 0 \\
0 & 0 & 1 & -x & 1 & 0 \\
0 & 0 & 0 & 1 & -x & 1 \\
1 & 0 & 0 & 0 & 1 & -x
\end{vmatrix} = 0 \qquad (2.282)
$$

---

[34] As a general rule, the number of nodal planes increases for the higher π orbitals, while the deepest bonding MO has no nodal planes (except for the molecular plane, which is common to all molecules considered here).

where 1 and 6 are now *adjacent* atoms. By expanding the determinant we obtain a sixth degree equation in x that can be easily factorized into the three quadratic equations:

$$D_6 = x^6 - 6x^4 + 9x^2 - 4 = (x^2 - 4)(x^2 - 1)^2 = 0 \qquad (2.283)$$

with the roots, written in ascending order:

$$x = 2, \quad 1, \quad 1, \quad -1, \quad -1, \quad -2 \qquad (2.284)$$

Because of the high symmetry of the molecule, two levels are now doubly degenerate. The calculation of the MO coefficients can be done using elementary algebraic methods in solving the linear homogeneous system corresponding to Equation (2.282). With reference to Figure 2.29, a rather lengthy calculation (Section 2.9.3) shows that the *real* MOs are:

$$
\begin{cases}
\phi_1 = \dfrac{1}{\sqrt{6}}(\chi_1 + \chi_2 + \chi_3 + \chi_4 + \chi_5 + \chi_6) \\[2ex]
\phi_2 = \dfrac{1}{2}(\chi_1 - \chi_3 - \chi_4 + \chi_6) \propto x \\[2ex]
\phi_3 = \dfrac{1}{\sqrt{12}}(\chi_1 + 2\chi_2 + \chi_3 - \chi_4 - 2\chi_5 - \chi_6) \propto y \\[2ex]
\phi_4 = \dfrac{1}{\sqrt{12}}(\chi_1 - 2\chi_2 + \chi_3 + \chi_4 - 2\chi_5 + \chi_6) \propto x^2 - y^2 \\[2ex]
\phi_5 = \dfrac{1}{2}(\chi_1 - \chi_3 + \chi_4 - \chi_6) \propto xy \\[2ex]
\phi_6 = \dfrac{1}{\sqrt{6}}(\chi_1 - \chi_2 + \chi_3 - \chi_4 + \chi_5 - \chi_6).
\end{cases}
\qquad (2.285)
$$

The first degenerate MOs[35] ϕ_2 and ϕ_3 transform like (x, y) and are *bonding* MOs (HOMOs), the second degenerate MOs ϕ_4 and ϕ_5 transform like $(x^2 - y^2, xy)$ and are *antibonding* MOs (LUMOs).

---

[35] Loosely speaking, we attribute to MOs a property (degeneracy) of energy levels.
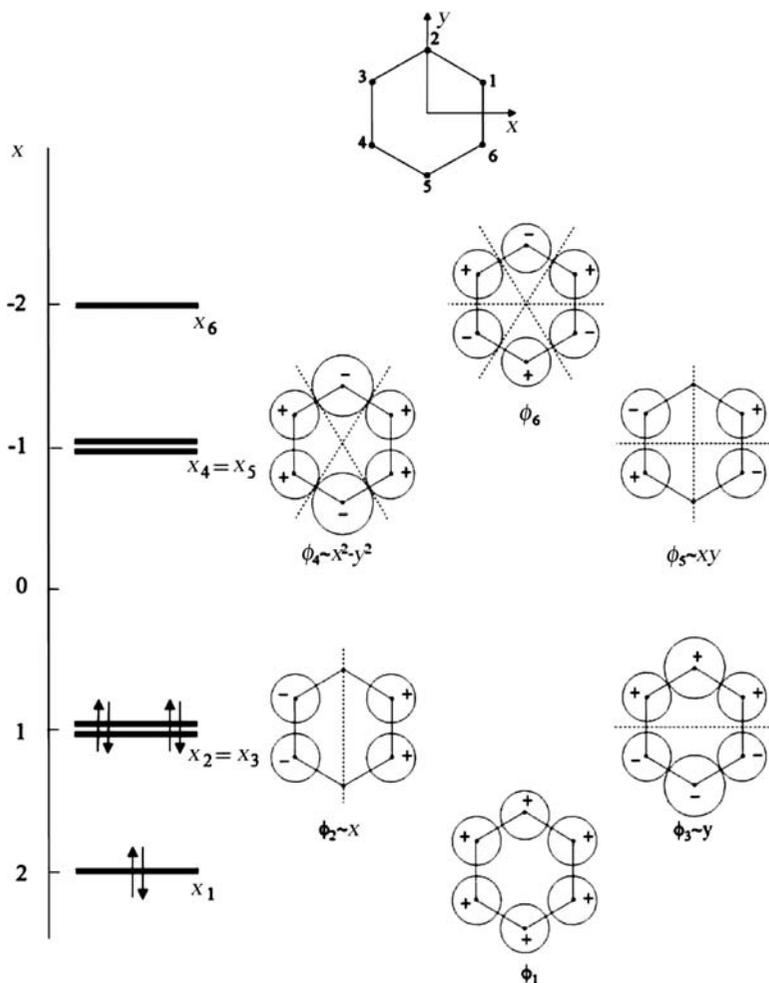
Figure 2.29 Numbering of carbon atoms and coordinate system (top), energy levels (left) and real Hückel MOs (right) for the π electrons in benzene (ring with $N = 6$)

The ρ^{α} and ρ^{β} components of the electron distribution function for benzene are equal:

$$
\begin{cases}
\rho^{\alpha} = \rho^{\beta} = \phi_1^2 + \phi_2^2 + \phi_3^2 \\
\quad = \chi_1^2\left(\dfrac{1}{6} + \dfrac{1}{4} + \dfrac{1}{12}\right) + \chi_2^2\left(\dfrac{1}{6} + \dfrac{4}{12}\right) + \chi_3^2\left(\dfrac{1}{6} + \dfrac{1}{4} + \dfrac{1}{12}\right) \\
\quad + \chi_4^2\left(\dfrac{1}{6} + \dfrac{1}{4} + \dfrac{1}{12}\right) + \chi_5^2\left(\dfrac{1}{6} + \dfrac{4}{12}\right) + \chi_6^2\left(\dfrac{1}{6} + \dfrac{1}{4} + \dfrac{1}{12}\right)
\end{cases}
$$

$$(2.286)$$

so that:

$$\rho^\alpha = \rho^\beta = \frac{1}{2}\left(\chi_1^2 + \chi_2^2 + \chi_3^2 + \chi_4^2 + \chi_5^2 + \chi_6^2\right) \qquad (2.287)$$

We then have for the electron density:

$$P(\mathbf{r}) = \rho^\alpha(\mathbf{r}) + \rho^\beta(\mathbf{r}) = \chi_1^2 + \chi_2^2 + \chi_3^2 + \chi_4^2 + \chi_5^2 + \chi_6^2 \qquad (2.288)$$

and the charge distribution of the π electrons in benzene is *uniform* (one electron onto each carbon atom), as expected for an alternant hydrocarbon; whereas the spin density is zero:

$$Q(\mathbf{r}) = \rho^\alpha(\mathbf{r}) - \rho^\beta(\mathbf{r}) = 0 \qquad (2.289)$$

as it must be for a singlet state.

The π bond energy (units of β) for benzene is:

$$\Delta E^\pi = 2 \times 2 + 4 \times 1 = 8 \qquad (2.290)$$

When the π bond energy of three ethylenes:

$$3\Delta E^\pi \text{ (ethylene)} = 3 \times 2 = 6 \qquad (2.291)$$

is subtracted from Equation (2.290) we obtain for the delocalization energy of the three double bonds in benzene:

$$\Delta E^\pi(\text{benzene}) - 3\Delta E^\pi(\text{ethylene}) = 8 - 6 = 2 \qquad (2.292)$$

the highest value obtained so far among the molecules studied. This energy lowering is responsible for the great stability of the π electron system of the benzene molecule, where the three *aromatic* π bonds are fully delocalized and bear no resemblance at all to three *ethylenic* double bonds. Further stability in benzene arises from the fact that, at variance with its homologues cyclobutadiene[36] ($N = 4$) and cyclooctatetraene[37] ($N = 8$), its σ skeleton has no internal strain.

---

[36] In cyclobutadiene the ring bond angles are 30° less than the value expected for sp^2 hybridization, so that its ground state is a very unstable triplet.

[37] Cyclooctatetraene is not aromatic, since it is not planar but has a 'tube' conformation (Magnasco, 2007).

2.9   APPENDICES

2.9.1   The Second Derivative of the Hückel Energy

Putting $\beta_{sh} = \beta_{oh} = \beta$ the second derivative of the Hückel energy, Equation (2.207), becomes:

$$
\begin{cases}
\dfrac{d^2E}{d\theta^2} = \dfrac{4}{\Delta_2}\beta^2 \sin 2\,\omega \cos\theta + 8\,\beta^2 \cos 2\theta \left(\dfrac{\cos^2\omega}{\Delta_2} - \dfrac{1}{\Delta_3} \right) \\[3mm]
\quad + \dfrac{16}{\Delta_2^{\,3}}\beta^4 (\sin 2\,\omega \sin\theta + \cos^2\omega \sin 2\theta)^2 + \dfrac{16}{\Delta_3^{\,3}}\beta^4 (\sin 2\theta)^2
\end{cases}
$$

$$(2.293)$$

where:

$$
\begin{cases}
\Delta_2 = [(\alpha_b - \alpha_h)^2 + 8\beta^2 (\sin\omega + \cos\omega \cos\theta)^2]^{1/2} \\[2mm]
\Delta_3 = [(\alpha_p - \alpha_h)^2 + 8\beta^2 \sin^2\theta]^{1/2}
\end{cases}
$$

$$(2.294)$$

Since, for $\omega = 40°$, $2\theta = 105°$,

$$(\alpha_b - \alpha_h)^2 > (\alpha_p - \alpha_h)^2, \ (\sin\omega + \cos\omega \cos\theta)^2 > \sin^2\theta \qquad (2.295)$$

surely:

$$\Delta_2 > \Delta_3 \qquad\qquad (2.296)$$

Therefore, a fortiori it is true that:

$$\frac{\cos^2\omega}{\Delta_2} < \frac{1}{\Delta_3} \qquad\qquad (2.297)$$

and all terms of Equation (2.293) are *positive*, so that:

$$\left(\frac{d^2E}{d\theta^2} \right)_{\omega=40°, 2\theta=105°} > 0 \qquad\qquad (2.298)$$

and we have a true minimum there.

2.9.2   The Set of Three Coulson's Orthogonal Hybrids

If ω' is a hybridization parameter, Coulson's hybrids can be written as:

$$\begin{cases} b_1' = s\sin\omega' + z\cos\omega'\cos\theta + y\cos\omega'\sin\theta \\ b_2' = s\sin\omega' + z\cos\omega'\cos\theta - y\cos\omega'\sin\theta \\ l' = s\cos\omega' - z\sin\omega'. \end{cases} \qquad (2.299)$$

Comparison with our set (Equations 2.219) shows that, if the two sets have to be *equivalent*, we must have:

$$\sin\omega' = \frac{1}{\sqrt{2}}\sin\omega, \;\; \cos\omega'\cos\theta = \frac{1}{\sqrt{2}}\cos\omega, \;\; \cos\omega'\sin\theta = \frac{1}{\sqrt{2}} \quad (2.300)$$

so establishing the relation between Coulson's ω' and our (ω) hybridization parameters.

We notice, first, that hybrids (Equations 2.299) are correctly normalized, and that:

$$S_{12} = \langle b_1'|b_2'\rangle = \sin^2\omega' + \cos^2\omega'\cos 2\theta = 0 \qquad (2.301)$$

provided Coulson's relation is satisfied:

$$\cos 2\theta = -\left(\frac{\sin\omega'}{\cos\omega'}\right)^2 < 0 \qquad (2.302)$$

but that the lone pair hybrid l' is *not* orthogonal to either b_1' or b_2':

$$S_{13} = S_{23} = \sin\omega'\cos\omega'(1-\cos\theta) \neq 0 \qquad (2.303)$$

Schmidt orthogonalization of l' to b_1 or b_2 can be done using the explicit formulae given elsewhere (Magnasco, 2007), so obtaining:

$$\begin{cases} b_1 = b_1', \; b_2 = b_2', \\ l = (1-2S^2)^{-1/2}(l'-Sb_2'-Sb_1') \end{cases} \qquad (2.304)$$

It can be seen that, in doing the orthogonalization process, the coefficient of y in (Equatrions 2.304) becomes identically zero, and we obtain

the *orthogonalized* lone pair in the form:

$$l = (1-2S^2)^{-1/2}[s(\cos\omega'-2S\sin\omega')-z(\sin\omega'+2S\cos\omega'\cos\theta)] \quad (2.305)$$

Using Equations (2.300) and (2.214) it is further easily verified that:

$$\begin{cases} (1-2S^2)^{-1/2}(\cos\omega'-2S\sin\omega') = \cos\omega \\ (1-2S^2)^{-1/2}(\sin\omega'+2S\cos\omega'\cos\theta) = \sin\omega \end{cases} \quad (2.306)$$

so that Coulson's orthogonalized set (2.304) coincides with our set (2.219). Hence we may say that our main result (2.214) is just another way of expressing Coulson's result (2.302), and that our Equations (2.219) are the simplest way of expressing the set of *three* orthonormal sp^2 hybrids equivalent under C_{2v} symmetry.

2.9.3   Calculation of Coefficients of Real MOs for Benzene

We give in the following an elementary derivation of the coefficients occurring in the *real* MOs for benzene, Equations (2.285), based on the direct solution of the system of linear homogeneous equations giving (2.282). We start by considering each eigenvalue in turn, making reference to numbering of carbon atoms and coordinate system of Figure 2.29. We recall that each equation must be used once.

(a) $x_1 = 2$ (first eigenvalue)

The homogeneous system corresponding to this eigenvalue is:

$$\begin{cases} 1. & -2c_1 + c_2 + c_6 = 0 \\ 2. & c_1 - 2c_2 + c_3 = 0 \\ 3. & c_2 - 2c_3 + c_4 = 0 \\ 4. & c_3 - 2c_4 + c_5 = 0 \\ 5. & c_4 - 2c_5 + c_6 = 0 \\ 6. & c_1 + c_5 - 2c_6 = 0 \end{cases} \quad (2.307)$$

We express all ratios between the coefficients in terms of c_5/c_1, assuming $c_1 \neq 0$.

1. and 6. in Equations (2.307) give:

$$\frac{c_6}{c_1} = 2 - \frac{c_2}{c_1} = \frac{1}{2}\left(1 + \frac{c_5}{c_1}\right)$$

so that:

$$\frac{c_2}{c_1} = 2 - \frac{1}{2}\left(1 + \frac{c_5}{c_1}\right) = \frac{1}{2}\left(3 - \frac{c_5}{c_1}\right)$$

2. gives:

$$\frac{c_3}{c_1} = 2\frac{c_2}{c_1} - 1 = \left(3 - \frac{c_5}{c_1}\right) - 1 = 2 - \frac{c_5}{c_1}$$

4. gives:

$$\frac{c_4}{c_1} = \frac{1}{2}\left(\frac{c_3}{c_1} + \frac{c_5}{c_1}\right) = \frac{1}{2}\left(2 - \frac{c_5}{c_1} + \frac{c_5}{c_1}\right) = 1$$

5. gives:

$$\frac{c_5}{c_1} == \frac{1}{2}\left(\frac{c_4}{c_1} + \frac{c_6}{c_1}\right) = \frac{1}{2} + \frac{1}{4}\left(1 + \frac{c_5}{c_1}\right) = \frac{1}{4}\left(3 + \frac{c_5}{c_1}\right)$$

and therefore:

$$c_5/c_1 = 1$$

So, we finally get:

$$\frac{c_6}{c_1} = \frac{1}{2}(1+1) = 1; \ \frac{c_2}{c_1} = \frac{1}{2}(3-1) = 1; \ \frac{c_3}{c_1} = 2-1 = 1; \ \frac{c_4}{c_1} = 1; \ \frac{c_5}{c_1} = 1$$

$$c_1 = c_2 = c_3 = c_4 = c_5 = c_6$$

The additional constraint of coefficient normalization gives:

$$c_1^2 + c_2^2 + c_3^2 + c_4^2 + c_5^2 + c_6^2 = 1 \Rightarrow 6c_1^2 = 1 \Rightarrow c_1 = \frac{1}{\sqrt{6}}$$

thereby giving for the eigenvector ϕ_1 corresponding to the first eigenvalue:

$$c_1 = c_2 = c_3 = c_4 = c_5 = c_6 = \frac{1}{\sqrt{6}}. \qquad (2.308)$$

(b) $x_2 = 1$ (first degenerate eigenvalue)
The homogeneous system is:

$$\begin{cases} 1. & -c_1 + c_2 + c_6 = 0 \\ 2. & c_1 - c_2 + c_3 = 0 \\ 3. & c_2 - c_3 + c_4 = 0 \\ 4. & c_3 - c_4 + c_5 = 0 \\ 5. & c_4 - c_5 + c_6 = 0 \\ 6. & c_1 + c_5 - c_6 = 0 \end{cases} \qquad (2.309)$$

Again assume $c_1 \neq 0$. Then:
1. and 6. in Equations (2.309) give:

$$\frac{c_6}{c_1} = 1 - \frac{c_2}{c_1} = 1 + \frac{c_5}{c_1}$$

so that:

$$\frac{c_2}{c_1} = -\frac{c_5}{c_1}$$

2. gives:

$$\frac{c_3}{c_1} = \frac{c_2}{c_1} - 1 = -1 - \frac{c_5}{c_1}$$

3. gives:

$$\frac{c_4}{c_1} = \frac{c_3}{c_1} - \frac{c_2}{c_1} = -1 - \frac{c_5}{c_1} + \frac{c_5}{c_1} = -1$$

4. gives:

$$\frac{c_5}{c_1} = \frac{c_4}{c_1} - \frac{c_3}{c_1} = -1 + 1 + \frac{c_5}{c_1} = \frac{c_5}{c_1}$$

nothing new.
  Hence c_5/c_1 is *arbitrary*, and we choose to put it equal to zero.

$$c_5/c_1 = 0$$

gives:

$$\frac{c_6}{c_1} = 1; \ \frac{c_2}{c_1} = 0; \ \frac{c_3}{c_1} = -1; \ \frac{c_4}{c_1} = -1; \ \frac{c_5}{c_1} = 0$$

Therefore:

$$c_2 = c_5 = 0; \ c_3 = c_4 = -c_1; \ c_6 = c_1$$

and the normalization condition gives:

$$c_1^2 + c_2^2 + c_3^2 + c_4^2 + c_5^2 + c_6^2 = 1 \Rightarrow 4c_1^2 = 1 \Rightarrow c_1 = \frac{1}{2}$$

$$c_1 = c_6 = \frac{1}{2}, \ c_2 = c_5 = 0, \ c_3 = c_4 = -\frac{1}{2} \qquad (2.310)$$

In this way, we obtain the first (normalized) eigenvector ϕ_2 corresponding to the first degenerate eigenvalue, and we see that it has the same transformation properties of the coordinate x. Because of the necessary orthogonality in the xy plane between the two basic vectors, the second (normalized) eigenvector ϕ_3 belonging to the first degenerate eigenvalue must therefore transform like y. Hence we must have:

$$\frac{c_6}{c_1} = -1; \ \frac{c_5}{c_1} = -2; \ \frac{c_2}{c_1} = 2; \ \frac{c_3}{c_1} = 1; \ \frac{c_4}{c_1} = -1$$

Hence, orthogonality gives:

$$c_1; \ c_2 = 2c_1; \ c_3 = c_1; \ c_4 = -c_1; \ c_5 = -2c_1; \ c_6 = -c_1$$

and, normalizing to unity:

$$c_1^2(1 + 4 + 1 + 1 + 4 + 1) = 12c_1^2 = 1 \Rightarrow c_1 = \frac{1}{\sqrt{12}}$$

so that we finally obtain for the eigenvector transforming like y:

$$c_1 = c_3 = -c_4 = -c_6 = \frac{1}{\sqrt{12}}, \quad c_2 = -c_5 = \frac{2}{\sqrt{12}} \qquad (2.311)$$

(c) $x_4 = -1$ (second degenerate eigenvalue)

The homogeneous system is:

$$\begin{cases} 1. & c_1 + c_2 + c_6 = 0 \\ 2. & c_1 + c_2 + c_3 = 0 \\ 3. & c_2 + c_3 + c_4 = 0 \\ 4. & c_3 + c_4 + c_5 = 0 \\ 5. & c_4 + c_5 + c_6 = 0 \\ 6. & c_1 + c_5 + c_6 = 0 \end{cases} \qquad (2.312)$$

Again assume $c_1 \neq 0$. Then:
1. and 6. in Equations (2.312) give:

$$\frac{c_6}{c_1} = -1 - \frac{c_2}{c_1} = -1 - \frac{c_5}{c_1}$$

and therefore:

$$\frac{c_2}{c_1} = \frac{c_5}{c_1}.$$

2. gives:

$$\frac{c_3}{c_1} = -1 - \frac{c_2}{c_1} = -1 - \frac{c_5}{c_1}$$

3. gives:

$$\frac{c_4}{c_1} = -\frac{c_2}{c_1} - \frac{c_3}{c_1} = -\frac{c_5}{c_1} + 1 + \frac{c_5}{c_1} = 1$$

4. gives:

$$\frac{c_5}{c_1} = -\frac{c_3}{c_1} - \frac{c_4}{c_1} = 1 + \frac{c_5}{c_1} - 1 = \frac{c_5}{c_1}$$

nothing new.

Hence c_5/c_1 is *arbitrary*, and we choose to put it equal to -2. Then:

$$\frac{c_6}{c_1} = -1 + 2 = 1; \ \frac{c_5}{c_1} = -2; \ \frac{c_4}{c_1} = 1; \ \frac{c_3}{c_1} = -1 + 2 = 1; \ \frac{c_2}{c_1} = -2$$

Therefore:

$$c_2 = -2c_1; \; c_3 = c_1; \; c_4 = c_1; \; c_5 = -2c_1; \; c_6 = c_1$$

and the normalization condition gives:

$$c_1^2 + c_2^2 + c_3^2 + c_4^2 + c_5^2 + c_6^2 = 1 \Rightarrow 12c_1^2 = 1 \Rightarrow c_1 = \frac{1}{\sqrt{12}}$$

$$c_1 = c_3 = c_4 = c_6 = \frac{1}{\sqrt{12}}; \; c_2 = c_5 = -\frac{2}{\sqrt{12}} \qquad (2.313)$$

In this way, we obtain the first (normalized) eigenvector ϕ_4 corresponding to the second degenerate eigenvalue, and we see that it has the same transformation properties as $(x^2 - y^2)$. Because of the necessary orthogonality in the xy plane between the two basic vectors, the second (normalized) eigenvector ϕ_5 belonging to the second degenerate eigenvalue must therefore transform like xy. Hence we must have:

$$\frac{c_6}{c_1} = -1; \; \frac{c_5}{c_1} = 0; \; \frac{c_4}{c_1} = 1; \; \frac{c_3}{c_1} = -1; \; \frac{c_2}{c_1} = 0$$

Hence, orthogonality gives:

$$c_2 = c_5 = 0; \; c_3 = -c_1; \; c_4 = c_1; \; c_6 = c_1$$

and, normalizing to unity:

$$c_1^2 + c_2^2 + c_3^2 + c_4^2 + c_5^2 + c_6^2 = 1 \Rightarrow 4c_1^2 = 1 \Rightarrow c_1 = \frac{1}{2}$$

so that we finally obtain for the eigenvector transforming like xy:

$$c_1 = -c_3 = c_4 = -c_6 = \frac{1}{2}; \; c_2 = c_5 = 0 \qquad (2.314)$$

d) $x_6 = -2$ (last eigenvalue)

We proceed in the same way as we did for the first eigenvalue. The homogeneous system corresponding to this eigenvalue is:

$$\begin{cases} 1. & 2c_1 + c_2 + c_6 = 0 \\ 2. & c_1 + 2c_2 + c_3 = 0 \\ 3. & c_2 + 2c_3 + c_4 = 0 \\ 4. & c_3 + 2c_4 + c_5 = 0 \\ 5. & c_4 + 2c_5 + c_6 = 0 \\ 6. & c_1 + c_5 + 2c_6 = 0 \end{cases} \qquad (2.315)$$

1. and 6. in Equations (2.315) now give:

$$\frac{c_6}{c_1} = -2 - \frac{c_2}{c_1} = \frac{1}{2}\left(-1 - \frac{c_5}{c_1}\right)$$

so that:

$$\frac{c_2}{c_1} = -2 + \frac{1}{2}\left(1 + \frac{c_5}{c_1}\right) = \frac{1}{2}\left(-3 + \frac{c_5}{c_1}\right)$$

2. gives:

$$\frac{c_3}{c_1} = -1 - 2\frac{c_2}{c_1} = -1 + \left(3 - \frac{c_5}{c_1}\right) = 2 - \frac{c_5}{c_1}$$

4. gives:

$$\frac{c_4}{c_1} = \frac{1}{2}\left(-\frac{c_3}{c_1} - \frac{c_5}{c_1}\right) = \frac{1}{2}\left(-2 + \frac{c_5}{c_1} - \frac{c_5}{c_1}\right) = -1$$

5. gives:

$$\frac{c_5}{c_1} = \frac{1}{2}\left(-\frac{c_4}{c_1} - \frac{c_6}{c_1}\right) = \frac{1}{2} + \frac{1}{4}\left(1 + \frac{c_5}{c_1}\right) = \frac{1}{4}\left(3 + \frac{c_5}{c_1}\right)$$

Hence:

$$4\frac{c_5}{c_1} = 3 + \frac{c_5}{c_1} \Rightarrow \frac{c_5}{c_1} = 1$$

So, we finally get:

$$\frac{c_6}{c_1} = -\frac{1}{2} - \frac{1}{2} = -1; \frac{c_2}{c_1} = -\frac{3}{2} + \frac{1}{2} = -1; \frac{c_3}{c_1} = 2 - 1 = 1;$$

$$\frac{c_4}{c_1} = -1; \frac{c_5}{c_1} = \frac{3}{4} + \frac{1}{4} = 1$$

namely:

$$c_2 = -c_1; c_3 = c_1; c_4 = -c_1; c_5 = c_1; c_6 = -c_1$$

Normalizing to unity we obtain:

$$c_1^2 + c_2^2 + c_3^2 + c_4^2 + c_5^2 + c_6^2 = 1 \Rightarrow 6c_1^2 = 1 \Rightarrow c_1 = \frac{1}{\sqrt{6}}$$

thereby giving for the eigenvector ϕ_6 corresponding to the last eigenvalue:

$$c_1 = -c_2 = c_3 = -c_4 = c_5 = -c_6 = \frac{1}{\sqrt{6}} \qquad (2.316)$$

Following what was said for cyclobutadiene, it is left as an easy exercise for the reader to verify that all MOs, Equations (2.285), are normalized and orthogonal and not interacting in pairs. Furthermore, even if their form is different, each pair of MOs belonging to the respective degenerate eigenvalue gives the same value for the corresponding orbital energy.

3

An Introduction to Bonding in Solids

In the previous chapter, we saw that immediate solution of the N-dimensional (D_N) Hückel secular equation was possible for the first members of the series, ethylene ($N = 2$), allyl radical ($N = 3$) and butadiene ($N = 4$), but for higher values of N only symmetry can help in finding the solutions, unless we have at our disposal the general solution for the linear polyene chain of N atoms. The secular equations for linear and closed polyene chains, even with different βs for single and double bonds, were first solved by Lennard-Jones (1937) and rederived by Coulson (1938). In the following, we present a simple derivation of the general solution for the N-atom linear and closed polyene chains (*equal* βs) which are useful for introducing the general theory of bonding in solids. We follow here the lines sketched in McWeeny's book on valence theory (1979).

3.1   THE LINEAR POLYENE CHAIN

We want to find the general solution for the system of homogeneous linear equations for the *linear* polyene chain with N atoms yielding the Nth degree secular equation

$$D_N = \begin{vmatrix} -x & 1 & 0 & \cdots & 0 & 0 & 0 \\ 1 & -x & 1 & \cdots & 0 & 0 & 0 \\ \cdots & \cdots & \cdots & \cdots & \cdots & \cdots & \cdots \\ 0 & 0 & 0 & \cdots & 1 & -x & 1 \\ 0 & 0 & 0 & \cdots & 0 & 1 & -x \end{vmatrix} = 0 \qquad (3.1)$$

The homogeneous system corresponding to Equation (3.1) is:

$$\begin{cases} -xc_1 + c_2 = 0 \\ \cdots \\ c_{m-1} - xc_m + c_{m+1} = 0 \\ \cdots \\ c_{N-1} - xc_N = 0 \end{cases} \qquad (3.2)$$

The general equation is:

$$c_{m-1} - xc_m + c_{m+1} = 0 \qquad m = 1, 2, \cdots, N \qquad (3.3)$$

with the boundary conditions

$$c_0 = c_{N+1} = 0 \qquad (3.4)$$

The general solution is the *standing* wave

$$c_m = A \exp(im\,\theta) + B \exp(-im\,\theta) \qquad (3.5)$$

where i is the imaginary unit ($i^2 = -1$), provided

$$x = 2 \cos \theta \qquad (3.6)$$

(i) From the first boundary condition it is in fact obtained:

$$c_0 = A + B = 0 \Rightarrow B = -A \qquad (3.7)$$

$$c_m = A[\exp(im\,\theta) - \exp(-im\,\theta)] = 2iA \sin m\theta = C \sin m\theta \qquad (3.8)$$

where $C = 2iA$ is a normalization factor. The general equation then gives:

$$
\begin{cases}
A\{\exp[i(m-1)\theta] - x\exp(im\,\theta) + \exp[i(m+1)\theta]\} \\
+ B\{\exp[-i(m-1)\theta] - x\exp(-im\,\theta) + \exp[-i(m+1)\theta]\} \\
= A\exp(im\,\theta)[\exp(-i\theta) - x + \exp(i\theta)] \\
+ B\exp(-im\,\theta)[\exp(i\theta) - x + \exp(-i\theta)] \\
= [A\exp(im\,\theta) + B\exp(-im\,\theta)][\exp(-i\theta) - x + \exp(i\theta)] \\
= c_m(2\cos\theta - x) = 0
\end{cases}
\tag{3.9}
$$

so that, for $c_m \neq 0$:

$$
2\cos\theta - x = 0 \Rightarrow x = 2\cos\theta
\tag{3.10}
$$

as required.

(ii) From the second boundary condition it is obtained:

$$
c_{N+1} = C\sin(N+1)\theta = 0
\tag{3.11}
$$

therefore it must be:

$$
(N+1)\theta = k\pi \qquad k = 1, 2, 3, \cdots, N
\tag{3.12}
$$

with k a *quantum number*:

$$
\theta_k = \frac{k\pi}{N+1}
\tag{3.13}
$$

so that angle θ is *quantized*.

In conclusion, we see that the general solution for the linear chain will be:

$$
\begin{cases}
x_k = 2\cos\dfrac{k\pi}{N+1} \qquad k = 1, 2, \cdots, N \\[2ex]
c_{mk} = c_k \sin m\dfrac{k\pi}{N+1}
\end{cases}
\tag{3.14}
$$

the first being the π bond energy of the kth level (in units of β), the second the coefficient of the mth AO in the kth MO. All previous results for ethylene, allyl radical and butadiene given in Section 2.8 of Chapter 2 are easily rederived from the general formula (Equation 3.14).

We give below the derivation of the detailed formulae for the open linear chain with $N = 4$ (butadiene).

3.1.1   Butadiene $N = 4$

$$\theta_k = k\frac{\pi}{5}, \quad x_k = 2\cos k\frac{\pi}{5}, \quad k = 1, 2, 3, 4 \tag{3.15}$$

The roots in ascending order are:

(i) Bonding levels

$$\begin{cases} x_1 = 2\cos\dfrac{\pi}{5} = 2\cos 36° = 1.618 \\[2ex] x_2 = 2\cos\dfrac{2\pi}{5} = 2\cos 72° = 0.618 \end{cases} \tag{3.16}$$

(ii) Antibonding levels

$$\begin{cases} x_3 = 2\cos\dfrac{3\pi}{5} = 2\cos 108° = -0.618 \\[2ex] x_4 = 2\cos\dfrac{4\pi}{5} = 2\cos 144° = -1.618 \end{cases} \tag{3.17}$$

which coincide with those of Equations (2.272) of Chapter 2.

For the MOs, we have:

$$\phi_k = \sum_m \chi_m c_{mk} = C\sum_m \chi_m \sin m\frac{k\pi}{5} \tag{3.18}$$

where C is a normalization factor.
Then:

$$\begin{cases} \phi_1 = C\displaystyle\sum_{m=1}^{4}\chi_m \sin m\frac{\pi}{5} = C\left(\chi_1\sin\frac{\pi}{5} + \chi_2\sin\frac{2\pi}{5} + \chi_3\sin\frac{3\pi}{5} + \chi_4\sin\frac{4\pi}{5}\right) \\[2ex] \quad = C(0.5878\chi_1 + 0.9510\chi_2 + 0.9510\chi_3 + 0.5878\chi_4) \tag{3.19} \\[2ex] \quad = 0.3718\chi_1 + 0.6015\chi_2 + 0.6015\chi_3 + 0.3718\chi_4 \end{cases}$$

the deepest bonding MO (no nodal planes);

$$
\left\{
\begin{aligned}
\phi_2 &= C\sum_{m=1}^{4}\chi_m \sin m\frac{2\pi}{5} = C\left(\chi_1 \sin\frac{2\pi}{5} + \chi_2 \sin\frac{4\pi}{5} + \chi_3 \sin\frac{6\pi}{5} + \chi_4 \sin\frac{8\pi}{5}\right) \\
&= C(0.9510\chi_1 + 0.5878\chi_2 - 0.5878\chi_3 - 0.9510\chi_4) \\
&= 0.6015\chi_1 + 0.3718\chi_2 - 0.3718\chi_3 - 0.6015\chi_4 \tag{3.20}
\end{aligned}
\right.
$$

the second bonding MO (HOMO, one nodal plane);

$$
\left\{
\begin{aligned}
\phi_3 &= C\sum_{m=1}^{4}\chi_m \sin m\frac{3\pi}{5} = C\left(\chi_1 \sin\frac{3\pi}{5} + \chi_2 \sin\frac{6\pi}{5} + \chi_3 \sin\frac{9\pi}{5} + \chi_4 \sin\frac{12\pi}{5}\right) \\
&= C(0.9510\chi_1 - 0.5878\chi_2 - 0.5878\chi_3 + 0.9510\chi_4) \\
&= 0.6015\chi_1 - 0.3718\chi_2 - 0.3718\chi_3 + 0.6015\chi_4 \tag{3.21}
\end{aligned}
\right.
$$

the first antibonding MO (LUMO, two nodal planes);

$$
\left\{
\begin{aligned}
\phi_4 &= C\sum_{m=1}^{4}\chi_m \sin m\frac{4\pi}{5} = C\left(\chi_1 \sin\frac{4\pi}{5} + \chi_2 \sin\frac{8\pi}{5} + \chi_3 \sin\frac{12\pi}{5} + \chi_4 \sin\frac{16\pi}{5}\right) \\
&= C(0.5878\chi_1 - 0.9510\chi_2 + 0.9510\chi_3 - 0.5878\chi_4) \\
&= 0.3718\chi_1 - 0.6015\chi_2 + 0.6015\chi_3 - 0.3718\chi_4 \tag{3.22}
\end{aligned}
\right.
$$

the last antibonding MO, highest in energy (three nodal planes). These MOs coincide with those given in Equations (2.272) of Chapter 2, and whose shapes are sketched in Figure 2.27.

3.2   THE CLOSED POLYENE CHAIN

Next, we want to find the general solution for the system of homogeneous linear equations for the *closed* polyene chain with N atoms yielding the Nth degree secular equation

$$D_N = \begin{vmatrix} -x & 1 & 0 & \cdots & 0 & 0 & 1 \\ 1 & -x & 1 & \cdots & 0 & 0 & 0 \\ \cdots & \cdots & \cdots & \cdots & \cdots & \cdots & \cdots \\ 0 & 0 & 0 & \cdots & 1 & -x & 1 \\ 1 & 0 & 0 & \cdots & 0 & 1 & -x \end{vmatrix} = 0 \qquad (3.23)$$

The homogeneous system corresponding to Equation (3.23) is:

$$\begin{cases} -xc_1 + c_2 + \cdots + c_N = 0 \\ \cdots \\ c_{m-1} - xc_m + c_{m+1} = 0 \\ \cdots \\ c_1 + \cdots + c_{N-1} - xc_N = 0 \end{cases} \qquad (3.24)$$

The general equation for the coefficients is the same as that for the linear chain:

$$c_{m-1} - xc_m + c_{m+1} = 0 \quad m = 1, 2, \cdots, N \qquad (3.25)$$

but with the different boundary conditions:

$$c_0 = c_N, \quad c_1 = c_{N+1} \Rightarrow c_m = c_{m+N} \qquad (3.26)$$

the last being a periodic boundary condition.

The general solution is now the *progressive* wave in complex form:

$$c_m = A \exp(im\,\theta) \qquad (3.27)$$

where i is the imaginary unit ($i^2 = -1$), and the general Equation (3.25) gives:

$$\begin{cases} A\{\exp[i(m-1)\theta] - x\exp(im\theta) + \exp[i(m+1)\theta]\} & = & 0 \\ A\exp(im\,\theta)[\exp(-i\theta) - x + \exp(i\theta)] = c_m(2\cos\theta - x) & = & 0 \end{cases} \qquad (3.28)$$

namely, for $c_m \neq 0$:

$$x = 2\cos\theta \qquad (3.29)$$

as before.

(i) The periodic boundary condition gives:

$$A \exp(im\,\theta) = A \exp[i(m+N)\theta] \tag{3.30}$$

$$\begin{cases} \exp(iN\theta) = \cos N\theta + i\sin N\theta = 1 \\ N\theta = k2\pi \end{cases} \tag{3.31}$$

$$k = 0, \pm1, \pm2, \cdots \begin{cases} \dfrac{N}{2} & N = \text{even} \\[2ex] \pm\dfrac{N-1}{2} & N = \text{odd} \end{cases} \tag{3.32}$$

where k is the *quantum number* for the ring. In this case, all energy levels are doubly degenerate except those for $k = 0$ and $k = N/2$ for $N = $ even.

Therefore, the general solution for the N-atom ring will be:

$$\begin{cases} x_k = 2\cos\theta_k = 2\cos k\dfrac{2\pi}{N} \\[2ex] c_{mk} = A_k \exp\left(im\dfrac{2\pi k}{N}\right) & \text{anticlockwise} \\[2ex] c_{mk} = A_k \exp\left(-im\dfrac{2\pi k}{N}\right) & \text{clockwise} \end{cases} \tag{3.33}$$

If A_k is a normalization factor, the form of the general MO in *complex* form will be:

$$\phi_k = A_k \sum_m \chi_m c_{mk} \tag{3.34}$$

with:

$$c_{mk} = A_k \exp\left(im\dfrac{2\pi k}{N}\right), \qquad c_{mk}^* = A_k \exp\left(-im\dfrac{2\pi k}{N}\right) \tag{3.35}$$

The coefficients can be expressed in *real* form, using Euler's formulae[1], through the transformation:

---

[1] $\exp(\pm i\,\alpha x) = \cos\alpha x \pm i\sin\alpha x$.

$$\begin{cases} \dfrac{c_{mk}-c_{mk}^*}{2i} = A_k \sin m\dfrac{2\pi k}{N} = a_{mk} \\[4mm] \dfrac{c_{mk}+c_{mk}^*}{2} = A_k \cos m\dfrac{2\pi k}{N} = b_{mk} \end{cases} \qquad (3.36)$$

giving the *real* MOs in the form:

$$\phi_k^s = \sum_m \chi_m a_{mk}, \qquad \phi_k^c = \sum_m \chi_m b_{mk} \qquad (3.37)$$

The previous results for cyclobutadiene and benzene given in Section 2.8 of Chapter 2 can be rederived from the general formula (Equation 3.37).

We give below the derivation of the detailed formulae for the closed chain with $N = 6$ (benzene).

3.2.1   Benzene $N = 6$

$$N = 6, \quad \theta_k = k\frac{2\pi}{6} = k\frac{\pi}{3}, \quad x_k = 2\cos k\frac{\pi}{3}, \quad k = 0, \pm 1, \pm 2, 3 \quad (3.38)$$

The roots in ascending order are:

(i) Bonding levels

$$\begin{cases} x_0 = 2 \\[2mm] x_1 = x_{-1} = 2\cos\dfrac{\pi}{3} = 1 \end{cases} \qquad (3.39)$$

(ii) Antibonding levels

$$\begin{cases} x_2 = x_{-2} = 2\cos\dfrac{2\pi}{3} = -1 \\[4mm] x_3 = 2\cos\dfrac{3\pi}{3} = -2 \end{cases} \qquad (3.40)$$

which coincide with those of Equations (2.284) of Chapter 2.

For the *real* coefficients, we have:

$$a_{mk} = A \sin m\frac{k\pi}{3}, \quad b_{mk} = A \cos m\frac{k\pi}{3} \tag{3.41}$$

with A a normalization factor.

For the MOs in real form, we then have:

$$\phi_0 = \phi_0^c = A \sum_{m=1}^{6} \chi_m \cos\theta = \frac{1}{\sqrt{6}}(\chi_1 + \chi_2 + \chi_3 + \chi_4 + \chi_5 + \chi_6) \tag{3.42}$$

the deepest bonding MO (no nodal planes);

$$\begin{cases} \phi_1^s = A\sum_{m=1}^{6}\chi_m \sin m\frac{\pi}{3} = \frac{1}{2}(\chi_1 + \chi_2 - \chi_4 - \chi_5) \\ \phi_1^c = A\sum_{m=1}^{6}\chi_m \cos m\frac{\pi}{3} = \frac{1}{\sqrt{12}}(\chi_1 - \chi_2 - 2\chi_3 - \chi_4 + \chi_5 + 2\chi_6) \end{cases} \tag{3.43}$$

the second bonding doubly degenerate MOs (HOMOs, one nodal plane);

$$\begin{cases} \phi_2^s = A\sum_{m=1}^{6}\chi_m \sin m\frac{2\pi}{3} = \frac{1}{2}(\chi_1 - \chi_2 + \chi_4 - \chi_5) \\ \phi_2^c = A\sum_{m=1}^{6}\chi_m \cos m\frac{2\pi}{3} = \frac{1}{\sqrt{12}}(-\chi_1 - \chi_2 + 2\chi_3 - \chi_4 - \chi_5 + 2\chi_6) \end{cases}$$

$$\tag{3.44}$$

the first antibonding doubly degenerate MOs (LUMOs, two nodal planes);

$$\phi_3 = \phi_3^c = A \sum_{m=1}^{6} \chi_m \cos\frac{3\pi}{3} = \frac{1}{\sqrt{6}}(-\chi_1 + \chi_2 - \chi_3 + \chi_4 - \chi_5 + \chi_6) \tag{3.45}$$

the last antibonding MO, highest in energy (three nodal planes). The MOs obtained in this way differ by an orthogonal transformation from those

given in Equations (2.285) of Chapter 2. This transformation was derived elsewhere (Magnasco, 2007), and was shown to be given by the orthogonal matrix:

$$
\mathbf{U} = \begin{pmatrix}
1 & 0 & 0 & 0 & 0 & 0 \\
0 & \dfrac{1}{2} & \dfrac{\sqrt{3}}{2} & 0 & 0 & 0 \\
0 & \dfrac{\sqrt{3}}{2} & -\dfrac{1}{2} & 0 & 0 & 0 \\
0 & 0 & 0 & \dfrac{\sqrt{3}}{2} & \dfrac{1}{2} & 0 \\
0 & 0 & 0 & \dfrac{1}{2} & -\dfrac{\sqrt{3}}{2} & 0 \\
0 & 0 & 0 & 0 & 0 & -1
\end{pmatrix}
\tag{3.46}
$$

the two sets of MOs being connected by the matrix transformation:

$$
\phi = \phi' U \tag{3.47}
$$

where the row vector:

$$
\phi' = (\phi_0^c \ \phi_1^s \ \phi_1^c \ \phi_2^s \ \phi_2^c \ \phi_3^c) \tag{3.48}
$$

is the actual set, and:

$$
\phi = (\phi_1 \ \phi_2 \phi_3 \ \phi_4 \ \phi_5 \ \phi_6) \tag{3.49}
$$

is that resulting from Equations (285).

Since matrix (3.46) has a block-diagonal form, its larger blocks being matrices of order 2, matrix multiplications in Equation (3.47) can be easily done block-by-block involving matrices of order 2 at most.

So that, while it is immediately evident that:

$$
\phi_1 = \phi_0^c \tag{3.50}
$$

$$
\phi_6 = \phi_3^c \tag{3.51}
$$

we have for the first degenerate block (E_1 symmetry, bonding HOMOs):

$$(\phi_2 \phi_3) = (\phi_1^s \phi_1^c) \begin{pmatrix} \dfrac{1}{2} & \dfrac{\sqrt{3}}{2} \\[2ex] \dfrac{\sqrt{3}}{2} & -\dfrac{1}{2} \end{pmatrix} \tag{3.52}$$

giving the second real MO as:

$$\begin{cases} \dfrac{1}{2}\phi_1^s + \dfrac{\sqrt{3}}{2}\phi_1^c = \\[2ex] = \dfrac{1}{4}\left[\begin{array}{l} \chi_1(1+1)+\chi_2(1-1)+\chi_3(0-2)+ \\ +\chi_4(-1-1)+\chi_5(-1+1)+\chi_6(0+2) \end{array} \right] \\[3ex] = \dfrac{1}{4}(2\chi_1 - 2\chi_3 - 2\chi_4 + 2\chi_6) \\[2ex] = \dfrac{1}{2}(\chi_1 - \chi_3 - \chi_4 + \chi_6) = \phi_2 \propto \mathrm{x} \end{cases} \tag{3.53}$$

which coincides with the second MO of Equations (2.285), transforming like x. It is seen that this transformed MO corresponds to an anticlockwise rotation by $2\pi/6$ around an axis perpendicular to the molecular plane of benzene of the second MO of Equations (3.43).

For the third real MO calculation gives:

$$\begin{cases} \dfrac{\sqrt{3}}{2}\phi_1^s - \dfrac{1}{2}\phi_1^c = \\[2ex] = \dfrac{\sqrt{3}}{4}\left[\begin{array}{l} \chi_1\left(1-\dfrac{1}{3}\right)+\chi_2\left(1+\dfrac{1}{3}\right)+\chi_3\left(0+\dfrac{2}{3}\right)+ \\[2ex] +\chi_4\left(-1+\dfrac{1}{3}\right)+\chi_5\left(-1-\dfrac{1}{3}\right)+\chi_6\left(0-\dfrac{2}{3}\right) \end{array} \right] \\[3ex] = \dfrac{\sqrt{3}}{4}\left(\dfrac{2}{3}\chi_1 + \dfrac{4}{3}\chi_2 + \dfrac{2}{3}\chi_3 - \dfrac{2}{3}\chi_4 - \dfrac{4}{3}\chi_5 - \dfrac{2}{3}\chi_6\right) \\[2ex] = \dfrac{1}{\sqrt{12}}(\chi_1 + 2\chi_2 + \chi_3 - \chi_4 - 2\chi_5 - \chi_6) = \phi_3 \propto \mathrm{y} \end{cases} \tag{3.54}$$

and we obtain the third MO of Equations (2.285), transforming like y.

In a similar way, we obtain for the second degenerate block (symmetry E_2, antibonding LUMOs):

$$(\phi_4 \phi_5) = (\phi_2^s \phi_2^c) \begin{pmatrix} \dfrac{\sqrt{3}}{2} & \dfrac{1}{2} \\[3mm] \dfrac{1}{2} & -\dfrac{\sqrt{3}}{2} \end{pmatrix} \tag{3.55}$$

giving first:

$$\left\{ \begin{aligned} & \frac{\sqrt{3}}{2}\phi_2^s + \frac{1}{2}\phi_2^c = \\[2mm] & = \frac{\sqrt{3}}{4}\left[\begin{aligned} & \chi_1\left(1-\frac{1}{3}\right) + \chi_2\left(-1-\frac{1}{3}\right) + \chi_3\left(0+\frac{2}{3}\right) \\[2mm] & + \chi_4\left(1-\frac{1}{3}\right) + \chi_5\left(-1-\frac{1}{3}\right) + \chi_6\left(0+\frac{2}{3}\right) \end{aligned} \right] \\[2mm] & = \frac{\sqrt{3}}{4}\left(\frac{2}{3}\chi_1 - \frac{4}{3}\chi_2 + \frac{2}{3}\chi_3 + \frac{2}{3}\chi_4 - \frac{4}{3}\chi_5 + \frac{2}{3}\chi_6\right) \\[2mm] & = \frac{1}{\sqrt{12}}(\chi_1 - 2\chi_2 + \chi_3 + \chi_4 - 2\chi_5 + \chi_6) = \phi_4 \propto x^2 - y^2 \end{aligned} \right. \tag{3.56}$$

the first antibonding LUMO transforming like $(x^2 - y^2)$ and, next:

$$\left\{ \begin{aligned} & \frac{1}{2}\phi_2^s - \frac{\sqrt{3}}{2}\phi_2^c = \\[2mm] & = \frac{1}{4}\left[\begin{aligned} & \chi_1(1+1) + \chi_2(-1+1) + \chi_3(0-2) \\[2mm] & + \chi_4(1+1) + \chi_5(-1+1) + \chi_6(0-2) \end{aligned} \right] \\[2mm] & = \frac{1}{2}(\chi_1 - \chi_3 + \chi_4 - \chi_6) = \phi_5 \propto xy \end{aligned} \right. \tag{3.57}$$

the second antibonding LUMO, transforming like xy. In this way, we reobtain all results of Equations (2.285) of Chapter 2.

3.3 A MODEL FOR THE ONE-DIMENSIONAL CRYSTAL

Increasing the number of interacting AOs increases the number of resulting MOs (Figure 3.1). For the $C_N H_{N+2}$ polyene chain the molecular orbital levels, which always range between $\alpha + 2\beta$ and $\alpha - 2\beta$, become closer and closer, eventually transforming in *bands* (a continuous succession of molecular levels) which are characteristic of solids.

The first (bonding) and the last (antibonding) energy levels of the linear polyene chain are reported with respect to N in Table 3.1 in units of β. In the last column of the table is the difference in energy between two successive levels. The asymptotic approach of x_1 towards 2 and of x_N towards -2 is apparent from the numbers given in the table, as well as is the decreasing distance between two successive levels, which tends to zero for $N \rightarrow \infty$.

These results can be easily established in general as follows. Using formula (3.14) for the orbital energy of the kth MO of the N-atom linear polyene chain:

$$\varepsilon_k = \alpha + 2\beta \cos \frac{\pi}{N+1} k \qquad (3.58)$$

we obtain the following results.

(i) First level ($k = 1$):

$$\varepsilon_1 = \alpha + 2\beta \cos \frac{\pi}{N+1} \qquad \lim_{N \to \infty} \varepsilon_1 = \alpha + 2\beta \qquad (3.59)$$
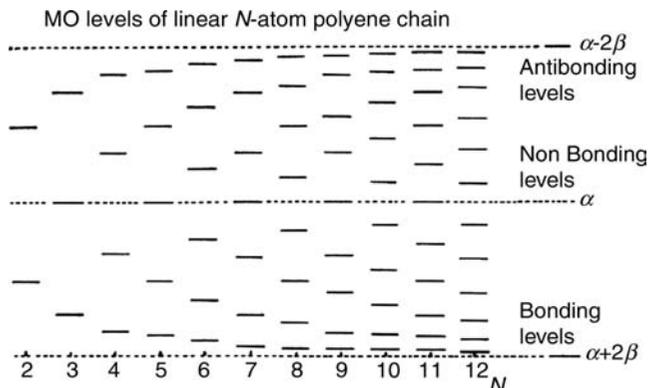
Figure 3.1 Showing the origin of electronic bands in solids as the limit for $N \rightarrow \infty$ of the linear N–atom polyene chain

Table 3.1   Orbital energies (units of β) of first and last level and energy difference between two successive levels in a linear polyene chain as a function of the number of carbon atoms N

N	x_N	x_{N+1}	$x_{N+1} - x_N$
1	0	0	
2	1	−1	1
3	1.414	−1.414	0.414
4	1.618	−1.618	0.204
5	1.732	−1.732	0.114
6	1.802	−1.802	0.070
7	1.848	−1.848	0.046
8	1.879	−1.879	0.031
9	1.902	−1.902	0.023
10	1.919	−1.919	0.017
11	1.932	−1.932	0.011
12	1.942	−1.942	0.010
13	1.950	−1.950	0.008
14	1.956	−1.956	0.006
∞	2	−2	0

(ii) Last level ($k = N$):

$$\varepsilon_N = \alpha + 2\beta \cos \frac{\pi N}{N+1} = \alpha + 2\beta \cos \frac{\pi}{1 + \frac{1}{N}} \qquad \lim_{N \to \infty} \varepsilon_N = \alpha - 2\beta$$

$$(3.60)$$

(iii) Difference between two successive levels:

$$\left\{ \begin{array}{l} \Delta\varepsilon = \varepsilon_{k+1} - \varepsilon_k \\ \quad = 2\beta\left(\cos\frac{\pi}{N+1}(k+1) - \cos\frac{\pi}{N+1}k\right) = -4\beta \sin\frac{\pi}{2}\frac{2k+1}{N+1} \sin\frac{\pi}{2}\frac{1}{N+1} \end{array} \right.$$

$$(3.61)$$

where use was made of the trigonometric identity (see Section 3.6):

$$\cos\alpha - \cos\beta = -2 \sin\frac{\alpha+\beta}{2} \sin\frac{\alpha-\beta}{2} \qquad (3.62)$$

Hence, for $N \to \infty$, $\Delta\varepsilon \to 0$, and we have formation of a continuous band of molecular levels. The limiting values $\alpha + 2\beta$ and $\alpha - 2\beta$ are reached asymptotically when $N \to \infty$. This gives a generalization of the results of Table 3.1 and of the plots of Figure 3.1.

(iv) For $N \to \infty$, therefore, the polyene chain becomes the model for the one-dimensional crystal. We have a bonding band with energy
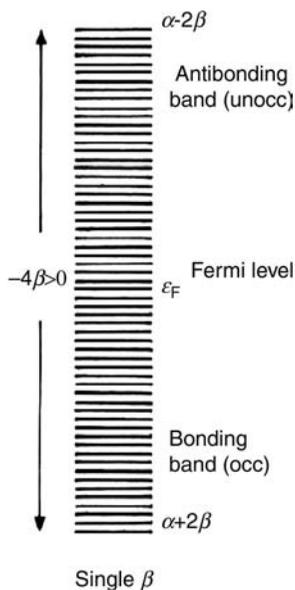
Figure 3.2 Electronic bands in linear polyene chain (single β)

ranging from $\alpha + 2\beta$ to α, and an antibonding band with energy ranging from α to $\alpha - 2\beta$, which are separated by the so-called Fermi level, the top of the bonding band occupied by electrons. It is important to notice that using just one β, equal for single and double bonds as we have done, there is no band gap between bonding and antibonding levels (Figure 3.2). If we admit $|\beta_d| > |\beta_s|$, as reasonable and done by Lennard-Jones in his original work (1937), we have a *band gap* $\Delta = 2(\beta_d - \beta_s)$, which is of great importance in the properties of solids. Figure 3.3 shows the origin of this band gap. In the figure, ε_F is the Fermi level, that is the negative of minimum energy required to ionize the system. Metals and covalent solids, conductors and insulators, semiconductors, can all be traced back to the model of the infinite polyene chain extended to three dimensions (McWeeny, 1979).

3.4 ELECTRONIC BANDS IN CRYSTALS

From Equation (3.61), we can define a density of energy levels or *density of states* $N(\varepsilon)$ in the crystal as $\Delta \varepsilon^{-1}$. $N(\varepsilon)$ is a function giving the number or
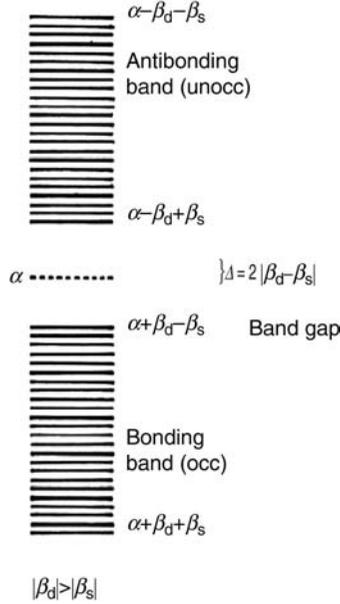
Figure 3.3   Electronic bands in linear polyene chain (double β)

levels (or states) in an infinitesimal range of ε, and is quantitatively defined as:

$$N(\varepsilon) = \frac{\partial k}{\partial \varepsilon} = \left(\frac{\partial \varepsilon}{\partial k}\right)^{-1} = -\frac{1}{2\beta}\frac{N+1}{\pi}\operatorname{cosec}\frac{\pi k}{N+1} \tag{3.63}$$

In fact, from Equation (3.14):

$$\varepsilon = \alpha + 2\beta\cos\frac{\pi k}{N+1} \tag{3.64}$$

$$\frac{\partial \varepsilon}{\partial k} = -2\beta\frac{\pi}{N+1}\sin\frac{\pi k}{N+1} \tag{3.65}$$

$$\left(\frac{\partial \varepsilon}{\partial k}\right)^{-1} = -\frac{1}{2\beta}\frac{N+1}{\pi}\operatorname{cosec}\frac{\pi k}{N+1} \tag{3.66}$$

or, by expressing k as $f(\varepsilon)$:

$$\cos\frac{\pi k}{N+1} = \frac{\varepsilon - \alpha}{2\beta} \tag{3.67}$$

$$\frac{\pi k}{N+1} = \cos^{-1}\left(\frac{\varepsilon-\alpha}{2\beta}\right) \tag{3.68}$$

where $^{-1}$ denotes the *inverse* function.

Hence, remembering from elementary analysis that:

$$\frac{\mathrm{d}\cos^{-1}u}{\mathrm{d}u} = -(1-u^2)^{-1/2} \tag{3.69}$$

we have:

$$k = \frac{N+1}{\pi}\cos^{-1}\left(\frac{\varepsilon-\alpha}{2\beta}\right) \tag{3.70}$$

$$\begin{cases} \dfrac{\partial k}{\partial \varepsilon} = -\dfrac{1}{2\beta}\dfrac{N+1}{\pi}\left[1-\left(\dfrac{\varepsilon-\alpha}{2\beta}\right)^2\right]^{-1/2} \\[4mm] = -\dfrac{1}{2\beta}\dfrac{N+1}{\pi}\left(\sin^2\dfrac{\pi k}{N+1}\right)^{-1/2} = -\dfrac{1}{2\beta}\dfrac{N+1}{\pi}\mathrm{cosec}\dfrac{\pi k}{N+1} \end{cases} \tag{3.71}$$

the same result as before.

To introduce further details of the theory of solids in an elementary way, we can resort to the results given in Section 3.2 for the closed chain with N atoms. We have shown there that the general solution in complex form for the N-atom closed chain with $N = $ odd is:

$$\begin{cases} x_k = 2\cos\dfrac{2\pi k}{N+1} \qquad k = 0, \pm 1, \pm 2, \cdots, \pm\left(\dfrac{N-1}{2}\right) \\[4mm] c_{mk} \propto \exp\left(2\pi i\dfrac{mk}{N}\right) \end{cases} \tag{3.72}$$

where i is the imaginary unit. Apart from the ground state $(k = 0)$, roots (3.72) occur in pairs, each level being hence doubly degenerate.

Let consider as an example the cases $N = 5$ and $N = 15$. We have the numerical results of Table 3.2 which are plotted in Figure 3.4.

For solids, the quantum number k is replaced by the wave vector $\boldsymbol{\kappa}$:

$$\boldsymbol{\kappa}a = \frac{2\pi k}{N}, \quad \boldsymbol{\kappa} = 0, \pm\frac{\pi}{a}\frac{2}{N}, \cdots, \pm\frac{\pi}{a}\left(1-\frac{1}{N}\right) \tag{3.73}$$

where a is the lattice spacing.

Table 3.2   Roots of the closed chains for $N = 5$ and $N = 15$

$N = 5$			$N = 15$
k	$x_k = 2 \cos \frac{2\pi k}{5}$	k	$x_k = 2 \cos \frac{2\pi k}{15}$
0	2	0	2
± 1	0.618	± 1	1.827
± 2	-1.618	± 2	1.338
		± 3	0.618
		± 4	-0.219
		± 5	-1
		± 6	-1.618
		± 7	-1.956

For $N \to \infty$, we have the plots sketched in Figure 3.5, that on the left giving $x(\kappa)$ versus κ, that on the right the energy levels $\varepsilon(\kappa)$ versus the density of states $N(\varepsilon)$, and where the Fermi level ε_F is apparent.

In the crystal, the periodic potential of the nuclei will perturb the energy levels, removing the double degeneracy of the two states corresponding to $\pm \pi / a$, the splitting manifesting itself as a band gap in the energy spectrum. For the values of κ for which $\lambda = 2a$ this originates discontinuities in the spectrum, giving gaps that divide the $|\kappa|$ space into zones called *Brillouin zones*. The region from $|\kappa| = 0$ is the first break, called the first Brillouin zone, from there up to the second break is the second Brillouin zone, and so on. These zones have the dimensions of reciprocal length, and are schematically plotted in Figure 3.6.
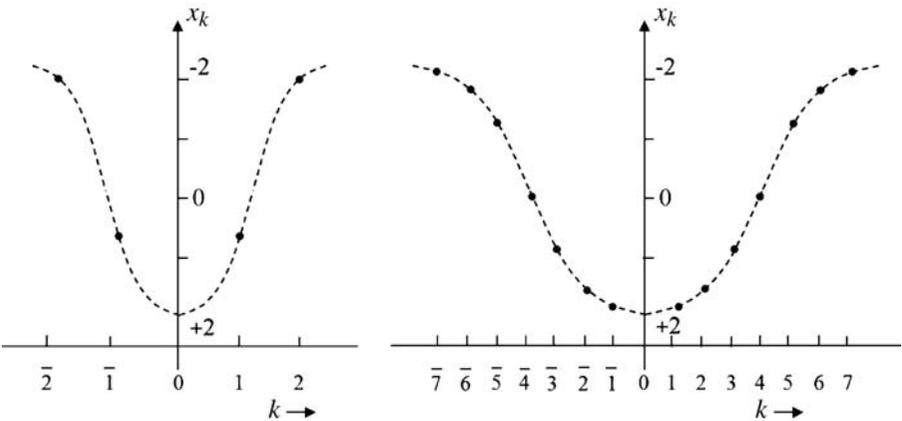
Figure 3.4   Plots of the roots for the closed chain with $N = 5$ (left) and $N = 15$ (right)
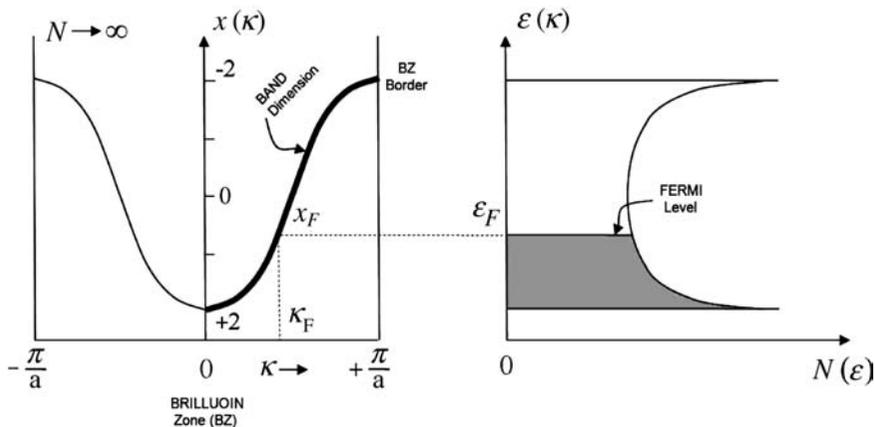
Figure 3.5 Energy levels versus κ (left), and energy levels versus density of states (right)
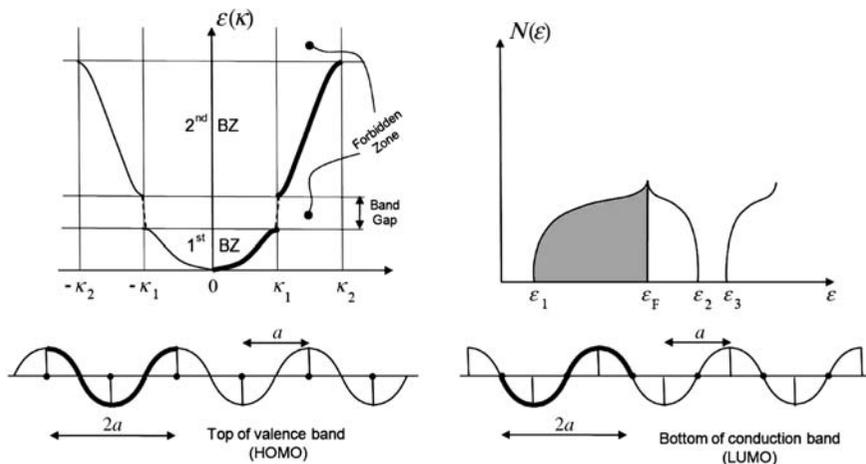
Figure 3.6 One-dimensional Brillouin zones

Figure 3.7 gives a sketch of the $N(\varepsilon)$–ε curve for the d-band of the bcc[2] $Fe(3d^6 4s^2)$ crystal as calculated numerically via the APW[3] method by Wood (1962).

---

[2] Body-centred cubic.

[3] The APW (augmented plane wave) method was devised by Slater (1937, 1965), and is based on the solution of the Schrödinger equation for a spherical periodic potential using an expansion of the wavefunction in terms of solutions of the atomic problem *near* the nucleus, and an expansion in plane waves *outside* a predetermined sphere in the crystal.
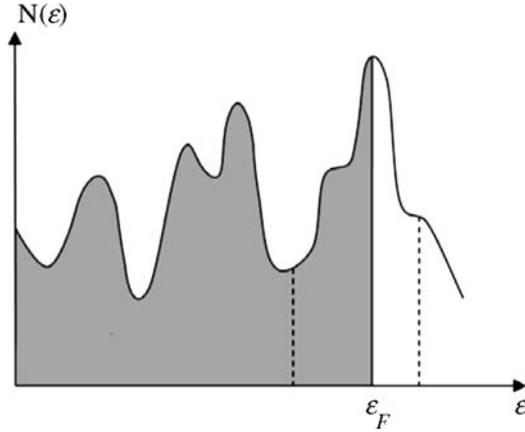
Figure 3.7 Sketch of the $N(\varepsilon)$–ε curve for the bcc Fe($3d^6 4s^2$) crystal

Table 3.3 Electrical conductivity ($ohm^{-1} cm^{-1}$) of different materials

Conductivity	10^{-12}	10^{-2}	10^5	$\gg 10^5$
Material	Insulator	Semiconductor	Conductor	Superconductor
Substance	Si or C	Si or Ge	Metals	$YBa_2Cu_3O_9$

3.5 INSULATORS, CONDUCTORS, SEMICONDUCTORS AND SUPERCONDUCTORS

Insulators can be distinguished from conductors or semiconductors in terms of their different conductivity at room temperature ($T = 293$ K) as shown in Table 3.3.

To give a general description of covalent solids and metals, the band theory arising from the infinite polyene chain must be extended to three dimensions. The properties of solids depend largely on the way in which electrons fill the different available bands.

Figure 3.8 shows the behaviour of the electronic bands in crystalline Be as a function of the lattice spacing R. When the spacing in the (hcp)[4] crystal lattice is very large, the energy bands will be very narrow and centred on the atomic levels of energy ε_{2s} and ε_{2p}. When spacing is reduced, electronic bands enlarge until they begin to overlap. At the equilibrium distance in the crystal lattice R_{eq}, the electronic bands

---

[4] Hexagonal close-packed.
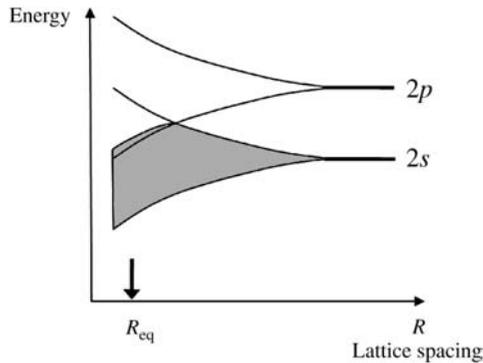
Figure 3.8   Overlap of electronic bands in solid Be

originating from the $2s$ and $2p$ atomic levels will overlap, while the inner $1s$ band will still be very separated because of its large difference in energy. Each Be $(1s^2 2s^2)$ atom will contribute four electrons to the solid. Two electrons come from the inner shell and are sufficient to fill the $1s$ band completely. The other two electrons come from the valence $2s$ orbital, and suffice to fill the $2s$ band completely. At large lattice spacings, the ground state of the solid will have a completely filled $1s$ band and a completely filled $2s$ band, and there will be a gap between the $2s$ filled band and the $2p$ empty band. At variance with what occurs in metals, a large amount of energy, the Δ_{2s-2p} band gap, will be needed to transfer electrons from filled to empty orbitals, so that solid Be with a large value of R will be an insulator. However, at R_{eq} in solid Be, the two $2s$ and $2p$ bands partially overlap and the crystal orbitals will have both s and p character, so that the overlapping bands can now contain eight electrons from each atom. The two electrons that each Be atom can contribute at the valence level will only partially fill the combined bands, so that there will be no energy gap among occupied and empty levels, and solid Be at its equilibrium lattice distance R_{eq} will be a typical metal.

The fact that a solid is a metal or a nonmetal will therefore depend on three factors: (i) the separation of the orbital energies in the free atom; (ii) the lattice spacing; and (iii) the number of electrons provided by each atom. For a realistic description of the three-dimensional crystal, we must therefore extend our simple Hückel theory[5] in two respects. First, we must consider more than a single type of AOs (e.g. $2s$, $2p$, $3d$, $\cdots$), and, second, we must consider more than an electron per atom. By increasing the

---

[5] In solid state theory called the tight-binding approximation (TBA) (see Table 3.4).
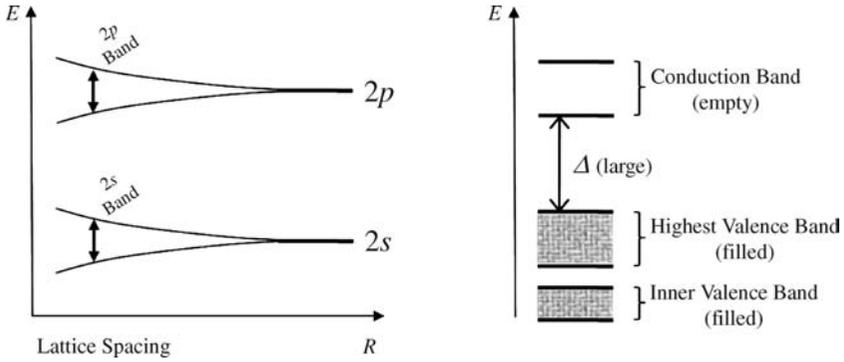
Figure 3.9   Band structure of covalent solids (insulators)

external pressure on a solid, namely by compressing it, will reduce the
lattice spacing, widening the bands, so that under sufficient pressure, all
solids will display metallic character (as first claimed by J.D. Bernal,
quoted in Wigner and Huntington, 1935; see also Yakovlev, 1976).

A *covalent* solid (insulator, such as diamond, pure state carbon) has
electronic bands which are either completely filled or completely empty,
with a large band gap Δ between the highest level occupied by electrons
and the lowest empty one (Figure 3.9). We have no band overlap at R_{eq},
the valence band being completely filled by electrons that cannot be
excited to the conduction band.

Metals (conductors), instead, have bands that are only partially occu-
pied by electrons (Figure 3.10), this being the reason that gives them their
typical properties of high electrical and thermal conductivity, and metallic
brightness. The energy needed to excite electrons from occupied to empty
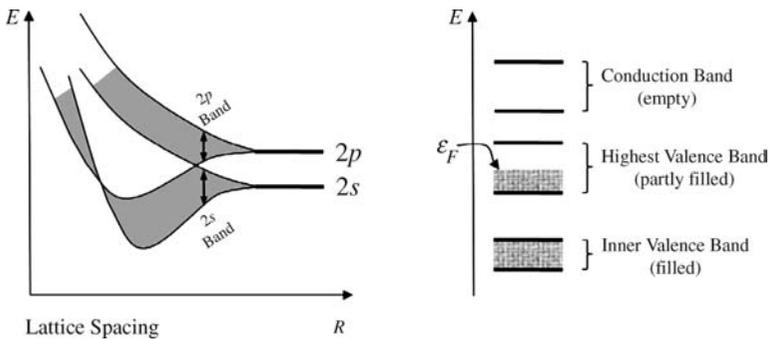
Figure 3.10   Band structure of metals (conductors)
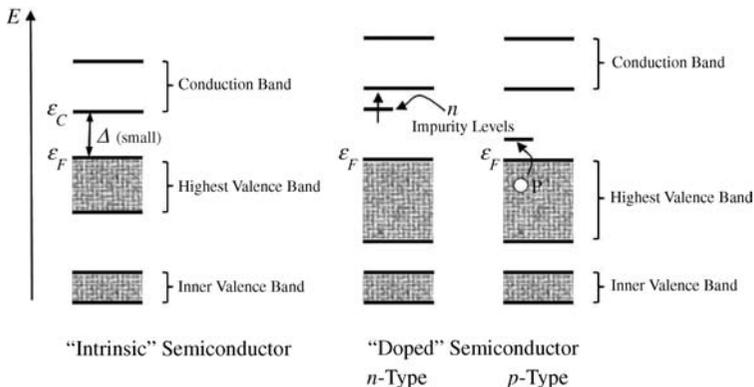
Figure 3.11 Band structure of intrinsic and doped semiconductors

bands is extremely small, their energy being readily distributed over the entire metal because of fully MO delocalization. Furthermore, a metal can absorb light of any wavelength. The highest valence band is only partially filled, and electrons may flow easily under the action of an external field, except for the collisions with the positive ions of the lattice. Increasing temperature increases lattice vibrations and electron collisions, so that electrical conductivity decreases.

Semiconductors have a small band gap, $60–100\,\mathrm{kJ\,mol^{-1}}$, namely $0.6–1\,\mathrm{eV}$ for Ge or Si (Figure 3.11). The electrons of the last valence band are easily excited to the conduction band (empty) under the effect of temperature ($kT \approx \varepsilon_C - \varepsilon_F$) or light ($h\nu \approx \varepsilon_C - \varepsilon_F$), the latter effect being known as photoconductivity. The electronic population in the conduction band will increase with temperature according to the statistical equilibrium described by the Fermi–Dirac statistics, so that conductivity will increase with temperature (the opposite of what was found for metals).

Besides conduction due to the electrons thermally excited to the conduction band (*n*-type, negative charge), there may be conduction due to vacancies occurring in the valence band (*p*-type, where *p* stands for a positive hole). Germanium and silicon are typical intrinsic semiconductors (left-hand side of Figure 3.11), whose properties are due to the pure elements. But also of great importance are the so-called impurity semiconductors, where small amounts of impurity in a perfect crystal lattice can modify the structure of the Brillouin zones, giving products whose properties may be of commercial interest. The 'doping' of silicon or germanium can be done using elements with one *more* electron in their valence shell, such as phosphorus or arsenic, or elements with one *less*
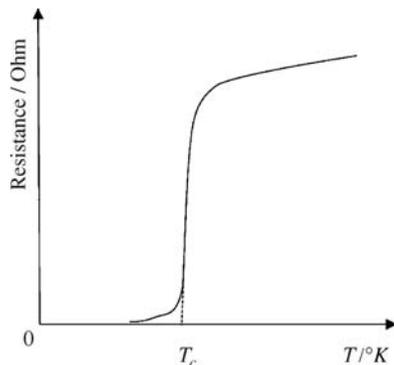
Figure 3.12   Plot of resistance versus temperature for common metals

electron in their valence shell, such as gallium or indium[6]. Conduction now arises from excitation of the electrons *out of* (*n*-type) or *into* (*p*-type) the impurity levels (right-hand side of Figure 3.11). For more information the reader is referred to elsewhere (see, for instance, Murrell *et al.*, 1985).

As we have seen, at low temperatures, resistance to the current flow decreases for all crystal conductors (metals) and, therefore, electric conductivity increases. At a given critical temperature T_c, resistance disappears completely and the metal becomes a *superconductor*, with an infinitely large conductivity (Figure 3.12). For metals, this occurs at rather low temperatures (<30 K), but Bednorz and Müller (1986)[7] prepared new substances exhibiting high-temperature superconductivity (above 77 K, the boiling temperature of liquid N_2). These are alloys containing Cu, O, La (where La may be replaced by Ba, Sr and Y) with a perovskite (La_2CuO_4) lattice structure.

They are structurally homogeneous, perfectly diamagnetic, with a very small band gap, Δ less than 0.1 eV. These materials were prepared by doping perovskites in two ways, either by introducing oxygen-deficient compounds (such as La_2CuO_{4-x}) or by replacing La by other atoms X (such as Ba, Sr, Y). On the theoretical side, Mattheiss (1987) did ab initio calculations of the electronic band structure of tetragonal La_2CuO_4 and of superconductors derivatives of it, such as $La_{2-y}X_yCuO_4$, that throw some light on the factors determining superconductivity at high temperature. The electronic bands at the Fermi surface show a substantially *p*-character. These *p* AOs give strong σ bonds with the $3d$ orbitals of Cu of

---

[6] Ground state valence electron configurations of the elements are: Si($3s^23p^2$) and Ge($4s^24p^2$), P ($3s^23p^3$) and As($4s^24p^3$), Ga($4s^24p$) and In($5s^25p$).
[7] 1987 Nobel Prize for Physics.

Table 3.4 Connection between molecular and solid state terminologies

Molecular theory	Solid state theory
MO (molecular orbital)	Bloch orbital (crystal orbital)
Energy levels	Energy band
HOMO	Valence band
LUMO	Conduction band
HOMO/LUMO energy difference	Band gap
Hückel theory	Tight-binding approximation (TBA)
MO models with electron repulsion	Hückel–Hubbard Hamiltonian
Resonance integral β	Hopping integral t
Jahn–Teller distortion	Peierls distortion
High spin	Magnetic material
Low spin	Nonmagnetic material

appropriate symmetry[8]. The breathing lattice vibrations of the four coplanar O atoms are strongly coupled with the electron conduction band at ε_F, giving a high value for the coupling electron–phonon constant λ that occurs in the Bardeen–Cooper–Schrieffer (BCS) theory of super-conductivity (Tinkham, 1975), with a band gap at ε_F (0.2–0.5 eV) determining a large value of the deformation potential (1.6–3.9 eV/Å). Because of the small mass of the oxygen atoms and the high-frequency ω of lattice vibrations, the pre-exponential factor in the BCS equation for T_c is magnified, thus generating the high T_c values observed for these compounds. The effect is magnified for $X = $ Sr, Ba.

To end this section, it may be useful to the reader to give a table collecting some analogies between molecular and solid state theory (Table 3.4). The table is taken from Albright *et al.* (1985), and is useful in connecting quantum theorist terminology to that of solid state physicists.

3.6 APPENDIX: THE TRIGONOMETRIC IDENTITY

The trigonometric identity (Equation 3.62) can be easily derived as follows. We start from the well-known trigonometric formulae:

$$\cos(x-y) = \cos x \cos y + \sin x \sin y \qquad (3.74)$$

$$\cos(x+y) = \cos x \cos y - \sin x \sin y \qquad (3.75)$$

---

[8] The O_h octahedral symmetry of Cu is distorted to a D_{4h} tetragonal symmetry, with four stronger planar dp–σ bonds and two weaker apical dp–σ bonds.

$$\sin x \, \sin y = \frac{1}{2}\left[\cos(x-y)-\cos(x+y)\right] \qquad (3.76)$$

Subtracting Equation (3.75) from (3.74), immediately gives (3.76). If we put:

$$\begin{cases} x-y = \alpha \\ x+y = \beta \end{cases} \qquad (3.77)$$

then:

$$\begin{cases} x = \dfrac{\alpha+\beta}{2} \\[2ex] y = -\dfrac{\alpha-\beta}{2} \end{cases} \qquad (3.78)$$

and, substituting in Equation (3.76):

$$\sin\frac{\alpha+\beta}{2}\,\sin\left(-\frac{\alpha-\beta}{2}\right) = \frac{1}{2}\left(\cos\alpha-\cos\beta\right) \qquad (3.79)$$

so that we obtain Equation (3.62):

$$\cos\alpha-\cos\beta = -2\sin\frac{\alpha+\beta}{2}\sin\frac{\alpha-\beta}{2} \qquad (3.80)$$

since $\sin x$ is an *odd* function of x, namely:

$$\sin(-x) = -\sin x \qquad (3.81)$$

Part 2

Long-Range Interactions

4

The van der Waals Bond

4.1 INTRODUCTION

In the previous chapters we sketched an elementary model of the chemical bond occurring between atoms in terms of a simple Hückel theory mostly involving solution of 2×2 secular equations. The theory, first concerned with σ-bonding in H_2^+, H_2, He_2^+, He_2, was next extended to σ- and π-bonding in first-row homonuclear diatomics and to the study of multiple bonds, the fundamental quantity being a bond integral β, whose form is

unspecified, but was assumed to depend on positive overlap between AOs of like symmetry on the interacting atoms. Thereafter, the method was extended to consideration of the heteropolar chemical bond with introduction of a further parameter, the atomic energy difference $\alpha_B - \alpha_A$ between A and B, to the study of bond stereochemistry in first-row hydrides (HF, H_2O, NH_3, and CH_4), and to the investigation of delocalization effects in the π electrons of a few conjugated and aromatic hydrocarbons. After giving the general solution for linear and closed N-atom polyene chains, in Chapter 3 the theory was extended to an elementary theory of the electronic bands in solids.

It was shown there that *a chemical bond can be established at short range between overlapping atoms through the linear superposition of their valence atomic orbitals of like symmetry, provided the number of electrons in the resulting bonding MOs is greater than the number of electrons in antibonding MOs.* When this is not the case, as for the dimers X_2 of rare gases, where the number of electrons in antibonding (more repulsive) MOs equals the number of electrons in bonding (less attractive) MOs, we have what is called a Pauli repulsion between closed shells and the formation of any chemical bond is no longer possible. This also happens for the interaction of closed-shell molecules (e.g. H_2, N_2, HF, H_2O) or for atoms in some excited states (e.g. two H or Li atoms interacting with like spin).

On the other hand, Pauli *repulsion* decreases exponentially ($\propto \exp(-aR)$ with $a > 0$) with the distance R between the centres of mass of the interacting molecules and, at large distances, is sufficiently small to be overbalanced by the effect of other *attractive* interactions which decrease more slowly as R^{-n} ($n \geq 6$ for *neutral* systems)[1], and which we call van der Waals (VdW) interactions (Magnasco and McWeeny, 1991; Magnasco, 2007, 2009a). At variance with what observed before in the case of the chemical bond, *VdW interactions occur at long range and can be described in terms of small interaction integrals βs involving orthogonal states[2] having different symmetries and largely different energies.* At least in some simple cases, the form of these βs can be derived in terms of classical electrostatic concepts.

In Section 4.2, we introduce, first, a few elements of Rayleigh–Schrödinger perturbation theory for stationary states (Magnasco, 2007, 2009a), the fundamental theory needed for studying in a quantitative way the weak interactions occurring at long range between atoms and

---

[1] $n \geq 3$ for the dipolar molecules generating the hydrogen bond described in Chapter 5.
[2] Usually, the ground state and some excited states of higher energy.

molecules, just to define unequivocally the physical meaning of the different components of the interactions. An outline of these interactions for molecules is presented in Section 4.3.

In Section 4.4, we introduce a simple two-state model of these weak interactions (Magnasco, 2004b), which expresses the energy lowering in terms of a long-range interaction parameter β, with an application to the case of the dipole polarizability of the H atom. The explicit form of these βs for atom–atom dispersion, atom–linear molecule dispersion, and atom–linear molecule induction, is presented in Section 4.5, avoiding any calculation of matrix elements (Magnasco *et al.*, 1990b) and giving a rather detailed, yet simple, explanation of the nature of the VdW bond occurring between closed-shell atoms and molecules. In this way, we derive the C_6 coefficients and their dependence on the relative molecular orientation for these systems. A detailed calculation of the C_6 dispersion coefficient for the H–H interaction is presented in Section 4.6, while Section 4.7 introduces the reader to an understanding of the nature of the van der Waals bond. A comparison between C_6 dispersion and induction coefficients, and a tabulation of VdW bond strengths and shapes in homodimers of atoms and molecules using data from the literature is included to emphasize the difference occurring between chemical and VdW bonds.

The chapter ends with a short outline of the theory of the temperature-dependent Keesom interactions in polar gases.

4.2   ELEMENTS OF RAYLEIGH–SCHRÖDINGER (RS) PERTURBATION THEORY

Since this important method of approximation is fully described elsewhere (Magnasco, 2007, 2009a), we limit ourselves here to the main elements of the RS theory for stationary states.

We want to solve the Schroedinger eigenvalue equation:

$$(\hat{H}-E)\psi = 0 \qquad (4.1)$$

for a *Hermitian* decomposition of the Hamiltonian $\hat{H}$ into:

$$\hat{H} = \hat{H}_0 + \lambda\hat{H}_1 \qquad (4.2)$$

where: (i) λ is a parameter giving the *orders* in perturbation theory[3] ; (ii) $\hat{H}_0$ the *unperturbed* Hamiltonian, namely the Hamiltonian of a

---

[3] Orders are here indicated by the suffixes or their sum.

previously solved problem (either physical or model); and (iii) $\hat{H}_1$ the *small* first-order difference between $\hat{H}$ and $\hat{H}_0$, called the *perturbation*.

We now expand both eigenvalue E and eigenfunction ψ into powers of λ:

$$E = E_0 + \lambda E_1 + \lambda^2 E_2 + \lambda^3 E_3 + \cdots \tag{4.3}$$

$$\psi = \psi_0 + \lambda \psi_1 + \cdots \tag{4.4}$$

where the coefficients of the different powers of λ are, respectively, the *corrections* of the various orders to energy and wavefunction (e.g., E_2 is the second-order energy correction, ψ_1 the first-order correction to the wavefunction, and so on). It is often useful to define corrections up to a given order, which we write, for example:

$$E^{(3)} = E_0 + E_1 + E_2 + E_3 \tag{4.5}$$

meaning that we add corrections *up to* the third order.

By substituting the expansions into the Schrödinger equation (4.1):

$$[(\hat{H}_0 - E_0) + \lambda(\hat{H}_1 - E_1) - \lambda^2 E_2 - \lambda^3 E_3 - \cdots] (\psi_0 + \lambda \psi_1 + \lambda^2 \psi_2 + \cdots) = 0 \tag{4.6}$$

separating the orders, we obtain a set of ordered equations:

$$\begin{cases} \lambda^0 & (\hat{H}_0 - E_0)\psi_0 = 0 \\ \lambda & (\hat{H}_0 - E_0)\psi_1 + (\hat{H}_1 - E_1)\psi_0 = 0 \\ \lambda^2 & (\hat{H}_0 - E_0)\psi_2 + (\hat{H}_1 - E_1)\psi_1 - E_2\psi_0 = 0 \\ & \quad \cdots \end{cases} \tag{4.7}$$

which are known as Rayleigh–Schrödinger (RS) perturbation equations of the various orders specified by the power of λ.

Because of the Hermitian property of $\hat{H}_0$, bracketing Equations (4.7) on the left by $\langle \psi_0|$, all the first terms in the RS equations are zero, and we are left with:

$$\begin{cases} \lambda^0 & \langle \psi_0 | \hat{H}_0 - E_0 | \psi_0 \rangle = 0 \\ \lambda & \langle \psi_0 | \hat{H}_1 - E_1 | \psi_0 \rangle = 0 \\ \lambda^2 & \langle \psi_0 | \hat{H}_1 - E_1 | \psi_1 \rangle - E_2 \langle \psi_0 | \psi_0 \rangle = 0 \\ & \quad \cdots \end{cases} \tag{4.8}$$

Taking ψ_0 normalized to 1, we then obtain from Equations (4.8) the RS energy corrections of the various orders as:

$$\begin{cases} \lambda^0 & E_0 = \langle\psi_0|\hat{H}_0|\psi_0\rangle \\ \lambda & E_1 = \langle\psi_0|\hat{H}_1|\psi_0\rangle \\ \lambda^2 & E_2 = \langle\psi_0|\hat{H}_1-E_1|\psi_1\rangle = -\langle\psi_1|\hat{H}_0-E_0|\psi_1\rangle \\ \lambda^3 & E_3 = \langle\psi_0|\hat{H}_1-E_1|\psi_2\rangle-E_2\langle\psi_0|\psi_1\rangle = \langle\psi_1|\hat{H}_1-E_1|\psi_1\rangle \\ & \qquad\qquad \cdots \end{cases} \qquad (4.9)$$

E_0 and E_1 are nothing but the average value of $\hat{H}_0$ and $\hat{H}_1$, respectively, over the unperturbed function ψ_0, while E_2 is given as a *nondiagonal* term, often referred to as *transition integral*, connecting ψ_0 to ψ_1 through the operator $\hat{H}_1$, the last expression in Equations (4.9), showing that E_2 is always greater than zero for the ground state. The equations above show that knowledge of ψ_1 (the solution of the first-order RS differential equation) determines the energy corrections up to third order[4]. In solving the first-order RS differential equation, we impose on ψ_1 the *orthogonality* condition:

$$\langle\psi_0|\psi_1\rangle = 0 \qquad (4.10)$$

which follows in first order from the normalization condition on the total wavefunction and the fact that we assume a normalized ψ_0. The detailed explanation of the symmetric forms resulting for E_2 an E_3 in Equations (4.9) is given elsewhere (Magnasco, 2007, 2009a).

Variational approximations to the second-order energy E_2 are obtained using the Hylleraas variational method outlined in Section 1.3 of Chapter 1.

It is important to stress that the leading term of the RS perturbation Equations (4.7), the zeroth- order equation $(\hat{H}_0-E_0)\psi_0 = 0$, must be satisfied *exactly*, otherwise uncontrollable errors will affect the whole chain of equations. Furthermore, it must be observed that only energy in first order gives an upper bound to the true energy of the ground state, so that the energy in second order, $E^{(2)}$, may be *below* the true value.

4.3 MOLECULAR INTERACTIONS

We now apply our RS perturbation equations to the interaction between two molecules A and B whose non-expanded intermolecular potential V

---

[4] Likely, ψ_n determines the energy corrections up to order $2n + 1$. We recall that all $\psi_n(n \neq 0)$ corrections are *not* normalized but are normalizable.
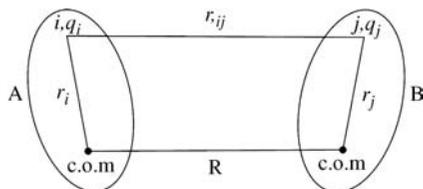
Figure 4.1 Interparticle distances in the intermolecular potential. Reprinted from Magnasco, V., Methods of Molecular Quantum Mechanics: An Introduction to Electronic Molecular Structure. Copyright (2009) with permission from John Wiley and Sons

arises from the Coulombic interactions between all pairs i, j of charged particles (electrons + nuclei) in the molecules (Figure 4.1):

$$V = \sum_i \sum_j \frac{q_i q_j}{r_{ij}} \tag{4.11}$$

where q_i and q_j are the charges of particles i (belonging to A) and j (belonging to B) interacting at the distance r_{ij}. In a previous book (Magnasco, 2009a) a readable introduction was given to the interatomic interactions occurring at long range between two ground state H atoms.

4.3.1   Non-expanded Energy Corrections up to Second Order

If A_0, B_0 are the unperturbed wavefunctions of molecules A (N_A electrons) and B (N_B electrons), and A_i, B_j a pair of excited pseudostates describing single excitations on A and B, all fully antisymmetrized within the space of A and B, we have to second order of RS perturbation theory:

$$E_1^{cb} = \langle A_0 B_0 | V | A_0 B_0 \rangle = E_1(es) \tag{4.12}$$

the semiclassical *electrostatic* energy arising in first order from the interactions between undistorted A and B;

$$\tilde{E}_2^{ind,A} = -\sum_i \frac{|\langle A_i B_0 | V | A_0 B_0 \rangle|^2}{\varepsilon_i} = -\sum_i \frac{|(A_0 A_i | U^B)|^2}{\varepsilon_i} \tag{4.13}$$

the *polarization* (distortion) of A by the static field of B, described by U^B:

$$U^B = \langle B_0 | V | B_0 \rangle \tag{4.14}$$

the molecular electrostatic potential (MEP) of B;

$$\tilde{E}_2^{ind,B} = -\sum_j \frac{|\langle A_0 B_j | V | A_0 B_0 \rangle|^2}{\varepsilon_j} = -\sum_j \frac{|(B_0 B_j | U^A)|^2}{\varepsilon_j} \tag{4.15}$$

the *polarization* (distortion) of B by the static field of A, described by the MEP U^A;

$$\tilde{E}_2^{disp} = -\sum_i \sum_j \frac{\left|\langle A_i B_j | V | A_0 B_0 \rangle\right|^2}{\varepsilon_i + \varepsilon_j} = -\sum_i \sum_j \frac{\left|\langle A_i B_j \left| \sum_{i < j} r_{i'j'}^{-1} \right| A_0 B_0 \rangle\right|^2}{\varepsilon_i + \varepsilon_j}$$

(4.16)

the *dispersion* interaction, a purely electronic term arising from the density fluctuations of the electrons on A and B which are coupled together through the intermolecular electron repulsion operator r_{12}^{-1} (1 on A, 2 on B).

eneralization of the H–H results to molecules is possible in terms of the charge-density operator (Longuet-Higgins, 1956) and of static and transition electron densities, $P^A(00|\mathbf{r}_1;\mathbf{r}_1)$ and $P^B(00|\mathbf{r}_2;\mathbf{r}_2)$, $P^A(0i|\mathbf{r}_1;\mathbf{r}_1)$ and $P^B(0j|\mathbf{r}_2;\mathbf{r}_2)$, respectively on A and B. The non-expanded dispersion energy between molecules A and B then takes the simple integral form:

$$\tilde{E}_2^{disp} = -\sum_i \sum_j \frac{\left|\int \int d\mathbf{r}_1 d\mathbf{r}_2 \frac{P^A(0i|\mathbf{r}_1;\mathbf{r}_1)P^B(0j|\mathbf{r}_2;\mathbf{r}_2)}{r_{12}}\right|^2}{\varepsilon_i + \varepsilon_j}$$

(4.17)

4.3.2 Expanded Energy Corrections up to Second Order

In molecules, the interaction depends on the distance R between their centres of mass (c.o.m.) as well as on the relative orientation of the interacting partners, which can be specified in terms of the five independent angles[5] $(\theta_A, \theta_B, \varphi, \chi_A, \chi_B)$ shown in Figure 4.2. The first three angles describe the orientation of the principal symmetry axes of the two molecules, the latter two the rotation about these axes.

Expansion at long range gives rise to the typical R^{-n} dependence of the intermolecular interactions. The first components of the long-range intermolecular interaction were studied by the author and coworkers in two papers (Magnasco *et al.*, 1988, 1990b), where the first few coefficients of the R^{-n} expansion were determined explicitly for atom–atom, atom–linear molecule, and linear molecule–linear molecule systems.

In the first order of perturbation theory, the expanded electrostatic energy gives rise to what is known as the interaction between *permanent*

---

[5] These angles are simply related to the Euler angles describing the rotation of a rigid body (Brink and Satchler, 1993).
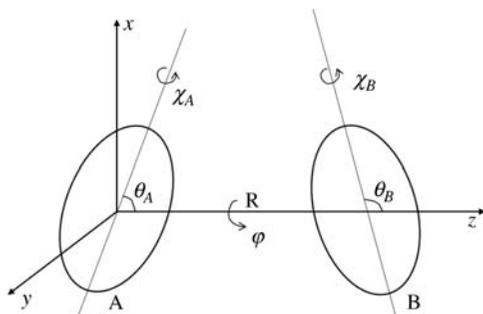
Figure 4.2 The five angles specifying in general the relative orientation of two polyatomic molecules. Reprinted from Magnasco, V., Methods of Molecular Quantum Mechanics: An Introduction to Electronic Molecular Structure. Copyright (2009) with permission from John Wiley and Sons

multipoles[6]. Since atoms have no permanent electric moments, their electrostatic interaction at long range is zero. The values of the first three electric moments at their equilibrium distances for a few molecules are given in Table 5.2 of the next chapter, while Section 5.2.1 gives the explicit expressions of the angular dependence of the first three terms of the expanded electrostatic interaction beteween two hydrogen fluoride molecules.

The two papers cited above also give explicit expressions for the polarization (induction) energies between polar molecules. They are expressed in terms of permanent moments and static polarizabilities of the interacting molecules. Both are observable quantities that can be measured by experiment.

In what follows, we shall limit ourselves mostly to consideration of the long-range dispersion interaction between: (i) two atoms; (ii) two linear molecules A and B; and (iii) an atom A, at the origin of the intermolecular coordinate system, and a linear molecule B, whose orientation with respect to the z axis is specified by the single angle θ (Figure 5.3 in the next chapter).

The expanded dispersion energy involves the interaction between *induced* moments on two atoms, the leading term describing the interaction between induced dipoles on A and B being:

$$E_2^{disp}(6) = -\frac{C_6}{R^6} = -\frac{6}{R^6} \times \frac{1}{4} \sum_i \sum_j \alpha_i^A \alpha_j^B \frac{\varepsilon_i^A \varepsilon_j^B}{\varepsilon_i^A + \varepsilon_j^B} = -\frac{6}{R^6} C_{11} \quad (4.18)$$

---

[6] An electric multipole is specified by its value of l as 2^l−pole ($l = 1$ dipole, $l = 2$ quadrupole, $l = 3$ octupole, etc.). Hence, the electrostatic interaction is between 2^l−$2^{l'}$ poles, the leading term for two dipolar molecules ($l = l' = 1$) being the dipole–dipole interaction.

where C_6 is the London dispersion coefficient, and:

$$C_{11} = \frac{1}{4} \sum_i \sum_j \alpha_i^A \alpha_j^B \frac{\varepsilon_i^A \varepsilon_j^B}{\varepsilon_i^A + \varepsilon_j^B} \tag{4.19}$$

is the dipole–dipole *dispersion constant* in London form. It involves knowledge of the *pseudostate* components[7] of the static dipole polarizabilities of A and B:

$$\alpha^A = \sum_i \alpha_i^A \tag{4.20}$$

$$\alpha^B = \sum_j \alpha_j^B \tag{4.21}$$

where:

$$\alpha_i^A = \frac{2\mu_i^2}{\varepsilon_i} \tag{4.22}$$

is the *i*th pseudostate contribution to the static dipole polarizability of atom A, and:

$$\alpha_j^B = \frac{2\mu_j^2}{\varepsilon_j} \tag{4.23}$$

is the *j*th pseudostate contribution to the static dipole polarizability of atom B. μ_i and μ_j are the *transition* dipole moments on A and B, $\varepsilon_i > 0$ and $\varepsilon_j > 0$ are the excitation energies from the ground states to the excited pseudostates *i* and *j*. We notice that the pseudostate components of the polarizabilities are *not* observable quantities, so that they cannot be measured.

An alternative, yet equivalent, expression for the dipole dispersion constant is the Casimir–Polder formula (Casimir and Polder, 1948):

$$C_{11} = \frac{1}{2\pi} \int_0^\infty du\, \alpha^A(iu)\, \alpha^B(iu) \tag{4.24}$$

which involves integration over the frequency *u* of the frequency-dependent polarizabilities (FDPs) at imaginary frequencies of the two atoms[8].

---

[7] See Section 1.3 of Chapter 1
[8] *u* is the *real* frequency and *i* the imaginary unit ($i^2 = -1$).

While the polarizability of the atom is isotropic, the linear molecule has *two* dipole polarizabilities, $\alpha_{||}$, the parallel or longitudinal component directed along the intermolecular axis, and $\alpha_\perp$, the perpendicular or transverse component perpendicular to the intermolecular axis (McLean and Yoshimine, 1967). The molecular *isotropic* polarizability can be compared to that of atoms, and is defined as:

$$\alpha = \frac{\alpha_{||} + 2\alpha_\perp}{3} \tag{4.25}$$

while:

$$\Delta\alpha = \alpha_{||} - \alpha_\perp \tag{4.26}$$

is the polarizability *anisotropy*, which is zero for $\alpha_\perp = \alpha_{||}$.

The composite system of two *different* linear molecules has hence four independent elementary dipole dispersion constants, which in London form can be written as:

$$\begin{cases} A = \frac{1}{4}\sum_i\sum_j \alpha_{i||}\alpha_{j||}\frac{\varepsilon_{i||}\varepsilon_{j||}}{\varepsilon_{i||}+\varepsilon_{j||}}, & B = \frac{1}{4}\sum_i\sum_j \alpha_{i||}\alpha_{j\perp}\frac{\varepsilon_{i||}\varepsilon_{j\perp}}{\varepsilon_{i||}+\varepsilon_{j\perp}}, \\[2mm] C = \frac{1}{4}\sum_i\sum_j \alpha_{i\perp}\alpha_{j||}\frac{\varepsilon_{i\perp}\varepsilon_{j||}}{\varepsilon_{i\perp}+\varepsilon_{j||}}, & D = \frac{1}{4}\sum_i\sum_j \alpha_{i\perp}\alpha_{j\perp}\frac{\varepsilon_{i\perp}\varepsilon_{j\perp}}{\varepsilon_{i\perp}+\varepsilon_{j\perp}} \end{cases} \tag{4.27}$$

For two *identical* linear molecules, there are three independent dispersion constants since $C = B$.

It has been shown elsewhere (Wormer, 1975; Magnasco and Ottonelli, 1999) that the leading (dipole–dipole) term of the long-range dispersion interaction between two linear molecules has the form:

$$\tilde{E}_2^{disp} = -R^{-6}C_6(\theta_A, \theta_B, \varphi) \tag{4.28}$$

$C_6(\theta_A, \theta_B, \varphi)$ being an *angle-dependent* dipole dispersion coefficient, which can be expressed (Meyer, 1976) in terms of associated Legendre polynomials on A and B as:

$$C_6(\theta_A, \theta_B, \varphi) = C_6 \sum_{L_A L_B M} \gamma_6^{L_A L_B M} P_{L_A}^M(\cos\theta_A) P_{L_B}^M(\cos\theta_B) \tag{4.29}$$

where L_A, $L_B = 0, 2$ and $M = |M| = 0, 1, 2$. In Equation (4.29), C_6 is the isotropic coefficient and γ_6 is an anisotropy coefficient defined as:

$$\gamma_6^{L_A L_B M} = \frac{C_6^{L_A L_B M}}{C_6} \tag{4.30}$$

The different components of the C_6 dispersion coefficients in the $L_A L_B M$ scheme for: (i) two *different* linear molecules, and (ii) an atom and a linear molecule, are given in Table 11.2 of Magnasco and Ottonelli (1999) in terms of the symmetry-adapted combinations of the elementary dispersion constants (Equations (4.27). For *identical* molecules, $C = B$ in (4.27), and the (020) and (200) coefficients are equal.

Therefore, the determination of the elementary dispersion constants (the quantum mechanical relevant part of the calculation) allows for a detailed analysis of the angle-dependent dispersion coefficients between molecules.

4.4   THE TWO-STATE MODEL OF LONG-RANGE INTERACTIONS

We turn now to the more recently proposed two-state model of long-range interactions (Magnasco, 2004b). It is of interest in so far as it avoids completely explicit calculation of the matrix elements (Equations 4.12–4.17) occurring in RS perturbation theory, being based only on the fundamental principles of variation theorem and on a classical electrostatic approach.

For the sake of simplicity, we mix in just two normalized states, an initial state ψ_0 and a final (orthogonal) state ψ_1, the coefficients in the resulting quantum state ψ:

$$\psi = \psi_0 C_0 + \psi_1 C_1 \tag{4.31}$$

being determined by the Ritz method of Chapter 1, giving the 2×2 secular equation:

$$\begin{vmatrix} H_{00}-E & H_{01} \\ H_{01} & H_{11}-E \end{vmatrix} = 0 \tag{4.32}$$

which has the real roots:

$$\begin{cases} E_{\pm} = \dfrac{H_{00}+H_{11}}{2} \pm \dfrac{\Delta}{2} \\[2ex] \Delta = \left[(H_{11}-H_{00})^2 + 4(H_{01})^2 \right]^{1/2} \end{cases} \tag{4.33}$$

Since now $0 < |H_{01}| \ll H_{11}-H_{00}$, the Taylor expansion of Δ we did in Chapter 2 gives for the lowest root the approximate form:

$$E \approx H_{00} - \frac{|H_{01}|^2}{H_{11}-H_{00}} \tag{4.34}$$

$$\Delta E = E - H_{00} \approx -\frac{|H_{01}|^2}{H_{11} - H_{00}} = -\frac{\beta^2}{\Delta\varepsilon} \qquad (4.35)$$

where the energy lowering ΔE is properly described as a small effect, second order in $|H_{01}| = |\beta|$, which involves a transition from ψ_0 to ψ_1 with a (positive) excitation energy $H_{11} - H_{00} = \Delta\varepsilon$.

As an example, explicit expressions of β can be given in the case of the dipole polarizability of the H atom and for a few simple VdW interactions which depend on the electrical properties of the molecules such as electric dipole moments and polarizabilities (Stone, 1996). As we have already said, these dipole moments, and the higher ones known generally as multipole moments, can be *permanent* (when they persist in absence of any external field) or *induced* (when due, temporarily, to the action of an external field and disappear when the field is removed).

An atom or molecule distorts under the action of an external field, the measure of distortion being expressed through a second-order electrical quantity called the (dipole) polarizability α, which we define in terms of a transition moment μ_i from state ψ_0 to ψ_1 and an excitation energy ε_i as:

$$\alpha = \frac{2\mu_i^2}{\varepsilon_i} \qquad (4.36)$$

The interaction of the induced dipole μ_i with the external field F is:

$$\beta = -\mu_i F \qquad (4.37)$$

with a second-order energy lowering that, for a small field, is given by:

$$\Delta E = -\frac{\beta^2}{\Delta E} = -\frac{\mu_i^2 F^2}{\varepsilon_i} = -\frac{1}{2}\left(\frac{2\mu_i^2}{\varepsilon_i}\right)F^2 = -\frac{1}{2}\alpha F^2 \qquad (4.38)$$

where α is the dipole polarizability of the atom. From this relation follows that we can define α as the negative of the second derivative of the energy with respect to the field F evaluated at $F = 0$:

$$\alpha = -\left(\frac{d^2 \Delta E}{dF^2}\right)_{F=0} \qquad (4.39)$$

We have seen that polarizabilities are *isotropic* for atoms, but are *anisotropic* for molecules, showing different response for different directions of the field. For linear molecules we have parallel or longitudinal, $\alpha_{||}$, and transverse or perpendicular, $\alpha_{\perp}$, components in terms of which the isotropic polarizability α and the anisotropy factor $\Delta\alpha$ are defined (Equations 4.25 and 4.26 of Section 4.3.2). For nonlinear molecules α is

given by a polarizability tensor whose nonvanishing components depend on molecular symmetry (Buckingham, 1967). The isotropic polarizability of molecules can be directly compared with the polarizability of atoms. The key role of atomic polarizabilities in assessing intermolecular potentials in a variety of systems has been widely documented (Cambi et al., 1991; Aquilanti et al., 1996).

We now turn to consideration of VdW interactions.

4.5   THE van der WAALS INTERACTIONS

As we have seen, the second-order VdW interactions are: (i) the *distortion* (induction or polarization) interaction, where an atom or molecule is distorted by the permanent electric field provided by a second molecule; and (ii) the *dispersion* interaction, whose leading term arises from the simultaneous coupling of the mutually induced dipoles on the two molecules (Buckingham, 1967; Stone, 1996; Magnasco, 2007, 2009a). The dispersion energy, whose name is derived from the fact that the physical quantities involved are the same as those determining the dispersion of the refractive index in media, is recognized as an interatomic or intermolecular electron correlation (Magnasco and McWeeny, 1991), and is called *London attraction* from the name of the scientist who first explained why two ground state H atoms attract each other in long range (London, 1930a, 1930b).

At the *large* distances at which they usually occur, VdW forces result mostly from *weak* attractive interactions described by second-order processes whose energy lowering is:

$$\Delta E = -\frac{\beta^2}{\Delta\varepsilon} < 0 \qquad (4.40)$$

as we have shown before. Here, $\Delta\varepsilon = \varepsilon_i$ or ε_j for induction (single excitation on A *or* B), $\Delta\varepsilon = \varepsilon_i + \varepsilon_j$ for dispersion (double simultaneous excitations on A *and* B), and, for the leading terms, $\beta^2 = \mu_i^2(F_B)^2$, where μ_i is the dipole on A induced by the field of B.

Let us consider in greater detail the long-range interaction of an atom A (at the origin of the coordinate system) with an atom (or linear molecule) B, whose centre of mass has coordinates R, θ, φ. The problem has been fully treated by Buckingham (1967) using Rayleigh–Schrödinger perturbation theory in terms of cartesian tensors, and by Magnasco et al. (1988, 1990b) in terms of spherical tensors. For the sake of simplicity, we shall give here an elementary derivation in terms of classical electrostatics by considering the

field at A due to a point-like dipole (permanent or induced) at B. The electric potential at A due to the dipole μ_i at B (Coulson, 1958):

$$V_B = \frac{\boldsymbol{\mu}_j \cdot \mathbf{R}}{R^3} = \frac{1}{R^2}\left[\sin\theta(\mu_{jx}\cos\varphi + \mu_{jy}\sin\varphi) + \mu_{jz}\cos\theta\right] \qquad (4.41)$$

originates the electric field (a vector):

$$\mathbf{F}_B = -\nabla V_B \qquad (4.42)$$

having spherical components:

$$(F_B)_R = -\frac{\partial V_B}{\partial R} = \frac{2}{R^3}\left[\sin\theta(\mu_{jx}\cos\varphi + \mu_{jy}\sin\varphi) + \mu_{jz}\cos\theta\right] \qquad (4.43)$$

$$(F_B)_\theta = -\frac{\partial V_B}{R\,\partial\theta} = -\frac{1}{R^3}\left[\cos\theta(\mu_{jx}\cos\varphi + \mu_{jy}\sin\varphi) - \mu_{jz}\sin\theta\right] \qquad (4.44)$$

$$(F_B)_\varphi = -\frac{\partial V_B}{R\sin\theta\,\partial\varphi} = -\frac{1}{R^3}(-\mu_{jx}\sin\varphi + \mu_{jy}\cos\varphi) \qquad (4.45)$$

The square of the electric field of B at A will be:

$$\left\{\begin{array}{l} (F_B)^2 = \mathbf{F}_B \cdot \mathbf{F}_B = (F_B)_R^2 + (F_B)_\theta^2 + (F_B)_\varphi^2 \\[2mm] \qquad = \dfrac{1}{R^6}\left[\begin{array}{l}(3\cos^2\theta + 1)\mu_{jz}^2 + (4-3\cos^2\theta)(\mu_{jx}^2\cos^2\varphi + \mu_{jy}^2\sin^2\varphi) \\[1mm] + (\mu_{jx}^2\sin^2\varphi + \mu_{jy}^2\cos^2\varphi)\end{array}\right]\end{array}\right.$$

$$(4.46)$$

where only diagonal terms have been retained, since off-diagonal terms do not contribute to the integral β.

Different local symmetries on B generate different fields.

(i) Isotropic dipole: $\mu_{jz} = \mu_{jx} = \mu_{jy} = \mu_j$

$$(F_B)^2 = \frac{6\mu_j^2}{R^6} \qquad (4.47)$$

(ii) Cylindrical dipole: $\mu_{jz} = \mu_j, \quad \mu_{jx} = \mu_{jy} = \mu_{j\perp}$

$$(F_B)^2 = \frac{1}{R^6}\left[(3\cos^2\theta + 1)\mu_{j\parallel}^2 + (5-3\cos^2\theta)\mu_{j\perp}^2\right] \qquad (4.48)$$

(iii) Unidimensional dipole: $\mu_{jz} = \mu_B, \quad \mu_{jx} = \mu_{jy} = 0$

$$(F_B)^2 = \frac{\mu_B^2}{R^6}(3\cos^2\theta + 1) \qquad (4.49)$$

We are now in a position to discuss, in a unified way, atom–atom dispersion, atom–linear molecule dispersion, and atom–linear dipolar molecule induction.

4.5.1   Atom–Atom Dispersion

In this case, μ_i, μ_j are both isotropic *induced* dipoles, and we have for the energy lowering:

$$
\begin{cases}
\Delta E = -\dfrac{\beta^2}{\Delta\varepsilon} = -\dfrac{6}{R^6}\dfrac{\mu_i^2\mu_j^2}{\varepsilon_i+\varepsilon_j} \\[2ex]
\quad = -\dfrac{6}{R^6}\dfrac{1}{4}\left(\dfrac{2\mu_i^2}{\varepsilon_i}\right)\left(\dfrac{2\mu_j^2}{\varepsilon_j}\right)\dfrac{\varepsilon_i\varepsilon_j}{\varepsilon_i+\varepsilon_j} \\[2ex]
\quad = -\dfrac{6}{R^6}\dfrac{1}{4}\alpha_i\alpha_j\dfrac{\varepsilon_i\varepsilon_j}{\varepsilon_i+\varepsilon_j} = -\dfrac{C_6}{R^6}
\end{cases}
\tag{4.50}
$$

which is the well-known London dispersion formula. Generally speaking, we can have *several* simultaneous dipole excitations on A and B (the corresponding final states are often referred to as dipole pseudostates), so that we can write:

$$
C_6 = 6 \times \frac{1}{4}\sum_i\sum_j \alpha_i\alpha_j\frac{\varepsilon_i\varepsilon_j}{\varepsilon_i+\varepsilon_j} = 6C_{11}
\tag{4.51}
$$

where C_6 is the London dispersion coefficient, and:

$$
C_{11} = \frac{1}{4}\sum_i\sum_j \alpha_i\alpha_j\frac{\varepsilon_i\varepsilon_j}{\varepsilon_i+\varepsilon_j}
\tag{4.52}
$$

is the *dispersion constant* in London form, while 6 is a geometrical factor.

The leading term of London attraction has an R^{-6} dependence on R, the C_6 coefficient involving knowledge of the individual *nonobservable* (i.e., nonmeasurable) contributions from each excited pseudostate to the polarizabilities of A and B, as given by Equations (4.22) and (4.23).

Accurate values of C_6 dispersion coefficients can be calculated through a generalization of the London formula in terms of the so called N-term dipole pseudospectra $\{\alpha_i, \varepsilon_i\}(i = 1, 2, \cdots, N)$ of the monomers (Magnasco and Ottonelli, 1999). Less important higher terms, going as $R^{-8}, R^{-10}, \cdots$ arise from the coupling of higher induced moments on A and B (Buckingham, 1967; Magnasco and McWeeny, 1991).

4.5.2 Atom–Linear Molecule Dispersion

μ_i is now an *isotropic induced* dipole on atom A, μ_j a *cylindrically induced* dipole on the linear molecule B[9] with components $\mu_{j\parallel}$, $\mu_{j\perp}$. We then have for the energy lowering the sum of separate contributions from parallel and perpendicular components:

$$\begin{cases} \Delta E = -\dfrac{\beta_\parallel^2}{\Delta\varepsilon_\parallel} - \dfrac{\beta_\perp^2}{\Delta\varepsilon_\perp} = -\dfrac{1}{R^6}\left[(3\cos^2\theta+1)\dfrac{\mu_i^2\mu_{j\parallel}^2}{\varepsilon_i+\varepsilon_{j\parallel}} + (5-3\cos^2\theta)\dfrac{\mu_i^2\mu_{j\perp}^2}{\varepsilon_i+\varepsilon_{j\perp}}\right] \\[2mm] \qquad = -\dfrac{1}{R^6}\left[\dfrac{3\cos^2\theta+1}{4}\alpha_i\alpha_{j\parallel}\dfrac{\varepsilon_i\varepsilon_{j\parallel}}{\varepsilon_i+\varepsilon_{j\parallel}} + \dfrac{5-3\cos^2\theta}{4}\alpha_i\alpha_{j\perp}\dfrac{\varepsilon_i\varepsilon_{j\perp}}{\varepsilon_i+\varepsilon_{j\perp}}\right] \end{cases}$$
$$(4.53)$$

Considering several dipole excitations, we can write for the *two* dispersion constants in London form:

$$\begin{cases} A = \dfrac{1}{4}\sum_i\sum_j \alpha_i\alpha_{j\parallel}\dfrac{\varepsilon_i\varepsilon_{j\parallel}}{\varepsilon_i+\varepsilon_{j\parallel}} \\[3mm] B = \dfrac{1}{4}\sum_i\sum_j \alpha_i\alpha_{j\perp}\dfrac{\varepsilon_i\varepsilon_{j\perp}}{\varepsilon_i+\varepsilon_{j\perp}} \end{cases} \qquad (4.54)$$

so that the angle-dependent C_6 dispersion coefficient for the atom-linear molecule interaction will be:

$$C_6(\theta) = (3\cos^2\theta+1)A + (5-3\cos^2\theta)B \qquad (4.55)$$

This expression is usually written in terms of the Legendre polynomial $P_2(\cos\theta)$ (Abramowitz and Stegun, 1965):

$$C_6(\theta) = C_6[1+\gamma_6 P_2(\cos\theta)] \qquad (4.56)$$

where:

$$C_6 = 2A + 4B \qquad (4.57)$$

is the isotropic coefficient for dispersion, and:

$$\gamma_6 = \frac{A-B}{A+2B} \qquad (4.58)$$

---

[9] A is at the origin of the coordinate system, while molecule B is at an angle θ with respect to the intermolecular z axis.

the anisotropy coefficient for dispersion. C_6 can be obtained from the previous angle-dependent expression by averaging over angle θ, whereas γ_6 describes in a standard way the orientation dependence of the coefficient.

In fact, since $(\cos \theta = x)$:

$$\langle \cos^2 \theta \rangle = \frac{\int\limits_{-1}^{1} dx\, x^2}{\int\limits_{-1}^{1} dx} = \frac{1}{3} \tag{4.59}$$

averaging Equation (4.55) over θ, we obtain for the *isotropic* C_6 dispersion coefficient:

$$\langle C_6 \rangle = \left(3 \times \frac{1}{3} + 1 \right) A + \left(5 - 3 \times \frac{1}{3} \right) B = 2A + 4B = C_6 \tag{4.60}$$

The same result is obtained from Equation (4.56), since the average of $P_2(\cos \theta)$ over angle θ is zero:

$$\langle P_2(\cos \theta) \rangle = \frac{3}{2} \langle \cos^2 \theta \rangle - \frac{1}{2} = \frac{3}{2} \times \frac{1}{3} - \frac{1}{2} = 0 \tag{4.61}$$

4.5.3 Atom–Linear Dipolar Molecule[10] Induction

μ_i is now an *isotropic induced* dipole on atom A, $\mu_j = \mu_{jz} = \mu_B$ the *unidimensional permanent* dipole of a noncentrosymmetric neutral linear molecule B. We then have for the energy lowering (induction, B polarizes A):

$$\Delta E_{BA} = -\frac{\beta^2}{\varepsilon_i} = -\frac{3\cos^2\theta + 1}{R^6} \frac{\mu_i^2}{\varepsilon_i} \mu_B^2 = -\frac{3\cos^2\theta + 1}{2} \frac{\alpha_i \mu_B^2}{R^6} = -\frac{C_6(\theta)}{R^6} \tag{4.62}$$

where $C_6(\theta)$ is the angle-dependent *induction* coefficient:

$$\begin{cases} C_6(\theta) = \alpha_i \mu_B^2 \dfrac{3\cos^2\theta + 1}{2} \\ \qquad = \alpha_i \mu_B^2 [1 + P_2(\cos \theta)] \\ \qquad = C_6 [1 + \gamma_6 P_2(\cos \theta)] \end{cases} \tag{4.63}$$

---

[10] Namely, a molecule possessing a *permanent* dipole moment.

Here:

$$C_6 = \alpha_i \mu_B^2 \qquad (4.64)$$

is the isotropic coefficient, and:

$$\gamma_6 = 1 \qquad (4.65)$$

the anisotropy coefficient for induction. Averaging over angle θ, we get for the isotropic polarization of A by B ($\alpha_i = \alpha_A$):

$$\Delta E_{BA} = -\frac{\alpha_A \mu_B^2}{R^6} \qquad (4.66)$$

We have a similar result for a dipolar molecule A distorting B, so that on average:

$$\Delta E = \Delta E_{BA} + \Delta E_{AB} = -\frac{\alpha_A \mu_B^2 + \alpha_B \mu_A^2}{R^6} \qquad (4.67)$$

and, for identical molecules:

$$\Delta E = -\frac{2\alpha \mu^2}{R^6} = -\frac{C_6}{R^6} \qquad (4.68)$$

Even the leading term of the induction (polarization) energy has an R^{-6} dependence on R with an isotropic $C_6 = 2\alpha\mu^2$, but the coefficient depends now on *observable* quantities (α, μ) that can be measured by experiment. This makes an important difference from dispersion coefficients that should be noted.

Isotropic C_6 dispersion and induction coefficients (in atomic units) for some homodimers of atoms and molecules taken from the literature are compared in Table 4.1. We see from the table that the distortion energy is zero for atoms, which do not have permanent moments, and is always smaller than the dispersion energy for the molecules considered, with the only exception of $(LiH)_2$. The dispersion energy (London attraction) is therefore the dominant VdW interaction,[11] the only one for atoms. The large value for the distortion energy in $(LiH)_2$ is due to the combined large values of μ and α for LiH, $-2.29ea_0$ and $28.5a_0^3$, respectively (Bendazzoli et al., 2000).

---

[11] Note, however, the importance of the temperature-dependent Keesom effect for dipolar molecules in the gas phase.

Table 4.1 Comparison between isotropic C$_6$ dispersion and induction coefficients $\left(E_h a_0^6\right)$ for some homodimers of atoms and molecules

Atom–atom	Dispersion	Induction	Molecule–molecule	Dispersion	Induction
He$_2$	1.46	0	(H$_2$)$_2$	12.1	0
Ne$_2$	6.28	0	(N$_2$)$_2$	73.4	0
H$_2$	6.50	0	(CO)$_2$	81.4	0.05
Ar$_2$	64.3	0	(CO$_2$)$_2$	159	0
Kr$_2$	130	0	(CH$_4$)$_2$	130	0
Be$_2$	213	0	(NH$_3$)$_2$	89.1	9.82
Xe$_2$	286	0	(H$_2$O)$_2$	45.4	10.4
Mg$_2$	686	0	(HF)$_2$	19.0	6.30
Li$_2$	1450	0	(LiH)$_2$	125	299

4.6   THE C$_6$ DISPERSION COEFFICIENT FOR THE H–H INTERACTION

The excited pseudostates occurring in Equations (4.18) and (4.19) can be obtained using the extension of the Ritz method to the calculation of second-order energies introduced in Chapter 1.

The dipole pseudospectra of H(1s) for $N = 1$ through $N = 4$ are given in Table 4.2. The two-term approximation gives the exact result for the dipole polarizability α, the same being true for the three-term and the higher N-term $(N > 3)$ approximations. In all such cases, the dipole polarizability of the atom is partitioned into an increasing number N of contributions arising from the different pseudostates:

$$\alpha = \sum_{i=1}^{N} \alpha_i \qquad (4.69)$$

Table 4.2 Dipole pseudospectra of H(1s) for $N = 1$ through $N = 4$

i	α_i/a_0^3	ε_i/E_h	$\sum \alpha_i$
1	$4.000\,000 \times 10^0$	$5.000\,000 \times 10^{-1}$	4.0
1	$4.166\,667 \times 10^0$	$4.000\,000 \times 10^{-1}$	
2	$3.333\,333 \times 10^{-1}$	$1.000\,000 \times 10^0$	4.5
1	$3.488\,744 \times 10^0$	$3.810\,911 \times 10^{-1}$	
2	$9.680\,101 \times 10^{-1}$	$6.165\,762 \times 10^{-1}$	
3	$4.324\,577 \times 10^{-2}$	$1.702\,333 \times 10^0$	4.5
1	$3.144\,142 \times 10^0$	$3.764\,643 \times 10^{-1}$	
2	$1.091\,451 \times 10^0$	$5.171\,051 \times 10^{-1}$	
3	$2.564\,244 \times 10^{-1}$	$9.014\,629 \times 10^{-1}$	
4	$7.982\,236 \times 10^{-3}$	$2.604\,969 \times 10^0$	4.5

This increasingly fine subdivision of the exact polarizability value into different pseudostate contributions is of fundamental importance for the increasingly refined evaluation of the London dispersion coefficients for two H atoms interacting at long range. It can only be said that, in general, the N-term approximation will involve diagonalization of the $(N \times N)$ matrix $\mathbf{M}$ generalizing Equation (1.64) of Chapter 1, its eigenvalues being the excitation energies ε_i and its eigenvectors the corresponding N-term pseudostates $\{\psi_i\}\, i = 1, 2, \cdots, N$. For a given atom (or molecule), knowledge of the so-called N-term pseudospectrum $\{\alpha_i, \varepsilon_i\}\, i = 1, 2, \cdots, N$, allows for the *direct* calculation of the dispersion coefficients of the interacting atoms (or molecules).

In this way, for *each* H atom, the calculated *dipole pseudospectra* $\{\alpha_i, \varepsilon_i\}\, i = 1, 2, \cdots, N$ of Table 4.2 can be used to obtain better and better values for the C_6 London dispersion coefficient for the H$-$H interaction: a molecular (two-centre) quantity C_6 can be evaluated in terms of atomic (one-centre), *nonobservable*, quantities, α_i (α alone is useless). The coupling between the different components of the polarizabilities occurs through the denominator in the London formula (4.19), so that we cannot sum over i or j to get the full, *observable*,[12] α^A or α^B.

Using the London formula and the pseudospectra derived previously, we obtain for the leading term of the H–H interaction the results collected in Table 4.3. The table shows that convergence is very rapid for the H–H interaction.[13] Unfortunately, the convergence rate for C_6 (as well as that for α) is not so good for other systems (Magnasco, 2009a).

We have already said that an alternative, yet equivalent, formula for the dispersion constant is due to Casimir and Polder (1948) in terms of the frequency-dependent polarizabilities (FDPs) at imaginary frequen-

Table 4.3 N-term results for the C_{11} dipole dispersion constant and the C_6 London dispersion coefficients for the H–H interaction

N	$C_{11}/E_h a_0^6$	$C_6/E_h a_0^6$	Accuracy(%)
1	1	6	92.3
2	1.080 357	6.4821	99.7
3	1.083 067	6.4984	99.99
4	1.083 167	6.499 00	99.999
5	1.083 170	6.499 02	100

[12] That is, measurable.

[13] The first approximate value (6.47) of the C_6 dispersion coefficient for the H–H interaction was obtained by Eisenschitz and London (1930) from a perturbative calculation using the *complete* set of H eigenstates following early work by Sugiura (1927).

cies of A and B, Equation (4.24). In this case, we must know the dependence of the FDPs on the real frequency u, and the coupling occurs now via the integration over the frequencies. When the necessary data are available, however, the London formula (4.19) is preferable because use of the Casimir–Polder formula (4.24) presents some problems in the accurate evaluation of the integral through numerical quadrature techniques (Figari and Magnasco, 2003; Magnasco and Figari, 2009).

We give below the explicit London-type calculation for $N = 2$:

$$C_{11}(\text{two-term}) = \frac{1}{8}\left(\frac{25}{6}\right)^2 \times \frac{2}{5} + \frac{1}{8}\left(\frac{2}{6}\right)^2 \times 1 + \frac{1}{2} \times \frac{25}{6} \times \frac{2}{6} \times \frac{\frac{2}{5} \times 1}{\frac{2}{5} + 1}$$

$$= \frac{5 \times 5 \times 25 \times 2}{2 \times 4 \times 36 \times 5} + \frac{4}{2 \times 4 \times 36} + \frac{5 \times 5 \times 2 \times 5}{36 \times 5 \times 7}$$

$$= \frac{125}{4 \times 36} + \frac{1}{2 \times 36} + \frac{50}{7 \times 36} = \frac{1089}{1008} = \frac{121}{112} = 1.080\,357$$

so that the two-term approximation gives the dispersion constant as the ratio between two integers that are not divisible! However, this explicit calculation is no longer possible for $N > 2$ so that we must resort to the numerical method.[14]

4.7   THE van der WAALS BOND

On the basis of what we have said so far, we conclude that a *van der Waals bond* between two closed-shell atoms can be formed, at the minimum point of the potential energy surface, as a result of the overwhelming at long range of a weak Pauli repulsion ($\propto \exp(-aR)$) by a weak London attraction ($\propto R^{-6}$). Figure 4.3 shows the formation of the VdW minimum for two ground state He atoms as a result of the first-order Pauli repulsion E_1 and the second-order London attraction E_2. A small potential well with $D_e = -33.4 \times 10^{-6}E_h$ is then formed at the rather large interatomic distance of $R_e = 5.6a_o$. For neutral molecules, electrostatic interactions are important as well, giving contributions going as R^{-3} for the leading dipole–dipole interaction (non-centrosymmetric molecules), and R^{-4} for

---

[14] We must diagonalize the matrix representative of the excitation operator $H_0 - E_0$ over the appropriate basis.
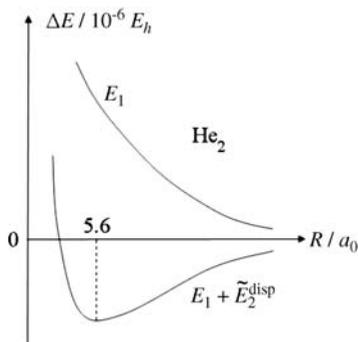
Figure 4.3   Origin of the VdW bond in He$_2$ ($^1\sum_g^+$)

the quadrupole–quadrupole interactions (centrosymmetric molecules). The latter are responsible for the typical T-structure observed for the dimers of H$_2$, N$_2$ and F_2, as will be seen in Section 5.3 of the next chapter.

An approximate non-expanded potential energy curve of the $(H_2O)_2$ dimer evaluated by Magnasco *et al.* (1985) is schematically shown in Figure 4.4. We see that the first-order interaction E_1 already shows, in this range of internuclear distances, a minimum, chiefly due to the first-order electrostatic component, while second-order interactions (induction plus dispersion) simply deepen such a minimum, strengthening the bond. It is appropriate in this case to speak of formation of a *hydrogen bond*, essentially electrostatic in origin. It is of interest to notice the change in the scale factor for energy, from $10^{-6}E_h$ for He$_2$ (VdW bond) to $10^{-3}E_h$ for $(H_2O)_2$ (H-bond), even though roughly in the same region of
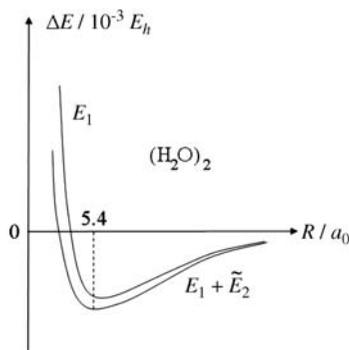
Figure 4.4   Origin of the hydrogen bond in $(H_2O)_2$ ($^1A_1$)

Table 4.4 Bond distances R_e and bond strengths D_e (atomic units) at the minimum of the potential energy surface for some homodimers of atoms and molecules

Atom–atom	R_e/a_0	$D_e/10^{-6}E_h$	Molecule–molecule	R_e/a_0	$D_e/10^{-3}E_h$
$H_2(^3\sum_u^+)$	7.8	20.5	$(H_2)_2$	6.5	0.12
He_2	5.6	33.4	$(N_2)_2$	8.0	0.39
Ne_2	5.8	133	$(CH_4)_2$	7.3	0.69
Ar_2	7.1	449	$(NH_3)_2$	6.2	6.47
Kr_2	7.6	633	$(H_2O)_2$	5.4	10.3
Xe_2	8.2	894	$(HF)_2$	5.1	11.4
$Li_2(^3\sum_u^+)$	8.0	1332	$(BeH_2)_2$		52.2
Be_2	4.7	2694	$(LiH)_2$	4.0	75.8

intermolecular distances ($5.6a_0$ for He_2, $5.4a_0$ for the H_2O dimer), just to outline that the H-bond has an energy comparable to that of a weak chemical bond. H-bonding will be treated in detail in the next chapter.

The structures of VdW dimers, considered as weakly bounded complexes in which each monomer maintains its original structure (Buckingham, 1982), are studied at low temperatures by sophisticated experimental techniques, such as far infrared spectra, high-resolution rotational spectroscopy in the microwave region, and molecular beams. Distances R_e between the centres of mass and bond strengths D_e at the VdW minimum for some homodimers of atoms and molecules taken from Literature are collected in Table 4.4.

We notice from the table how large R_e and how small D_e values characterize our VdW dimers with respect to the corresponding values of the chemical bonds reported in Table 2.1 of Chapter 2. The sensibly larger D_e values observed for the dimers of first-row hydrides $(NH_3)_2$, $(H_2O)_2$, $(HF)_2$, $(BeH_2)_2$, $(LiH)_2$ denote formation of a $XH-X$ *hydrogen* bond, particularly strong in $(LiH)_2$, where it is of the order of a chemical bond.

4.8   THE KEESOM INTERACTION

The electrostatic energy $E_1(es)$ is zero when averaged over the angles describing the relative orientation of the two interacting molecules. However, Keesom (1921) showed that if two dipolar molecules undergo thermal motions, they *attract* each other according to:

$$E_6(\text{Keesom}) = -\frac{C_6(T)}{R^6} \tag{4.70}$$

$C_6(T)$ being the temperature-dependent coefficient:

$$C_6(T) = \frac{2\mu_A^2\mu_B^2}{3kT} \tag{4.71}$$

where T is the absolute temperature and k the Boltzmann constant. The corresponding attractive energies (4.70) are the *isotropic* electrostatic contributions to the interaction energy and are temperature-dependent.

The Keesom formula (4.70) is easily derived (Magnasco, 2009a) by taking the Boltzmann average of the dipolar interaction over the angles of relative orientation of the two molecules for *small* values of the dimensionless parameter:

$$a = -\frac{\mu_A\mu_B}{R^3 kT} < 0 \tag{4.72}$$

It may be helpful for the reader to recall briefly the derivation of the Keesom formula.

The interaction between point-like dipoles (Coulson, 1958) is:

$$V = \frac{\mu_A\mu_B}{R^3}(\sin\theta_A \sin\theta_B \cos\varphi - 2\cos\theta_A \cos\theta_B) \tag{4.73}$$

where $\varphi = \varphi_A - \varphi_B$ is the dihedral angle between the planes specified by μ_A, μ_B and R.

We put:

$$\begin{cases} \Omega = \theta_A, \theta_B, \varphi \\ F(\Omega) = \sin\theta_A \sin\theta_B \cos\varphi - 2\cos\theta_A \cos\theta_B \end{cases} \tag{4.74}$$

If all orientations were *equally probable*, the average potential energy $\langle V \rangle$, and hence the first-order electrostatic C_3 coefficient (Magnasco 2007, 2009a; Magnasco *et al.*, 1988), would be zero. In fact:

$$\langle V \rangle_\Omega = \frac{\mu_A\mu_B}{R^3}\frac{\int_\Omega d\Omega\, F(\Omega)}{\int_\Omega d\Omega} = 0 \tag{4.75}$$

since, putting:

$$x_A = \cos\theta_A, \; x_B = \cos\theta_B \tag{4.76}$$

we have:

$$\int_\Omega d\Omega = \int_0^{2\pi} d\varphi \int_0^\pi d\theta_A \sin\theta_A \int_0^\pi d\theta_B \sin\theta_B = 2\pi \int_{-1}^1 dx_A \int_{-1}^1 dx_B = 8\pi \tag{4.77}$$

$$\int_{\Omega} d\Omega \ F(\Omega) = \int_{0}^{2\pi} d\varphi \ \cos\varphi \left[\int_{-1}^{1} dx \left(1-x^2 \right)^{1/2} \right]^2 -2\int_{0}^{2\pi} d\varphi \left[\int_{-1}^{1} dx \ x \right]^2 = 0$$

(4.78)

The vanishing of the average potential energy for *free* orientations is true for all multipoles (dipoles, quadrupoles, octupoles, hexadecapoles, etc.).

The Boltzmann probability for a dipole arrangement whose potential energy is V is proportional to:

$$W \propto \exp(-V/kT) \qquad (4.79)$$

We now average the quantity $V\exp(-V/kT)$ over all possible orientations Ω assumed by the dipoles:

$$\langle V\exp(-V/kT)\rangle_{\Omega} = \frac{\mu_A\mu_B}{R^3} \frac{\int_{\Omega} d\Omega \ F(\Omega) \exp[aF(\Omega)]}{\int_{\Omega} d\Omega \ \exp[aF(\Omega)]} \qquad (4.80)$$

where the parameter a was introduced in Equation (4.72).

We then obtain:

$$\left\{ \begin{aligned} \langle V\exp(-V/kT)\rangle_{\Omega} &= \frac{\mu_A\mu_B}{R^3} \frac{\int_{\Omega} d\Omega \ F(\Omega) \exp[aF(\Omega)]}{\int_{\Omega} d\Omega \ \exp[aF(\Omega)]} \\ &= \frac{\mu_A\mu_B}{R^3} \frac{d}{da} \ln K(a) \end{aligned} \right. \qquad (4.81)$$

where

$$K(a) = \int_{\Omega} d\Omega \exp\left[aF(\Omega)\right] \qquad (4.82)$$

is called the Keesom integral.

We evaluate Equation (4.81) for $a = small$ (high temperatures and large distances between the dipoles), by expanding the exponential in

Equation (4.82):

$$\int_{\Omega} d\Omega \, \exp[aF(\Omega)] \approx \int_{\Omega} d\Omega \left\{ 1 + a\,F(\Omega) + \frac{a^2}{2}\,F(\Omega)^2 + \cdots \right\} \qquad (4.83)$$

where we have just seen that, in the expansion, the second integral vanishes, so that only the quadratic term can contribute to the Keesom integral.

We have:

$$\begin{cases} \displaystyle\int_{\Omega} d\Omega \, F(\Omega)^2 \\[2mm] = \displaystyle\int_0^{2\pi} d\varphi \int_0^{\pi} d\theta_A \sin\theta_A \int_0^{\pi} d\theta_B \, \sin\theta_B \, \left(\sin^2\theta_A \sin^2\theta_B \cos^2\varphi + 4\cos^2\theta_A \cos^2\theta_B \right) \\[3mm] = 8\pi\dfrac{2}{3} \end{cases}$$

$$(4.84)$$

so that

$$\int_{\Omega} d\Omega \, \frac{a^2}{2} F(\Omega)^2 = 8\pi\frac{a^2}{3} \qquad (4.85)$$

Then:

$$\int_{\Omega} d\Omega \left[1 + \frac{a^2}{2} F(\Omega)^2 \right] = 8\pi\left(1 + \frac{a^2}{3} \right) \qquad (4.86)$$

$$\frac{d}{da} \ln\left[8\pi\left(1 + \frac{a^2}{3} \right) \right] = \frac{1}{1 + \frac{a^2}{3}} \times \frac{2}{3} a \approx \frac{2}{3} a \qquad (4.87)$$

for $a = small$. Hence, we obtain the final result for the average attraction energy between the dipoles:

$$\langle V \exp(-V/kT) \rangle_{\Omega} \approx \frac{\mu_A \mu_B}{R^3}\frac{2}{3} a = -\frac{2}{3kT}\frac{\mu_A^2 \mu_B^2}{R^6} \qquad (4.88)$$

which is known as Keesom or dipole orientation energy, Equations (4.70) and (4.71). Even this term depends on R^{-6}, but is temperature-dependent and decreases in importance with increasing T.

It is of interest to compare the relative importance of all *attractive* contributions to the intermolecular energy in the VdW region. For atoms and centrosymmetric molecules, induction is zero, so that the only

Table 4.5 Comparison between isotropic C_6 coefficients ($E_h a_0{}^6$) for some homo-dimers of atoms and molecules at $T = 293 \, K$

Atom–atom	Dispersion	Molecule–molecule	Dispersion	Induction	Keesom
He_2	1.46	$(H_2)_2$	12.1	0	0
Ne_2	6.35	$(N_2)_2$	73.4	0	0
H_2	6.50	$(CO)_2$	81.4	0.05	0.002
Ar_2	64.9	$(NO)_2$	69.8	0.08	0.009
Kr_2	129	$(N_2O)_2$	184.9	0.19	0.017
Be_2	213	$(NH_3)_2$	89.1	9.82	81.3
Xe_2	268	$(H_2O)_2$	45.4	10.4	204
Mg_2	686	$(HF)_2$	19.0	6.3	227
Li_2	1450	$(LiH)_2$	125	299	8436

contribution comes from attractive dispersion. For dipolar molecules induction is usually negligible with respect to dispersion except perhaps for $(LiH)_2$. The electrostatic energy is not zero when its thermal average is taken. The corresponding Keesom attractive energies (Equation 4.70) are hence the *isotropic* electrostatic contributions to the interaction energy and are temperature-dependent. A comparison between isotropic C_6 coefficients for some homodimers at $T = 293 \, K$ is given in Table 4.5. It is seen that Keesom $C_6(T)$ is negligible compared with dispersion and induction coefficients for the homodimers of CO, NO, N_2O, while for $(NH_3)_2$, $(HF)_2$, $(H_2O)_2$ Keesom dipole orientation forces become increasingly dominant at room temperature, so they cannot be neglected in assessing collective gas properties such as the equation of state for real gases and virial coefficients.

Battezzati and Magnasco (2004) gave an asymptotic evaluation of the Keesom integral (4.82) for $a = large$ (low temperatures and small distances between the dipoles), obtaining the formula:

$$K(a) \cong \frac{4\pi}{3} \frac{\exp(-2a)}{a^2} \left(1 - \frac{2}{3a}\right) \qquad (4.89)$$

Magnasco *et al.* (2006) recently extended Keesom's calculations up to the R^{-10} term, showing that deviations of the Keesom approximation[15] from the full series expansion are less important than consideration of the higher-order terms in the R^{-2n} expansion of the intermolecular potential. The validity of the Keesom two-term approximation with respect to the complete series expansion is thus very good, and is best studied by comparing the respective logarithmic derivatives.

---

[15] Expansion of the exponential stopped to the second power of $\Omega = \theta_A, \theta_B, \varphi$.

Table 4.6 Dimensionless Keesom parameters $|a_{ll'}|$ and T-dependent $C_{2n}(l, l')$ Keesom coefficients

l	l'	$|a_{ll'}|$	$C_{2n}(l, l')$
1	1	$\dfrac{\mu_1^A \mu_1^B}{R^3 kT}$	$\dfrac{2(\mu_1^A)^2(\mu_1^B)^2}{3kT}$
1	2	$\dfrac{3\mu_1^A \mu_2^B}{2R^4 kT}$	$\dfrac{(\mu_1^A)^2(\mu_2^B)^2}{kT}$
2	1	$\dfrac{3\mu_2^A \mu_1^B}{2R^4 kT}$	$\dfrac{(\mu_2^A)^2(\mu_1^B)^2}{kT}$
1	3	$\dfrac{\mu_1^A \mu_3^B}{2R^5 kT}$	$\dfrac{4(\mu_1^A)^2(\mu_3^B)^2}{3kT}$
3	1	$\dfrac{\mu_3^A \mu_1^B}{2R^5 kT}$	$\dfrac{4(\mu_3^A)^2(\mu_1^B)^2}{3kT}$
2	2	$\dfrac{3\mu_2^A \mu_2^B}{4R^5 kT}$	$\dfrac{14(\mu_2^A)^2(\mu_2^B)^2}{5kT}$

Table 4.6 gives the dimensionless Keesom parameters $|a_{ll'}|$ and the T-dependent $C_{2n}(l, l')$ Keesom coefficients for $l, l' = 1, 2, 3$ calculated from the electrostatic potentials given in Equations (5.3–5.8) of the next chapter, using the same techniques as we did before for the dipole–dipole term.

The numerical values of the Keesom coefficients for some homodimers in the gas phase at $T = 293$ K are collected in Table 4.7.

The long-range electrostatic Keesom attractive energies up to the R^{-10} term ($10^{-6}E_h$) for some homodimers in the gas phase at $R = 10a_0$ and $T = 293$ K are reported in Table 4.8, while the R^{-6} electrostatic contributions $E_6(es)$ are compared in Table 4.9 with the corresponding dispersion contributions $E_6(\text{disp})$. It must be noted that the R^{-10} contribution is complete only for the homodimers of CO, HCl and HF, the

Table 4.7 Numerical values of Keesom coefficients (atomic units) for some homodimers in the gas phase at $T = 293$ K

Molecule	$C_6(1, 1)/E_h a_0^6$	$C_8(1, 2)/E_h a_0^8$	$C_{10}(1, 3)/E_h a_0^{10}$	$C_{10}(2, 2)/E_h a_0^{10}$
CO	2.693×10^{-3}	4.508×10^0	3.330×10^1	1.409×10^4
HCl	2.300×10^1	1.374×10^3	3.991×10^3	1.533×10^5
NH_3	8.074×10^1	2.168×10^3		1.087×10^5
HF	1.765×10^2	1.562×10^3	4.451×10^3	2.580×10^4
H_2O	2.007×10^2	5.695×10^0		3.017×10^{-1}
LiH	1.989×10^4	5.439×10^4		2.766×10^5
H_2				1.131×10^2
N_2				3.530×10^3
O_2				2.444×10^1
CO_2				3.085×10^5

Table 4.8 Long-range electrostatic Keesom attractive energies ($10^{-6}E_h$) for some homodimers in the gas phase at $R = 10a_0$ and $T = 293\,\mathrm{K}$

Molecule	$-E_6$	$-E_8$	$-E_{10}$	$-E(\mathrm{es})$
CO	2.693×10^{-3}	9.016×10^{-2}	1.416×10^{0}	1.509×10^{0}
HCl	2.300×10^{1}	2.748×10^{1}	1.613×10^{1}	6.661×10^{1}
NH$_3$	8.074×10^{1}	4.336×10^{1}	1.087×10^{1}	1.350×10^{2}
HF	1.765×10^{2}	3.124×10^{1}	3.470×10^{0}	2.112×10^{2}
H$_2$O	2.007×10^{2}	1.139×10^{-1}	3.017×10^{-5}	2.008×10^{2}
LiH	1.989×10^{4}	1.088×10^{3}	2.776×10^{1}	2.101×10^{4}
H$_2$			1.131×10^{-2}	1.131×10^{-2}
N$_2$			3.530×10^{-1}	3.530×10^{-1}
O$_2$			2.444×10^{-3}	2.444×10^{-3}
CO$_2$			3.085×10^{1}	3.085×10^{1}

remaining values giving only the quadrupole–quadrupole contribution. It is well known (Magnasco, 2007, 2009a) that, except for LiH, induction energies are always sensibly smaller than dispersion.

It is seen from the tables that the electrostatic contribution $E_6(\mathrm{es})$ is smaller than dispersion only for CO and HCl ($|a_{11}| = 2.086 \times 10^{-3}$ and 0.1928, respectively), being of the same order of dispersion for NH$_3$ (0.3612), and decidedly larger for HF, H$_2$O (0.5341 and 0.5695) and LiH (5.671). The Keesom series is apparently divergent for CO, practically a quadrupolar molecule, so that it might be not unexpected that the largest contribution to the electrostatic energy comes from the quadrupole–quadrupole term. Convergence seems rather poor for HCl, all higher-order terms being of the same order as the leading term, while it is better for NH$_3$ and HF. HF is the only case where the dipole–quadrupole contribution is one order less than the leading dipole–dipole term. The dipole–octupole plus quadrupole–quadrupole contribution for HF is one

Table 4.9 Comparison between R^{-6} attractive electrostatic and dispersion energies ($10^{-6}E_h$) for some homodimers at $R = 10a_0$ and $T = 293\,\mathrm{K}$

Molecule	$-E_6(\mathrm{es})$	$-E_6(\mathrm{disp})$
CO	2.693×10^{-3}	8.140×10^{1}
HCl	2.300×10^{1}	1.304×10^{2}
NH$_3$	8.074×10^{1}	8.908×10^{1}
HF	1.765×10^{2}	1.900×10^{1}
H$_2$O	2.007×10^{2}	4.537×10^{1}
LiH	1.989×10^{4}	1.250×10^{2}
H$_2$		1.211×10^{1}
N$_2$		7.339×10^{1}
O$_2$		6.201×10^{1}
CO$_2$		1.587×10^{2}

order less than the dipole–quadrupole, and two orders less than dipole–dipole. So, the series expansion in R^{-n} for HF–HF shows very good convergence. Anyway, it must not be forgotten that the series in R^{-n} has asymptotic properties, though it may converge also for finite R, provided that the charge distributions are sufficiently concentrated around their centres. H_2O is left with a large axial dipole–dipole contribution only, since, as already said, its large dipole–transverse quadrupole contribution cannot be accounted for at the present level of the theory.[16]

As expected, Tables 4.8 and 4.9 show that for centrosymmetric molecules the electrostatic contribution (going as R^{-10}) is practically negligible with respect to dispersion (going as R^{-6}), being four orders smaller for O_2, three for H_2, two for N_2, and only one for CO_2.

The case of LiH is a very particular one, because of its very large value of $|a_{11}|$. The corresponding C_6 Keesom coefficient is hardly reliable, the complete series expansion showing that a reduction of over 57% is needed for C_6 ($8.475 \times 10^3\, E_h a_0^6$ with $n = 17$) and about 5% for C_8 ($5.169 \times 10^4\, E_h a_0^8$ with $n = 7$). The two-term asymptotic formula (4.89) given by Battezzati and Magnasco (2004) yields $8.436 \times 10^3\, E_h a_0^6$, which is within 0.5% of the complete series expansion result. So, the simple two-term formula (4.89) is expected to work well for other fluorides and chlorides of the alkaline metals (considered as gaseous diatomic molecules), all of which have even larger values of the dipole–dipole constant $|a_{11}|$.

---

[16] Only linear point-like multipoles directed along the main symmetry axis are considered.

5

The Hydrogen Bond

In this chapter, we shall examine two different approaches to explain the nature of the hydrogen bond and the structure of H-bonded dimers. First, a qualitative MO model where H-bonding is assumed to stem from electron transfer from an electron-rich donor MO[1] on one partner to an electron acceptor MO[2] centred at the H atom of the partner molecule. Second, a quantitative electrostatic approach, where the H-bond and the shape resulting therefrom for the dimers, can be understood in terms of the long-range interactions between the first few *permanent* multipole moments of the interacting molecules, yielding the electrostatic model.

---

[1] HOMO, mostly a lone pair or a multiple bond.
[2] An empty MO (LUMO).

5.1   A MOLECULAR ORBITAL MODEL OF THE HYDROGEN BOND

The possibility of electron transfer from a donor to an acceptor molecule is shown schematically for some homo- and heterodimers in the drawings of Figure 5.1. Figures 5.1(a,b) on $(HF)_2$ show the possibility of favourable electron transfer from F lone pairs (doubly occupied HOMOs) to a vacant (empty LUMO) orbital on H, (a) suggesting σ charge transfer from F to H, (b) π charge transfer from F to H (doubled because of the degeneracy of the π level). As a result, the dimer would acquire the non-collinear C_s geometric structure depicted in Figure 5.5 and observed by experiment ($\theta = 60°$). The same can be said for Figures 5.1(c,d) which suggest a possible explanation for the observed C_s structure of Figure 5.6 for the $(H_2O)_2$ dimer ($\alpha = 60°$). Figure 5.1(e) shows the possible formation of a T-shaped C_{2v} structure of the dimer C_2H_2-HF, where the triple bond of acetylene acts as electron donor to H, as suggested by ab initio calculations by Pople (1982). Finally, Figures 5.1(f,g) show the possibility of H-bonding of NH_3 and CO_2 with HF, where σ HOMO lone pairs on N and O act as electron donors to the empty LUMO of HF.

   To get an idea of the energy lowering involved in the formation of the hydrogen bond in some typical dimers, we use the model long-range formula:
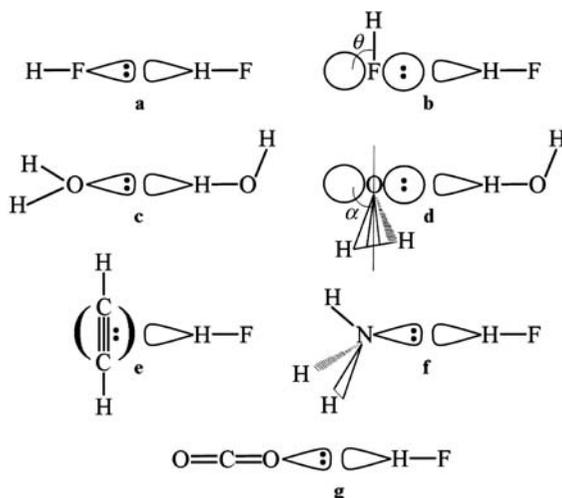
Figure 5.1   Possible HOMO-LUMO electron donation for some H-bonded dimers

$$\Delta E = -2\frac{\beta^2}{\Delta\alpha} = -D_e \tag{5.1}$$

where, as usual, the αs replace the appropriate molecular orbital energies ε, $\Delta\alpha = \alpha_{LUMO} - \alpha_{HOMO} \approx \varepsilon_{LUMO} - \varepsilon_{HOMO}$, and the bond strength D_e is taken as the negative of the intermolecular energy at the minimum of the potential energy curve. From Equation (5.1), an estimate of the intermolecular interaction integral $|\beta|$ is obtained if we use the data from the last column of Table 4.4 of the previous chapter in conjunction with calculated values of $\Delta\alpha$:

$$|\beta| = \left(\frac{D_e \cdot \Delta\alpha}{2}\right)^{1/2} \tag{5.2}$$

Table 5.1 gives for four simple molecules the values of HOMO/LUMO orbital energies calculated with accurate augccpVTZ-GTO[3] basis sets at the University of Modena and the values of the intermolecular $|\beta|$s resulting from Equation (5.2).

In the table, R is the distance between the centres of mass of the interacting molecules, roughly corresponding to the sum of the van der Waals radii of each monomer. It is seen that the estimated values of $|\beta|$ for the H-bonded dimers between the two dipolar molecules, $(HF)_2$ and $(H_2O)_2$, are 5–10 times larger than the values resulting for the VdW dimers of the centrosymmetric molecules H_2 and N_2, whose first non-vanishing electric moment is the quadrupole. This suggests the electrostatic interaction as a possible source of H-bonding, as we shall see in the next section. These values of $|\beta|$ have nearly the same order of magnitude as those occurring for the corresponding monomers (see Table 2.8 of Chapter 2), suggesting that the H-bond has a strength not far from that of a weak chemical bond.

5.2 ELECTROSTATIC INTERACTIONS AND THE HYDROGEN BOND

The Rayleigh–Schrödinger perturbation theory of the previous chapter (see Magnasco, 2007, 2009a) suggests that, in the VdW region, two typical factors can originate a *hydrogen bond* in a dimer: (1) the first-order electrostatic interaction in the case of homo- and heterodimers of

---

[3] Augmented-correlation-consistent polarized-valence triple zeta GTOs (Magnasco, 2009a).

Table 5.1 Best values of HOMO/LUMO orbital energies from accurate augccpVTZ-MO calculations[a] and estimated intermolecular interaction integral $\beta(E_h)$

Molecule	R/a_0	α_{HOMO}	α_{LUMO}	$\Delta\alpha$	$\lvert\beta\rvert = \left(\frac{D_e \cdot \Delta\alpha}{2}\right)^{1/2}$
H_2	6.50	$-0.59\,(1\sigma_g)$	$0.049\,(1\sigma_u)$	0.639	6.19×10^{-3}
N_2	8.00	$-0.61\,(1\pi_u)$	$0.081\,(4\sigma_g)$	0.691	11.61×10^{-3}
HF	5.09	$-0.65\,(1\pi)$	$0.030\,(4\sigma)$	0.680	62.26×10^{-3}
H_2O	5.40	$-0.51\,(1b_1)$	$0.029\,(4a_1)$	0.539	52.69×10^{-3}

[a] Pelloni (2008) private communication to V.Magnasco.

the first-row hydrides XH_n; and (2) the second-order interactions for the dimers between a rare gas atom and HX, which will be examined later in Section 5.4.

In the first case, the hydrogen bond and the shape resulting therefrom for these dimers can be understood in terms of the long-range interactions between the first few *permanent* multipole moments of the interacting molecules (Magnasco *et al.*, 1989b).

Equilibrium bond distances and electric properties (permanent moments[4] up to $l = 3$ and isotropic dipole polarizabilities) of a few polar molecules are collected in Table 5.2 (Magnasco *et al.*, 2006). Data for H_2O are taken from recent accurate work by Torheyden and Jansen (2006).

A few comments on Table 5.2 seem appropriate at this point. CO has such a small dipole moment C^-O^+ that can be considered a 'quasi-quadrupolar' molecule. NH_3 has large axial quadrupole and octupole moments directed along the z symmetry axis. Besides by its dipole moment, H_2O is characterized by a rather small ($0.06ea_0^2$) axial quadrupole moment and by a large transverse quadrupole moment ($2.19ea_0^2$) perpendicular to the z symmetry axis, mostly due to the couple of lone pair electrons. LiH has the largest dipole moment and dipole polarizability.

Figure 5.2 sketches a comparison between HOMO/LUMO and electrostatic descriptions of the H-bonded structure observed for $(HF)_2$. The correspondence between the two descriptions is evident from the figure.

---

[4] The dipole moment μ_1 is a vector always directed along the main symmetry axis z, being positive for $A^{-\delta}B^{+\delta}$ with the heaviest atom A taken at the origin of the coordinate system.

Table 5.2 Equilibrium bond distances and electric properties (au) of a few polar molecules

Molecule	R_e/a_0	μ_1/ea	$\mu_2/ea_0{}^2$	$\mu_3/ea_0{}^3$	$\alpha/a_0{}^3$
OC	2.132	−0.044	−1.47	−3.46	13.08
NH$_3$	1.913	−0.579	−2.45	2.462	14.56
H$_2$O	1.836	−0.726	0.06(2.19)	1.98(−4.25)	9.51
FH	1.733	0.704	1.71	2.50	5.60
ClH	2.409	0.4	2.8		17.75
LiH	3.015	−2.294	−3.097	−6.326	28.31
H$_2$	1.40		0.44		5.43
N$_2$	2.074		−1.04		11.74
O$_2$	2.282		−0.30		10.59
F$_2$	2.71		0.536		9.31
CO$_2$	2.192		−3.18		17.51
C$_2$H$_2$	6.213		4.03		21.21
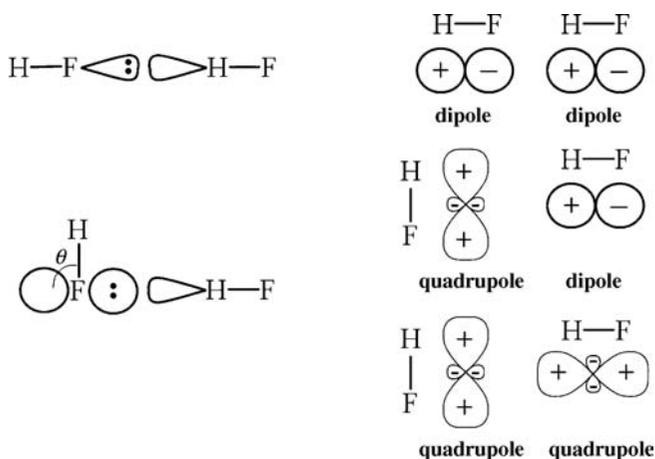
Figure 5.2   HOMO/LUMO (left) and electrostatic (right) descriptions of the origin of the H-bonded structure of $(HF)_2$

The shapes of some H-bonded dimers resulting from electrostatic calculations involving *permanent* multipole moments[5] up to R^{-6} are shown in Table 5.3, where angles refer to the coordinate system of Figure 5.3. Apart from the $(NH_3)_2$ dimer, a substantial agreement is found between theoretical predictions and experiment.

---

[5] The R^{-6} term of the expanded electrostatic energy involves interaction between dipole–hexadecapole ($l = 1$, $l' = 4$),   hexadecapole-dipole($l = 4$, $l' = 1$),   quadrupole-octupole ($l = 2$, $l' = 3$) and octupole–quadrupole ($l = 3$, $l' = 2$) moments.

Table 5.3 Theoretical angular shapes from calculated electrostatic interaction expanded to R^{-6} versus experimental results for some H-bonded VdW dimers

Dimer	R/a_0	Theoretical		Experimental	
		$\theta_A/^o$	$\theta_B/^o$	$\theta_A/^o$	$\theta_B/^o$
$(HF)_2$	5.09	104	194	117	190
$(H_2O)_2$	5.40	118	117	128	120
$(NH_3)_2$	6.31	11	75	49	115
$(LiH)_2$	3.98	51	126	50	130
H_2O-HF	5.03	52	185	46	180
H_3N-HF	5.38	0	180	0	180
$C_2H_2 - HF$	5.81	90	180	90	180
CO_2-HF	7.47	0	180	0	180
$H_2O-C_2H_2$	7.48	0	0	0	0
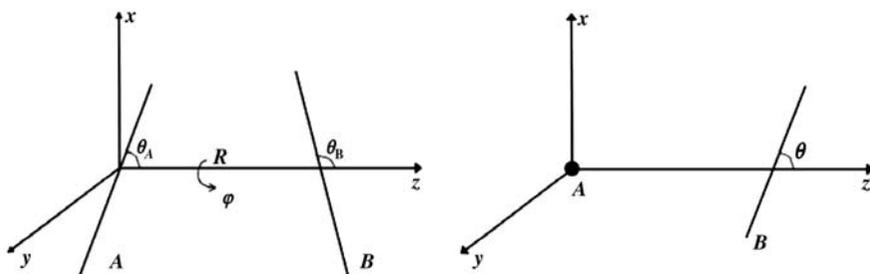
Figure 5.3 The three angles specifying the relative orientation of two linear molecules (left), and the system atom A–linear molecule B (right)

In the following, we shall consider in little more detail, first, quantitative calculations on the hydrogen bond occurring in the homodimers $(HF)_2$ and $(H_2O)_2$, next, the electrostatic model we proposed some time ago (Magnasco *et al.*, 1990a) for the hydrogen bond, and, finally, a discussion of the hydrogen bond occurring between rare gases and HF, Rg–HF (Rg = He, Ne, Ar, Kr, Xe), where the structure of the dimer is seen to depend mostly on second-order induction.

5.2.1 The Hydrogen Fluoride Dimer $(HF)_2$

As a typical quantitative example of formation of a H-bonded structure as a consequence of the electrostatic interactions between the individual molecules, we choose the $(HF)_2$ homodimer. To give the best description

of the shape of $(HF)_2$ we must take into account the long-range interaction of at least the first three permanent moments of HF. The first-order electrostatic interaction goes as R^{-n} (Magnasco, 2007, 2009a) with $n = l + l' + 1$, and l, $l' = 1$, 2, 3 for the dipole, quadrupole and octupole moments, respectively. The first three terms of the expanded electrostatic interaction showing explicitly their angular dependence for the two *linear* molecules depicted in the left part of Figure 5.3 are[6] (Magnasco *et al.*, 1990b):

$$E_1^{11}(es) = \frac{\mu_1^A \mu_1^B}{R^3} (\sin\theta_A \sin\theta_B \cos\varphi - 2\cos\theta_A \cos\theta_B) \qquad (5.3)$$

$$E_1^{12}(es) = \frac{\mu_1^A \mu_2^B}{R^4} \frac{3}{2} \left[\cos\theta_A (3\cos^2\theta_B - 1) - \sin\theta_A \sin 2\theta_B \cos\varphi\right] \quad (5.4)$$

$$E_1^{21}(es) = \frac{\mu_2^A \mu_1^B}{R^4} \frac{3}{2} \left[(1 - 3\cos^2\theta_A)\cos\theta_B + \sin 2\theta_A \sin\theta_B \cos\varphi\right] \quad (5.5)$$

$$E_1^{13}(es) = \frac{\mu_1^A \mu_3^B}{R^5} \frac{1}{2} \left[\begin{array}{l} 4\cos\theta_A (3 - 5\cos^2\theta_B)\cos\theta_B \\ + 3\sin\theta_A \sin\theta_B (5\cos^2\theta_B - 1)\cos\varphi \end{array}\right] \qquad (5.6)$$

$$E_1^{31}(es) = \frac{\mu_3^A \mu_1^B}{R^5} \frac{1}{2} \left[\begin{array}{l} 4\cos\theta_A (3 - 5\cos^2\theta_A)\cos\theta_B \\ + 3\sin\theta_A (5\cos^2\theta_A - 1)\sin\theta_B \cos\varphi \end{array}\right] \qquad (5.7)$$

$$E_1^{22}(es) = \frac{\mu_2^A \mu_2^B}{R^5} \frac{3}{4} \left[\begin{array}{l} 1 - 5(\cos^2\theta_A + \cos^2\theta_B) + 17\cos^2\theta_A \cos^2\theta_B \\ + 2\sin^2\theta_A \sin^2\theta_B \cos^2\varphi - 4\sin 2\theta_A \sin 2\theta_B \cos\varphi) \end{array}\right]$$
$$(5.8)$$

where spherical tensor notation (Magnasco, 2007) is used for the multipole moments of the linear molecules.

Choosing $\theta_B = 180°$, for $(HF)_2$, the above formulae simplify to:

$$E_1^{11}(es) = 2\frac{(\mu_1^{HF})^2}{R^3} \cos\theta_A \qquad (5.9)$$

$$E_1^{12}(es) + E_1^{21}(es) = \frac{3}{2} \frac{\mu_1^{HF} \mu_2^{HF}}{R^4} \left[2\cos\theta_A + (3\cos^2\theta_A - 1)\right] \quad (5.10)$$

---

[6] Point-like linear multipoles are assumed to be placed in the centre of mass of the molecule.
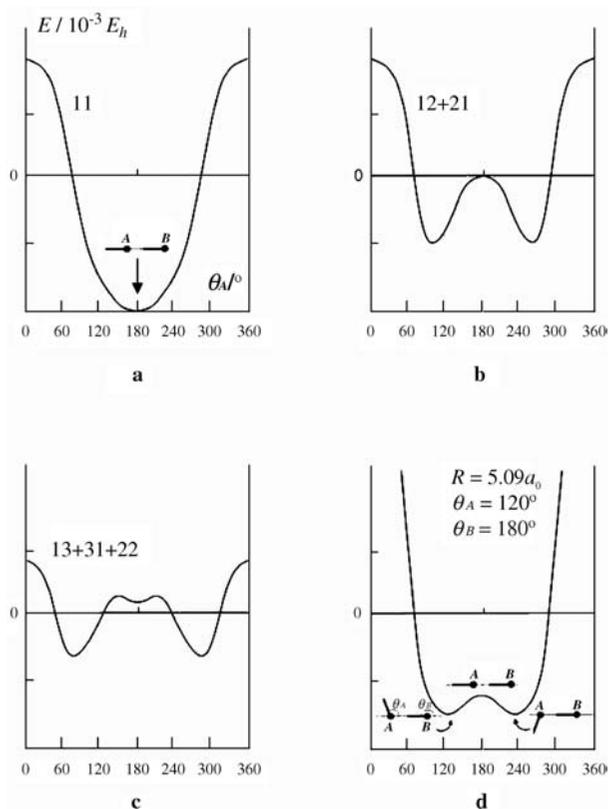
Figure 5.4   Angular dependence on θ_A of the first three terms of the expanded electrostatic interaction in linear $(HF)_2$

$$E_1^{13}(es) + E_1^{31}(es) + E_1^{22}(es)$$

$$= \frac{1}{R^5}\left[8\,\mu_1^{HF}\mu_3^{HF}\cos\theta_A + 3(\mu_2^{HF})^2(3\cos^2\theta_A - 1)\right] \tag{5.11}$$

The angular dependence on θ_A of the first three terms ($n = 3,\ 4,\ 5$) of the expanded electrostatic interaction in linear $(HF)_2$ is sketched in the drawings of Figure 5.4. In all the plots there, molecule B is kept fixed at $\theta_B = 180°$. It is seen that, while the dipole–dipole term would favour the head-to-tail shape of the dimer with a collinear H-bond (H–F...H–F, Figure 5.4(a) with $\theta_A = \theta_B = 180°$), the higher multipole interactions lead to the final L-shape of the dimer depicted in Figure 5.4(d), in agreement with the structure of the dimer observed by molecular beams techniques (Howard *et al.*, 1984) and reported in Figure 5.5. Figure 5.4(a) gives the
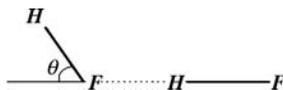
Figure 5.5 Experimental structure[7] ($\theta \approx 60°$) of the $(HF)_2$ linear dimer. Reprinted from Magnasco, V., Methods of Molecular Quantum Mechanics: An Introduction to Electronic Molecular Structure. Copyright (2009) with permission from John Wiley and Sons

behaviour with respect to θ_A of the 11 dipole–dipole contribution ($l = l' = 1$) going as R^{-3}; Figure 5.4(b) the 12 dipole–quadrupole ($l = 1$, $l' = 2$) plus the 21 quadrupole–dipole ($l = 2$, $l' = 1$) contribution going as R^{-4}; Figure 5.4(c) the 13 dipole–octupole ($l = 1$, $l' = 3$) plus the 31 octupole–dipole ($l = 3$, $l' = 1$) plus the 22 quadrupole–quadrupole ($l = 2$, $l' = 2$) contribution going as R^{-5}; Figure 5.4(d) the resultant of adding all contributions up to R^{-5}. It is apparent that the collinear H-bonded structure (a) would be the more stable considering just the dipole–dipole interaction, while adding higher multipole contributions the dimer acquires the characteristic L-shaped structure that agrees with experiment (Figure 5.5).

5.2.2   The Water Dimer $(H_2O)_2$

With reference to the coordinate system of Figure 5.6, the leading dipole–dipole term of the expanded first-order electrostatic interaction between the two H_2O molecules is given by (Magnasco *et al.*, 1988):

$$E_1(es) = -\frac{(\mu_1^{H_2O})^2}{R^3}(\sin\theta \sin\alpha + 2\cos\theta \cos\alpha) \qquad (5.12)$$

where 2θ is the valence angle. Molecule A is taken to lie in the zx plane, while α is the inclination of the molecular plane of B with respect to the yz plane (for $\alpha = 0°$ molecule B lies in the yz plane). Experimentally (Dyke and Muenter, 1974) it is found $\alpha = 60°$. For $2\theta = 105°$, $R = 5.4a_0$, $\mu_1^{H_2O} = 0.73ea_0$, Equation (5.12) has a minimum of about $-4.9 \times 10^{-3}E_h$ at $\alpha = 30°$, so indicating that, as in the case of $(HF)_2$, interaction between higher multipoles is important. Inclusion of such higher terms gives the results reported in Table 5.3.

---

[7] Angle θ in this figure is the supplement of angle θ_A of Figure 5.3**d**.
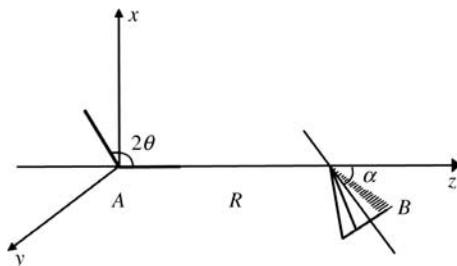
Figure 5.6   Geometry[8] of the $(H_2O)_2$ linear water dimer

5.3   THE ELECTROSTATIC MODEL OF THE HYDROGEN BOND

Buckingham and Fowler (1983) asked whether electrostatic interactions could predict structures of van der Waals molecules. The answer is 'yes they can', not only for hydrogen-bonded systems but generally for VdW complexes. All considerations we made before, in fact, led us to propose a simple *electrostatic model* for the elementary prediction of the angular geometries of VdW dimers based on the characterization of a molecule by just its first two observable electric moments (Magnasco *et al.*, 1990a). The relative stability of different angular geometries of 35 VdW dimers was correctly predicted just from the pictorial analysis of the electrostatic interactions between these moments. We enter in some detail in the following.

   For small molecules (such as HF, H_2O, NH_3, CO, H_2 and N_2) the electrostatic model is based on the following rules. It is assumed that molecules in the dimer be kept a distance R apart not less than the sum of their Van der Waals radii.

1. Each molecule is characterized by its first two observable electric moments (quadrupole alone for centrosymmetric molecules, terms higher than R^{-5} not being considered in the formulation of the model).
2. Qualitative evaluation (attractive or repulsive) is made of the dipole–dipole (R^{-3}), dipole–quadrupole plus quadrupole–dipole (R^{-4}), and quadrupole–quadrupole (R^{-5}) electrostatic interactions for the different angular geometries of the dimer.

---

[8] Angle α in this figure is the supplement of angle θ_B of Table 5.3d.

3. A scale is given of the relative importance of such electrostatic interactions in the order $\sigma\sigma > \sigma\pi > \pi\pi$, where σ is a multipole moment directed along the intermolecular axis and π a moment perpendicular to it.[9]
4. Highest stability (vs, very stable) is obtained for the angular configuration of the dimer when all three contributions are favourable.
5. Secondary stability (s, stable) is obtained when terms beyond the first are repulsive, opposing the largest attractive contribution of the leading term.
6. Unstable (ns, not stable) angular configurations are obtained when all three terms (or the leading term, at least) are repulsive.

   For elongated molecules (such as CO_2, C_2H_2 and HCN) below the sum of their VdW radii a further rule is introduced.
7. Of two angular configurations possible on the basis of the previous rules, the configuration having smaller Pauli steric repulsions will be more stable.

These rules are simple and immediately intuitive, once the electrical characterization of a molecule in terms of its point-like multipoles is accepted. The underlying physical assumption is that the electrostatic interaction is the dominant *attractive* component of the intermolecular potential determining the angular shape of the dimer, while short-range forces are assumed to provide a *repulsive* uniform background balancing attraction at the VdW minimum. Monomer size enters the model through rule 7, which corrects for deviation from uniform repulsion when steric interactions occur below the sum of the respective VdW radii.[10]

Figures 5.7 and 5.8 sketch a picture of the first two permanent electric moments (au) for a selection of noncentrosymmetric and centrosymmetric molecules, respectively. The notation is the same as that given in Magnasco *et al.* (1988). It is understood that the point-like multipoles are placed at the centre of mass of the molecule, their sign in relation to the molecular structure of the monomer being of fundamental importance in determining the nature of the electrostatic interaction (attractive or repulsive). The numbers shown in each figure are from SCF calculations and so are little larger than those given in Table 5.2.

---

[9] This σ, π definition, strictly correct for dipoles, is here loosely extended to higher multipoles with $m = 0$.

[10] Provided this situation is avoided, the exact value of the intermolecular distance R is not particularly relevant for the qualitative prediction of the angular shapes of the dimers.
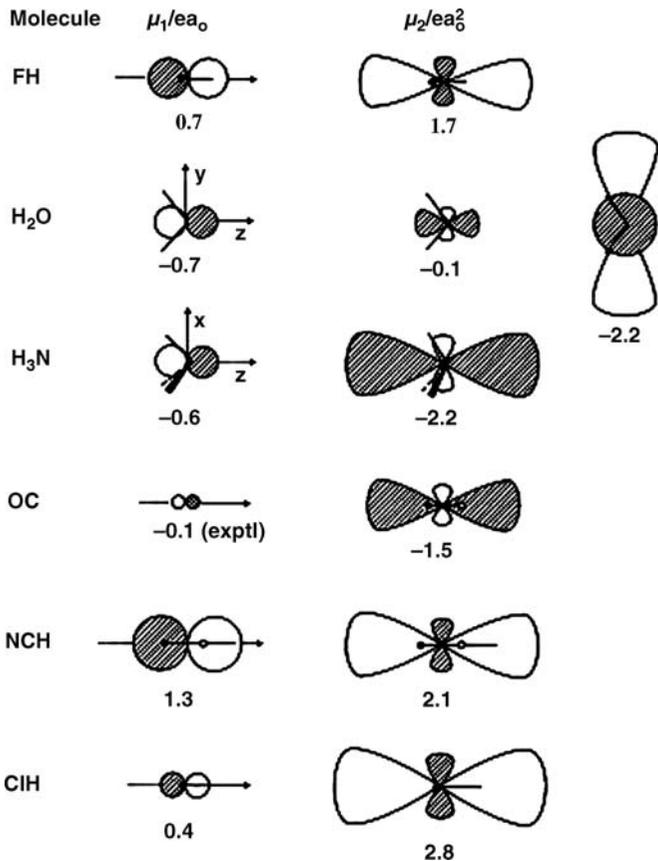
Figure 5.7 The first two permanent electric moments of some noncentrosymmetric molecules

In the figures, a pictorial representation is given of the angular shape of the molecular multipoles in terms of a polar diagram schematically close to that of the corresponding atomic orbitals of quantum number l (white for the positive lobe, dashed for the negative lobe) given in Figure 1.1 of Chapter 1.

For H_2O and C_2H_4 both nonvanishing quadrupole moments are given in the figures, to outline the greater importance of $\mu_{22} \approx \mu_{x^2-y^2}$ for H_2O, and the similar importance, and the different sign, of $\mu_{20}(=\mu_{zz})$ and μ_{22} for C_2H_4.

As an example of the operative use of the model, a classification of the first few multipole interactions with their relative stability for some selected shapes of VdW dimers is given in Figure 5.9. The interactions are classified according to rule 2 into attractive (a) or repulsive (r), (0) denoting the case when the interaction vanishes by symmetry. Stability is
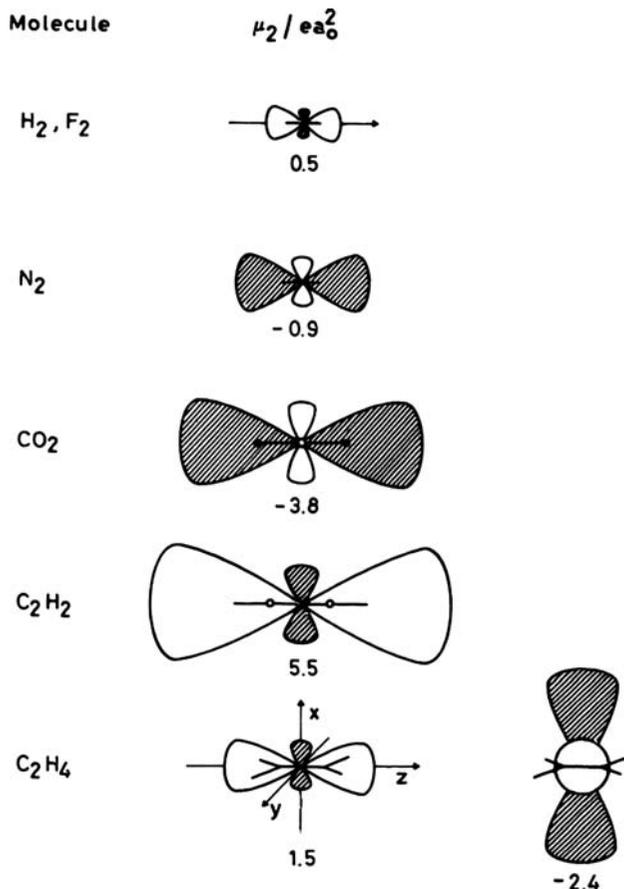
Figure 5.8 The first permanent electric moments of some centrosymmetric molecules

classified according to rules 3–7. It should be clear that the model can be used only to predict stability of sufficiently symmetric configurations.

A total of 69 angular geometries of 35 VdW dimers, classified according to a tabulation like that illustrated in Figure 5.9, are collected in Table 5.4 and compared, when possible, with geometries resulting from experiment, mostly by IR or microwave rotational spectra, or molecular beam electric resonance spectra.

In the table, and also elsewhere in the present chapter, we use the notation H-bonded to specify a structure bound by a hydrogen bond, and anti-H-bonded to specify a structure where VdW binding is opposite to that of a hydrogen bond.

We see from the table that the most stable angular geometries predicted by the model agree almost perfectly with experiment. In a few cases, as for

Figure 5.9 Classification of the first few multipole interactions and stability of the resultant angular geometries of some dimers. Reprinted from Journal of Molecular Structure: THEOCHEM, 204, Magnasco, V. *et al.*, *A model for the elementary prediction of the angular shape of Van der Waals dimers*. 229–246, Copyright (1990), with permission from Elsevier

the linear dimers $(HF)_2$, $(H_2O)_2$ and H_2O-HF, the experimentally observed geometries are somewhat intermediate between the two specific (symmetrical) structures given in the table.

It is of some interest to compare the different structures resulting from linear monomers: $(HF)_2$ (bent) and $(HCN)_2$ (collinear). In both dimers, the observed intermolecular separations[11] are such that rule 7 is ineffective, even for the collinear structure of $(HCN)_2$, where steric effects might be expected to be important. As already seen in Section 5.2.1 and

---

[11] $5.09a_0$ for $(HF)_2$ (Howard *et al.*, 1984) and $8.29a_0$ for $(HCN)_2$ (Legon *et al.*, 1977).

Table 5.4 Comparison of the model structural predictions with experiment. Reprinted from Journal of Molecular Structure: THEOCHEM, 204, Magnasco, V. *et al.*, *A model for the elementary prediction of the angular shape of Van der Waals dimers.* 229–246, Copyright (1990), with permission from Elsevier

Dimer	Structure	Electrostatic model	Stability	Experiment
$(HF)_2$[a]	Linear, $C_{\infty v}$		s	
	Bent, C_S		s	
$(HCN)_2$[b]	Bent, C_S		s	
	Linear, $C_{\infty v}$		vs	
$(H_2O)_2$[c]	Bifurcated, C_{2v}		s	
	Bifurcated crossed, C_2		s	
	Linear $\theta = 90°$, C_s		s	
	Linear $\theta = 180°$, C_s		s	
$H_2O \cdot HF$[d]	Bent, C_S		s	
	Coplanar, C_{2v}		s	
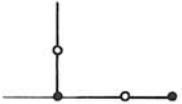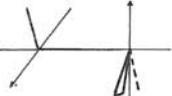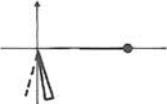
[a] Howard et al. (1984); [b] Legon et al. (1977); [c] Dyke and Muenter (1974); [d] Kisiel et al. (1982).

Table 5.4   (*Continued*)

Dimer	Structure	Electrostatic model	Stability	Experiment
$(CO)_2$	Linear, $C_{\infty v}$		ns	
	Linear, $C_{\infty v}$		ns	
	T-shape, C_s		ns	
	T-shape, C_s		s	
OC·HX[e] X=F, Cl, CN	Linear, $C_{\infty v}$ H-bonded		vs	
OC·F_2	T-shape, C_s		ns	
	T-shape, C_s		ns	
	Linear, $C_{\infty v}$		s	
HX·HCN X=F, Cl	Linear, $C_{\infty v}$ H-bonded		s	
HCN·HX[f]	Linear, $C_{\infty v}$ H-bonded		vs	
NCH·F_2	Linear, $C_{\infty v}$ H-bonded		ns	
HCN·F_2	T-shape, C_{2v}		ns	
	Linear, $C_{\infty v}$ Anti-H		s	
F_2·HCN	T-shape, C_{2v}		vs	

[e] Legon et al. (1981); Legon, Soper et al. (1980, 1981); Soper et al. (1981); Goodwin and Legon (1984); [f] Legon, Millen et al. (1980); Legon et al. (1982).

Table 5.4 (*Continued*)

Dimer	Structure	Electrostatic model	Stability	Experiment
$H_3N \cdot HX$[g] $X=F, Cl, CN$	Pyramidal, C_{3v} H-bonded		vs	
$H_3N \cdot F_2$	Symmetry Cs		ns	
	Pyramidal, C_{3v}		vs	
$H_3N \cdot N_2$	Pyramidal, C_{3v}		ns	
	Symmetry Cs		s	
$C_2H_2 \cdot HF$	Linear, $C_{\infty v}$ Anti-H, C_{2v}		ns	
$C_2H_2 \cdot FH$	Linear, $C_{\infty v}$		s	
$C_2H_2 \cdot HF$[h]	T-shape, C_{2v}		vs	
$C_2H_2 \cdot OH_2$[i]	Coplanar, C_{2v}		s	
$C_2H_2 \cdot NH_3$[j]	Pyramidal, C_{3v}		vs	

[g] Howard, unpublished; [h] Read and Flygare (1982); [i] Peterson and Klemperer (1984a); [j] Fraser et al. (1984a).

Table 5.4 (*Continued*)

Dimer	Structure	Electrostatic model	Stability	Experiment
$CO_2 \cdot FH$[k]	T-shape, C_{2v} Anti-H		s	
	Linear, $C_{\infty v}$ H-bonded		vs	
$CO_2 \cdot NCH$[l]	T-shape, C_{2v} Anti-H		s	
$CO_2 \cdot OH_2$[m]	Coplanar, C_{2v} Anti-H		s	
	Coplanar, C_s H-bonded		vs	
$CO_2 \cdot NH_3$[n]	H-bonded, C_s		s	
	Anti-H, C_s		vs	
$(H_2)_2$[o], $(N2)_2$[p]	Linear, $D_{\infty h}$		ns	
	Parallel, D_{2h}		ns	
	Canted Parallel, C_{2h}		s	$(F_2)_2$
	T-shape, C_{2v}		vs	$(H_2)_2$, $(N_2)_2$

[k] Baiocchi et al. (1981); [l] Leopold et al. (1984); [m] Peterson and Klemperer (1984b); [n] Fraser et al. (1984b); [o] Gegenbach et al. (1974); [p] Long et al. (1973).

Table 5.4   (*Continued*)

Dimer	Structure	Electrostatic model	Stability	Experiment
$N_2 \cdot F_2$	Linear, $C_{\infty v}$		vs	
$N_2 \cdot HX^q$ X=F, Cl	Linear, $C_{\infty v}$ H-bonded		vs	
$N_2 \cdot HCN^r$	Linear, $C_{\infty v}$ H-bonded		vs	
$F_2 \cdot HF$	Linear, $C_{\infty v}$ H-bonded		ns	
$F_2 \cdot FH$	Linear, $C_{\infty v}$ Anti-H		s	
$F_2 \cdot HF$	T-shape, C_{2v}		s	
$F_2 \cdot H_2$	Canted Parallel. C_s		s	
	T-shape, C_{2v}		s	
$C_2H_4 \cdot HX^s$ X=F, Cl, CN	HX perpendicular to molecular plane, C_{2v}		vs	
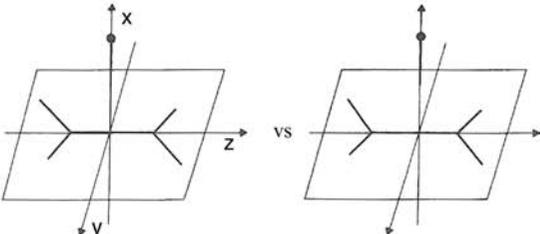
[q] Soper et al. (1982); Altman et al. (1983); [r] Goodwin and Legon (1985); [s] Shea and Flygare (1982); Aldrich et al. (1981); Kukolich et al. (1983).

Figure 5.4(a), strong $\sigma\sigma$ dipole–dipole attraction (R^{-3}) would favour the collinear H-bonded structure HF–HF, which is however destabilized by the quadrupole–quadrupole repulsion $(R^{-5}$, Figure 5.4c). In the collinear configuration, the mixed dipole–quadrupole attraction (R^{-4}) exactly compensates the quadrupole–dipole repulsion $(R^{-4}$, Figure 5.4b). The L-shaped bent configuration is favoured by $\pi\sigma$ quadrupole-dipole (R^{-4}) and quadrupole–quadrupole (R^{-5}) attractions, with the other components vanishing by symmetry. As a result of these competing effects, the bent structure of Figure 5.4(d) is observed, in qualitative agreement with experiment (Howard et al., 1984).

On the other hand, the collinear H-bonded structure is the more stable for $(HCN)_2$ (Legon et al., 1977). This is due, first, to the larger value of the dipole moment for HCN, about twice that of HF, increasing dipole–dipole attraction, and, second, to the larger intermolecular separation, due to the large size of the monomers, which results in a faster decay with R of the quadrupole–quadrupole interaction (repulsive in the linear case, attractive in the bent form). These examples show that the model must always be handled with care before sound theoretical predictions can be made.

NH_3 gives complexes with a C_{3v} pyramidal structure with HF (Figure 5.1f), HCl and HCN, all bound by a H-bond to the nitrogen atom, complexes of C_{3v} symmetry with F_2 and of C_s symmetry with N_2. The latter behaviour depends on F_2 being a positive and N_2 a negative quadrupole.

For complexes between C_2H_2 and HF, the model correctly predicts the T-shaped C_2 structure of the dimer (Figure 5.1e), having the proton of the proton-donor HF molecule directly H-bonded to the π bond of acetylene, be more stable than the linear $C_{\infty v}$ structure, where acetylene would act as proton donor in forming a H-bonded structure with the σ lone pair of fluorine. In the first case, in fact, both quadrupole-dipole (R^{-4}) and quadrupole-quadrupole $(R^{-5})\pi\sigma$ interactions are attractive.

The anti-H-bonded structure of the complexes $CO_2-XH_n(X = NC, O, N)$ (Baiocchi et al., 1981; Leopold et al., 1984; Peterson and Klemperer, 1984b; Fraser et al., 1984b) follows directly from postulate 7. The corresponding electrostatically possible H-bonded structures are highly destabilized by the strong steric repulsions occurring when the intermolecular separation decreases below the sum of the VdW radii of the monomers. On the contrary, in CO_2-HF the intermolecular separation $(7.47\, a_0)$ is large enough to avoid severe steric repulsions, thereby allowing the linear H-bonded structure of Figure 5.1g to be the most stable.

Finally, we observe that the electrostatic model, characterizing centrosymmetric molecules by their (first) quadrupole moment alone,

necessarily predicts for the corresponding homodimers that stability increases in the order linear (L) < parallel (P) < canted parallel (CP) < T-shaped configurations. This order directly follows from the quadrupole–quadrupole interaction in its various form. While this is true for $(H_2)_2$ (Gegenbach *et al.*, 1974; Long *et al.*, 1973) and $(N_2)_2$, the inversion in stability between the last two structures, expected for $(F_2)_2$ and its higher homologues (Buckingham and Fowler, 1983), but not experimentally observed as yet, would only be possible by taking the next moment (the hexadecapole, large for F_2) into account. A CP configuration was in fact found to be stable for $(C_2H_2)_2$ in terms of a spheroidal quadrupole interaction mimicking quicker convergence of the multipole expansion (Aubert-Frécon, 1978a, 1978b). While the linear (L) structure is always unstable for *homodimers* of quadrupolar molecules, in the N_2-F_2 *heterodimer* this structure is expected to be stabilized by the opposite sign of the quadrupole moments of the two molecules.

The formation of T-shaped complexes between C_2H_4 and HX molecules (Shea and Flygare, 1982; Aldrich *et al.*, 1981; Kukolich *et al.*, 1983), where HX is bound by a H-bond perpendicular to the molecular plane of ethylene having the π bond of the olefin as proton acceptor, is favoured by attractive quadrupole-dipole (R^{-4}) and quadrupole–quadrupole (R^{-5}) interactions, those involving the out-of-plane quadrupole moment of ethylene $(\mu_{x^2-y^2})$ being particularly large (Figure 5.8). For the ethylene homodimer, a similar T-shaped structure, with one of the ethylene units twisted by 90° out of the molecular plane, is predicted by the model, in agreement with the results of ab initio calculations (Alberts *et al.*, 1988). This is what we expect from our model in view of the prevalent favourable attraction between the large out-of-plane quadrupole moments of the two ethylene molecules. A similar structure is expected for the benzene dimer (Janda *et al.*, 1975; Pawliszyn *et al.*, 1984).

So, we conclude that our electrostatic model, although simple, is capable of reasonably accurate qualitative predictions which may be confidently used, even for cases not yet theoretically or experimentally studied.

5.4 THE Rg–HF HETERODIMERS

Lastly, we turn to consideration of the Rg–HF heterodimers (the atom–diatomic molecule system of the right-hand side of Figure 5.2), where a crucial role is played by the induction interaction occurring between the higher multipole moments of HF and the induced dipoles originating the polarizability of the rare gas (Magnasco *et al.*, 1989a).

Since atom A (Rg) has no permanent electric moments, the expanded electrostatic interaction energy and the polarization of HF by Rg are both zero:

$$E_1(es) = E_2^{ind}(\text{Rg polarizes HF}) = 0 \qquad (5.13)$$

In this case, the possibility of forming a hydrogen bond comes from second-order induction (polarization of the Rg atom by the *permanent* electric moments of HF) and dispersion (the mutual interaction between fluctuating *induced* moments on both partners).

As far as induction is concerned, the leading R^{-6} term describing polarization of a Rg atom by the dipolar HF molecule as given by Equation (4.63) of Chapter 4:

$$E_2{}^{ind}(6) = -\frac{\alpha^{\text{Rg}}(\mu_1{}^{\text{HF}})^2}{R^6} \, \frac{3\cos^2\theta + 1}{2} \qquad (5.14)$$

cannot discriminate between H-bonded ($\theta = 180°$) and anti-H-bonded ($\theta = 0°$) structures, giving in both cases:

$$E_2{}^{ind}(6) = -2\frac{\alpha^{\text{Rg}}(\mu_1{}^{\text{HF}})^2}{R^6} \qquad (5.15)$$

The next term in R^{-7}, implying further polarization of the Rg atom by the *mixed* dipole–quadrupole moments of HF, contains a $\cos^3\theta$ term:

$$E_2{}^{ind}(7) = \frac{3\,\alpha^{\text{Rg}}\,\mu_1{}^{\text{HF}}\mu_2{}^{\text{HF}}}{R^7} \, \cos^3\theta \qquad (5.16)$$

which stabilizes the H-bonded structure Rg−HF($\theta = 180°$), so that we can properly speak of formation of a H-bond between Rg and HF.

The same is true for dispersion, whose first two terms in Casimir–Polder form (Magnasco, 2007, 2009a) are:

$$E_2^{disp}(6) = -\frac{1}{2\pi R^6}\int_0^\infty du[6\alpha^{\text{Rg}}(iu)\alpha^{\text{HF}}(iu) + (3\cos^2\theta - 1)\alpha^{\text{Rg}}(iu)\Delta\alpha^{\text{HF}}(iu)]$$

$$(5.17)$$

$$E_2^{disp}(7) = \frac{1}{2\pi R^7}\int_0^\infty du\,\alpha^{\text{Rg}}(iu)\left[\cos^3\theta\,\alpha_{210}^{\text{HF}}(iu) + \frac{\sqrt{3}}{3}(3 - 2\cos^2\theta)\cos\theta\,\alpha_{211}^{\text{HF}}(iu)\right]$$

$$(5.18)$$

Table 5.5 Dipole polarizabilities α and relative stabilities Δ of H-bonded with respect to anti-H bonded structures in Rg-HF interactions (atomic units)

Rg	α/a_0^3	R/a_0	$\Delta/10^{-6}E_h$
He	1.38	7.00	46.8
Ne	2.67	7.25	60.8
Ar	11.08	6.41	396.7
Kr	16.71	6.65	456.3
Xe	27.16	7.01	515.8

with Equation (5.17) unable to distinguish between the two structures and Equation (5.18) stabilizing the H-bonded form ($\theta = 180°$). In Equation (5.18), $\alpha_{210}^{HF}(iu)$ and $\alpha_{211}^{HF}(iu)$ are the nonvanishing *mixed* quadrupole–dipole frequency-dependent polarizabilities (FDPs) of HF. A more detailed analysis in Magnasco *et al.* (1989a) shows further that, even if *smaller* in absolute value than dispersion, induction has a *larger* angular change than dispersion, being therefore the main contributor to the shape of such H-bonded dimers.

From the data reported in this work, we obtain Table 5.5, which gives the relative stability Δ of H-bonded with respect to anti-H-bonded structures in the whole series of heterodimers. The distances for the heavier rare gases (Ar, Kr, Xe) are those given by Hutson and Howard (1982) for the well depths of the potentials at the absolute minima of the H-bonded structures. The experimental values of the dipole polarizabilities α of the Rg gases taken from Soldán *et al.* (2001) are given in the second column of the table. It is seen that the stability of the H-bonded structures increases with the dipole polarizability of the heavier rare gases.

References

Abramowitz, M. and Stegun, I.A. (1965) *Handbook of Mathematical Functions*, Dover, New York.

Alberts, I.L., Rowlands, T.W., and Handy, N.C. (1988) Stationary points on the potential energy surfaces of $(C_2H_2)_2$, $(C_2H_2)_3$, and $(C_2H_4)_2$. *J. Chem. Phys.*, **88**, 3811–3816.

Albright, T.A., Burdett, J.K., and Whangbo, M.H. (1985) *Orbital Interactions in Chemistry*, John Wiley & Sons, Inc, New York.

Aldrich, P.D., Legon, A.C., and Flygare, W.H. (1981) The rotational spectrum, structure and molecular properties of ethylene–HCl dimer. *J. Chem. Phys.*, **75**, 2126–2134.

Altman, R.S., Marshall, M.D., and Klemperer, W. (1983) The microwave spectrum and molecular structure of N_2–HCl. *J. Chem. Phys.*, **79**, 57–64.

Amos, R.D. (1982) Multipole moments and polarizabilities of hydrogen fluoride. A comparison of configuration interaction and perturbation theory methods. *Chem. Phys. Lett.*, **88**, 89–94.

Aquilanti, V., Cappelletti, D., and Pirani, F. (1996) Range and strength of interatomic forces: dispersion and induction contributions to the bonds of dications and of ionic molecules. *Chem. Phys.*, **209**, 299–311.

Aubert-Frécon, M. (1978a) Spheroidal multipolar expansions for intermolecular energy in crystal theory. I. Formalism. *Chem. Phys.*, **34**, 341–357.

Aubert-Frécon, M. (1978b) Spheroidal multipolar expansions for intermolecular energy in crystal theory. II. Lattice energy of the orthorombic structure of acetylene crystal. *Chem. Phys.*, **34**, 359–364.

Baiocchi, F.A., Dixon, T.A., Joyner, C.H., and Klemperer, W. (1981) CO_2–HF: a linear molecule. *J. Chem. Phys.*, **74**, 6544–6549.

Bartell, L.S. and Carroll, B.L. (1965) Electron-diffraction study of diborane and deuterodiborane. *J. Chem. Phys.*, **42**, 1135–1139.

Battezzati, M. and Magnasco, V. (2004) Asymptotic evaluation of the Keesom integral. *J. Phys. A: Math. Gen.*, **37**, 9677–9684.

Bednorz, J.G. and Müller, K.A. (1986) Possible high T_c superconductivity in the Ba–La–Cu–O system. *Z. f. Phys. Ser. B*, **64**, 189–193.

Bendazzoli, G.L., Magnasco, V., Figari, G., and Rui, M. (2000) Full-CI calculation of imaginary frequency-dependent dipole polarizabilities of ground state LiH and the C_6 dispersion coefficients of LiH–LiH. *Chem. Phys. Lett.*, **330**, 146–151.

Branton, G.R., Frost, D.C., Makita, T., McDowell, C.A., and Stenhouse, I.A. (1970) Photoelectron spectra of ethylene and ethylene-d$_4$. *J. Chem. Phys.*, **52**, 802–806.

Brink, D.M. and Satchler, G.R. (1993) *Angular Momentum*, 3rd edn, Oxford Clarendon Press, Oxford.

Buckingham, A.D. (1967) Permanent and induced molecular moments and long-range intermolecular forces. *Adv. Chem. Phys.*, **12**, 107–142.

Buckingham, A.D. (1982) Closing remarks. *Faraday Discuss. Chem. Soc.*, **73**, 421–423.

Buckingham, A.D. and Fowler, P.W. (1983) Do electrostatic interactions predict structures of van der Waals molecules? *J. Chem. Phys.*, **79**, 6426–6428.

Cambi, R., Cappelletti, D., Liuti, G., and Pirani, F. (1991) Generalized correlations in terms of polarizability for van der Waals interaction potential parameter calculations. *J. Chem. Phys.*, **95**, 1852–1861.

Casimir, H.B.G. and Polder, D. (1948) The influence of retardation on the London-van der Waals forces. *Phys. Rev.*, **73**, 360–372.

Christiansen, P.A. and McCullough, E.A. (1977) Numerical Hartree–Fock calculations for N_2, FH and CO: comparison with optimized LCAO results. *J. Chem. Phys.*, **67**, 1877–1882.

Clementi, E. and Roetti, C. (1974) Roothaan–Hartree–Fock atomic wavefunctions. *Atom. Data Nucl. Data Tables*, **14**, 177–478.

Coulson, C.A. (1938) The electronic structure of some polyenes and aromatic molecules. IV. The nature of the links of certain free radicals. *Proc. R. Soc. London Ser. A*, **164**, 383–396.

Coulson, C.A. (1958) *Electricity*, 5th edn, Oliver and Boyd, Edinburgh.

Coulson, C.A. (1961) *Valence*, 2nd edn, Oxford University Press, Oxford.

Dyke, T.R. and Muenter, J.S. (1974) Microwave spectrum and structure of hydrogen bonded water dimer. *J. Chem. Phys.*, **60**, 2929–2930.

Eisenschitz, R. and London, F. (1930) Über das Verhältnis der van der Waalsschen Kräfte zu den homöopolaren Bindungskräfte. *Z. f. Phys.*, **60**, 491–527.

Feller, D. and Dixon, D.A. (2001) Extended benchmark studies of coupled cluster theory through triple excitations. *J. Chem. Phys.*, **115**, 3484–3496.

Feltgen, R., Kirst, H., Köhler, K.A., Pauly, H., and Torello, F. (1982) Unique determination of the He$_2$ ground state potential from experiment by use of a reliable potential model. *J. Chem. Phys.*, **76**, 2360–2378.

Figari, G. and Magnasco, V. (2003) On the interpolation of frequency-dependent polarizabilities through a readily integrable expression. *Chem. Phys. Lett.*, **374**, 527–533.

Fraser, G.T., Leopold, K.R., and Klemperer, W. (1984a) The structure of NH$_3$–acetylene. *J. Chem. Phys.*, **80**, 1423–1426.

Fraser, G.T., Leopold, K.R., and Klemperer, W. (1984b) The rotational spectrum, internal rotation, and structure of NH$_3$–CO$_2$. *J. Chem. Phys.*, **81**, 2577–2584.

Gegenbach, R., Hahn, C., Schrader, W., and Toennies, J.P. (1974) Determination of the H$_2$–H$_2$ potential from absolute cross section measurements. *Theor. Chim. Acta Berlin*, **34**, 199–212.

Goodwin, E.J. and Legon, A.C. (1984) The rotational spectrum of the weakly bound molecular complex OC–HCN investigated by pulsed-nozzle, Fourier transform microwave spectroscopy. *Chem. Phys.*, **87**, 81–92.

Goodwin, E.J. and Legon, A.C. (1985) The rotational spectrum and properties of N_2–HCN. *J. Chem. Phys.*, **82**, 4434–4441.

Herzberg, G. (1956) *IR and Raman Spectra of Polyatomic Molecules*, Van Nostrand, New York.

Howard, B.J., Dyke, T.R., and Klemperer, W. (1984) The molecular beam spectrum and the structure of the hydrogen fluoride dimer. *J. Chem. Phys.*, **81**, 5417–5425.

Huber, K.P. and Herzberg, G. (1979) *Molecular Spectra and Molecular Structure: IV. Constants of Diatomic Molecule*, Van Nostrand-Reinhold, New York.

Hückel, E. (1930) Zur Quantentheorie der Doppelbindung. *Z. f .Phys.*, **60**, 423–456.

Hückel, E. (1931) Quantentheoretische Beiträge zum Benzolproblem. I. Die Elektronen-konfiguration des Benzols und verwandter Verbindungen. *Z. f .Phys.*, **70**, 204–286.

Hückel, E. (1932) Quantentheoretische Beiträge zum Problem der aromatischen und ungesättigten Verbindungen. III. *Z. f .Phys.*, **76**, 628–648.

Hutson, J.M. and Howard, B.J. (1982) Anisotropic intermolecular forces. II. Rare gas–hydrogen fluoride systems. *Mol.Phys.*, **45**, 791–805.

Janda, K.C., Hemminger, J.C., Winn, J.S., Novick, S.E., Harris, S.J., and Klemperer, W. (1975) Benzene dimer: a polar molecule. *J. Chem. Phys.*, **63**, 1419–1421.

Keesom, W.H. (1921) Die van der Waalsschen Kohäsionkräfte. *Phys. Z.*, **22**, 129–141.

Kisiel, Z., Legon, A.C., and Millen, D.J. (1982) Spectroscopic investigations of hydrogen bonding interactions in the gas phse. VII. The equilibrium conformation and out-of-plane bending potential energy function of the hydrogen-bonded heterodimer H_2O–HF determined from its microwave rotational spectrum. *Proc. R. Soc. London Ser. A*, **381**, 419–442.

Klessinger, M. (1965) Self-consistent group calculations on polyatomic molecules. II. Hybridization and optimum orbitals in water. *J. Chem. Phys.*, **43**, S117–S119.

Kukolich, S.G., Read, W.G., and Aldrich, P.D. (1983) Microwave spectrum, structure and quadrupole coupling for the ethylene–hydrogen cyanide complex. *J. Chem. Phys.*, **78**, 3552–3556.

Kutzelnigg, W. (1990) The Physical Origin of the Chemical Bond. In *Theoretical Models of Chemical Bonding*, Part 2, Z. B. Maksic, Ed, Springer, Berlin. pp 1–43.

Legon, A.C., Campbell, E.J., and Flygare, W.H. (1982) The rotational spectrum and molecular properties of a hydrogen-bonded complex formed between hydrogen cyanide and hydrogen chloride. *J. Chem. Phys.*, **76**, 2267–2274.

Legon, A.C., Millen, D.J., and Mjöberg, P.J. (1977) The hydrogen cyanide dimer: identification and structure from microwave spectroscopy. *Chem. Phys.Lett.*, **47**, 589–591.

Legon, A.C., Millen, D.J., and Rogers, S.C. (1980) Spectroscopic investigations of hydrogen bonding interactions in the gas phase. I. The determination of the geometry, dissociation energy, potential constants and electric dipole moment of the hydrogen-bonded heterodimer HCN–HF from its microwave rotational spectrum. *Proc. R. Soc. London Ser. A*, **370**, 213–237.

Legon, A.C., Soper, P.D., and Flygare, W.H. (1981) The rotational spectrum, H–^{19}F nuclear spin–nuclear spin coupling, D nuclear quadrupole coupling, and molecular geometry of a weakly bound dimer of carbon monoxide and hydrogen fluoride. *J. Chem. Phys.*, **74**, 4944–4950.

Legon, A.C., Soper, P.D., Keenan, M.R., Minton, T.K., Balle, T.J., and Flygare, W.H. (1980) The rotational spectrum of weakly bound dimers of carbon monoxide and the hydrogen halides HX (X = F, Cl, and Br). *J. Chem. Phys.*, **73**, 583–584.

Lempka, H.J., Passmore, T.R., and Price, W.C. (1968) The photoelectron spectra and ionized states of the halogen acids. *Proc.R.Soc.London Ser. A*, **304**, 53–64.

Lennard-Jones, J.E. (1937) The electronic structure of some polyenes and aromatic molecules. I. The nature of the links by the method of molecular orbitals. *Proc. R. Soc. London Ser. A*, **158**, 280–296.

Leopold, K.R., Fraser, G.T., and Klemperer, W. (1984) Rotational spectrum and structure of the complex $HCN–CO_2$. *J. Chem. Phys.*, **80**, 1039–1046.

Liu, B. and McLean, A.D. (1973) Accurate calculation of the attractive interaction of two ground state helium atoms. *J. Chem. Phys.*, **59**, 4557–4558.

Lloyd, D.R. and Lynaugh, N. (1970) Photoelectron studies of Boron compounds: I. Diborane, borazine and B-trifluoroborazine. *Phil.Trans.R.Soc.London Ser. A*, **268**, 97–109.

London, F. (1930a) Zur Theorie und Systematik der Molekularkräfte. *Z.f.Phys.*, **63**, 245–279.

London, F. (1930b) Über einige Eigenschaften und Anwendungen der Molekularkräfte. *Z. f. phys. Chem. Ser. B*, **11**, 222–251.

Long, C.A., Henderson, G. and Ewing, G.E. (1973) The infrared spectrum of the $(N_2)_2$ Van der Waals molecule. *Chem. Phys.*, **2**, 485–489.

Longuet-Higgins, H.C. (1956) The electronic states of composite systems. *Proc. R. Soc. London Ser. A*, **235**, 537–543.

MacRobert, T.M. (1947) *Spherical Harmonics*, 2nd edn, Methuen, London.

Magnasco, V. (2002) On the α and β parameters in Hückel theory including overlap for simple molecular systems. *Chem. Phys.Lett.*, **363**, 544–549.

Magnasco, V. (2003) A model for the heteropolar bond. *Chem. Phys. Lett.*, **380**, 397–403.

Magnasco, V. (2004a) A model for the chemical bond. *J. Chem. Edu.*, **81**, 427–435.

Magnasco, V. (2004b) A model for the van der Waals bond. *Chem. Phys. Lett.*, **387**, 332–338.

Magnasco, V. (2005) On the principle of maximum overlap in molecular orbital theory. *Chem. Phys.Lett.*, **407**, 213–216.

Magnasco, V. (2007) *Elementary Methods of Molecular Quantum Mechanics*, Elsevier, Amsterdam.

Magnasco, V. (2008) Orbital exponent optimization in elementary VB calculations of the chemical bond in the ground state of simple molecular systems. *J. Chem. Edu.*, **85**, 1686–1691.

Magnasco, V. (2009a) *Methods of Molecular Quantum Mechanics (An Introduction to Electronic Molecular Structure)*, John Wiley & Sons, Ltd, Chichester.

Magnasco, V. (2009b) On the hybridization problem in H_2O by Hückel transformation theory. *Chem. Phys. Lett.*, **474**, 212–216.

Magnasco, V. (2009c) Hückel transformation theory of the hybridization problem in NH_3. *Chem. Phys. Lett.*, **477**, 392–396.

Magnasco, V. (2009d) Hückel transformation theory of ground state HF. *Chem. Phys. Lett.*, **477**, 397–401.

Magnasco, V., Battezzati, M., Rapallo, A., and Costa, C. (2006) Keesom coefficients in gases. *Chem. Phys. Lett.*, **428**, 231–235.

Magnasco, V., Costa, C., and Figari, G. (1989a) Long-range second-order interactions and the shape of the He–HF and Ne–HF complexes. *Chem. Phys. Lett.*, **156**, 585–591.

Magnasco, V., Costa, C., and Figari, G. (1989b) On the angular shape of van der Waals dimers of small polar molecules. *Chem. Phys. Lett.*, **160**, 469–478.

Magnasco, V., Costa, C., and Figari, G. (1990a) A model for the elementary prediction of the angular geometries of van der Waals molecules. *J. Mol. Struct. Theochem*, **204**, 229–246.

Magnasco, V., Costa, C., and Figari, G. (1990b) Long-range coefficients for molecular interactions. II. *J. Mol .Struct. Theochem*, **206**, 235–252.

Magnasco, V. and Figari, G. (2009) Reduced dipole pseudospectra for the accurate tabulation of C_6 dispersion coefficients. *Theoret. Chem. Acc.*, **123**, 257–263.

Magnasco, V., Figari, G., and Costa, C. (1988) Long-range coefficients for molecular interactions. *J. Mol .Struct. Theochem*, **164**, 49–66.

Magnasco, V. and McWeeny, R. (1991) Weak Interactions Between Molecules, In *Theoretical Models of Chemical Bonding*, Part 4, Z.B.Maksic, Ed, Springer, Berlin. pp 133–169.

Magnasco, V. and Musso, G.F. (1981) H_2-H_2 revisited. Orthogonalization, polarization and delocalization effects within a bond-orbital scheme. *Chem. Phys. Lett.*, **84**, 575–579.

Magnasco, V., Musso, G.F., Costa, C., and Figari, G. (1985) A minimal basis bond-orbital investigation of the linear water dimer. *Mol. Phys.*, **56**, 1249–1269.

Magnasco, V. and Ottonelli, M. (1999) Long-range dispersion coefficients from a generalization of the London formula. *Trends Chem. Phys.*, **7**, 215–232.

Magnasco, V., Ottonelli, M., Figari, G., Rui, M., and Costa, C. (1998) Polarizability pseudospectra and dispersion coefficients for H(1s)–H(1s). *Mol. Phys.*, **94**, 905–908.

Magnasco, V. and Perico, A. (1967) Uniform localization of atomic and molecular orbitals. I. *J. Chem. Phys.*, **47**, 971–981.

Magnasco, V. and Perico, A. (1968) Uniform localization of atomic and molecular orbitals. II. *J. Chem. Phys.*, **48**, 800–808.

Mattheiss, L.F. (1987) Electronic band properties and superconductivity in $La_{2-y}X_yCuO_4$. *Phys. Rev. Lett.*, **58**, 1028–1030.

McLean, A.D. and Yoshimine, M. (1967) Theory of molecular polarizabilities. *J. Chem. Phys.*, **47**, 1927–1935.

McWeeny, R. (1979) *Coulson's Valence*, 3rd edn, Oxford University Press, Oxford.

Meyer, W. (1976) Dynamic polarizabilities of H_2 and He and long-range interaction coefficients for H_2-H_2, H_2–He and He–He. *Chem. Phys.*, **17**, 27–33.

Mohr, P.J. and Taylor, B.N. (2003) The fundamental physical constants. *Phys. Today*, **56**, BG6–BG13.

Muenter, J.S. and Klemperer, W. (1970) Hyperfine structure constants of HF and DF. *J. Chem. Phys.*, **52**, 6033–6037.

Mulliken, R.S. (1951) Overlap and bonding power of 2s,2p hybrid orbitals. *J. Chem. Phys.*, **19**, 900–912.

Mulliken, R.S. (1955) Electronic population analysis on LCAO-MO molecular wave functions. *J. Chem. Phys.*, **23**, 1833–1840.

Murrell, J.N., Kettle, S.F.A., and Tedder, J.M. (1985) *The Chemical Bond*, 2nd edn, John Wiley & Sons, Ltd, Chichester.

Musso, G.F. and Magnasco, V. (1982) Bond-orbital analysis of rotation barriers. Polarization and delocalization effects in ethane. *J. Chem. Soc. Faraday Trans. II*, **78**, 1609–1616.

Palke, W.E. (1986) Double bonds are bent equivalent hybrid (banana) bonds. *J.Am.Chem. Soc.*, **108**, 6543–6544.

Palke, W.E. and Lipscomb, W.N. (1966) Molecular SCF calculations on CH_4, C_2H_2, C_2H_4, C_2H_6, BH_3, B_2H_6, NH_3 and HCN. *J. Am .Chem. Soc.*, **88**, 2384–2393.

Pawliszyn, J., Szczęśniak, M.M., and Scheiner, S. (1984) Interaction between aromatic systems: dimers of benzene and *s*-tetrazine. *J. Phys. Chem.*, **88**, 1726–1730.

Pelloni, S. (2008) Private communication to V. Magnasco.

Peterson, K.I. and Klemperer, W. (1984a) Water-hydrocarbon interactions: rotational spectroscopy and structure of the water–acetylene complex. *J. Chem. Phys.*, **80**, 2439–2445.

Peterson, K.I. and Klemperer, W. (1984b) Structure and internal rotation of H_2O–CO_2, HDO–CO_2, and D_2O–CO_2 van der Waals complexes. *J. Chem. Phys.*, **81**, 3842–3845.

Pople, J.A. (1982) Intermolecular binding. *Faraday Discuss. Chem. Soc.*, **73**, 7–17.

Pople, J.A. and Santry, D.P. (1964) A molecular orbital theory for hydrocarbons. I. Bond delocalization in paraffins. *Mol. Phys.*, **7**, 269–286.

Pople, J.A. and Santry, D.P. (1965) A molecular orbital theory for hydrocarbons. II. Ethane, ethylene and acetylene. *Mol. Phys.*, **9**, 301–310.

Potts, A.W. and Price, W.C. (1972) Photolectron spectra and valence shell orbital structures of groups V and VI hydrides. *Proc. R. Soc. London Ser. A*, **326**, 181–197.

Price, W.C. (1974) Photoelectron spectroscopy. *Adv. Atom. Mol. Phys.*, **10**, 131–171.

Read, W.G. and Flygare, W.H. (1982) The microwave spectrum and molecular structure of the acetylene-HF complex. *J. Chem. Phys.*, **76**, 2238–2246.

Ruedenberg, K. (1962) The physical nature of the chemical bond. *Rev. Mod. Phys.*, **34**, 326–376.

Shea, J.A. and Flygare, W.H. (1982) The rotational spectrum and molecular structure of the ethylene–HF complex. *J. Chem. Phys.*, **76**, 4857–4864.

Sileo, R.N. and Cool, T.A. (1976) Overtone emission spectroscopy of HF and DF: vibrational matrix elements and dipole moment function. *J. Chem. Phys.*, **65**, 117–133.

Slater, J.C. (1937) Wave functions in a periodic potential. *Phys. Rev.*, **51**, 846–851.

Slater, J.C. (1965) *Quantum Theory of Molecules and Solids, Vol. 2. Symmetry and Energy Bands in Crystals*, McGraw-Hill Book Co., New York.

Smirnov, V.I. (1993) *Corso di Matematica Superiore, Vol. I*, Editori Riuniti, Roma.

Soldán, P., Lee, E.P.F., and Wright, T.G. (2001) Static dipole polarizabilities (α) and static second hyperpolarizabilities (γ) of the rare gas atoms. *Phys. Chem. Chem. Phys.*, **3**, 4661–4666.

Soper, P.D., Legon, A.C., and Flygare, W.H. (1981) Microwave rotational spectrum, molecular geometry, and intermolecular interaction potential of the hydrogen-bonded dimer OC–HCl. *J. Chem. Phys.*, **74**, 2138–2142.

Soper, P.D., Legon, A.C., Read, W.G., and Flygare, W.H. (1982) The microwave rotational spectrum, molecular geometry, ^{14}N nuclear quadrupole coupling constants, and H–^{19}F nuclear spin–nuclear spin coupling constant of the nitrogen–hydrogen fluoride dimer. *J. Chem. Phys.*, **76**, 292–300.

Stone, A.J. (1996) *The Theory of Intermolecular Forces*, Clarendon Press, Oxford.

Sugiura, Y. (1927) Sur le nombre des électrons de dispersion pour les spectres continus et pour les spectres de séries de l'hydrogène. *J. de Phys. et le Radium*, **8**, 113–124.

Sundholm, D., Pyykkö, P., and Laaksonen, L. (1985) Two-dimensional, fully numerical molecular calculations. X. Hartree–Fock results for He_2, Li_2, Be_2, HF, OH^-, N_2, CO, BF, NO^+ and CN^-. *Mol. Phys.*, **56**, 1411–1418.

Tinkham, M. (1975) *Introduction to Superconductivity*, McGraw-Hill, Inc, New York.

Torheyden, M. and Jansen, G. (2006) A new potential energy surface for the water dimer obtained from separate fits of *ab-initio* electrostatic, induction, dispersion and exchange energy contributions. *Mol. Phys.*, **104**, 2101–2138.

Torkington, P. (1951) The generalized valence orbitals derivable by sp^3 hybridization. *J. Chem. Phys.*, **19**, 528–533.

Walker, S. and Straw, H. (1966) *Spectroscopy*, paperback edn, Chapman & Hall, London.

Werner, H.-J. and Meyer, W. (1976) PNO-CI and PNO-CEPA studies of electron correlation effects V. Static dipole polarizabilities of small molecules. *Mol. Phys.*, **31**, 855–872.

Wigner, E. and Huntington, H.B. (1935) On the possibility of a metallic modification of hydrogen. *J. Chem. Phys.*, **3**, 764–770.

Wolniewicz, L. (1993) Relativistic energies of the ground state of the hydrogen molecule. *J. Chem. Phys.*, **99**, 1851–1868.

Wood, J.H. (1962) Energy bands in iron via the augmented plane wave method. *Phys. Rev.*, **126**, 517–527.

Wormer, P.E.S. (1975) Intermolecular Forces and the Group Theory of Many-Body Systems. PhD Dissertation, Katholicke Universiteit, Nijmegen, The Netherlands.

Yakovlev, Y. (1976) Hydrogen is a metal at last. *New Scientist*, **71**, 478–479.

Author Index

Subject Index